DTU Library

Model-Based Integrated Process Design and Controller Design of Chemical Processes

Abd Hamid, Mohd Kamaruddin Bin

Publication date:
2011

Document Version
Publisher's PDF, also known as Version of record

[Link back to DTU Orbit](#)

Model-Based Integrated Process Design and Controller Design of Chemical Processes

Mohd. Kamaruddin bin Abd. Hamid
Ph.D. Thesis
January 2011

DTU Chemical Engineering
Department of Chemical and Biochemical Engineering

Model-Based Integrated Process Design and Controller Design of Chemical Processes

Ph.D. Thesis
Mohd. Kamaruddin bin Abd. Hamid

January 2011

Computer Aided Process-Product Engineering Center
Department of Chemical and Biochemical Engineering
Technical University of Denmark

Preface

This dissertation was written as partial fulfillment of requirements for the degree of Doctor of Philosophy (*Ph.D.*) in Chemical Engineering at the Technical University of Denmark (*DTU*). The project has been carried out at the Computer Aided Process-Product Engineering Center (*CAPEC*) at the Department of Chemical and Biochemical Engineering, from Jun 2007 until January 2011, under the supervision of Professor Rafiqul Gani and Associate Professor Gürkan Sin.

This work has been financed by the Ministry of Higher Education (*MOHE*) of Malaysia and Universiti Teknologi Malaysia (*UTM*).

My sincerest thanks to my supervisors Professor Rafiqul Gani and Associate Professor Gürkan Sin who have provided all possible help and guidance when and where required. A special thanks to my main supervisor Professor Rafiqul Gani for his guidance, academic support and interest in my work. Also I am grateful to Associate Professor Gürkan Sin for all the fruitful discussions besides the support provided during the development of this work.

I would like to thank all the coworkers at *CAPEC*: Elisa, Rasmus, Sasha, Azizul, Fazli, Martin, Axel, Jacob, Oscar, Alicia, Katrine, Ricardo, Martina, Merlin, Philip, Alafiza, Igor, Amol, Alberto, and Ravendra, for their support, technical and non-technical discussions and encouragement in all those years of research.

Finally, I wish to thank to my family for their support and understanding during the writing of this thesis. I am grateful to my wife, Norazana Ibrahim and my lovely sons, Muhammad Afiq Zakwan and Muhammad Adam Zarif, for their unconditional support and love. Not forget to all my family members in Malaysia, thank you very much for the doa'.

MOHD. KAMARUDDIN BIN ABD. HAMID
Kgs. Lyngby, January 2011

Abstract

This thesis describes the development and application of a new systematic model-based methodology for performing integrated process design and controller design (*IPDC*) of chemical processes. The new methodology is simple to apply, easy to visualize and efficient to solve. Here, the *IPDC* problem that is typically formulated as a mathematical programming (optimization with constraints) problem is solved by the so-called reverse approach by decomposing it into four sequential hierarchical sub-problems: (i) pre-analysis, (ii) design analysis, (iii) controller design analysis, and (iv) final selection and verification. Using thermodynamic and process insights, a bounded search space is first identified. This feasible solution space is further reduced to satisfy the process design and controller design constraints in sub-problems 2 and 3, respectively, until in the final sub-problem all feasible candidates are ordered according to the defined performance criteria (objective function). The final selected design is then verified through rigorous simulation.

In the pre-analysis sub-problem, the concepts of attainable region and driving force are used to locate the optimal process-controller design solution in terms of optimal condition of operation from design and control viewpoints. The targets for the design-control solution are defined at the maximum point of the attainable region and driving force diagrams. Defining the targets at the maximum point of the attainable region and driving force diagram ensure the optimal solution not only for the process design but also for the controller design. From a process design point of view at these targets, the optimal design objectives can be obtained. Then by using the reverse solution approach, values of design-process variables that match those targets are calculated in Stage 2. Using model analysis, controllability issues are incorporated in Stage 3 to calculate the process sensitivity and to pair the identified manipulated variables with the corresponding controlled variables. From a controller design point of view, at targets defined in Stage 1, the sensitivity of controlled variables with respect to disturbances is at the minimum and the sensitivity of controlled variables with respect to manipulated variables is at the maximum. Minimum sensitivity with respect to disturbances means that the controlled variables are less sensitive to the effect of disturbances and maximum sensitivity with respect to manipulated variables determines the best controller structure. Since the optimization deals with multi-criteria objective functions, therefore, in Stage 4, the objective function is calculated to verify the best (optimal) solution that satisfies design, control and economic criteria. From an optimization point of view, solution targets at the maximum point of the attainable region and driving force diagrams are shown the higher value of the objective function, hence the optimal solution for the *IPDC* problem is verified. While other optimization methods may or may not be able to find the optimal solution, depending on the performance of their search algorithms and computational demand, this method using the attainable region and driving force concepts is simple and able to find at least near-optimal designs (if not optimal) to *IPDC* problems.

The developed methodology has been implemented into a systematic computer-aided framework to develop a software called *ICAS-IPDC*. The purpose of the software is to support engineers in solving process design and controller design problems in a systematic and efficient way. The proposed methodology has been tested using a series of case studies that represents three different systems in chemical processes: a single reactor system, a single separator system and a reactor-separator-recycle system.

Resumé på Dansk

Denne afhandling beskriver udviklingen og anvendelsen af en ny systematisk modelbaseret metode, der bruges i integreret procesdesign og regulatordesign (*IPDC*) af kemiske processer. Den nye metodik er simpel at anvende, let at visualisere og virksom til opgaveløsning. *IPDC* opgaver, der ofte tager form som matematisk programmeringsopgaver (optimering med begrænsninger), er her løst med den såkaldte omvendte fremgangsmåde ved at dele opgaven op i fire hierarkisk ordnede underopgaver: (i) for-analyse, (ii) design analyse, (iii) regulatordesign analyse og (iv) endelig udvælgelse og verifikation. Ved at anvende termodynamik og procesforståelse bliver et afgrænset undersøgelsesområde først identificeret. Det mulige løsningsområde er yderligere reduceret for at opfylde procesdesignene og regulatordesignenes begrænsninger, i henholdsvis underopgave 2 og 3, indtil at alle potentielle kandidater er ordnet i forhold til de definerede driftskriterier (optimeringsobjektet) i den endelige underopgave. Det udvalgte design er herefter verificeret gennem indgående simuleringer.

I for-analyse underopgaven bliver begreberne om det opnåelige operationsområde og drivende kræfter brugt til at finde det optimale procesregulatordesign med hensyn til optimale forhold for design og regulering. Målene for design-reguleringsløsningerne er defineret som maksimumpunktet i det opnåelige operationsområde og drivende kræfter-diagrammerne. Ved at definere målene som maksimumpunktet i det opnåelige operationsområde og drivende kræfter-diagrammet sikres den optimale løsning, ikke kun for procesdesignet, men også for regulatordesignet. Fra et procesdesign syn på disse mål kan de optimale designformål findes. Herefter kan værdier af designproces variablerne, som passer til målene, beregnes ved at anvende den omvendte fremgangsmåde i Fase 2. Ved at anvende modelanalyse bliver problemer med kontrollerbarheden integreret i Fase 3, hvor proces-sensitiviteten bliver beregnet for at parre de identificerede manipulerede variable med de tilsvarende regulerede variable. Fra et regulatordesign syn på målene, defineret i Fase 1, er sensitiviteten af de regulerede variable med hensyn til forstyrrelser på et minimum og sensitiviteten af de regulerede variable med hensyn til de manipulerede variable er på et maksimum. Minimum sensitiviteten med hensyn til forstyrrelser betyder, at de regulerede variable er mindre sensitive over for forstyrrelser og maksimum sensitiviteten med hensyn til manipulerede variable bestemmer den bedste reguleringsstruktur. Eftersom optimeringen anvender et optimeringsobjekt med flere kriterier bliver kost-funktionen beregnet i Fase 4 for at verificere den bedste (mest optimale) løsning i forhold til at opfylde design, regulering og økonomiske kriterier. Løsningerne i det opnåelige operationsområde og drivende kræfter-diagrammerne udløser også højere værdier i kost-funktionen, og den optimale løsning til *IPDC* opgaven er dermed verificeret. Mens andre optimeringsmetoder måske er brugbare til at finde den optimale løsning afhængig af deres søgnings-algoritme og computerkraftbehov, er denne metode, som anvender begreberne om det opnåelige operationsområde og drivende kræfter-

diagrammerne, enkel og kan finde (hvis ikke helt, så næsten) optimale design i *IPDC* opgaven.

Den udviklede metodik er blevet implementeret i en systematisk computerbaseret struktur og endt som softwaret, *ICAS-IPDC*. Formålet med softwaret er at hjælpe ingeniører med at løse opgaver inden for procesdesign og regulatordesign på en effektiv måde. Metodikken er blevet testet i en række case-studier som repræsenterer tre forskellige systemer inden for kemiske processer: Et enkelt reaktorsystem, et enkelt separationssystem og et reaktor-separation-recirkulationssystem.

Table of Contents

List of Tables

List of Figures

Introduction

1.1   **Introduction**

1.2   **Objective of the Work**

1.3   **Thesis Organization**

In this chapter, we begin in section 1.1 with an introduction to give an overview of the integrated process design and controller design problem. We then discuss the objective of the work in section 1.2, which consists of two main parts - development of a model-based methodology for integrated process design and controller design, and development of an *ICAS-IPDC* software, which is based on the developed methodology. Finally, we summarize the organization of this thesis (section 1.3).

1.1   Introduction

Chemical processes have been traditionally designed by a sequential approach consisting of initial process design, which is based on steady state economic calculations followed by the synthesis of a control structure that is generally based on heuristic controllability measures. Thus, the process design and process control aspects have been generally studied independently (Douglas, 1988). This traditional sequential design approach is often inadequate since the process design can significantly affect the process control. (Malcom et al, 2007, Miranda et al., 2008). Another drawback has to do with how process design decisions influence the controllability of the process. To assure that design decisions give the optimum economic and the best control performance, controller design issues need to be considered simultaneously with the process design issues. The research area of combining process design and controller design considerations is referred here as integrated process design and controller design (*IPDC*). One way to achieve *IPDC* is to identify variables together with their target values that have roles in process design (where the optimal values of a set of design variables are obtained to match specification on a set of process variables) and controller design (where the same set of design variables serve as the actuators or manipulated variables and the same set of

process variables become the controlled variables). Also, the optimal design values become the set-points for the controlled and manipulated variables. Using model analysis, controllability issues are incorporated to pair the identified actuators with the corresponding controlled variables. The integrated design problem is therefore reduced to identifying the dual purpose design-actuator variables, the process-controlled variables, their sensitivities, their target-setpoint values, and their pairing.

The importance of an integrated process-controller design approach, considering operability together with the economic issues, has been widely recognized (Sakizlis et al., 2004; Seferlis and Georgiadis, 2004). The objective has been to obtain a profitable and operable process, and control structure in a systematic manner. The *IPDC* has advantage over the traditional-sequential method because the controllability issues are considered together with the process design issues. In the *IPDC* problem, the controller parameters are optimized together with the system's design parameters to determine the optimal design and operating conditions of a process. The solution to this optimization problem must address the trade-offs between conflicting design and control objectives.

A number of methodologies have been proposed for solving *IPDC* problems (Sakizlis et al., 2004; Seferlis and Georgiadis, 2004). In these methodologies, a mixed-integer non-linear optimization problem (*MINLP*) is formulated and solved with standard *MINLP* solvers. The continuous variables are associated with design variables (flow rates, heat duties) and process variables (temperatures, pressures, compositions), while binary (decision) variables deal with flowsheet structure and controller structure. When an *MINLP* problem represents an *IPDC*, the process model considers only steady state conditions, while a *MIDO* (mixed-integer dynamic optimization) problem represents an *IPDC* where steady state as well as dynamic behavior are considered.

A number of algorithms have been developed to solve the *MIDO* problem. From a dynamic optimization point of view, the solution approaches for *MIDO* problems can be divided into simultaneous and sequential methods, where the original *MIDO* problem is reformulated into a mixed-integer nonlinear program (*MINLP*) problem (Sakizlis et al., 2004). The former method, also called complete discretization approach, transforms the original *MIDO* problem into a finite dimensional nonlinear program (*NLP*) by discretization of the state and control variables. However, this method typically generates a very large number of variables and equations, yielding large *NLPs* that may be difficult to solve reliably (Exler et al., 2008; Patel et al., 2008), depending on the complexity of the process models. As regards the sequential method, also called control vector parameterization approach, only control variables are discretized. The *MIDO* algorithm is decomposed into a sequence of primal problems (nonconvex *DO*s) and relaxed master problems (Bansal et al., 2003; Mohideen et al., 1997; Schweiger and Floudas, 1997; Sharif et al., 1998). Because of nonconvexity of the constraints in *DO* problems, such solution methods are possibly excluding large portions of the feasible region within which an optimal solution may occur, leading to suboptimal solutions (Chachuat et al., 2005). Several works have been done to overcome the suboptimal convergence problem. A number of works in the global optimization methods have shown that the region of global

solutions can be located with relative efficiency (Banga et al., 2003; Moles et al., 2003; Sendin et al., 2004), but they tend to be computationally expensive and have difficulties with highly constrained problems.

Solving *IPDC* problems using the dynamic optimization approach causes a combinatorial explosion due to alternative control formulations and the complexity of the optimization problem. To obtain solutions for this problem will require a huge computational effort which makes this approach impractical for solving real industrial problems (Ricardez-Sandoval et al., 2010). To overcome this complexity, an alternative solution strategy based on an embedded control optimization approach (Malcolm et al., 2007) has been proposed. This approach is based on a new mathematical formulation to reduce the combinatorial complexity of the *IPDC* problem. Accordingly, the *IPDC* problem is formulated as a bi-level optimization problem, which is then solved using a two sequential stage. This formulation separates design decisions from control decisions to keep the problem size manageable. The first stage (usually called master level) seeks optimal design decisions while the second stage tests the dynamic performance based on design decisions obtained previously by fixing a particular control strategy alongside its tuning parameters. Fixing a particular control strategy in the second stage, therefore, eliminates integer decisions for selecting controller structures, and the problem complexity is reduced. Different control techniques/strategies have been implemented such as feedback control (Malcom et al., 2007; Ricardez-Sandoval et al., 2008; Moon et al., 2009a,b), model predictive control (*MPC*) (Chawankul et al., 2007), optimal control with linear quadratic regulator (*LQR*) (Patel et al., 2008), and fuzzy control (Lu et al., 2010). More advanced control techniques can further improve the control performance for a particular design. However, these advanced control techniques come at the price of higher computational effort in each embedded control optimization, hence will deteriorate the performance of the proposed approach that may lead to suboptimal solutions (Malcom et al., 2007, Moon et al., 2009a,b).

In order to overcome the complexity of the *IPDC* problem and obtain an achievable optimal solution, a decomposition approach is proposed in this work. The decomposition approach has been applied in managing and solving the complexity of different optimization problems in chemical engineering such as design of optimal solvents and solvent mixtures (Karunanithi et al., 2005), solvent selection (Gani et al., 2008), sustainable process design (Carvalho et al., 2008), process intensification (Lutze et al., 2010) and product-process design (Conte et al., 2010), where optimal (or nearly optimal) solutions are obtained. The basic idea is that in optimization problems with constraints, the search space is defined by the constraints within which all feasible solutions lie and the objective function helps to identify one or more of the optimal solutions. In the decomposition-based approach (Karunanithi et al., 2005) the optimization problem is decomposed into several sequential sub-problems. The constraint equations are solved in a pre-determined sequence such that after every sequential sub-problem, the search space for feasible solutions is reduced and a sub-set of decision variables are fixed. When all the constraints are satisfied, it remains to calculate the objective function for all the identified feasible solutions to locate the optimal solution. In this work, the decomposition solution strategy has been adopted to develop a new model-based methodology for solving *IPDC* problem.

1.2   Objective of the Work

The objective for this work is to develop a new model-based methodology, which is able to identify and obtain an optimal solution for the *IPDC* problem for chemical processes in an easy, simple and efficient way. The methodology (Hamid et al., 2009a,b; 2010a,b) is based on decomposition of the complex *IPDC* problem into four sequential hierarchical sub-problems: (i) pre-analysis; (ii) design analysis; (iii) controller design analysis; and (iv) final selection and verification. Using thermodynamic and process insights, the bounded search space is first identified. This feasible solution space is further reduced to satisfy the process design and controller design constraints in sub-problems (ii) and (iii), respectively. As each sub-problem is being solved, a large portion of the infeasible solution of the search space is identified and eliminated, thereby leading to a final sub-problem that is significantly smaller, which can be solved more easily. In the pre-analysis sub-problem, the concepts of attainable region (Hildebrandt & Glasser, 1990; Glasser et al., 1987, 1990) and driving force (Gani & Bek-Pedersen, 2000; Bek-Pedersen, 2002; Bek-Pedersen & Gani, 2004) are used to locate the optimal process-controller design solution in terms of optimal condition of operation from design and control viewpoints. While other optimization methods may or may not be able to find the optimal solution, depending on the performance of their search space algorithms and computational demand, using of attainable region and driving force concepts it is possible to find at least near-optimal designs (if not optimal) to *IPDC* problems.

The other main objective is to develop a software that is based on the proposed methodology allowing a systematic, efficient and fast analysis of the *IPDC* problem. This software can be used for industrial and academic purposes.

1.3   Thesis Organization

This PhD-thesis is organized in six chapters including this chapter (Introduction), where the motivation and the objectives of the work are presented. Chapter 2 gives an overview about the methodologies available in solving the *IPDC* problem. This includes the importance of the *IPDC* for chemical processes and also addresses several solution strategies that have been developed to solve *IPDC* problems. The new proposed methodology for model-based *IPDC* is presented in Chapter 3. This chapter presents the formulation of the *IPDC* problem for chemical processes and describes the methodology for solving the *IPDC* problem, which is based on the decomposition approach. The description of the methodology and also the concepts for obtaining the optimal design-control targets are also discussed in detail. Simple illustrative examples are provided at the end of each section to highlight the main concepts and solution steps. In Chapter 4, the *ICAS-IPDC* software is presented in terms of the software framework and its implementation. The case studies, illustrating the application of the methodology through *ICAS-IPDC* are presented in Chapter 5. The objective of this chapter is to highlight the capability of the methodology and its implementation as the *ICAS-IPDC* in solving problems of different type and complexity. The chapter is divided into three sub-sections, which are (i) a single

reactor system; (ii) a single separator system; and (iii) a reactor-separator-recycle system where two case studies are presented for each sub-section. Finally, Chapter 6 presents conclusions and directions for future work.

In Appendix A, the detailed derivation of an alternative distillation column sensitivity analysis is presented. The detailed derivation of the attainable region equations used in the single reactor system for an ethylene glycol production process are given in Appendix B. The rate equations and kinetic models for the simultaneous saccharification and fermentation (*SSF*) process are given in Appendix C. Detailed derivation of the set of conditional constraints in terms of dimensionless variables used in the reactor-separator-recycle case studies are given in Appendices D and E for the theoretical consecutive reactions and an ethylene glycol process, respectively.

CHAPTER 2

Review of Integrated Process Design and Controller Design

In this chapter, we discuss in section 2.1 the importance of the integration of process design and controller design (*IPDC*). The *IPDC* implies the explicit inclusion of controllability considerations within the process design formulation in order to generate the profitable, sustainable and controllable process. However, the task of performing the *IPDC* is not straightforward since it involves multi-criteria optimization and needs trade-off between conflicting design and control objectives. In section 2.2, we discuss in details several solution strategies that have been developed to address the *IPDC* problems for chemical processes. Finally, the chapter ends with a set of concluding remarks (section 2.3).

2.1   Integrated Process Design and Controller Design

In this work, we will consider the case where the process flowsheet is known, as well as the feed and process specifications. The objective is to find the design variables, the operating conditions (including set-points for controlled variables) and controller structure that optimize the plant economics and, simultaneously, a measure of the plant controllability, subject to a set of constraints, which ensure appropriate dynamic behavior and process specifications. The general formulation of the problem is (Sendin et al., 2004):

$$\min_{\mathbf{x},\mathbf{y},\mathbf{u}} \quad F(\mathbf{x},\mathbf{y},\mathbf{u}) = \begin{bmatrix} F_1(\mathbf{x},\mathbf{y},\mathbf{u}) \\ F_2(\mathbf{x},\mathbf{y},\mathbf{u}) \end{bmatrix} \tag{2.1}$$

subject to:

$$\dot{\mathbf{x}}(t) = f(\mathbf{x},\mathbf{y},\mathbf{u},t) \tag{2.2}$$

$$0 = h(\mathbf{x},\mathbf{y},\mathbf{u}) \tag{2.3}$$

$$0 \leq g(\mathbf{x},\mathbf{y},\mathbf{u}) \tag{2.4}$$

$$\mathbf{x}(t_0) = \mathbf{x}_0 \tag{2.5}$$

$$\mathbf{u}(t_0) = \mathbf{u}_0 \tag{2.6}$$

$\mathbf{x}$ is the vector of state variables, $\mathbf{y}$ is the vector of process (controlled) variables, and $\mathbf{u}$ is the vector of design (manipulated) variables. $\mathbf{x}_0$ is the vector of initial conditions of the state variables and $\mathbf{u}_0$ is the vector of initial conditions of the design (manipulated) variables.

The objective function (2.1) to be minimized includes F_1 (the combination of capital and operating costs) and F_2 (the controllability measure i.e. the Integral Square Error). Eq. (2.2) refers to the set of differential and algebraic equality constraints describing the system dynamics (mass, energy and momentum balances, i.e. the nonlinear process model). Eqs. (2.3)-(2.4) are possible equality and inequality path and/or point constraints, which express additional requirements for the process performance.

Traditionally, initial research in the optimization of chemical processes focused mainly on the development of the process design and controller design as independent sequential problems (Douglas, 1988). The process is designed first to achieve the desired design objectives. Then, for a given solution of the steady state design, the operability and control aspects are analyzed and resolved to obtain the controller design, by assuming that the control system can be designed to maintain the process at the desired operating level and within the design constraints. This two step approach can be summarized as follows;

Step 1. Optimal Design Problem: The optimal design problem in steady state can be stated as:

$$
\left.
\begin{aligned}
&\min_{\mathbf{x}_0,\mathbf{y}_0,\mathbf{u}_0} \quad F_1(\mathbf{x},\mathbf{y},\mathbf{u}) \\
&s.t. \\
&0 = f\left(\mathbf{x},\mathbf{y},\mathbf{u}\right) \\
&0 = h(\mathbf{x},\mathbf{y},\mathbf{u}) \\
&0 \leq g(\mathbf{x},\mathbf{y},\mathbf{u})
\end{aligned}
\right\}
\tag{2.7}
$$

The basic idea of the solution of Eq. (2.7) is that the optimal steady state solutions $\mathbf{x}^*$, $\mathbf{y}^*$, $\mathbf{u}^*$ are obtained such that the objective function F_1 is minimized. Subsequently, these optimal steady state solutions are used to construct the initial condition of the optimal control design problem.

Step 2. Optimal Control Problem: The above obtained solutions ($\mathbf{x}^*$, $\mathbf{y}^*$, $\mathbf{u}^*$) are now evaluated dynamically in the presence of the perturbations and with consideration of dynamic control constraints. The objective is therefore to search for the optimal control rule that ensures the operability of the process according to the performance criteria. The optimal control problem can be formulated as:

$$
\left.
\begin{aligned}
&\min_{\mathbf{x}^*,\mathbf{y}^*,\mathbf{u}^*} \quad F_2(\mathbf{x}^*,\mathbf{y}^*,\mathbf{u}^*) \\
&s.t. \\
&\dot{\mathbf{x}}(t) = f\left(\mathbf{x}(t),\mathbf{y}(t),\mathbf{u}(t),t\right) \\
&0 = g(\mathbf{x}(t),\mathbf{y}(t),\mathbf{u}(t),t) \\
&0 \leq h(\mathbf{x}(t),\mathbf{y}(t),\mathbf{u}(t),t) \\
&\mathbf{x}(t_0) = \mathbf{x}^* \\
&\mathbf{u}(t_0) = \mathbf{u}^*
\end{aligned}
\right\}
\tag{2.8}
$$

The traditional-sequential approach (solving Eqs. (2.7)-(2.8) sequentially), is often judged on the basis of design and cost criteria alone, without taking controllability issues into consideration, and may lead to the elimination of easily controlled but slightly less economical design alternatives in favour of more economical design alternatives that may be extremely difficult to control (Luyben, 2004; Ricardez-Sandoval et al., 2009a,b). These more economical design alternatives may cause many process control challenges such as limitation of the effectiveness of the control system in attenuating the effect of disturbances leading to a process that is unable to meet its design specifications, dynamic constraint violations, and may not guarantee robust performance (López-Negrete & Flores-Tlacuahuac, 2009). Another drawback has to do with how process design decisions influence the controllability of the process. Recent results of research in this field have demonstrated that considering controller design issues simultaneously with the process design issues, provides considerable economic and operability benefits compared to the traditional approach.

The research area of combining process design and controller design considerations is referred here as integrated process design and controller design (*IPDC*). Using this approach, both process design and controller design will share the same variable(s) in their decisions. Accordingly, one way to achieve *IPDC* is to identify variables together with their target values that have roles in process design and controller design. In the process design the optimal values of a set of design variables are obtained to match specifications on a set of process variables, whereas, in the controller design, the same set of design variables serve as the actuators or manipulated variables and the same set of process variables become the controlled variables. Also, the optimal design values become the set points for the controlled and manipulated variables. Using model analysis, controllability issues are incorporated to pair the identified manipulated variables with the corresponding controlled variables. The integrated design problem is therefore reduced to identifying the dual purpose design-manipulated variables, the process-controlled variables, their sensitivities, their target - set point value, and their pairing. The optimal solutions (x^{opt}, y^{opt}, u^{opt}) are obtained by solving Eqs. (2.2)-(2.6) such that the objective function Eq. (2.1) is minimized.

The importance of an integrated process-controller design approach, considering controllability together with the economic issues, has been widely recognized (Allgor & Barton, 1999; Alhammadi & Romagnoli, 2004; Altimari & Bildea, 2009; Bansal et al., 2000; Bansal et al., 2003; Kookos & Perkins, 2001; Luyben, 2004; Luyben & Floudas, 1994; Meeuse & Grievink, 2004; Patel et al., 2008; Ricardez-Sandoval et al., 2008; Schweiger & Floudas, 1997; Swartz, 2004). The objective has been to obtain a profitable and operable process, and control structure in a systematic manner. The *IPDC* has advantage over the traditional-sequential approach because the controllability issues are resolved together with the optimal process design issues. The solution obtained from the *IPDC* not only considered the process costs, but also the process inherent controllability, which means "how well the process rejects disturbances, how severely the multiple variables interact, and how easily the system moves from one operating condition to another" (Luyben, 2004). However, the task of performing the *IPDC* is not straightforward since it involves multi-criteria optimization and needs a trade-off between conflicting design and control objectives (Ricardez-Sandoval et al., 2009a,b). For example, the process design issues point to design of smaller process units in order to minimize the capital and operating costs, while, process control issues point to larger process units in order to smooth out disturbances.

It has been recognized early that there are inherent conflicts between design and control objectives (Luyben, 2004). A simple example of this was shown by Luyben (2004). Luyben compared the steady state economic design and the dynamic controllability of two alternatives designs: Case 1 – a single large reactor, and Case 2 – two smaller reactors operating in series, in which the irreversible liquid-phase exothermic reaction A → B occurs, as shown in Fig. 2.1.
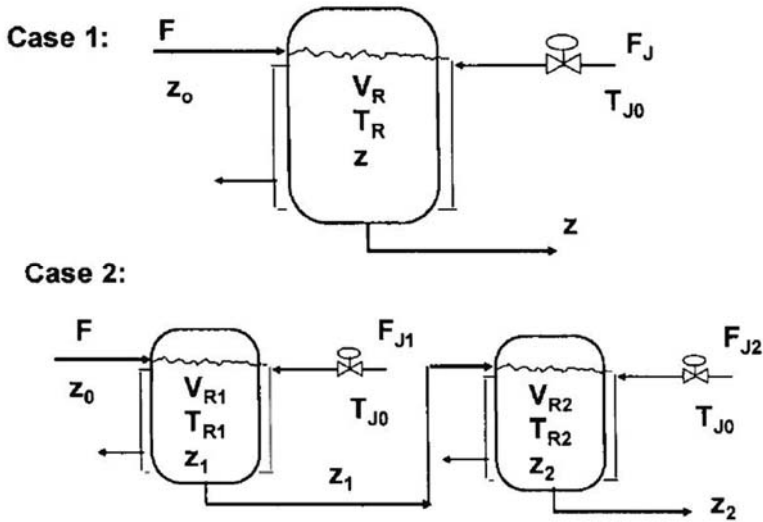
Fig. 2.1. Alternative designs for a simple *CSTR* example (adapted from Luyben, 2004).

Luyben found out that based on the steady state economics, the two-*CSTR* process of Case 2 is the best process since it has a lower capital cost (the capital cost of Case 1 is almost double). However, when the dynamic controllability is analyzed for the two alternatives designs, the controllability performance of a larger single *CSTR* process is seven times (in terms of overshoot) better than of the two-*CSTR* process, as shown in Fig. 2.2. It can be seen that a single *CSTR* is able to handle disturbance of 50% increase in the heat of reaction with only a 1.5 unit (unit used in this example is Fahrenheit) temperature deviation, while this disturbance causes a 10 unit jump in the temperature in the first reactor of a two-*CSTR* process. These results clearly demonstrate that the process that is the most economical from a steady state point of view is not necessarily the best from a dynamic controllability point of view. Therefore, this theoretical example illustrates clearly the importance of addressing the problem of both process design and controller design simultaneously (and not separately) for achieving better economic and operability benefits.
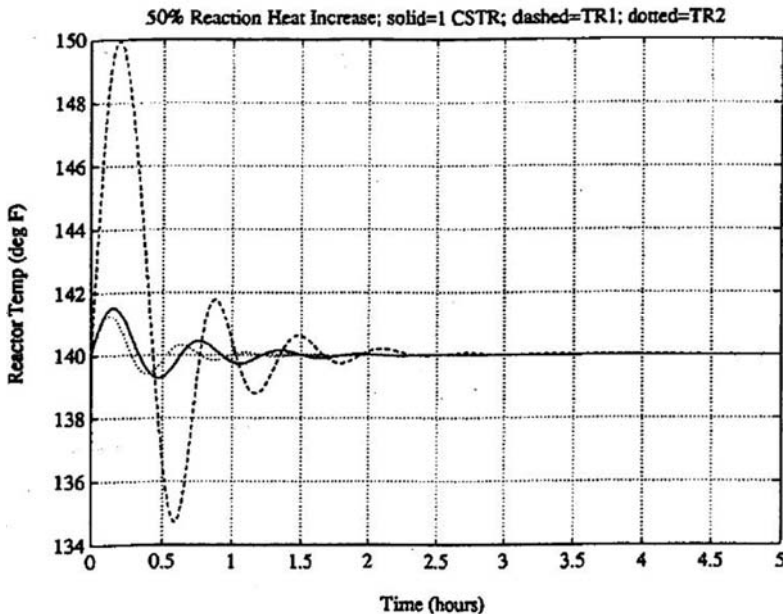
Fig. 2.2. One-*CSTR* and two-*CSTR* processes: responses to 50% increase in heat of reaction (adapted from Luyben, 2004).

2.2 Solution Strategies for Integrated Process Design and Controller Design

It has been recognized that a number of advantages can be obtained by predicting how well a given process meets the controllability issues as early as possible in the design process stage. For this reason, more and more researchers are now following the trend towards the *IPDC*. As a result, a number of new methodologies have been developed during the last years for addressing the solution of the *IPDC* problems (Sakizlis et al., 2004; Seferlis & Georgiadis, 2004; Ricardez-Sandoval et al., 2009b).

The methodologies that have been developed for addressing the solution of the *IPDC* problems of chemical processes can be classified as follows: 1) dynamic optimization approach, 2) embedded control optimization approach, and 3) decomposition approach. The following subsections present each of these strategies and outline the contributions that have been done in that area.

2.2.1   Dynamic Optimization Approach

In this approach, a mixed-integer non-linear optimization problem (*MINLP*) is formulated and solved with standard *MINLP* solvers. The continuous variables are associated with design variables (flow rates, heat duties) and process variables (temperatures, pressures, compositions), while binary (decision) variables are used to model logical decisions such as whether to choose between different possible flowsheet structures and/or controller structures. When a *MINLP* problem represents an *IPDC*, the process model considers only steady state conditions, while a *MIDO* (mixed-integer dynamic optimization) problem represents an *IPDC* where steady state as well as dynamic behaviour are considered. The popularity of this approach has increased due to advances in dynamic programming algorithms and the increasing computing power available to researchers in this area. (Seferlis & Georgiadis, 2004)

A number of algorithms have been developed to solve *MIDO* type problems as described in Table 2.1. From an optimization point of view, the solution approaches for *MIDO* problems can be divided into simultaneous and sequential methods, where the original *MIDO* problem is reformulated into a *MINLP* problem (Sakizlis et al., 2004). The former method, also called complete discretization approach, transforms the original *MIDO* problem into a finite dimensional nonlinear program (*NLP*) by discretization of the controlled and manipulated variables. Avraam et al. (1998), Avraam et al. (1999), Balakrishna and Biegler (1993), and Bahri et al. (1997) applied this complete discretization approach and solved the resulting *MINLP* problem using the Outer Approximation (*OA*) method. Mohideen et al. (1996), and Dimitriadis and Pistikopoulos (1995), on the other hand, solved the resulting *MINLP* problem using the Generalized Benders Decomposition (*GBD*) method. Androulakis (2000) also applied this complete discretization approach but solved the resulting *MINLP* problem using the Branch and Bound (*BB*) method.

However, this method typically generates a very large number of variables and equations, yielding large *NLP*'s that may be difficult to solve reliably even when a small number of process units are considered in the design. To circumvent this shortcoming, Bansal et al. (2000) proposed a different solution strategy based on a variant-2 of the Generalized Benders Decomposition (*v2-GBD*) technique for *MINLP*. This method was applied to design a double effect distillation column (Bansal et al., 2000), a high purity industrial distillation system (Ross et al., 1998), and a multi-component mixed-integer distillation column model (Bansal et al., 2002). In addition, López-Negrete and Flores-Tlacuahuac (2009) proposed a solution strategy that is based on solving relaxed versions of the optimization problem and using the results to initialize complex problem versions. They have successfully applied the proposed solution strategy to a binary distillation column carrying out the separation of the methanol-water system. The proposed strategy is capable of designing the optimal feed tray location, tray sizing, optimal operating steady states, the optimal open-loop trajectory, and also the best controller pairing that does the best tracking of the open-loop trajectory. However, the solution time required for the problem is very large and impractical for tackling industrial problems (Ricardez-Sandoval et al., 2009a,b; 2010).

Table 2.1
Methods for addressing MIDO problems.

Complete discretization	
Avraam et al. (1998), Avraam et al.,\ (1999), Balakrishna and Biegler (1993), Bahri et al. (1997)	Complete discretization on the dynamic system. The *MIDO* problem is transformed to a large *MINLP* problem. This problem is solved using the *OA* method.
Mohideen et al. (1996), Dimitriadis and Pistikopoulos (1995)	Complete discretization on the dynamic system. The transformed *MINLP* problem is solved using the *GBD* method.
Androulakis (2000)	Complete discretization on the dynamic system. The transformed *MINLP* problem is solved using the *BB* method.
Bansal et al. (2000), Ross et al. (1998), Bansal et al. (2002)	Complete discretization on the dynamic system. The transformed *MINLP* problem is solved using the v2-*GBD* method.
López-Negrete and Flores-Tlacuahuac (2009)	Solved relaxed versions of the optimization problem and using the results to initialize complex problem versions
Control vector parameterization	
Sharif et al. (1998), Schweiger and Floudas (1997)	Used control vector parameterization (*CVP*). *OA* method for treating the integers
Schweiger and Floudas (1997)	Used control vector parameterization (*CVP*). *GBD* method for treating the integers
Mohideen et al. (1997), Ross et al. (1998)	Applied similar approach to Schweiger and Floudas (1997) but used special integration gradient evaluation method in the master sub-problem formulation
Bansal et al. (2003)	Used control vector parameterization (*CVP*). *GBD* method for treating the integers with simplified master problem and no restriction to any integration or gradient evaluation method
Banga et al. (2003), Moles et al. (2003), Sendin et al. (2004)	Used stochastic global optimization (*GO*) method to locate the region of global solutions
Esposito and Floudas (2000), Moles et al. (2003)	Used deterministic *GO* methods to locate the optimal performance

As regards the sequential method, also called control vector parameterization approach, only controlled variables are discretized. In this approach, the *MIDO* algorithm is decomposed into a sequence of primal problems (nonconvex dynamic optimizations- *DO*s) and relaxed master problems. Sharif et al. (1998) and Schweiger and Floudas (1997) used control vector parameterization on the dynamic system and used the *OA* method for treating the integers. Schweiger and Floudas (1997) on the other hand used the *GBD* method for treating integers in the control vector parameterization approach. Mohideen et al. (1997) and Ross et al. (1998) applied a similar approach to Schweiger and Floudas (1997) but used a special integration gradient evaluation method in the master sub-problem formulation. Bansal et al. (2003) used control vector parameterization on the dynamic system and used *GBD* for treating the integers with a simplified master problem and no restriction to any integration or gradient evaluation method.

Because of nonconvexity of the constraints in *DO* problems, such solution methods are possibly excluding large portions of the feasible region within which an optimal solution may occur, leading to suboptimal solutions (Bansal et al., 2003). In order to overcome convergence to the suboptimal solution in *DO* or *MIDO* problems, stochastic and deterministic global optimization (*GO*) methods have also been proposed. Regarding stochastic *GO* methods, a number of works have shown that the region of global solutions can be located with relative efficiency (Banga et al., 2003; Moles et al., 2003; Sendin et al., 2004), but they tend to be computationally expensive and have difficulties with highly constrained problems. Most importantly, their major drawback is that global optimality cannot be guaranteed. While deterministic *GO* methods can guarantee that the optimal performance has been found (Esposito & Floudas, 2000), however their applicability is limited only to problems with a small number of process units (Moles et al., 2003).

In summary, the computational complexity associated with the resulting nonlinear dynamic optimization problems is a key drawback of these methodologies. The huge computational times involved make these strategies impractical for solving industrial problems (Ricardez-Sandoval et al., 2009a,b; 2010).

2.2.2 Embedded Control Optimization Approach

In the dynamic optimization approach, integer decisions for each possible pairing between controlled and manipulated variables causes a combinatorial explosion of design alternatives and introduces discontinuities in the search space (Malcolm et al., 2007) - see Fig. 2.3. Solving these integer decisions together with the already challenging dynamic design optimization with additional structural and continuous control variables may not be the best strategy. Therefore, an alternative solution strategy based on the embedded control optimization approach (Malcolm et al., 2007) has been proposed to solve the *IPDC* problems. This approach is based on a new mathematical formulation to reduce the combinatorial complexity of the *IPDC* problem. Accordingly, the *IPDC* problem is formulated as a bi-level optimization problem, which is then solved using a two-stage sequential approach. This formulation separates design decisions from control decisions to keep the problem size manageable. The first stage (usually called master level) seeks optimal design decisions while the second stage tests the dynamic performance based on design decisions obtained previously by fixing a particular control strategy alongside its tuning parameters. Fixing a particular control strategy in the second stage, therefore, eliminates integer decisions for selecting controller structures, and the problem complexity is reduced.
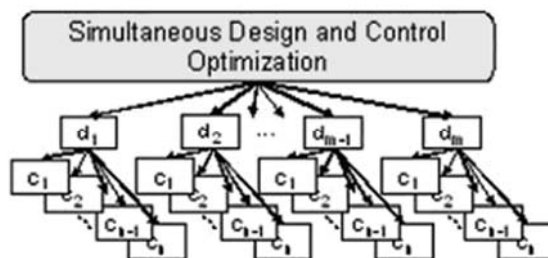
Fig. 2.3. Combinatorial explosion due to alternative control formulations and challenging optimization problems (adapted from Malcolm et al., 2007), where d is design decision and c is control decision.

Malcolm et al. (2007) and Moon et al. (2009a,b) proposed an embedded control optimization approach, which is used to recast the *IPDC* problem into a solvable mathematical programming format. This approach allows reduction of the combinatorial complexity of the *IPDC* problem by separating the design decisions from the control decisions as shown in Fig. 2.4. At the master level, the main design decisions such as reactor sizes and residence time that govern the dynamic process performance are obtained using stochastic design optimization. At this master level, no control decisions are made. Control decisions are delegated to the embedded control optimization at the second level. After the main design decisions have been obtained, the dynamic process performances are assessed by using a simplified, yet reasonably competitive control schemes based on full state space identification and least square regulation. According to Fig. 2.4, for every design decision, the embedded control problem is solved with the help of dynamically adaptive control optimization operating under uncertain conditions. The use of simpler adaptive state space models replacing the full nonlinear system equations eases the mathematical complexity of the optimal control problem. Hence, the complete system dynamics is reduced adaptively to a suitable linear state space model. The linearized state model is then used to compute optimal control actions in each time using a linear quadratic regulator (*LQR*). Since this approach is implemented based on simple state space identification, its applicability for highly nonlinear processes is limited. In order to improve the quality of identification, more advanced identification algorithms may be used. However, these advanced algorithms are computationally expensive, hence will deteriorate the performance of the proposed approach (Moon et al., 2009a,b).
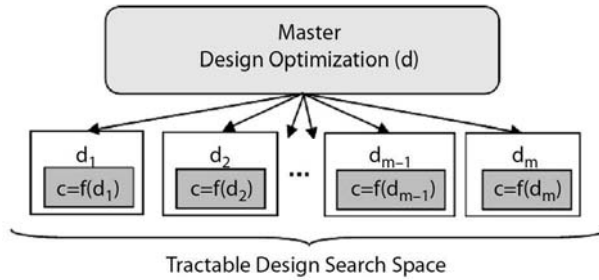
Fig. 2.4. Proposed embedded control optimization structure for the *IPDC* problem (adapted from Malcolm et al., 2007), where d is design decision and c is control decision.

Patel et al. (2008) introduced an optimal-control-based approach for achieving *IPDC* in a practical manner. The principal idea proposed is to utilize an optimal controller (a modified linear quadratic regulator, *mLQR*) to practically evaluate the best achievable control performance for each design candidate. In this approach, the *IPDC* problem is formulated as a bi-level optimization problem. This new problem consists of a main optimization step with respect to static (design) variables, subject to the solution of the dynamic optimization with respect to dynamic (control) variables in the second step. Initially, values of design variables are assumed. With the initial design values, the *mLQR* is used as the solution of the dynamic optimization at the second step. The main optimization then acquires the evaluation of the dynamic performance, combines this information with the static criteria such as cost and flexibility constraints, and produces a new candidate by adjusting the vector of design variables. Then, the new candidate is evaluated in the dynamic optimization step (with a new optimal controller based on the new design). This step is repeated until the iterations converge to a feasible design that cannot be improved further. However, the *mLQR* formulation does not allow for the inclusion of inequality constraints in the dynamic optimization. Ideally, these constraints should be imposed within the dynamic optimization. Thus, as the control problem is implemented within the design problem, it is possible to encounter designs that cannot satisfy these constraints (infeasible designs). This has been accepted as a trade-off to avoid the exponential increase in the problem complexity and computational burden.

Ricardez-Sandoval et al. (2009a,b; 2010) proposed a robust modeling approach to *IPDC* problems for large-scale chemical processes. This approach is based on the approaches proposed by Chawankul et al. (2007) and Ricardez-Sandoval et al. (2008) that address *IPDC* problems of a relatively simple one unit process. The key idea in these proposed approaches is to represent the closed loop nonlinear dynamic model of the process as a nominal linear closed loop state space model complemented with uncertain model parameters to circumvent some of the intensive computational burden and combinatorial complexity of *IPDC* problems. Robust control tools are then applied to calculate bounds on the closed loop process stability, the process feasibility and the worst-case scenario. Accordingly, these approaches require the assumption that the control structure used to control the system has to be known a *priori*. Different control algorithms have been used such as model predictive control

(*MPC*) (Chawankul et al., 2007) and a feedback proportional-integral (*PI*) controller (Ricardez-Sandoval et al., 2008). Although these approaches are attractive from a computational point of view, the solutions obtained from these approaches are local solutions only. Thus, the optimizations have to be conducted for several sets of initial guesses in order to ensure the global solution. As each initial guess leads to a different optimal solution, process knowledge is required to guess initial values of optimization variables.

Lu et al. (2010) proposed an intelligence-based method to solve *IPDC* problems, which combines fuzzy modeling/control and particle swarm optimization (*PSO*). The proposed method as shown in Fig. 2.5 decomposes the *IPDC* problem into two nested optimizations: embedded control optimization (inner loop) and master design optimization (outer loop) based on the framework proposed by Malcolm et al. (2007). In the embedded control optimization, a linear matrix inequality (*LMI*) is used to solve the fuzzy-modeling based controller design problem. In the master design optimization, a *PSO* method is developed to solve the process design problem. Since the control optimization is embedded into the master design optimization, successive iterations of the master design problem will gradually improve the integration performance. Since the *PSO*-based design is integrated with the fuzzy modeling/control, the proposed method has combined the merits of both fuzzy modeling/control and *PSO*. Thus, it has the ability to deal with the complex nonlinear problem in a large operating region.
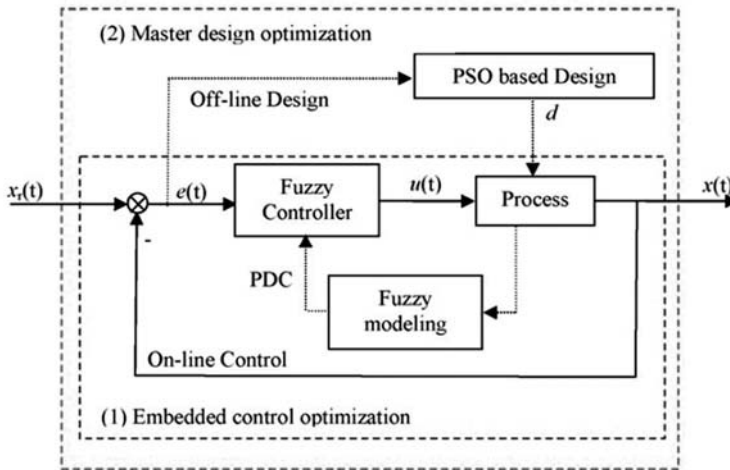
Fig. 2.5. *IPDC* intelligence-based method (adapted from Lu et al., 2010).

From a computational point of view, the above mentioned solution strategies have a capability to reduce the combinatorial complexity of the *IPDC* problem and therefore require less effort for solving the *IPDC* problem compared to the dynamic optimization-based solution strategies. Although the design solution obtained from the embedded control optimization approach may result in suboptimal design solutions, it

is attractive from a computational point of view and offers better practicality for solving industrial problems.

2.2.3   Decomposition Approach

Even though the embedded control optimization approach is attractive from a computational point of view, it is not guaranteed that the solution obtained is the global solution. This is because the objective here is to reduce the complexity of the *IPDC* problem by separating the design decisions from the control decisions. On the other hand, the dynamic optimization approach is capable of achieving the global solution but needs to overcome the combinatorial complexity and the resulting computational demand. Therefore, a new solution strategy for solving *IPDC* problems, which has the ability to find optimal design solutions at improved numerical and computational efficiency, is required. In most *IPDC* problems, the feasible solutions to the problem may lie in a relatively small portion of the search space due to the large number of constraints involved. The ability to solve this problem depends on the effectiveness of the employed solution strategy to identify and locate the feasible solutions one of which is the optimal. Hence, one approach to solve this *IPDC* problem is to apply a decomposition method.

The decomposition approach has been applied to manage and resolve the complexities associated with different optimization problems in chemical engineering, such as, design of optimal solvents and solvent mixtures (Karunanithi et al., 2005), computer aided molecular design (Karunanithi et al., 2006), solvent selection (Gani et al., 2008), sustainable process design (Carvalho et al., 2008), process flowsheet design and reverse approach (d'Anterroches & Gani, 2006; Alvarado-Morales et al., 2010), process intensification (Lutze et al., 2010) and product-process design (Conte et al., 2010) where optimal (or nearly optimal) solutions could easily be obtained. The basic idea here is that in optimization problems with constraints, the search space is defined by the constraints within which all feasible solutions lie and the objective function helps to identify one or more of the optimal solutions. In the decomposition-based approach (Karunanithi et al., 2005) the constraint equations are solved in a pre-determined sequence such that after every sequential sub-problem, the search space for feasible solutions is reduced and a sub-set of design-manipulated and/or decision variables are fixed. When all the constraints are satisfied, it remains to calculate the objective function for all the identified feasible solutions to locate the optimal. The solution approach could be termed as identify-define target and then match target.

Fig. 2.6 shows the decomposition methodology applied for a computer-aided molecular/mixture design (*CAMD*) (Karunanithi et al., 2005). Accordingly, the general *CAMD* problem can be formulated as a *MINLP* problem, where a (process/product) performance index is optimized subject to constraints (molecular structural constraints, molecular property constraints, mixture property constraints, process models). Then, an *MINLP* problem is decomposed into an ordered set of subproblems. Each subproblem (except the final) requires only solution of a subset of the constraints from the original set. The final subproblem contains the objective function and the remaining constraints. In this way, the solution of the decomposed set of subproblems is equivalent to that of the original *MINLP* problem. As each

subproblem is being solved, a large portion of the infeasible search space is identified and thus eliminated, thereby leading to a final subproblem that is a significantly smaller *MINLP* or *NLP* problem, which can be solved more easily.
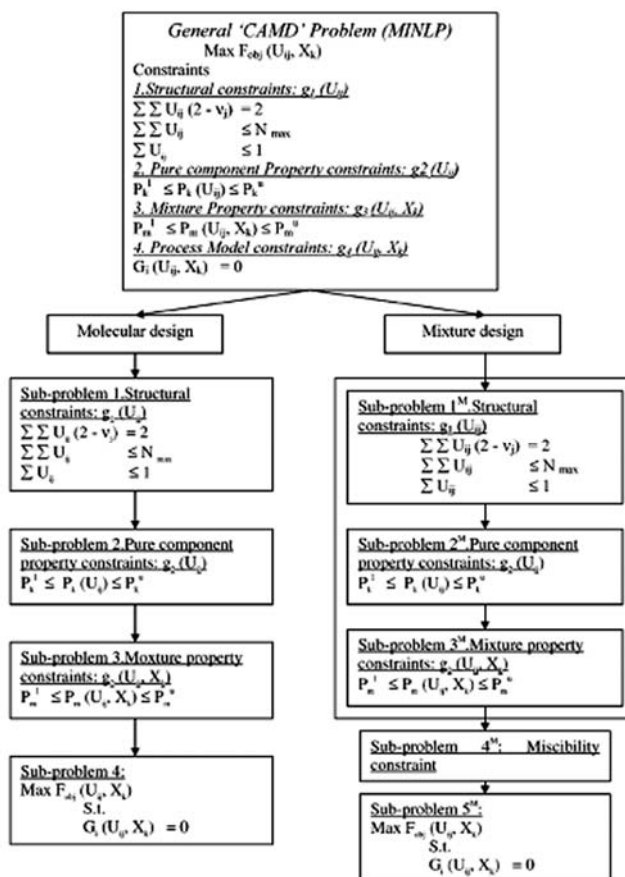
Fig. 2.6. Decomposition-based methodology for a computer-aided molecular/mixture design (*CAMD*) problem (adapted from Karunanithi et al., 2005).

Another application of the decomposition methodology is in solvent selection (Gani et al., 2008) as shown in Fig. 2.7. The search for suitable solvents is closely related to the set of search criteria defined in terms of a set of properties and their corresponding target values. The search is decomposed into a sequence of subproblems each consisting of a subset of the property constraints. The hierarchy of the properties is selected in terms of availability and reliability of data, need for the use of property models and the type of properties that need to be estimated. Since the search space can be potentially very large, the decomposition helps to reduce the search space for every subproblem.
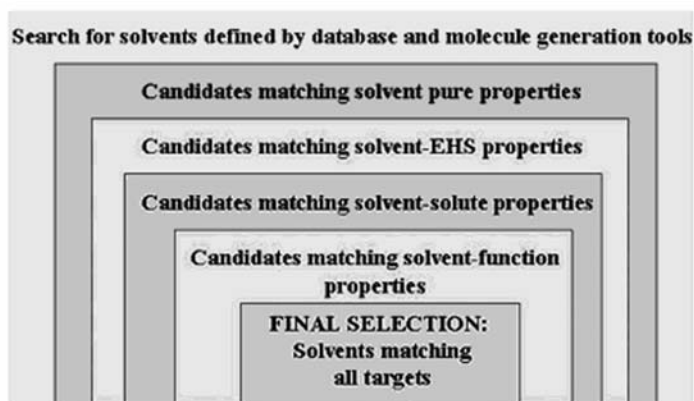
Fig. 2.7. General procedure for solvent selection. The solvent search starts from the outer level with a large search space and every subsequent set of constraints representing different solvent search subproblems, reduce the search space until for a small search space, a well-defined optimization problem can be solved (adapted from Gani et al., 2008).

2.3 Conclusion

Initial research in the optimization of chemical processes focused mainly on the development of the process design and controller design as independent sequential procedures. Recent results of research in this field have demonstrated that process design and controller design performed simultaneously may result in numerous economic and operability benefits over the traditional sequential design approach. As a result, a number of new methodologies have been developed. From the discussion of the previous solution strategies for addressing *IPDC* problems of chemical processes, it is clear that there are different solution approaches:

1. Dynamic optimization approach.
   This approach can be divided into simultaneous and sequential methods depending on how the original *MIDO* problem is reformulated into a *MINLP* problem. In the simultaneous method, also called complete discretization approach, all state and control variables are discretized, whereas in the sequential method (control vector parameterization), only control variables are discretized. This approach is capable of finding the optimal solution but suffers from its computational complexity that requires a huge computational effort. This is a key drawback that makes methodologies of this type impractical for solving industrial problems.

2. Embedded control optimization approach.
   In this approach, the *IPDC* problem is formulated as a bi-level optimization problem, which is then solved using two sequential stages to reduce the combinatorial complexity of the *IPDC* problem. In order to keep the problem

size manageable, this approach separates design decisions with control decisions. The first stage (usually called master level) seeks optimal design decisions while the second stage tests the dynamic performance based on design decisions obtained previously by fixing a particular control strategy alongside its tuning parameters. By fixing a particular control strategy in the second stage, integer decisions for selecting controller structures are eliminated, and therefore the problem complexity is reduced. From the computational point of view, methodologies of this type are attractive and have better practicability for solving industrial problems, but may result in suboptimal design solutions.

3. Decomposition approach.
   The main idea in this approach is to decompose the optimization problem into an ordered set of sub-problems. Each subproblem, except the final requires only the solution of a subset from the original constraints set. The final subproblem contains the objective function and the remaining constraints. In this way, the solution of the decomposed set of subproblems is equivalent to that of the original optimization problem. The advantage is a more flexible solution approach together with relatively easy to solve subproblems.

Even though the decomposition approach offers an effective solution strategy and several applications of this approach have been reported in the literature in solving different optimization problems in chemical engineering, no methodology based on the decomposition-based approach has been reported for solving the *IPDC* problems. Therefore, there is a need for a decomposition-based methodology to solve the *IPDC* problem and to facilitate its application in practice. The new model-based methodology based on the decomposition approach for solving *IPDC* problems is proposed and described in detail in Chapter 3.

CHAPTER 3

Methodology for Model-Based Integrated Process Design and Controller Design

In this chapter, we present in section 3.1 the general formulation of the integrated process design and controller structure design (*IPDC*) problem of chemical processes. In section 3.2, we describe in detail a model-based methodology which is based on the decomposition approach for solving the *IPDC* problem. After the description of the methodology, we present two important concepts used in this methodology for obtaining the optimal design-control solutions (section 3.3). Then, we summarize the

algorithm of the decomposition-based methodology for solving the *IPDC* problem in section 3.4. Finally, we present the main conclusion in section 3.5.

3.1   Problem Formulation

The *IPDC* problem is typically formulated as a generic optimization problem in which a performance objective in terms of design, control and cost is optimized subject to a set of constraints: process (dynamic and steady state), constitutive (thermodynamic states) and conditional (process-control specifications) constraints

$$\max \quad J = \sum_{i=1}^{m} \sum_{j=1}^{n} w_{i,j} P_{i,j} \tag{3.1}$$

subjected to:

Process (dynamic and/or steady state) constraints

$$\frac{d\mathbf{x}}{dt} = f(\mathbf{x}, \mathbf{y}, \mathbf{u}, \mathbf{d}, \boldsymbol{\theta}, Y, t) \tag{3.2}$$

Constitutive (thermodynamic) constraints

$$0 = g_1(\mathbf{v}, \mathbf{x}, \mathbf{y}) - \boldsymbol{\theta} \tag{3.3}$$

Conditional (process-control) constraints

$$0 = h_1(\mathbf{u}, \mathbf{x}, \mathbf{y}) \tag{3.4}$$

$$0 \leq h_2(\mathbf{u}, \mathbf{x}, \mathbf{y}, \mathbf{d}) \tag{3.5}$$

$$CS = \mathbf{y} + \mathbf{u}Y \tag{3.6}$$

In the above equations, $\mathbf{x}$ and $\mathbf{y}$ are usually regarded as the set of process variables in the process design and as the set of state and/or controlled variables in the controller design; usually temperatures, pressures and compositions. $\mathbf{u}$ is the set of design variables (for process design) and/or the set of manipulated variables (for controller design). $\mathbf{d}$ is the set of disturbance variables, $\boldsymbol{\theta}$ is the set of constitutive variables (physical properties, reaction rates), $\mathbf{v}$ is the set of chemical system variables (molecular structure, reaction stoichiometry, etc.) and t is the independent variable (usually time). The performance function, Eq. (3.1) includes design, control and economic criteria, where i indicates a specific term of each category. $w_{i,j}$ is the weight factor assigned to each objective term $P_{i,j}$ ($i = 1$-3; $j = 1,2$).

Eq. (3.2) represents a generic process model from which the steady state model is obtained by setting $d\mathbf{x}/dt = 0$. Eq. (3.3) represents constitutive equations which relate the constitutive variables to the process. Eqs. (3.4) and (3.5) represent sets of equality and inequality constraints (such as product purity, chemical ratio in a specific stream) that must be satisfied for feasible operation – they can be linear or non-linear. In Eq. (3.6), Y is the set of binary decision variables for the controller structure selection (corresponds to whether a controlled variable is paired with a particular manipulated variable or not).

Different optimization scenarios can be generated as follows:

- To achieve process design objectives, $P_{1,j}$ is maximized. $P_{1,1}$ is the performance criterion for reactor design and $P_{1,2}$ is the performance criterion for separator design.
- To achieve controller design objectives, $P_{2,1}$ is minimized by minimizing $(d\mathbf{y}/d\mathbf{d})$ the sensitivity of controlled variables $\mathbf{y}$ with respect to disturbances $\mathbf{d}$, and $P_{2,2}$ is maximized by maximizing $(d\mathbf{y}/d\mathbf{u})$ the sensitivity of the controlled variables $\mathbf{y}$ with respect to manipulated variables $\mathbf{u}$ for the best controller structure.
- To achieve economic objectives, $P_{3,j}$ is minimized. Here, $P_{3,1}$ is minimized by minimizing the capital costs and $P_{3,2}$ is minimized by minimizing the operating costs.

The multi-objective function in Eq. (3.1) is then reformulated as

$$\max \quad J = w_{1,j}P_{1,j} + w_{2,1}\left(\frac{1}{P_{2,1}}\right) + w_{2,2}P_{2,2} + w_{3,j}\left(\frac{1}{P_{3,j}}\right) \quad j = 1,2 \qquad (3.7)$$

From a process design point of view, for specified $\mathbf{u}$ and $\mathbf{d}$, values for $\mathbf{x}$ and $\mathbf{y}$ that satisfy a set of design specifications (process design objectives) are determined. In this case, $\mathbf{x}$ and $\mathbf{y}$ also define some of the operational conditions for the process. From a controller design point of view, for any changes in $\mathbf{d}$ and/or set point values in $\mathbf{y}$, values of $\mathbf{u}$ that restores the process to its optimal designed condition are determined. It should be noted that the solution for $\mathbf{x}$ and $\mathbf{y}$ is directly influenced by $\boldsymbol{\theta}$ (the constitutive variables such as reaction rate or equilibrium constant). For example, the optimal solution for $\mathbf{x}$ and $\mathbf{y}$ can be obtained at the maximum point of the attainable region (for reactor) and driving force (for separator) diagrams which are based on $\boldsymbol{\theta}$. By using model analysis, the corresponding derivative information with respect to $\mathbf{x}$, $\mathbf{y}$, $\mathbf{u}$, $\mathbf{d}$ and $\boldsymbol{\theta}$ can be obtained (to satisfy controller design objectives). Since $\mathbf{x}$ and $\mathbf{y}$ are intensive variables, they also can be used to determine the operational and capital costs of the process (to satisfy economic objectives) with respect to optimal energy consumption as they directly determine the energy consumption (for separator) and indirectly influence the equipment sizing variables such as tank volume (for reactor).

3.2 Decomposition-Based Solution Strategy

In most of the *IPDC* problems, the feasible solutions to the problems may lie in a relatively small portion of the search space due to the large number of constraints involved. The ability to solve such problems depends on the effectiveness of the method of solution in identifying and locating the feasible solutions (one of these is the optimal solution). Hence, one approach to solve this *IPDC* problem is to apply a decomposition method as illustrated in Fig. 3.1 (Hamid et al., 2010a,b).
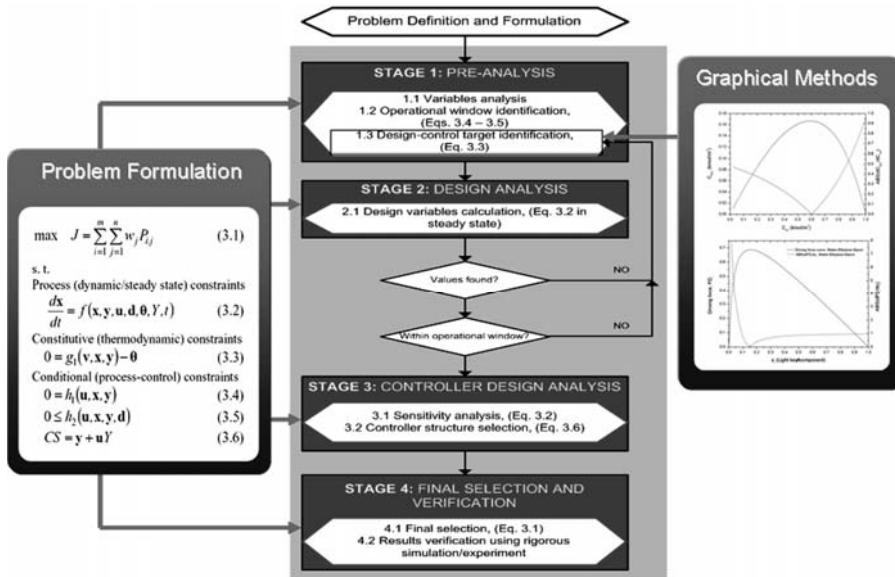
Fig. 3.1. Decomposition method for *IPDC* problem (adapted from Hamid et al., 2010a).

The basic idea here is that in optimization problems with constraints, the search space is defined by the constraints within which all feasible solutions lie and the objective function helps to identify one or more of the optimal solutions. In the simultaneous approach, all the constraint equations are solved together with the objective function to determine the values of the optimization variables (design-manipulated and decision variables) that satisfy the constraints and lead to the optimal objective function value. In the decomposition-based approach (Karunanithi et al., 2005), the constraint equations are solved in a pre-determined sequence such that after every sequential sub-problem, the search space for feasible solutions is reduced and a sub-set of design-manipulated and/or decision variables are fixed. When all the constraints are satisfied, it remains to calculate the objective function for all the identified feasible solutions to locate the optimal solution (see Fig. 3.2).
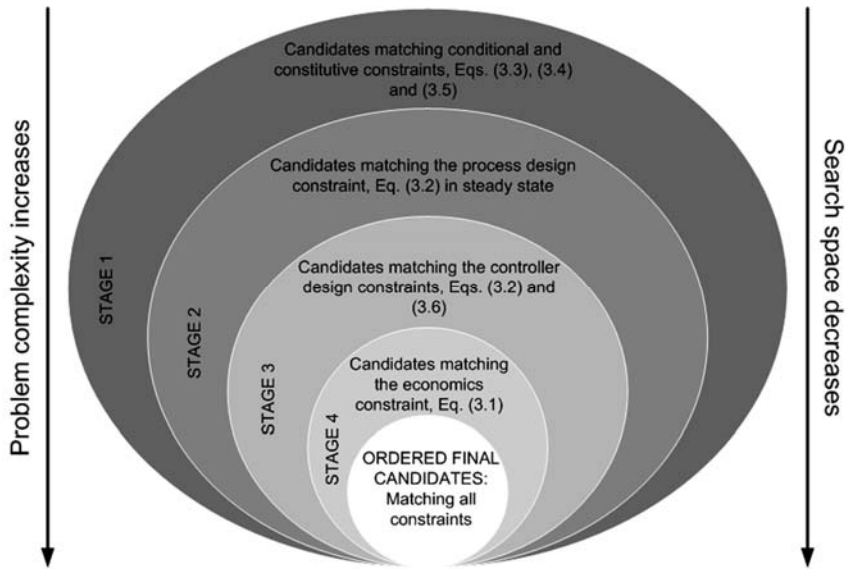
Fig. 3.2. The number of feasible solution is reduced to satisfy constraints at every sub-problems (adapted from Hamid et al., 2010a).

The *IPDC* problem is decomposed into four hierarchical stages: (1) pre-analysis, (2) design analysis, (3) controller design analysis, and (4) final selection and verification. As shown in Fig. 3.1, the set of constraint equations in the *IPDC* problem is decomposed into four sub-problems which correspond to four hierarchical stages (see Figs. 3.1 and 3.2). In this way, the solution of the decomposed set of sub-problems is equivalent to that of the original problem. As each sub-problem is being solved, a large number of infeasible solutions within the search space is identified and eliminated, thereby leading to a final sub-problem that is significantly smaller, which can be solved more easily. Therefore, while the sub-problem complexity may increase with every subsequent stage, the number of feasible solutions is reduced at every stage, as illustrated in Fig. 3.2.

3.2.1 Stage 1: Pre-analysis

The objective of this stage is to define the operational window and set the targets for the design-controller solution. First, all **y** and **u** are analyzed and the important ones with respect to the multi-objective function, Eq. (3.7) are shortlisted. The operational window is defined in terms of **y** and **u** (note that **d** is known). A choice is made for **y** based on thermodynamic and process insights and Eq. (3.3) (also defines the optimal solution targets). Then, Eqs. (3.4) and (3.5) are solved (for **u**) to establish the operational window. For each reactor design task, the attainable region diagram is drawn and the location of the maximum in the attainable region is selected as the reactor design target (Fig. 3.3 left). This point gives the highest selectivity of the

reaction product with respect to the limiting and/or selected reactant. Similarly, for each separation design task, the design target is selected at the highest driving force (Fig. 3.3 right). At the highest driving force, the separation becomes easiest due to the large difference in composition between the phases and therefore, the energy necessary to maintain the two-phase is at a minimum. Note that, both plots of attainable region and driving force usually have a well-defined maximum (Fig. 3.3). It is important to note that, from a process design point of view at these targets, the optimal design objectives (maximum value of $P_{1,1}$ and $P_{1,2}$) can be obtained. From a controller design point of view, at these targets the controllability of the process is best satisfied. We verify in more detail the reasons of selecting these targets from both a process design and controller design viewpoints in section 3.3.
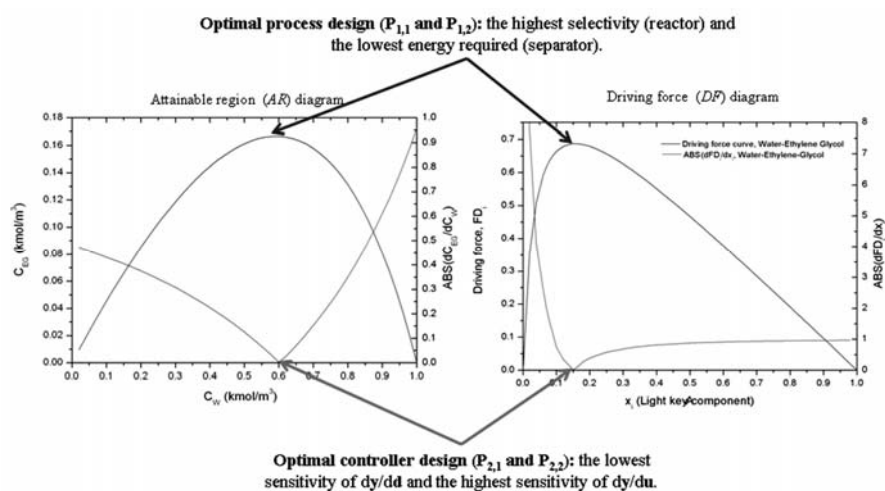
Fig. 3.3. Determination of optimal solution of design-control for a rector using the attainable region diagram at a specific temperature (left) and a separator using the driving force diagram at a specific pressure (right).

3.2.2 Stage 2: Design Analysis

The search space within the operational window identified in Stage 1 is further reduced in this stage. The objective is to validate the targets defined in Stage 1 by finding acceptable values (candidates) of **y** and **u** by considering Eq. (3.2) – steady state process model. If the acceptable values cannot be found or the solution is located outside the operational window, then a new target is selected and the procedure is repeated until a suitable match is found.

3.2.3   Stage 3: Controller Design Analysis

The search space is further reduced by considering now the feasibility of the process control. This sub-problem considers the process model constraints, Eq. (3.2) (dynamic and/or steady state forms) to evaluate the controllability performance of feasible candidates, and Eq. (3.6) for the selection of the controller structure. In this respect, two criteria are analyzed: (a) sensitivity ($d\mathbf{y}/d\mathbf{d}$) of controlled variable $\mathbf{y}$ with respect to disturbances $\mathbf{d}$, which should be low, and (b) sensitivity ($d\mathbf{y}/d\mathbf{u}$) of controlled variables $\mathbf{y}$ with respect to manipulated variables $\mathbf{u}$, which should be high. Lower value of $d\mathbf{y}/d\mathbf{d}$ means the process has lower sensitivity with respect to disturbances, hence the process is more robust in maintaining its controlled variables against disturbances. On the other hand, higher value of $d\mathbf{y}/d\mathbf{u}$ will determine the best pair of the controlled-manipulated variables (to satisfy Eq. (3.6)). According to the integrated design problem, the optimal design-process values become the set-points for the controlled and manipulated variables. Therefore, it is assumed by this methodology that the best set-point values of the controller are actually those already defined as design targets (at the maximum point of the attainable region diagram, for reactor, and the driving force diagram, for separator), since these targets are the optimal design solutions. It should be noted that the objective of this stage is not to find the optimal value of controller parameters or type of controller, but to generate the feasible controller structures.

3.2.4   Stage 4: Final Selection and Verification

The final stage is to select the best candidates by analyzing the value of the multi-objective function, Eq. (3.7). The best candidate in terms of the multi-objective function will be verified using rigorous simulations or by performing experiments. It should be noted that the rigorous simulation will be relatively easy because very good estimates of $\mathbf{y}$ and $\mathbf{u}$ are obtained from Stages 1 to 3. For controller performance, verification is made through open or closed loop simulations. For closed loop simulation, any tuning methods can be used to determine the value of controller parameters.

3.3   Defining Optimal Design Targets

In this section, we present two important concepts of finding the optimal solutions from process design and controller design viewpoints which are relatively straight forward to apply and which, in our opinion, have an important role in solving the *IPDC* problem. As mentioned in the previous section, the concepts of attainable region and driving force are used in order to obtain the optimal design solutions. In Stage 1 of this methodology, targets for the design-control solution are defined at the maximum point of the attainable region and driving force diagrams. Defining the targets at the maximum point of the attainable region and driving force diagram ensure the optimal solution not only for the process design but also for the controller design. From a process design point of view at these targets, the optimal design

objectives (maximum value of $P_{1,1}$ and $P_{1,2}$) are obtained (see Fig. 3.3). Then by using the reverse solution approach, values of design-process variables that match those targets are calculated in Stage 2. Using model analysis, controllability issues are incorporated in Stage 3 to calculate the process sensitivity and to pair the identified manipulated variables with the corresponding controlled variables. From a controller design point of view, at targets defined in Stage 1, the process sensitivity with respect to disturbances ($P_{2,1}$) is at the minimum and the sensitivity of controlled variables with respect to manipulated variables ($P_{2,2}$) is at the maximum (see Fig. 3.3). Since the optimization deals with multi-criteria objective functions, therefore, in Stage 4, the objective function is calculated to verify the best (optimal) solution that satisfies design, control and economic criteria. From an optimization point of view, solution targets at the maximum point of the attainable region and driving force diagrams should have the higher value of the objective function compared to design/operation at any other point.

3.3.1 Attainable Region Concept

The attainable region concept is used in this methodology to find the optimal (design target) values of the process variables for any reaction system. Glasser and coworkers (Glasser et al., 1987, 1990; Godorr et al., 1994) considered a reactor as a system where the only processes occurring are reaction and mixing. They have shown that once the attainable region is found the optimization of the problem is straight forward. If one knows the attainable region, one can then search over the entire region (often the boundary) to find the output conditions that maximize an objective function related to the yield or production. The attainable region concept has been successfully used for synthesizing and optimizing different reactor networks (Glasser et al., 1987, 1990; Godorr et al., 1994). The results of their works was the determination of optimum reactor networks in terms of different reaction processing units (reactors) and their interconnections (mixing strategies) for a number of different systems. They also identified the necessary conditions to which the attainable region must comply, one of which is that the profile of the attainable region always must be convex.

It should be noted that in this methodology, the attainable region concept is used to determine the maximum concentration of the reaction product for a specified reactor type, that is, continuous stirred tank reactor (*CSTR*) that maximizes the objective function ($P_{1,1}$) (for reactor design) without taking into consideration that the profile of the attainable region is convex, which is different from the original purpose of the concept of the attainable region.

Let **C** represent the state of process components such as reactants and products. The state **C** will provide information such as concentrations, mass fractions or partial pressures. Consider a reactor vector space comprising an instantaneous reaction rate vector at **C** as **r(C)**. The reaction rate vector **r(C)** contains information about the kinetics of the reaction taking place. The instantaneous change in the system state, **C** due to a change in the process residence time, $d\tau$ is expressed as

$$d\mathbf{C} = \mathbf{r}(\mathbf{C})d\tau \qquad\qquad (3.8)$$

For a plug flow reactor (*PFR*), the equation representing the rate changes of the state variable is given by

$$\frac{d\mathbf{C}}{d\tau} = \mathbf{r}(\mathbf{C}) \qquad\qquad (3.9)$$

In a *CSTR*, where reaction and mixing occur simultaneously, the equation representing the rate changes of the state variable is given by

$$\mathbf{C} - \mathbf{C}_0 = \mathbf{r}(\mathbf{C})\tau \qquad\qquad (3.10)$$

where $\mathbf{C}_0$ is the feed state and τ is the residence time.

The attainable region equation is expressed in terms of the state of desired product with respect to the limiting reactant, given by

for a *PFR*:
$$\frac{dC_P}{dC_R} = \frac{r_P}{r_R} \qquad\qquad (3.11)$$

for a *CSTR*:
$$\frac{C_P - C_{P,0}}{C_R - C_{R,0}} = \frac{r_P}{r_R} \qquad\qquad (3.12)$$

where C_P and C_R are the state of desired product and limiting reactant concentrations, respectively. r_P and r_R are the reaction rates for desired product and limiting reactant, respectively, and $C_{P,0}$ and $C_{R,0}$ are the feed concentrations.

Recall that, the concept of the attainable region is used in this methodology to locate the maximum value of the desired product concentration as the target for the reactor design. By using the reverse solution approach, starting from this target we calculate other reactor variables such as residence time, temperature, and reactor volume that match that target. There are three key steps for developing the graphical representation of the attainable region used in this methodology. The steps are based on modification of the Milne et al., (2006):

1. *Evaluation of the yield of product.*
   For a given set of reactions and their corresponding kinetics, evaluate the yield of the desired product with respect to the limiting reactant by considering only a *CSTR*. As an example, the attainable region equation for a *CSTR* is defined as:

$$\frac{C_B - C_{B,0}}{C_A - C_{A,0}} = \frac{r_B}{r_A} \qquad\qquad (3.13)$$

where C_B and C_A are the concentration of desired product and limiting reactant, respectively. $C_{A,0}$ and $C_{B,0}$ are initial concentrations of A and B, respectively. r_A and r_B are the rates of reaction for component A and B, respectively.

2. *Plotting the concentration of product with respect to the concentration of limiting reactant.*
   a) If the reaction rate is not a function of temperature, then plot the concentration of C_B as a function of C_A as shown in Fig. 3.4.
   b) If the reaction rate is a function of temperature, then:
      i.   Identify the allowable temperature range using Eq. (3.14)

$$T_{min} = \sum_i x_i T_m^i < T(K) < T_{max} = \sum_i x_i T_b^i \qquad (3.14)$$

where x_i is the mole fraction of component i in the feed, and T_m^i and T_b^i are the melting and boiling point, respectively.

      ii. Vary the temperature and then plot the concentration of C_B as a function of C_A as shown in Fig. 3.5.

3. *Finding the maximum.*
   The final step is to determine the maximum point which sets the target for the reactor design problem.

In Example 3.1, we demonstrate the development of the attainable region diagram based on the steps presented above for conceptual consecutive reactions.
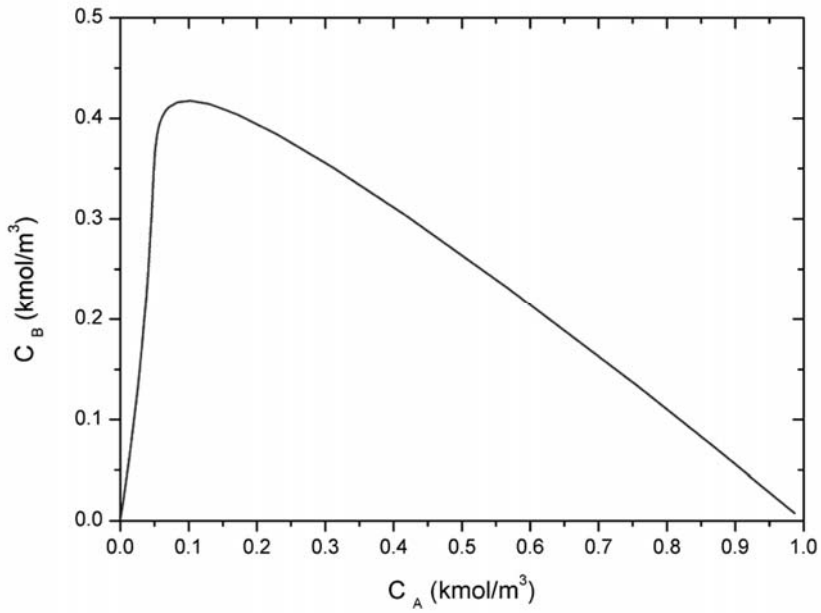
Fig. 3.4. Plot of concentration of *B* as a function of concentration of *A*.
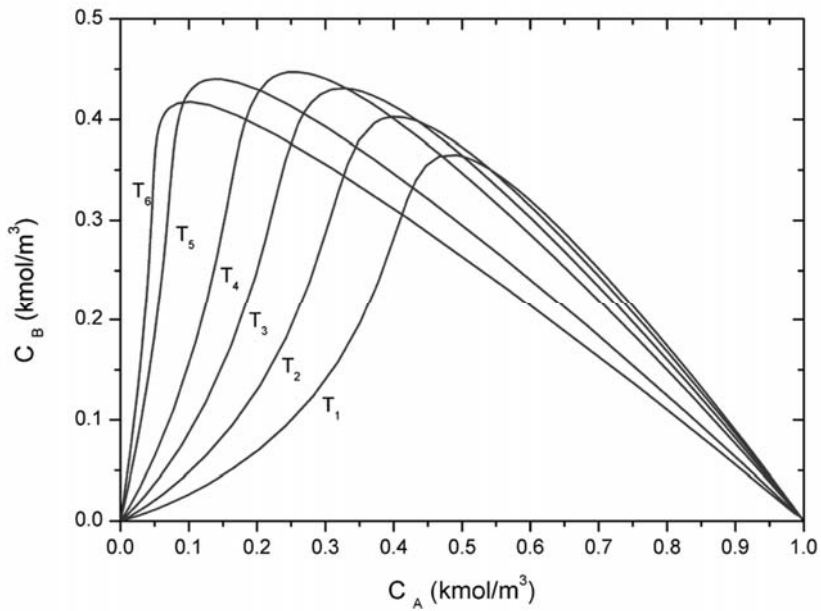
Fig. 3.5. Plot of concentration of *B* as a function of concentration of *A* at different temperatures.

Example 3.1: Attainable region diagram development

Consider the following liquid phase, constant density, isothermal reactions in a *CSTR*:

$$A \underset{k_{-1}}{\overset{k_1}{\longleftrightarrow}} B \overset{k_2}{\longrightarrow} C \tag{3.15}$$

The kinetic and initial feed concentrations are given in Table 3.1. The desired product *B* is produced from a pure reactant component *A* via a reversible reaction from *A*, and is further consumed by an irreversible reaction to *C*. The objective is to develop an attainable region diagram and then select the maximum point to be set as a target for the reactor design.

Table 3.1
Kinetic constants and feed concentration.

Kinetic constants	Value	Unit
k_1	3.06	1/h
k_2	0.066	1/h
k_{-1}	1.00	1/h
Feed concentrations	Value	Unit
C_{Af}	1.0	$kmol/m^3$
$C_{Bf}=C_{Cf}$	0.0	$kmol/m^3$
F	10.0	m^3/h

The mass balance equations are:

$$C_A - C_{Af} = (k_{-1}C_B + k_1 C_A)\tau \tag{3.16}$$

$$C_B - C_{Bf} = [k_1 C_A - (k_{-1} + k_2)C_B]\tau \tag{3.17}$$

where τ is the residence time.

The attainable region diagram for this reaction system is then developed using the three key steps as follows:

1. *Evaluation of the yield of product.*
   Using the known kinetic constants and feed concentrations, the yield of *B* is evaluated as a function of the concentration of *A* using Eq. (3.18). Eq. (3.18) is then solved by varying the value of C_A from its initial feed of 1.0 kmol/m³ to zero with a constant step size.

$$\frac{C_B - C_{Bf}}{C_A - C_{Af}} = \frac{k_1 C_A - (k_{-1} + k_2) C_B}{k_{-1} C_B + k_1 C_A} \tag{3.18}$$

2. *Plotting the concentration of product with respect to the concentration of limiting reactant.*

   Since the reaction rate is not a function of temperature, the concentration of B is then plotted as a function of the concentration of A, as shown in Fig. 3.6.
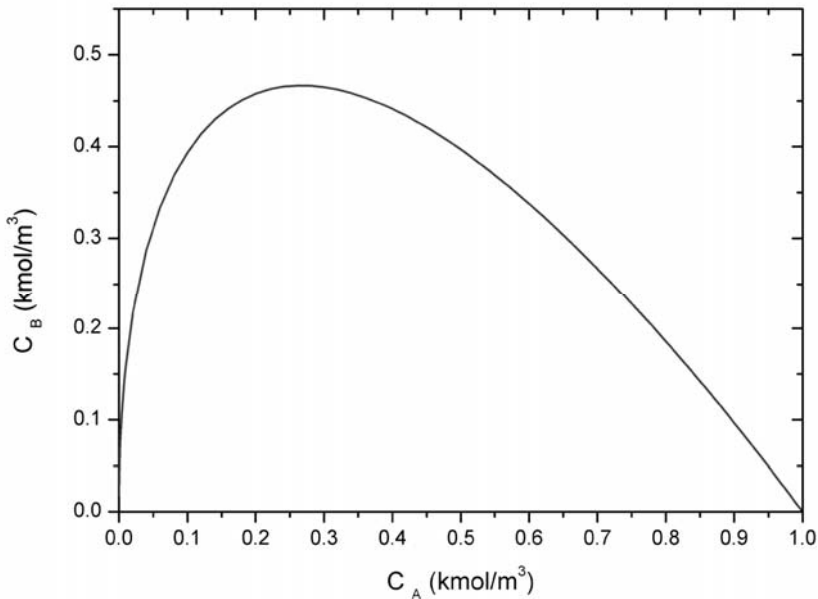
Fig. 3.6. Plot of concentration of B as a function of concentration of A for conceptual consecutive reactions.

3. *Finding the maximum.*

   The final step is to determine the maximum point which sets the target for the reactor design problem. In this example, the maximum yield of B is obtained at the highest concentration B, that is, at Point A as shown in Fig. 3.7. It can be seen that at that maximum point, 0.43 kmol/m^3 of component B can be produced with 0.26 kmol/m^3 of component A. This value of the desired concentration is then used as a basis for the reactor design to calculate other important variables such as residence time, temperature (in this example, temperature is already fixed), and reactor volume.
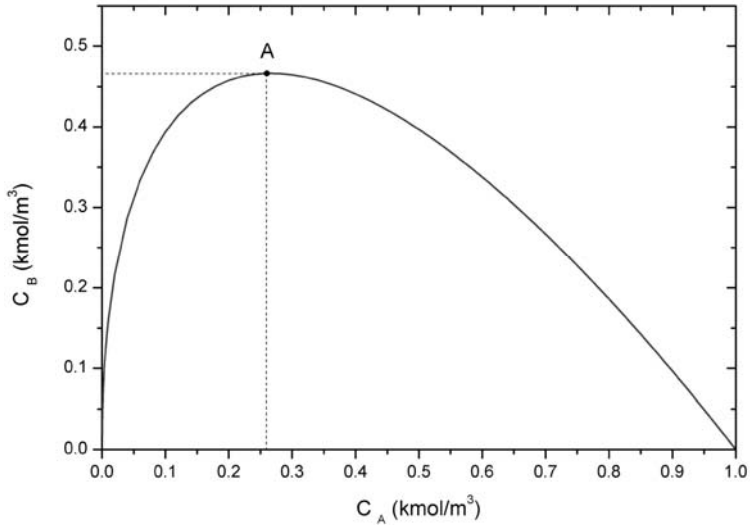
Fig. 3.7. Maximum point (Point A) which becomes a target for a reactor design for conceptual consecutive reactions.

3.3.2 Driving Force Concept

The driving force concept is used in this methodology to find the optimal (design target) values of the process variables for separation systems. Gani and Bek-Pedersen (Gani & Bek-Pedersen, 2000; Bek-Pedersen, 2002; Bek-Pedersen & Gani, 2004) proposed a design method of distillation separation systems based on identification of the largest driving force, defined as the difference in composition of a component i between the vapor phase and the liquid phase, which is caused by the difference in the volatilities of component i and all other components in the system as given in Eq. (3.19) below.

$$F_{Di} = y_i - x_i = \frac{x_i \alpha_{ij}}{1 + x_i(\alpha_{ij} - 1)} - x_i \qquad (3.19)$$

where α_{ij} is a parameter (relative volatility) that may or may not be composition dependent and provides a measure of the driving force. The parameter α_{ij} is obtained from a model describing the differences in composition between two co-existing phases, or measured composition data. As the driving force decreases, separation becomes difficult and becomes infeasible when the driving force approaches zero. On the other hand, as the driving force approaches its maximum value, the separation becomes easier, and the energy necessary to maintain the two-phase system is at a

minimum. Therefore, from a process design point of view, a separation process should be designed/selected at the highest possible driving force which will naturally lead to the most energy efficient design and the optimal objective function value ($P_{1,2}$).

The objective of a driving force based design is to design the distillation column to operate at the maximum of driving force, that is, utilize the largest possible area of the driving force diagram (Gani & Bek-Pedersen, 2000; Bek-Pedersen, 2002; Bek-Pedersen & Gani, 2004). This simple and visual approach forms the basis for the determination of important distillation column design variables, which can be determined by two important parameters, the location and the size of the maximum driving force, D_x and D. These D_x and D are then related to the feed stage location, N_F and the reflux ratio, RR (and/or the reboil ratio, RB). The starting point for the design of a simple distillation column is the vapor-liquid data, visualized in a driving force diagram, where the driving force between the vapor and liquid composition is plotted as a function of composition. A driving force diagram together with the distillation design parameters is illustrated in Fig. 3.8. Finding the important distillation column design variables involves the following six steps (Gani & Bek-Pedersen, 2000; Bek-Pedersen, 2002; Bek-Pedersen & Gani, 2004):
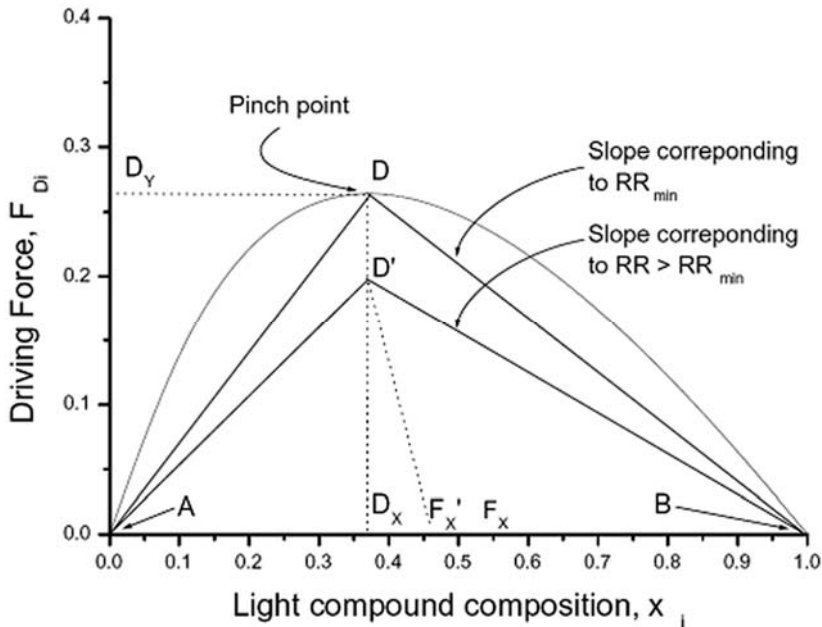
Fig. 3.8. Driving force diagram with illustration of the distillation design parameters, where the composition is in mole fractions (adapted from Gani & Bek-Pedersen, 2000).

Model-Based Integrated Process Design and Controller Design of Chemical Processes

1. Generate or retrieve from a database, the vapor-liquid data for the binary system. For a multi-component system, select the two key components to define the split and use them as the binary key mixture.

2. Compute F_{Di} using Eq. (3.19) and plot F_{Di} as a function of x_i, where i is the light key component.

3. Identify the point D and D_x graphically.

4. For a given number of stages, N, determine the feed stage, N_F from $N_F = (1 - D_x)N$.

5. If the product specifications are given, locate the points A and B. Determine the slopes of the lines AD and BD. Determine the corresponding RR_{min} and RB_{min}.

6. Determine the real RR and RB from $RR = 1.2(RR_{min})$ and $RB = 1.2(RB_{min})$.

With values of N_F, RR (or RB) and product purity, other design-process variables values can be calculated using any process model. Note that the driving force diagram shown in Fig. 3.8 is at a given pressure. Similar to Fig. 3.5 (for attainable regions), different driving force diagrams can be generated at different pressures. In this work, the effect of pressure has not been investigated and the pressure has been assumed to be fixed.

In Example 3.2, we demonstrate the development of the driving force diagram and finding the important distillation column design variables based on the steps presented above (and Fig. 3.8).

Example 3.2: Driving Force diagram development

Consider the reactor effluent from Example 3.1 to be purified into a product (consists of compounds *B* and *C*) and unreacted reactant (component *A*). The objective is to recover 99% of compound *A* as the bottom product in stream-B and 1% of compound *A* can be in the top product (stream-D) in a 15 equilibrium stages distillation column. The feed compositions and conditions are given in Table 3.2.

The driving force design method is then applied to this example. The split is between compounds *A* and *B* where compound *B* is the light key. The phase composition data have been calculated (using the vapour pressure data given in Table 3.2) and the driving force diagram for this system is shown in Fig. 3.9, in where the

mole-fraction of compound B is plotted on the x-axis (which is the light key compound).

Table 3.2
Feed composition and physical condition of the feed.

Component	Value		Unit
C_A	2.60		*kmol/h*
C_B	4.66		*kmol/h*
C_C	2.74		*kmol/h*
Total Flow	10.00		*kmol/h*
Physical Conditions			
Temperature (*K*)	433		
Pressure (*atm*)	6		
Antoine Coefficient	C_A	C_B	C_C
A	7.10	7.20	7.08
B	1381.68	1429.67	1342.79
C	228.79	239.77	239.50
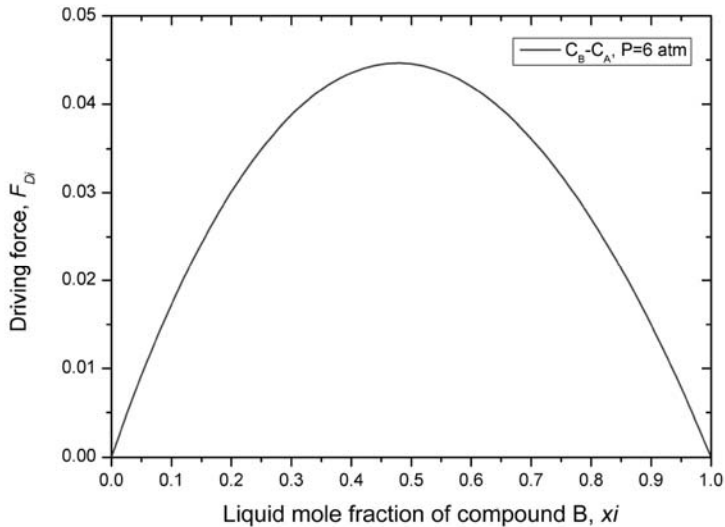
Fig. 3.9. Driving force diagram for Compound B – Compound A separation at 6 atm, where the liquid mole fraction of compound B is plotted on the x-axis.

From Fig. 3.9, the relative location of the largest driving force is determined to be $D_x = 0.48$. Along with a number of stages of $N = 15$, this leads to a prediction of an optimum feed location at stage, $N_F = 7$. A driving force diagram together with the distillation design parameters for compounds B-A separation is illustrated in Fig. 3.10. By taking product specifications at points A and B as 0.01 and 0.99, respectively,

values of RR_{min} and RB_{min} are calculated. The minimum reflux ratio is found to be $RR_{min} = 11.43$ and the minimum reboil ratio is calculated as $RB_{min} = 10.53$. The real reflux ratio and reboil ratio are then determined as 13.71 and 12.64, respectively.
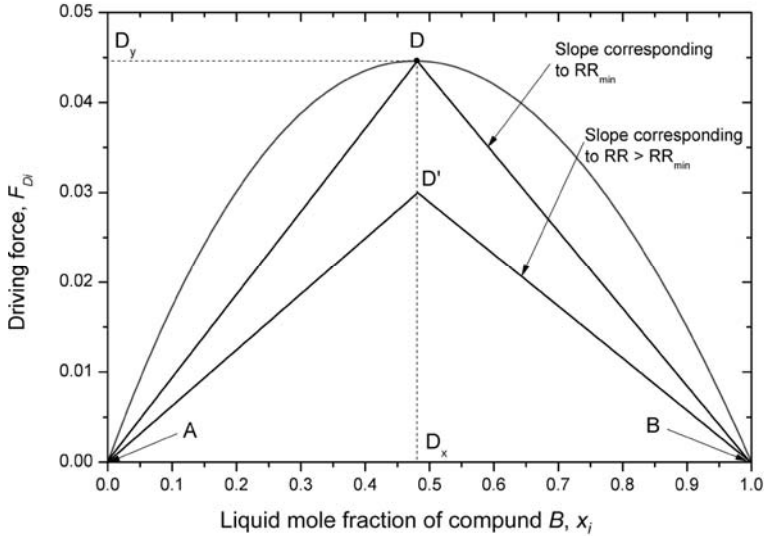
Fig. 3.10. Driving force diagram for Compound B – Compound A separation at 6 atm with illustration of the distillation design parameters.

With the known values of N_F, RR (or RB) and product purity, other design-process variables such as reboiler duty, condenser duty, bottom and top column temperatures and compositions are obtained by using any appropriate process model.

3.3.3 Optimal Design-Control Solutions

As previously explained in this chapter, for each reactor design problem, the attainable region is drawn and the location of the maximum in the attainable region is selected as the design target. Similarly, for each separator design problem, the driving force diagram is drawn and the design target is selected at the highest driving force. From a process design point of view, at these targets, the optimal design objectives ($P_{1,1}$ and $P_{1,2}$) can be obtained. From a controller design point of view, at these design targets the controllability of the process is best satisfied. The process sensitivity with respect to disturbances ($P_{2,1}$) is minimum and the sensitivity of controlled variables with respect to manipulated variables ($P_{2,2}$) is maximum. Minimum values of $P_{2,1}$ meaning that the controlled variables are less sensitive to the effect of disturbances and maximum values of $P_{2,2}$ determine the best controller structure.

According to Skogestad and coworkers (Larsson & Skogestad, 2000; Larsson et al., 2003; Skogestad 2000a,b; 2002; 2004), most (if not all) available control

theories assume that a controller structure is already defined. "They therefore fail to answer some basic questions, which a control engineer regularly meets in practice. Which variables should be controlled, which variables should be measured, which inputs should be manipulated, and which links should be made between them?" In Stage 3 (controller design analysis) of our methodology provides optimal solutions in terms of

1. Selection of controlled variables
2. Set-point values (controlled and manipulated variables)
3. Sensitivity of controlled variables with respect to disturbances
4. Selection of the controller structure (pairing between controlled-manipulated variables)

It has been discussed previously in this chapter that the value of the derivative of controlled variables $\mathbf{y}$ with respect to disturbances $\mathbf{d}$, $d\mathbf{y}/d\mathbf{d}$ and manipulated variables $\mathbf{u}$, $d\mathbf{y}/d\mathbf{u}$ will determine the process sensitivity and influence the controller structure selection. Accordingly, $d\mathbf{y}/d\mathbf{d}$ and $d\mathbf{y}/d\mathbf{u}$ are defined as (Russel et al., 2002)

$$\frac{d\mathbf{y}}{d\mathbf{d}} = \left(\frac{d\mathbf{y}}{d\boldsymbol{\theta}}\right)\left(\frac{d\boldsymbol{\theta}}{d\mathbf{x}}\right)\left(\frac{d\mathbf{x}}{d\mathbf{d}}\right) \tag{3.20}$$

$$\frac{d\mathbf{y}}{d\mathbf{u}} = \left(\frac{d\mathbf{y}}{d\boldsymbol{\theta}}\right)\left(\frac{d\boldsymbol{\theta}}{d\mathbf{x}}\right)\left(\frac{d\mathbf{x}}{d\mathbf{u}}\right) \tag{3.21}$$

Since values for $d\boldsymbol{\theta}/d\mathbf{x}$ can be obtained from Eq. (3.3), and values for $d\mathbf{y}/d\boldsymbol{\theta}$, $d\mathbf{x}/d\mathbf{d}$ and $d\mathbf{x}/d\mathbf{u}$ can be obtained from Eq. (3.2), it is possible to gain useful insights related to process sensitivity and controller structure without a rigorous solution of the process model equations. However, for a constant set of constitutive variables $\boldsymbol{\theta}$ (physical properties, reaction rates), which for example, is not a function temperature and/or pressure (since they are constant), Eqs. (3.20)-(3.21) can be reduced to Eqs. (3.22)-(3.23)

$$\frac{d\mathbf{y}}{d\mathbf{d}} = \left(\frac{d\mathbf{y}}{d\mathbf{x}}\right)\left(\frac{d\mathbf{x}}{d\mathbf{d}}\right) \tag{3.22}$$

$$\frac{d\mathbf{y}}{d\mathbf{u}} = \left(\frac{d\mathbf{y}}{d\mathbf{x}}\right)\left(\frac{d\mathbf{x}}{d\mathbf{u}}\right) \tag{3.23}$$

In general, values of $d\mathbf{y}/d\mathbf{d}$ (at optimal $\mathbf{y}$ values) will determine the process sensitivity and flexibility with respect to disturbances. If $d\mathbf{y}/d\mathbf{d}$ is small, the process sensitivity is low and the process flexibility is high. This means that, the process is more robust in maintaining its controlled variables in the presence of disturbances. If $d\mathbf{y}/d\mathbf{d}$ is high, the process sensitivity is high and the process flexibility is low. At this situation, the process will experience difficulty in maintaining its controlled variables in the presence of disturbances. On the other hand, the maximum value of $d\mathbf{y}/d\mathbf{u}$ will determine the best pair of the controlled-manipulated variables for the controller

structure selection. If $d\mathbf{y}/d\mathbf{u}$ is high, small changes in u will give large changes in y. This means that u has a large and direct effect on y, thus making controllability for y to be good. On the other hand, if $d\mathbf{y}/d\mathbf{u}$ is small, big changes in u will give small changes in y, which means that the effect of u on y is poor, leading to poor controllability.

Note that when the constitutive variables $\mathbf{\theta}$ are not constant, $d\mathbf{\theta}/d\mathbf{x}$ for a given chemical system is fixed and can be computed from Eq. 3.3, that is, from the corresponding constitutive (property or kinetic) models.

3.3.3.1 Controller Design Analysis for a Reactor

Let us revisit Example 3.1 to analyze the controller design problem for a single reactor.

a) Selection of controlled variables

It should be noted that, by using the attainable region concept, the selection of the primary controlled variable (y_1) is fixed at the y-axis of the attainable region diagram, since it is associated with the design objective function $P_{1,1}$. For this example, it is the desired product concentration C_B (see Fig. 3.11). However, in order to obtain an optimal controllability, in this methodology we select a secondary controlled variable (y_2) at the x-axis of the attainable region, which is a reactant concentration C_A (see Fig. 3.11). Here, C_A is controlled directly instead of C_B. The selection of controlled variables is summarized as follows:

- C_B (y_1) – a primary controlled variable (measured output)
- C_A (y_2) – a secondary controlled variable (measured and controlled output)

For this selection, an indirect control can be applied. The reason behind this selection is that by controlling C_A at its set-point value at Point A (at the maximum point of the attainable region – see Fig. 3.11), a good control of C_B can indirectly be achieved at its optimal set-point in the presence of disturbances or changes in the set-point of C_A compared to Points B and C. This statement will be verified later.

However, if C_A is difficult to measure, then other state variables such as reactor level, h or reactor temperature, T can be selected as an alternative secondary controlled variable (y^*_2). In this example, since the kinetic for the reaction rate is constant (not a function of temperature), therefore, reactor temperature is eliminated from the list of an alternative secondary controlled variable candidate. Thus, reactor level, h is selected as an alternative secondary controlled variable (y^*_2). Here, an indirect control can be applied. For an indirect control, the selection of controlled variables is summarized as follows:

- C_B (y_1) – a primary controlled variable (measured output)
- C_A (y_2) – a secondary controlled variable (desired output)

- $h\,(y^*_2)$ – an alternative secondary controlled variable (measured and controlled output)

The reason we control y^*_2 is to indirectly control y_2 to achieve a good control of y_1.

It should be noted that the objective here is to select the right controlled variables for the controller structure selection. According to this methodology and using control degree of freedom analysis, either controlling C_A or h using an indirect control, a good control of C_B can always be achieved at its optimal set-point in the presence of disturbances or changes in the set-point of C_A or h at Point A (at the maximum point of the attainable region – see Fig. 3.11) compared to Points B and C. This statement will be verified below.
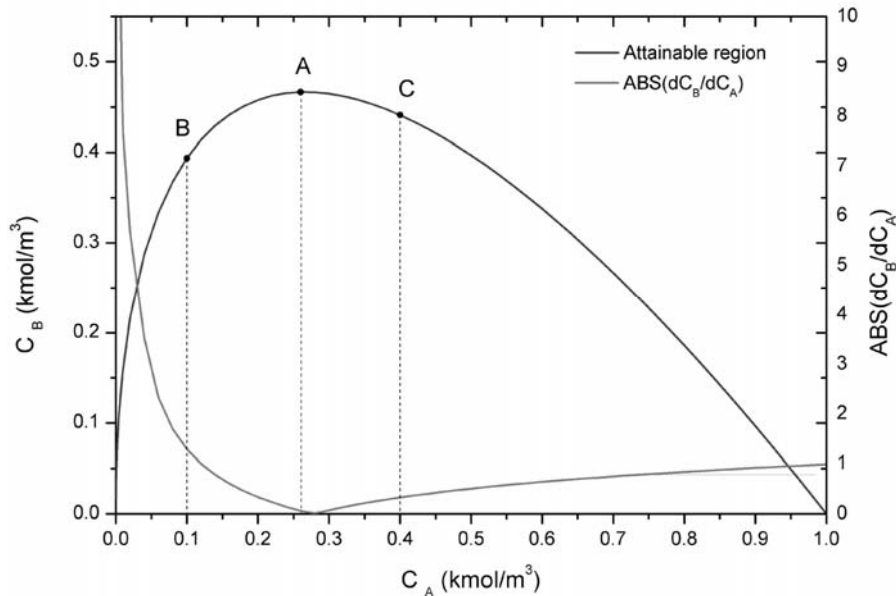
Fig. 3.11. Plot of concentration B as a function of concentration of A and its corresponding derivative of C_B with respect to C_A.

b) Set-points value for controlled and manipulated variables

For a reactor design problem, the target for the design solution is located at the maximum point of the attainable region diagram (Point A) – see Fig. 3.11. From this target, other values of controlled variables **y** and manipulated variables **u** are calculated using the reverse solution approach. The calculated values of **y** and **u** at this target are then assigned as set-point values. Since at this target, the design objective $P_{1,1}$ is maximum, therefore the set-point assigned values are the optimal ones.

Model-Based Integrated Process Design and Controller Design of Chemical Processes

c) <u>Sensitivity of controlled variables with respect to disturbances</u>

According to this methodology, at the maximum point of the attainable region, the sensitivity of the controlled variable with respect to disturbances is minimum, which satisfies the control objective $P_{2,1}$. For a reactor design problem (Example 3.1), variables **y** and **x** are scalar, which are selected at the axis of the attainable region diagram; $y = y_1 = C_B$ (at y-axis) and $x = y_2 = C_A$ (at x-axis). Variable **d**, on the other hand, is a vector, which consists of $\mathbf{d} = [F_f \; C_{Af}]$. Since the kinetic parameter for the reaction rate is constant, Eq. (3.22) is used in this example for sensitivity calculation. By taking $y_1 = f_1(y_2)$ or $C_B = f_1(C_A)$, then

$$\frac{dy}{dx} = \left[\frac{dy_1}{dy_2}\right] = \left[\frac{dC_B}{dC_A}\right] \tag{3.24}$$

Since $y_2 = f_2(\mathbf{d})$ or $C_A = f_2(\mathbf{d})$, where the vector **d** is $\mathbf{d} = [F_f \; C_{Af}]$, then

$$\frac{dx}{d\mathbf{d}} = \left[\frac{dy_2}{dd_1} \quad \frac{dy_2}{dd_2}\right] = \left[\frac{dC_A}{dF_f} \quad \frac{dC_A}{dC_{Af}}\right] \tag{3.25}$$

Multiplication of Eq. (3.24) with Eq. (3.25) yields

$$\frac{dy}{d\mathbf{d}} = \left[\frac{dC_B}{dF_f} \quad \frac{dC_B}{dC_{Af}}\right] = \left[\left(\frac{dC_B}{dC_A}\right)\left(\frac{dC_A}{dF_f}\right) \quad \left(\frac{dC_B}{dC_A}\right)\left(\frac{dC_A}{dC_{Af}}\right)\right] \tag{3.26}$$

From process models

$$0 = F_f C_{Af} - F C_A - k_1 C_A V + k_{-1} C_B V \tag{3.27a}$$

$$0 = -F C_B + k_1 C_A V - (k_{-1} + k_2) C_B V \tag{3.27b}$$

For a disturbance $d_1 = C_{Af}$, summing for Eqs. (3.27) and differentiating with respect to C_{Af} yields

$$(F_s + k_2 V_s)\frac{dC_B}{dC_{Af}} + F_s \frac{dC_A}{dC_{Af}} + k_2 C_{Bs} \frac{dV}{dC_{Af}} = F_{fs} + C_{Afs}\frac{dF_f}{dC_{Af}} - (C_{As} - C_{Bs})\frac{dF}{dC_{Af}} \tag{3.28}$$

where the subscript s denotes the steady-state value. By assuming $dF/dC_{Af} = dF_f/dC_{Af} = 0$, Eq. (3.28) is simplified to

$$(F_s + k_2 V_s)\frac{dC_B}{dC_{Af}} + F_s \frac{dC_A}{dC_{Af}} + k_2 C_{Bs} \frac{dV}{dC_{Af}} = F_{fs} \tag{3.29}$$

For a primary controlled variable $y_1 = C_B$ and a secondary controlled variable $y_2 = C_A$, Eq. (3.29) becomes

$$(F_s + k_2 V_s)\frac{dC_B}{dC_{Af}} + F_s \frac{dC_A}{dC_{Af}} = F_{fs} \tag{3.30}$$

where $dV/dC_{Af} = 0$, since the reactor volume (reactor level) is not the controlled variable. We will consider the reactor volume (reactor level) as a controlled variable later in this section.

Rearranging Eq. 3.30, we get the following equation

$$\left(\frac{dC_B}{dC_A}\right)\left(\frac{dC_A}{dC_{Af}}\right) + \frac{F_s}{F_s + k_2 V_s}\frac{dC_A}{dC_{Af}} = \frac{F_{fs}}{F_s + k_2 V_s} \tag{3.31a}$$

which then can be simplified to

$$\left(\frac{dC_A}{dC_{Af}}\right)\left[\left(\frac{dC_B}{dC_A}\right) + c_1\right] = c_2 \tag{3.31b}$$

where $c_1 = F_s / F_s + k_2 V_s$ and $c_2 = F_{fs} / F_s + k_2 V_s$.

Similarly, for a disturbance $d_2 = F_f$, we get:

$$\left(\frac{dC_B}{dC_A}\right)\left(\frac{dC_A}{dF_f}\right) + \frac{F_s}{F_s + k_2 V_s}\frac{dC_A}{dF_f} = \frac{C_{Afs}}{F_s + k_2 V_s} \tag{3.32a}$$

which then can be simplified to

$$\left(\frac{dC_A}{dF_f}\right)\left[\left(\frac{dC_B}{dC_A}\right) + c_1\right] = c_3 \tag{3.32b}$$

where $c_3 = C_{Afs} / F_s + k_2 V_s$.

Substituting Eqs. (3.31b) and (3.32b) into Eq. (3.26), then the sensitivity can be analyzed.

$$\frac{dy}{d\mathbf{d}} = \left[\begin{array}{cc} \dfrac{dC_B}{dF_f} & \dfrac{dC_B}{dC_{Af}} \end{array}\right] = \left[\begin{array}{cc} \left(\dfrac{dC_B}{dC_A}\right)\dfrac{c_1}{\dfrac{dC_B}{dC_A} + c_2} & \left(\dfrac{dC_B}{dC_A}\right)\dfrac{c_3}{\dfrac{dC_B}{dC_A} + c_2} \end{array}\right] \tag{3.33a}$$

Values of dC_B/dC_A are calculated and shown in Fig. 3.11. Note that in Fig. 3.11, two other points (Points B and C) which are not at the maximum are identified as candidate alternative designs for a reactor, which will be used for verification purposes.

It can be seen in Fig. 3.11 that, at the maximum point of the attainable region (Point A) $dC_B/dC_A \approx 0$, and bigger at all other points. It is important to note that values of dC_B/dC_A are directly related to the process sensitivity. At Point A, Eq. (3.33a) becomes

$$\frac{d\mathbf{y}}{d\mathbf{d}} = \begin{bmatrix} \dfrac{dC_B}{dF_f} & \dfrac{dC_B}{dC_{Af}} \end{bmatrix} \approx \left[(0)\left(\frac{c_1}{0+c_2}\right) \quad (0)\left(\frac{c_3}{0+c_2}\right) \right] \approx \begin{bmatrix} 0 & 0 \end{bmatrix} \tag{3.33b}$$

It can clearly be seen that in Eq. (3.33b), the primary controlled variable C_B is less sensitive to the effect of disturbances in the feed. On the other hand, since values of dC_B/dC_A are bigger at Points B and C, therefore, sensitivities of C_B with respect to disturbances at these points are bigger – see Eq. (3.34).

$$\left.\frac{dC_B}{dF_f}\right|_A , \left.\frac{dC_B}{dC_{Af}}\right|_A < \left.\frac{dC_B}{dF_f}\right|_{B,C} , \left.\frac{dC_B}{dC_{Af}}\right|_{B,C} \tag{3.34}$$

Smaller values of dC_B/dF_f and dC_B/dC_{Af} mean that the sensitivity of the desired product C_B with respect to disturbances C_{Af} and F_f is smaller. This means that at Point A, the optimal value of C_B is less sensitive to the effect of disturbances compared to Points B and C. Thus, the process is able to maintain C_B in the presence of disturbances at Point A more easily than at Points B and C, where more control action is required to maintain C_B. Therefore, it is verified that controlling C_A using an indirect control, a good control of C_B can always be achieved at its optimal set-point in the presence of disturbances at Point A (at the maximum point of the attainable region – see Fig. 3.11 and Eqs. (3.33)-(3.34)) compared to Points B and C. Thus, disturbance rejection performance is the best at the maximum point of the attainable region – Point A. Since the optimal C_B is insensitive to disturbances at Point A, which satisfies one of the requirements for the selection of controlled variables (Skogestad, 2000a,b), therefore, the selection of C_B as a primary controlled variable (y_1) is verified.

However, if C_A is difficult to measure, reactor level, h is selected as an alternative secondary controlled variable (y^*_2). Eq. (3.26) is then can be extended to

$$\frac{d\mathbf{y}}{d\mathbf{d}} = \begin{bmatrix} \dfrac{dC_B}{dF_f} & \dfrac{dC_B}{dC_{Af}} \end{bmatrix} = \left[\left(\frac{dC_B}{dC_A}\right)\left(\frac{dC_A}{dh}\right)\left(\frac{dh}{dF_f}\right) \quad \left(\frac{dC_B}{dC_A}\right)\left(\frac{dC_A}{dh}\right)\left(\frac{dh}{dC_{Af}}\right) \right] \tag{3.35}$$

Differentiating the process model with respect to h, and then after manipulation the derivative of dC_A/dh can be expressed as

$$\frac{dC_A}{dh} = -\frac{Ak_2C_{Bs}}{F_s} = c_4 \qquad (3.36)$$

Similarly, the derivative of dh/dF_f and dh/dC_{Af} can be expressed as

$$\frac{dh}{dF_f} = \frac{C_{Afs}}{Ak_2C_{Bs}} = c_5 \qquad (3.37a)$$

$$\frac{dh}{dC_{Af}} = \frac{F_{fs}}{Ak_2C_{Bs}} = c_6 \qquad (3.37b)$$

Substituting Eqs. (3.36)-(3.37) into Eq. (3.35), we get

$$\frac{d\mathbf{y}}{d\mathbf{d}} = \left[\frac{dC_B}{dF_f} \quad \frac{dC_B}{dC_{Af}} \right] = \left[\left(\frac{dC_B}{dC_A} \right)(c_4)(c_5) \quad \left(\frac{dC_B}{dC_A} \right)(c_4)(c_6) \right] \qquad (3.38)$$

From Eq. (3.38), it can be seen that the sensitivity of C_B with respect to disturbances is directly related to the value of dC_B/dC_A. Since at the maximum point of the attainable region (Point A), $dC_B/dC_A \approx 0$ and bigger at all other point, therefore, it is verified that the disturbance rejection performance at Point A is always better than other point.

As a summary, it has been shown that either controlling C_A or h at the maximum point of the attainable region – Point A, a good control of C_B in terms of disturbance rejection can always be achieved at its optimal set-point in the presence of disturbances compared to other point.

d) <u>Selection of the controller structure (pairing between controlled-manipulated variables)</u>

In this methodology we calculate the value of $d\mathbf{y}/d\mathbf{u}$ for the selection of the controller structure, which is a structure connecting controlled and manipulated variables, Previously, we have defined the primary controlled variable, y_1 as the desired product concentration C_B and the secondary controlled variable, y_2 as C_A which can be inferred with reactor level h (alternative secondary controlled variable, y^*_2). For this example the potential manipulated variable is u = F. Therefore Eq. (3.23) can be expressed as

$$\frac{dC_B}{dF} = \left(\frac{dC_B}{dC_A} \right)\left(\frac{dC_A}{dF} \right) \qquad (3.39)$$

for a controller structure of a direct control of the primary controlled variable C_B, where $C_A = f_2(F)$. On the other hand, for a controller structure of a direct control of the secondary controlled variable C_A and an alternative secondary controlled variable h can be expressed as dC_A/dF and dh/dF, respectively.

The effect of manipulated variable F can be expressed as

$$\left(F_s + k_2 V_s\right)\frac{dC_B}{dF} + F_s \frac{dC_A}{dF} + Ak_2 C_{Bs} \frac{dh}{dF} = -\left(C_{As} - C_{Bs}\right) + C_{Afs}\frac{dF_f}{dF} + F_{fs}\frac{dC_{Af}}{dF}$$

(3.40)

By assuming $dF_f/dF = dC_{Af}/dF = 0$, Eq. (3.40) is simplified to

$$\left(\frac{dC_A}{dF}\right)\left[\left(\frac{dC_B}{dC_A}\right) + c_1\right] + c_8 \frac{dh}{dF} = -c_7$$

(3.41)

where $c_7 = C_{As} - C_{Bs}/F_s + k_2 V_s$ and $c_8 = Ak_2 C_{Bs}/F_s + k_2 V_s$.

Then, dC_A/dF and dh/dF can be expressed as

$$\frac{dC_A}{dF} = \frac{-c_7}{\left(\frac{dC_B}{dC_A}\right) + c_1}$$

(3.42a)

$$\frac{dh}{dF} = \frac{-c_7}{c_8}$$

(3.42b)

Eqs. (3.39) and (3.42) are shown in the matrix form as

$$\frac{dy}{du} = \left[\frac{dC_B}{dF} \quad \frac{dC_A}{dF}\right] = \left[\left(\frac{dC_B}{dC_A}\right)\left(\frac{dC_A}{dF}\right) \quad \frac{dC_A}{dF}\right] = \left[\left(\frac{dC_B}{dC_A}\right)\frac{-c_7}{\left(\frac{dC_B}{dC_A}\right) + c_1} \quad \frac{-c_7}{\left(\frac{dC_B}{dC_A}\right) + c_1}\right]$$

(3.43a)

$$\frac{dy}{du} = \left[\frac{dC_B}{dF} \quad \frac{dC_A}{dF} \quad \frac{dh}{dF}\right] = \left[\left(\frac{dC_B}{dC_A}\right)\frac{-c_7}{\left(\frac{dC_B}{dC_A}\right) + c_1} \quad \frac{-c_7}{\left(\frac{dC_B}{dC_A}\right) + c_1} \quad \frac{-c_7}{c_8}\right]$$

(3.43b)

It has been mentioned that in order to obtain an optimal controllability, in this methodology we select a secondary controlled variable and control it directly instead of controlling the primary controlled variable. According to Skogestad (2000a,b), a large derivative value of controlled variable with respect to manipulated variable *dy/du* will determine the best pair of controlled-manipulated variable for a controller

structure selection, which satisfies the second control objective $P_{2,2}$. In Eq. (3.43a), expressions of dC_B/dF and dC_A/dF represent two controller structures – a direct control of the primary controlled variable and a direct control of the secondary control variable. The largest value among these two derivatives determines the best controller structure. On the other hand, in Eq. (3.43b), expressions of dC_B/dF, dC_A/dF and dh/dF represent three controller structures – a direct control of the primary controlled variable, a direct control of the secondary controlled variable and a direct control of an alternative secondary controlled variable. The selection for the best controller structure is determined by the largest value among these three derivatives.

From Fig. 3.11, at the maximum point of the attainable region (Point A), value of $dC_B/dC_A \approx 0$ whereas at Points B and C are much bigger. It is important to note that values of dC_B/dC_A are also directly related to the controller structure selection. Since at Point A value of dC_B/dC_A is smaller, therefore, values of dC_B/dF in Eqs. (3.43) is confirmed to be smaller than value of dC_A/dF and dh/dF as shown in Eq. (3.44).

$$\frac{dy}{du} = \begin{bmatrix} \dfrac{dC_B}{dF} & \dfrac{dC_A}{dF} \end{bmatrix} \approx \begin{bmatrix} 0 & \dfrac{-c_7}{c_1} \end{bmatrix} \approx \begin{bmatrix} 0 & \dfrac{C_{Bs} - C_{As}}{F_s} \end{bmatrix} \tag{3.44a}$$

$$\frac{dy}{du} = \begin{bmatrix} \dfrac{dC_B}{dF} & \dfrac{dC_A}{dF} & \dfrac{dh}{dF} \end{bmatrix} \approx \begin{bmatrix} 0 & \dfrac{-c_7}{c_1} & \dfrac{-c_8}{c_1} \end{bmatrix} \approx \begin{bmatrix} 0 & \dfrac{C_{Bs} - C_{As}}{Fs} & \dfrac{C_{Bs} - C_{As}}{Ak_s C_{Bs}} \end{bmatrix}$$
$$\tag{3.44b}$$

It can be seen that, C_A-F (for Eq. (3.44a)) and h-F and C_A-F (for Eq. (3.44b)) are the best controller structure (the best pair of controlled-manipulated variable) at Point A since values of dC_A/dF and dh/dF are always bigger. In Eq. (3.44b), h-F will become the best controller structure if and only if $Ak_2 C_{Bs} < F_s$, whereas if $Ak_2 C_{Bs} > F_s$, then C_A-F will become the best controller structure. On the other hand, since values of dC_B/dC_A are much bigger at Points B and C, therefore, values of dC_B/dF in Eqs. (3.43) may or may not be bigger than value of dC_A/dF and dh/dF. As a result, C_A-F (for Eq. (3.43a)) and h-F and C_A-F (for Eq. (3.43b)) may or may not be the best controller structure at Points B and C (note that since C_{Bs} at Point A is always larger that at Points B and C, the numerator for dC_A/dF and dh/dF in Eqs. (3.44a-b) are always larger at Point A than at Point B and C). As a summary, dC_A/dF and dh/dF are always being the best controller structure at Point A than other points – see Eq. (3.45).

$$\left.\frac{dC_A}{dF}\right|_A, \left.\frac{dh}{dF}\right|_A > \left.\frac{dC_B}{dF}\right|_A \qquad \left.\frac{dC_A}{dF}\right|_{B,C}, \left.\frac{dh}{dF}\right|_{B,C} \gtrless \left.\frac{dC_B}{dF}\right|_{B,C} \tag{3.45}$$

3.3.3.2 Controller Design Analysis for a Separator

Let us revisit Example 3.2 to analyze the controller design for a single separator problem.

a) <u>Selection of controlled variables</u>

In this methodology, the primary controlled variable is x_{imax}, which is the x-axis value corresponding to F_{Dimax}. The secondary controlled variables are the product purities, which are the desired product B composition at the top and bottom column, x_d and x_b – see Fig. 3.12. The reason behind this selection is that by controlling x_d and x_b at Point A (at the maximum point of the driving force – see Fig. 3.12) will require less control effort in terms of reflux ratio, RR and also reboil ratio, RB in the presence of disturbances compared to Points B and C. This statement will be verified below.

The selection of controlled variables for a direct control of product B composition is summarized as follows:

For the top column:

- x_{imax} (y_1) – a primary controlled variable (uncontrolled output)
- x_d (y_2) – a secondary controlled variable (measured and controlled output)

For the bottom column:

- x_{imax} (y_1) – a primary controlled variable (uncontrolled output)
- x_b (y_2) – a secondary controlled variable (measured and controlled output)

However, if x_d and x_b are difficult to measure, then they can be inferred with the top and bottom column temperatures. This is possible since at different points (x_i value) at the driving force diagram (see Fig. 3.12) correspond to different values of temperatures. In this example, top T_D and bottom T_B column temperatures are selected as alternative secondary controlled variable (y^*_2). Here, an indirect control can be applied. The selection of controlled variables is summarized as follows:

For the top column:

- x_{imax} (y_1) – a primary controlled variable (uncontrolled output)
- x_d (y_2) – a secondary controlled variable (desired output)
- T_D (y^*_2) – an alternative secondary controlled variable (measured and controlled output)

For the bottom column:

- x_{imax} (y_1) – a primary controlled variable (uncontrolled output)
- x_b (y_2) – a secondary controlled variable (desired output)
- T_B (y^*_2) – an alternative secondary controlled variable (measured and controlled output)

It should be noted that the objective here is to select the right controlled variables for the controller structure selection. According to this methodology, either controlling T_D and T_B or controlling x_d and x_b using an indirect control, less control effort can always be achieved in the presence of disturbances at Point A (at the maximum point of the driving force – see Fig. 3.12) compared to Points B and C. This statement will be verified later in this section.
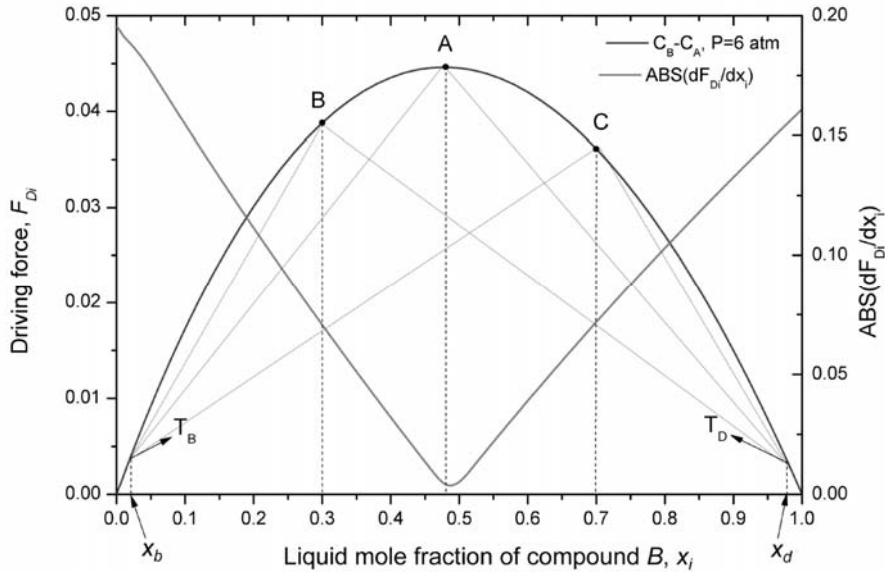

Fig. 3.12. Driving force diagram for Compound B – Compound A separation at 6 atm and its corresponding derivative of F_{Di} with respect to x_i.

b) Set-points value for controlled and manipulated variables

For a separator design problem, the target for the design solution is located at the maximum point of the driving force diagram (Point A) – see Fig. 3.12. From this target, other values of controlled **y** and manipulated variables **u** are calculated using the reverse solution approach. The calculated values of **y** and **u** at this target are then assigned as set-point values. Since at this target the value of the driving force F_{Di} is maximum, which maximizes the design objective $P_{1,2}$ is maximum, therefore the set-point assigned values are the optimal ones.

c) Sensitivity of controlled variables with respect to disturbances

It should be noted that, by using the driving force concept, the selection of the controlled variable is fixed at the x-axis of the driving force diagram, which is the desired product B composition at the top and bottom column, x_d and x_b – see Fig. 3.12. According to this methodology, at the maximum point of the driving force, the

sensitivity of x_d and x_b with respect to disturbances is minimum, which satisfy the control objective $P_{2.1}$. For a distillation column design problem (Example 3.2), variables $\mathbf{y}$ is a vector of $\mathbf{y} = [x_d \ x_b]$, $\mathbf{x}$ is a scalar, which is selected at the axis of the attainable region diagram; $\mathbf{x} = F_{Di}$ (at y-axis). Variables $\mathbf{d}$, on the other hand, are vector, which consist of $\mathbf{d} = [F_f \ z_{Bf}]$. By taking $\mathbf{y} = f_1(\mathbf{x})$ or $[x_d \ x_b] = f_1(F_{Di})$ and $\mathbf{x} = f_2(\mathbf{d})$ or $F_{Di} = f_2(\mathbf{d})$, , where the vector $\mathbf{d}$ is $\mathbf{d} = [F_f \ z_{Bf}]$, then $d\mathbf{y}/d\mathbf{d}$ can be expressed as

$$
\frac{d\mathbf{y}}{d\mathbf{d}} = \begin{bmatrix} \dfrac{dx_d}{dF_f} & \dfrac{dx_d}{dz_{Bf}} \\[2ex] \dfrac{dx_b}{dF_f} & \dfrac{dx_b}{dz_{Bf}} \end{bmatrix} = \begin{bmatrix} \left[\left(\dfrac{dx_d}{dF_{Di}}\right)\left(\dfrac{dF_{Di}}{dx_i}\right)\left(\dfrac{dx_i}{dF_f}\right) & \left(\dfrac{dx_d}{dF_{Di}}\right)\left(\dfrac{dF_{Di}}{dx_i}\right)\left(\dfrac{dx_i}{dz_{Bf}}\right)\right] \\[3ex] \left[\left(\dfrac{dx_b}{dF_{Di}}\right)\left(\dfrac{dF_{Di}}{dx_i}\right)\left(\dfrac{dx_i}{dF_f}\right) & \left(\dfrac{dx_b}{dF_{Di}}\right)\left(\dfrac{dF_{Di}}{dx_i}\right)\left(\dfrac{dx_i}{dz_{Bf}}\right)\right] \end{bmatrix} \tag{3.46}
$$

The operating line of the rectifying section is expressed as

$$
y = x_d \frac{D}{D+L} + x \frac{L}{D+L} \tag{3.47}
$$

By defining the external reflux ratio of the column as $RR = L/D$, Eq. (3.47) can be simplified to

$$
y = x_d \frac{1}{RR+1} + x \frac{RR}{RR+1} \tag{3.48}
$$

The driving force is expressed as

$$
F_D = y - x = x_d \frac{1}{RR+1} + x \frac{RR}{RR+1} - x \tag{3.49a}
$$

which can be simplified to

$$
F_D = x_d \frac{1}{RR+1} - x \frac{1}{RR+1} \tag{3.49b}
$$

Rearranging Eq. (3.49b), the top product composition x_d can be expressed as

$$
x_d = (RR+1)F_D + x \tag{3.50}
$$

Differentiating Eq. (3.50) with respect to F_D, we get

$$
\frac{dx_d}{dF_D} = (RR+1) + \frac{dx}{dF_D} = (RR+1) + \left(\frac{dF_D}{dx}\right)^{-1} \tag{3.51}
$$

Substituting Eq.(3.50) into the total material balance yields

$$F_f z_{Bf} = (RR+1)DF_D + Dx + x_b B \tag{3.52}$$

Differentiating Eq. (3.52) with respect to disturbance F_f in the feed yields

$$D_s(RR+1)\frac{dF_D}{dF_f} + D_s\frac{dx}{dF_f} + B_s\frac{dx_b}{dF_f} = z_{Bfs} + F_{fs}\frac{dz_{Bf}}{dF_f} - [(RR+1)F_{Ds} + x_s]\frac{dD}{dF_f} + x_{bs}\frac{dB}{dF_f} \tag{3.53}$$

By assuming $dz_{Bf}/dF_f = dD/dF_f = dB/dF_f = 0$, Eq. (3.53) is simplified to

$$D_s(RR+1)\frac{dF_D}{dF_f} + D_s\frac{dx}{dF_f} + B_s\frac{dx_b}{dF_f} = z_{Bfs} \tag{3.54a}$$

$$\frac{dx}{dF_f}\left[a_1\frac{dF_D}{dx} + a_2 + \left(\frac{dx_b}{dF_D}\right)\left(\frac{dF_D}{dx}\right) \right] = a_3 \tag{3.54b}$$

where $a_1 = D_s(RR+1)/B_s$, $a_2 = D_s/B_s$ and $a_3 = z_{Bfs}/B_s$.

On the other hand, differentiating Eq. (3.52) with respect to disturbance z_{Bf} in the feed yields

$$D_s(RR+1)\frac{dF_D}{dz_{Bf}} + D_s\frac{dx}{dz_{Bf}} + B_s\frac{dx_b}{dz_{Bf}} = F_{fs} + z_{Bfs}\frac{dF_f}{dz_{Bf}} - [(RR+1)F_{Ds} + x_s]\frac{dD}{dz_{Bf}} + x_{bs}\frac{dB}{dz_{Bf}} \tag{3.55}$$

By assuming $dF_f/dz_{Bf} = dD/dz_{Bf} = dB/dz_{Bf} = 0$, Eq. (3.55) is simplified to

$$D_s(RR+1)\frac{dF_D}{dz_{Bf}} + D_s\frac{dx}{dz_{Bf}} + B_s\frac{dx_b}{dz_{Bf}} = F_{fs} \tag{3.56a}$$

$$\frac{dx}{dz_{Bf}}\left[a_1\frac{dF_D}{dx} + a_2 + \left(\frac{dx_b}{dF_D}\right)\left(\frac{dF_D}{dx}\right) \right] = a_4 \tag{3.56b}$$

where $a_4 = F_{fs}/B_s$.

The operating line of the stripping section is expressed as

$$y = -x_b\frac{B}{V} + x\frac{V+B}{V} \tag{3.57}$$

By defining the external reboil ratio of the column as $RB = V/B$, Eq. (3.56) can be simplified to

$$y = -x_b \frac{1}{RB} + x \frac{RB+1}{RB} \tag{3.58}$$

The equation of the bottom product composition x_b in terms of F_D can be expressed as

$$x_b = x - RBF_D \tag{3.59}$$

Differentiating Eq. (3.59) with respect to F_D, we get

$$\frac{dx_b}{dF_D} = \frac{dx}{dF_D} - RB = \left(\frac{dF_D}{dx}\right)^{-1} - RB \tag{3.60}$$

Substituting Eq. (3.59) into the total material balance yields

$$F_f z_{Bf} = x_d D + Bx - RBF_D B \tag{3.61}$$

Differentiating Eq. (3.61) with respect to disturbance F_f in the feed yields

$$B_s RB \frac{dF_D}{dF_f} - B_s \frac{dx}{dF_f} - D_s \frac{dx_d}{dF_f} = x_{ds}\frac{dD}{dF_f} + \left(x_s - RBF_{Ds}\right)\frac{dB}{dF_f} - z_{Bfs} + F_{fs}\frac{dz_{Bf}}{dF_f} \tag{3.62}$$

By assuming $dz_{Bf}/dF_f = dD/dF_f = dB/dF_f = 0$, Eq. (3.62) is simplified to

$$B_s RB \frac{dF_D}{dF_f} - B_s \frac{dx}{dF_f} - D_s \frac{dx_d}{dF_f} = -z_{Bfs} \tag{3.63a}$$

$$\frac{dx}{dF_f}\left[a_5 \frac{dF_D}{dx} - a_6 - \left(\frac{dx_d}{dF_D}\right)\left(\frac{dF_D}{dx}\right)\right] = -a_7 \tag{3.63b}$$

where $a_5 = B_s RB/D_s$, $a_6 = B_s/D_s$ and $a_7 = z_{Bfs}/D_s$.

On the other hand, differentiating Eq. (3.62) with respect to disturbance z_{Bf} in the feed yields

$$B_s RB \frac{dF_D}{dz_{Bf}} - B_s \frac{dx}{dz_{Bf}} - D_s \frac{dx_d}{dz_{Bf}} = x_{ds}\frac{dD}{dz_{Bf}} + \left(x_s - RBF_{Ds}\right)\frac{dB}{dz_{Bf}} - F_{fs} + z_{Bfs}\frac{dF_f}{dz_{Bf}} \tag{3.64}$$

By assuming $dF_f/dz_{Bf} = dD/dz_{Bf} = dB/dz_{Bf} = 0$, Eq. (3.64) is simplified to

$$B_s RB \frac{dF_D}{dz_{Bf}} - B_s \frac{dx}{dz_{Bf}} - D_s \frac{dx_d}{dz_{Bf}} = -F_{fs} \tag{3.65a}$$

$$\frac{dx}{dz_{Bf}}\left[a_5\frac{dF_D}{dx}-a_6-\left(\frac{dx_d}{dF_D}\right)\left(\frac{dF_D}{dx}\right)\right]=-a_8 \tag{3.65b}$$

where $a_8 = F_{fs}/D_s$. Eq. (3.46) then becomes

$$\frac{d\mathbf{y}}{d\mathbf{d}}=\begin{bmatrix}\dfrac{dx_d}{dF_f}&\dfrac{dx_d}{dz_{Bf}}\\[2mm]\dfrac{dx_b}{dF_f}&\dfrac{dx_b}{dz_{Bf}}\end{bmatrix}=\begin{bmatrix}\left(\dfrac{dx_d}{dF_D}\right)\left(\dfrac{dF_D}{dx}\right)\left(\dfrac{dx}{dF_f}\right)&\left(\dfrac{dx_d}{dF_D}\right)\left(\dfrac{dF_D}{dx_i}\right)\left(\dfrac{dx}{dz_{Bf}}\right)\\[3mm]\left(\dfrac{dx_b}{dF_D}\right)\left(\dfrac{dF_D}{dx}\right)\left(\dfrac{dx}{dF_f}\right)&\left(\dfrac{dx_b}{dF_D}\right)\left(\dfrac{dF_D}{dx}\right)\left(\dfrac{dx}{dz_{Bf}}\right)\end{bmatrix}$$

$$=\begin{bmatrix}\left[\left((RR+1)+\left(\dfrac{dF_D}{dx}\right)^{-1}\right)\left(\dfrac{dF_D}{dx}\right)\left(\dfrac{-a_7}{\left[a_5\dfrac{dF_D}{dx}-a_6-\left(\dfrac{dx_d}{dF_D}\right)\left(\dfrac{dF_D}{dx}\right)\right]}\right)\right]&\left[\left((RR+1)+\left(\dfrac{dF_D}{dx}\right)^{-1}\right)\left(\dfrac{dF_D}{dx}\right)\left(\dfrac{-a_8}{\left[a_5\dfrac{dF_D}{dx}-a_6-\left(\dfrac{dx_d}{dF_D}\right)\left(\dfrac{dF_D}{dx}\right)\right]}\right)\right]\\[6mm]\left[\left(\left(\dfrac{dF_D}{dx}\right)^{-1}-RB\right)\left(\dfrac{dF_D}{dx}\right)\left(\dfrac{a_3}{\left[a_1\dfrac{dF_D}{dx}+a_2+\left(\dfrac{dx_b}{dF_D}\right)\left(\dfrac{dF_D}{dx}\right)\right]}\right)\right]&\left[\left(\left(\dfrac{dF_D}{dx}\right)^{-1}-RB\right)\left(\dfrac{dF_D}{dx}\right)\left(\dfrac{a_4}{\left[a_1\dfrac{dF_D}{dx}+a_2+\left(\dfrac{dx_b}{dF_D}\right)\left(\dfrac{dF_D}{dx}\right)\right]}\right)\right]\end{bmatrix}$$

$$(3.66)$$

Values of dF_D/dx are calculated and shown in Fig. 3.12. Note that in Fig. 3.12, two other points (Points B and C) which are not at the maximum are identified as candidate alternative designs for a distillation column which will be used for verification purposes.

Let us consider the effect of disturbances z_{Bf} and F_f to the process that will potentially move values of F_{Di} away from its set-points (Points A, B, C). Since at Point A dF_D/dx is smaller, therefore, any effect of z_{Bf} and F_f will move value of F_{Dimax} away from its set-point in a smaller value compared to Points B and C – see Fig. 3.12. Note that, expressions of $(dx_d/dF_D)(dF_D/dx)$ in Eq. (3.51b) and $(dx_b/dF_D)(dF_D/dx)$ in Eq. (3.60b) at Point A are 1 and greater than 1 at any other points. Therefore, Eq. (3.66) at Point A can be expressed as

$$\begin{bmatrix}\dfrac{dx_d}{dF_f}&\dfrac{dx_d}{dz_{Bf}}\\[2mm]\dfrac{dx_b}{dF_f}&\dfrac{dx_b}{dz_{Bf}}\end{bmatrix}\approx\begin{bmatrix}(1)\left(\dfrac{-a_7}{-a_6-1}\right)&(1)\left(\dfrac{-a_8}{-a_6-1}\right)\\[3mm](1)\left(\dfrac{a_3}{a_2+1}\right)&(1)\left(\dfrac{a_4}{a_2+1}\right)\end{bmatrix}\approx\begin{bmatrix}\dfrac{-a_7}{-a_6-1}&\dfrac{-a_8}{-a_6-1}\\[3mm]\dfrac{a_3}{a_2+1}&\dfrac{a_4}{a_2+1}\end{bmatrix} \tag{3.67}$$

Since values of $(dx_d/dF_D)(dF_D/dx)$ and $(dx_b/dF_D)(dF_D/dx)$ are bigger at any other points, numerator and denominator in Eq. (3.66) becomes bigger and smaller, respectively, which results in the bigger derivatives values. Therefore, it can clearly be seen that the secondary controlled variables x_d and x_b are less sensitive to the effect

of disturbances in the feed at Point A. Thus, disturbance rejection is the best at the maximum driving force (Point A) than other points.

On the other hand, there is another way of analyzing the distillation column sensitivity at the maximum driving force. This alternative way indicates half of the driving force area. Please refer to Appendix A for details of this alternative way.

However, if x_d and x_b are difficult to measure, other state variables such as column temperatures can be selected as an alternative secondary controlled variables and indirect control can be applied. The effect of the disturbance z_{Bf} to the column temperature can be simply expressed as

$$\frac{dT}{dz_{Bf}} = \frac{dF_D}{dz_{Bf}} \frac{d\alpha}{dF_D} \left(\frac{dP}{dT} \right)^{-1}$$

(3.68)

where $d\alpha/dF_D$ represents relationships between driving force and the relative volatility. On the other hand, $(dP/dT)^{-1}$ is representing the relationship between vapor pressure and temperature (note that if α is assumed constant, it is independent of temperature; therefore, representing the equilibrium constant as a function of the vapour pressure gives us the temperature dependence for the simplest model). It should ne noted that $d\alpha/dF_D$ and $(dP/dT)^{-1}$ are constant for a chemical system. Eq. (3.68) can be expended with respect to dF_D/dx as follows

$$\frac{dT}{dz_{Bf}} = \frac{dF_D}{dx} \frac{dx}{dz_{Bf}} \frac{d\alpha}{dF_D} \left(\frac{dP}{dT} \right)^{-1}$$

(3.69)

From Fig. 3.12, it can be seen that $dF_D/dx \approx 0$ at the maximum driving force. Irrespective of the value of $(dP/dT)^{-1}$ and $d\alpha/dF_D$, therefore, at the maximum driving force one gets the best disturbance rejection. Therefore, it can be seen by controlling column temperature, x_d and x_b can easily be maintained at its optimal set-point value in the presence of disturbances at Point A compared to other points.

d) <u>Selection of the controller structure (pairing between controlled-manipulated variables)</u>

In this methodology we calculate the value of $d\mathbf{y}/d\mathbf{u}$ for the selection of the controller structure, which is a structure connecting controlled and manipulated variables, Previously, we have defined the secondary controlled variable, y_2 as top and bottom compound B composition x_d and x_b which can be inferred with the top and bottom temperature T_D and T_B (an alternative secondary controlled variable, y^*_2). For this example the potential manipulated variable is $\mathbf{u} = [L \ V]$ which in this example is represented by RR and RB.

Differentiating the expression of the top product composition x_d – Eq. (3.50) with respect to RR yields

$$\frac{dx_d}{dRR} = F_{Ds} + (RR_s + 1)\frac{dF_D}{dRR} - \frac{dx}{dRR} \tag{3.70a}$$

which can be expressed as a function of dF_D/dx as

$$\frac{dx_d}{dRR} = F_{Ds} + (RR_s + 1)\frac{dF_D}{dx}\frac{dx}{dRR} - \frac{dx}{dRR} \tag{3.70b}$$

On the other hand, differentiating the expression of the top product composition x_D – Eq. (3.50) with respect to RB yields

$$\frac{dx_d}{dRB} = (RR_s + 1)\frac{dF_D}{dRB} + \frac{dx}{dRB} + F_{Ds}\frac{dRR}{dRB} \tag{3.71a}$$

Assuming that $dRR/dRB = 0$, Eq. (3.71a) is simplified to

$$\frac{dx_D}{dRB} = (RR_s + 1)\frac{dF_D}{dRB} + \frac{dx}{dRB} \tag{3.71b}$$

which can be expressed as a function of dF_D/dx as

$$\frac{dx_d}{dRB} = (RR_s + 1)\frac{dF_D}{dx}\frac{dx}{dRB} + \frac{dx}{dRB} \tag{3.71c}$$

Differentiating the expression of the bottom product composition x_b – Eq. (3.59) with respect to RR yields

$$\frac{dx_b}{dRR} = \frac{dx}{dRR} - RB_s\frac{dF_D}{dRR} - F_{Ds}\frac{dRB}{dRR} \tag{3.72a}$$

Assuming that $dRB/dRR = 0$, Eq. (3.72a) is simplified to

$$\frac{dx_b}{dRR} = \frac{dx}{dRR} - RB_s\frac{dF_D}{dRR} \tag{3.72b}$$

which can be expressed as a function of dF_D/dx as

$$\frac{dx_b}{dRR} = \frac{dx}{dRR} - RB_s\frac{dF_D}{dx}\frac{dx}{dRR} \tag{3.72c}$$

On the other hand, differentiating the expression of the bottom product composition x_b – Eq. (3.59) with respect to RB yields

$$\frac{dx_b}{dRB} = \frac{dx}{dRB} - F_{Ds} \tag{3.73}$$

Eqs. (3.70)-(3.73) are shown in the matrix form as

$$\frac{d\mathbf{y}}{d\mathbf{u}} = \begin{bmatrix} \dfrac{dx_d}{dRR} & \dfrac{dx_d}{dRB} \\ \dfrac{dx_b}{dRR} & \dfrac{dx_b}{dRB} \end{bmatrix} = \begin{bmatrix} F_{Ds} + (RR_s + 1)\dfrac{dF_D}{dx}\dfrac{dx}{dRR} - \dfrac{dx}{dRR} & (RR_s + 1)\dfrac{dF_D}{dx}\dfrac{dx}{dRB} + \dfrac{dx}{dRB} \\ \dfrac{dx}{dRR} - RB_s\dfrac{dF_D}{dx}\dfrac{dx}{dRR} & \dfrac{dx}{dRB} - F_{Ds} \end{bmatrix}$$
(3.74)

In Eq. (3.74), expressions of dx_d/dRR and dx_d/dRB represent two controller structures – a direct control of the secondary controlled variable x_d. The largest value among these two derivatives determines the best controller structure for x_d. On the other hand, expressions of dx_b/dRR and dx_b/dRB represent two controller structures – a direct control of the secondary controlled variable x_b. The selection for the best controller structure for x_b is determined by the largest value among these two derivatives. It can be seen from Fig. 3.12 that $dF_D/dx \approx 0$ at the maximum driving force (Point A). Thus, Eq. (3.74) is simplified to

$$\frac{d\mathbf{y}}{d\mathbf{u}} = \begin{bmatrix} \dfrac{dx_d}{dRR} & \dfrac{dx_d}{dRB} \\ \dfrac{dx_d}{dRR} & \dfrac{dx_d}{dRB} \end{bmatrix} = \begin{bmatrix} F_{Ds} - \dfrac{dx}{dRR} & \dfrac{dx}{dRB} \\ \dfrac{dx}{dRR} & \dfrac{dx}{dRB} - F_{Ds} \end{bmatrix}$$
(3.75a)

Assuming that $dx/dRR = dx/dRB \approx 0$, then Eq. (3.75a) becomes

$$\frac{d\mathbf{y}}{d\mathbf{u}} = \begin{bmatrix} \dfrac{dx_d}{dRR} & \dfrac{dx_d}{dRB} \\ \dfrac{dx_b}{dRR} & \dfrac{dx_b}{dRB} \end{bmatrix} = \begin{bmatrix} F_{Ds} & 0 \\ 0 & -F_{Ds} \end{bmatrix}$$
(3.75b)

It can be seen from Eq. (3.75b) that the best controller structure can easily be determined by looking at the value of $d\mathbf{y}/d\mathbf{u}$. Since values of dx_d/dRR and dx_b/dRB are bigger, controlling x_d by manipulating RR and controlling x_b by manipulating RB will require less control action. This is because only small changes in RR and RB are required to move x_d and x_b in a bigger direction.

As a summary, it has been shown that by designing a reactor and a separator (distillation column) at the maximum point of the attainable region (for reactor) and the driving force (for separator), the design objective and also the control objective can be best satisfied. At this point, the process sensitivity with respect to disturbance ($P_{2,1}$) is minimum, while the sensitivity with respect to the manipulated variable ($P_{2,2}$) is maximum. Minimum values of $P_{2,1}$ meaning that the controlled variables are less sensitive to the effect of disturbances (better disturbance rejection) and maximum values of $P_{2,2}$ determine the best controller structure.

3.4 Algorithm of Model-Based Integrated Process Design and Controller Design

A step-by-step algorithm of the proposed decomposition-based methodology for *IPDC* problems is presented in this section. The work flow of the methodology is seen in Fig. 3.13. The methodology is highlighted with a simple (theoretical) conceptual example of a single reactor design. Note, however, in Chapter 5 more elaborated application examples are presented.

3.4.1 Stage 1: Pre-analysis

The objective of this first stage is to define the operational window and set the targets for the design-control solution. The step-by-step algorithm for Stage 1 is presented below.

Step 1.1: Variables analysis
> Analyze all **y** and **u** and based on the multi-objective functions, Eq. (3.7), shortlist the important ones.

Step 1.2: Operational window identification
> Define the operational window in terms of **y** and **u** variables. **y** is selected based on thermodynamic-process insight and Eqs. (3.3) (also defines the optimal solution targets). Then, solve Eqs. (3.4) and (3.5) for **u** to establish the operational window.

Step 1.3: Design-control target identification
> Draw the attainable region and the driving force diagrams using Eq. (3.3) and identify design-control targets by locating the maximum points on the attainable region and the driving force diagrams.

3.4.2 Stage 2: Design Analysis

The objective of this stage is to validate the targets identified in Stage 1 by finding acceptable values (candidates) of **y** and **u**. If the acceptable values (candidates) cannot be obtained or the values are lying outside of the operational window, a new target is selected at Stage 1 and values are recalculated until a satisfactory match is obtained.
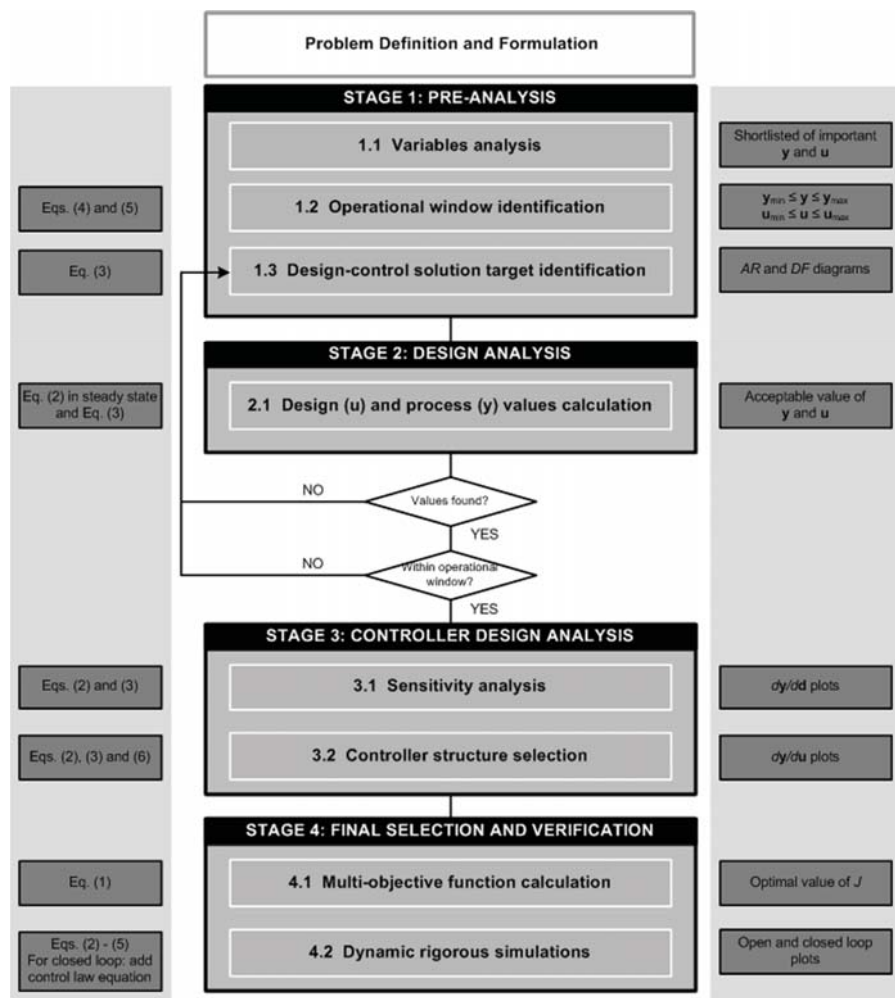
Fig. 3.13. Flow diagram of the model-based *IPDC* methodology for chemical processes.

Step 2.1: Design-process values calculation

Calculate the acceptable values (candidates) of $\mathbf{y}$ and $\mathbf{u}$ variables using steady state process model of Eq. (3.2).

a. For reactor design: at the maximum point of the attainable region, identify the corresponding value of concentrations of the desired products and limiting/selected reactant. Then find all other values of design-manipulated (reactor volume, reactor outlet flowrate, cooling water flowrate) and process-controlled (reactor temperature, concentrations, pressure) variables.

b. For separator design: at the maximum point of the driving force and given a desired product composition, then find all values of design variables (feed stage, reflux ratio, reboil ratio). By using the steady state process model find other design-manipulated (reflux flow, vapor boilup, reboiler and condenser duties) and process-controlled (top and bottom compositions, top and bottom temperature) variables.

3.4.3   Stage 3: Controller Design Analysis

The objective of this stage is to evaluate and validate the controllability performance of the feasible candidates. Two criteria are analyzed: (a) sensitivity ($d\mathbf{y}/d\mathbf{d}$) of controlled variable $\mathbf{y}$ with respect to disturbances $\mathbf{d}$, which should be low, and (b) sensitivity ($d\mathbf{y}/d\mathbf{u}$) of controlled variables $\mathbf{y}$ with respect to manipulated variables $\mathbf{u}$, which should be high.

Step 3.1: Sensitivity analysis

Calculate $d\mathbf{y}/d\mathbf{d}$ using Eq. (3.2) to determine the process sensitivity with respect to disturbances.

Step 3.2: Controller structure selection

Calculate $d\mathbf{y}/d\mathbf{u}$ using Eq. (3.2) to determine the best pair of the controlled-manipulated variables to satisfy Eq. (3.6). The best pair is selected based on the maximum value of $d\mathbf{y}/d\mathbf{u}$.

3.4.4   Stage 4: Final Selection and Verification

The objective of this stage is to select the best candidates by analyzing the value of the multi-objective function (refer to Eq. 3.7). The best candidate is then verified using rigorous simulations.

Step 4.1: Final selection: verification of design
    Evaluate the multi-objective function for the feasible candidates using Eq.
    (3.7) to select the optimal.

Step 4.2: Dynamic rigorous simulations: verification of controller performance
    Perform open or closed loop rigorous simulations. Solve Eqs. (3.2) – (3.5).
    For closed loop simulation, control law equations are needed.

The application of the step-by-step algorithm of the decomposition-based methodology for *IPDC* is illustrated by a conceptual example of a reactor design. We use this simple example as a motivation, with the aim of highlighting the capability of the proposed methodology.

Example 3.3: Conceptual example (Example 3.1 revisited)

The example presented here illustrates the step-by-step algorithm of the decomposition-based methodology for *IPDC* problems of a single reactor system as shown in Fig. 3.14. Let us revisit example 3.1. Consider the liquid phase, constant density, isothermal reactions (Eq. (3.8)) in a *CSTR* with the reaction kinetic and initial feed concentrations as shown in Table 3.1.
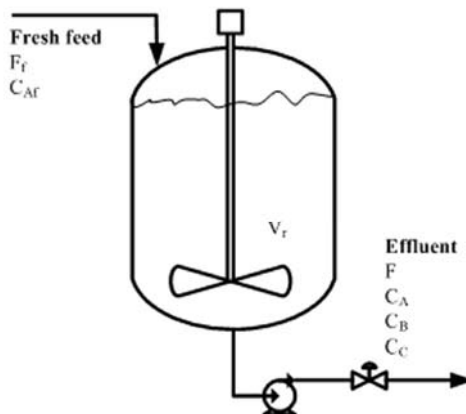
Fig. 3.14. *CSTR* for a component *B* production.

The objective of this process is to produce the highest and controllable of the concentration of the desired product of component B (C_B) in the presence of disturbances such as the feed flow rate, F_f and the feed concentration of component A, C_{Af}. In order to achieve that objective, we need to determine the optimal reactor volume that can produce the highest concentration of component B (C_B) as well as the optimal controller structure (the best pairing of controlled variable and manipulated variable) that is capable of maintaining C_B at its optimal set point value in the presence of disturbances, with the optimal capital and operating costs. This can be achieved by formulating the above problem as an *IPDC* problem as shown below.

Problem Formulation

The *IPDC* problem for the process described above is defined in terms of a performance objective (with respect to design, control and economics), and the three sets of constraints (process, constitutive and conditional).

$$\max \quad J = w_{1,1}P_{1,1} + w_{2,1}\left(\frac{1}{P_{2,1}}\right) + w_{2,2}P_{2,2} + w_{3,1}\left(\frac{1}{P_{3,1}}\right) \tag{3.76}$$

subjected to:

Process (dynamic and/or steady state) constraints

$$\frac{d(Ah_r)}{dt} = F_f - F \tag{3.77}$$

$$\frac{d(V_rC_A)}{dt} = F_fC_{Af} - FC_A - V_rR_A \tag{3.78}$$

$$\frac{d(V_rC_B)}{dt} = -FC_B + V_rR_B \tag{3.79}$$

$$\frac{d(V_rC_C)}{dt} = -FC_C + V_rR_C \tag{3.80}$$

Constitutive (thermodynamic) constraints

$$R_A = k_{-1}C_B + k_1C_A \tag{3.81}$$

$$R_B = k_1C_A - (k_{-1} + k_2)C_B \tag{3.82}$$

$$R_C = k_2C_B \tag{3.83}$$

Conditional (process-control) constraints

$$30 \geq V_r \tag{3.84}$$

$$3 \leq V_r \tag{3.85}$$

$$CS = \mathbf{y} + \mathbf{u}Y \tag{3.86}$$

Eq. (3.75) represents the multi-objective function, where $w_{1,1}$, $w_{2,1}$, $w_{2,2}$ and $w_{3,1}$ are the weight factors assigned to objective function terms of $P_{1,1}$, $P_{2,1}$, $P_{2,2}$ and $P_{3,1}$, respectively. The first objective function term $P_{1,1}$ is the performance criterion for the reactor design which in this problem is the concentration of the desired product (C_B). $P_{2,1}$ and $P_{2,2}$ are the sensitivities of the controlled variables $\mathbf{y}$ with respect to disturbances $\mathbf{d}$ and manipulated variables $\mathbf{u}$, respectively, which represent control objective functions. Lastly, $P_{3,1}$ is the real reactor volume V_r which represents the capital cost for the economic objective function.

Eqs. (3.77)-(3.80) are the dynamic process model equations for the reactor from which the steady-state models are obtained by setting the left hand side of the *ODEs* (ordinary differential equations) equal to zero. Eq. (3.77) represents the total mass balance for the reactor, Eq. (3.78) represents the mass balance for the reactant (component *A*), Eq. (3.79) represents the mass balance for the desired product (component *B*) while Eq. (3.80) represent of the mass balance for the by-product (component *C*). Eqs. (3.81)-(3.83) represent reaction rates of components *A*, *B* and *C*, respectively.

Eqs. (3.84)-(3.85) represent the real reactor volume V_r, by summing the reaction volume V_R with the headspace, where the headspace is calculated as 10% of the reaction volume (safety factor). The acceptable value of V_r for a *CSTR* is $3 \leq V_r$ (m^3) ≤ 30 (as defined in Table 6.2 of Sinnot (2005) as a relation between capacity and cost for estimation of purchased equipment costs). Eq. (3.86) represents the controller structure selection superstructure where $Y \in \{0,1\}$, which selected the pair of controlled-manipulated variables.

The *IPDC* problem formulated above is then solved using the proposed decomposition-based solution strategy as shown below.

Decomposition-based solution strategy

The summary of the decomposition-based solution strategy for this problem is shown in Table 3.3 and Fig. 3.15. It can be seen that the constraints in the *IPDC* problem are decomposed into four sub-problems that correspond to the four hierarchical stages. In this way, the solution of the decomposed set of sub-problems is equal to that of the original problem. Details of the step-by-step solutions are shown below.

Table 3.3
Mathematical equations and decomposition-based solution for a conceptual single reactor design.

Mathematical equations	Decomposition method	Corresponding variables
Multi-objective function: Eq. (3.75) *Process constraints:* Eqs. (3.76)-(3.80) *Constitutive constraints:* Eqs. (3.81)-(3.83) *Conditional constraints:* Volume range: Eqs. (3.84)-(3.85) Controller structure: Eq. (3.86)	*Stage 1: Pre-analysis.* a. Variable analysis b. Operational window: Eqs. (3.84)-(3.85) c. Design-control target Attainable region: Eqs. (3.81)-(3.83) *Stage 2: Design analysis.* Eqs. (3.81)-(3.83) and Eqs. (3.76)-(3.80) in steady state *Stage 3: Controller design analysis:* Sensitivity analysis: Eqs. (3.76)-(3.83) Controller structure selection: Eqs. (3.76)-(3.83) and Eq. (3.86) *Stage 4: Final selection and verification* Final selection: Eq. (3.75) Dynamic simulations verification: Eqs. (3.76)-(3.83)	C_A, C_B, V_r (h_r), F $3 \leq V \leq 30$ C_B/C_A F dC_B/dC_A, dC_B/dF_f dC_A/dF, dC_B/dF, dh_r/dF J
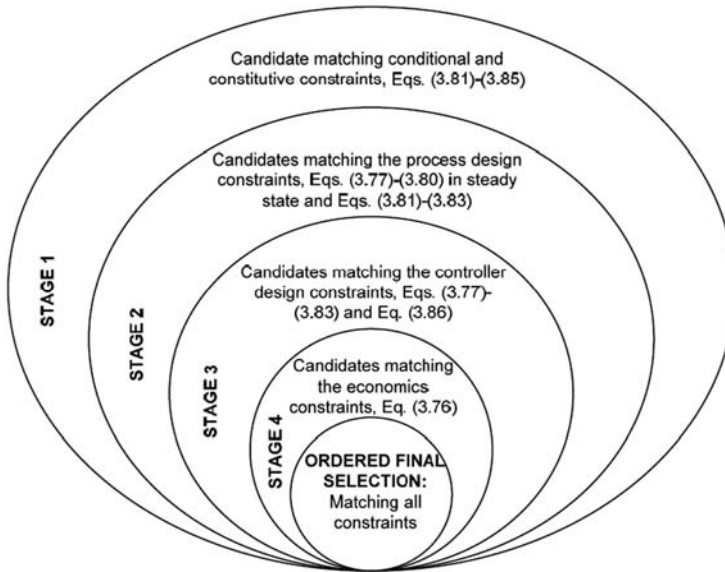
Fig. 3.15. Decomposition-based solution for a conceptual single reactor design.

Stage 1: Pre-analysis

The main objective of this stage is to define the operational window within which the optimal solution is located and set the targets for the optimal design-controller solution.

Step 1.1: Variables analysis

The first step in Stage 1 is to perform variable analysis. All variables involved in this process are analyzed and classified as design and manipulated variables $\mathbf{u}$, process-controlled variables $\mathbf{y}$, and disturbances $\mathbf{d}$ as shown in Table 3.4. V_r is considered as a design variable that needs to be adjusted in order to achieve the design objective and F is considered as a manipulated variable. On the other hand, four variables (C_A, C_B, C_C, h_r) are assigned as process variables and they also serve as the vector of measured/controlled variables. The remaining variables, F_f and C_{Af} are the known variables for the feed conditions which are assigned as disturbances. Then, the important $\mathbf{u}$ and $\mathbf{y}$ are selected with respect to the multi-objective function, Eq. (3.76), and shown in bold in Table 3.4. Design variable $\mathbf{u}_d = [V_r]$ is selected since V_r is directly related to the capital cost and manipulated variable $\mathbf{u}_m = [F]$ is selected since it is the potential candidate for the manipulated variable. Process-controlled variables $\mathbf{y}_m = [C_A, C_B, h_r]$, on the other hand, are selected since they are the important variables that need to be monitored and controlled in order to obtain the smooth, operable and controllable process.

Table 3.4
List of all design and manipulated variables, process-controlled variables and disturbances for a conceptual single reactor design. The important design and manipulated variables and process-controlled variables are shown in bold.

Design variable ($\mathbf{u}_d$)	$\mathbf{V_r}$
Manipulated variable ($\mathbf{u}_m$)	$\mathbf{F}$
Process-Controlled variables ($\mathbf{y}$)	$\mathbf{C_A}$, $\mathbf{C_B}$, C_C, $\mathbf{h_r}$
Disturbances ($\mathbf{d}$)	F_f, C_{Af}

Step 1.2: Operational window identification

The operational window is identified based on real reactor volume V_r. For a single reactor, its real volume should satisfy the constraints as defined in Eqs. (3.84)-(3.85). Therefore, for a single reactor design, the operational window (feasible solutions) within which the optimal solution is likely to exist is within the range of $3 \leq V_r$ (m^3) $\leq$ 30.

Step 1.3: Design-control target identification

For a reactor design, the attainable region diagram is drawn and the location of the maximum in the attainable region is selected as the reactor design target. This point gives the highest selectivity of the reaction product with respect to the limiting reactant. The attainable region is drawn from the feed points using Eq. (3.18). Solving Eq. (3.18) for specified values of reactant C_A with $C_{Af} = 1.00$ kmol/m^3, values for C_B are calculated. Then, the attainable region is created by plotting the concentration of C_B with respect to the concentration of C_A as shown in Fig. 3.11. The location of the maximum point at the attainable region diagram (Point A) is selected as the reactor design target. It can easily be seen from Fig. 3.11 that a maximum of 0.4665 kmol/m^3

of C_B can be achieved using a *CSTR*, with 0.26 kmol/m^3 of C_A in the outflow. Note that, in Fig. 3.11, two other points which are not at the maximum are identified as candidate alternative designs for a reactor which will be used for verification purposes in Stage 4.

Stage 2: Design analysis

The objective of this stage is to validate the target identified in Stage 1 by finding the acceptable values (candidates) of **y** and **u**. In this stage, the search space defined in Stage 1 is further reduced.

Step 2.1: Design-manipulated and process-controlled variables value calculation

The established targets (Points A, B, C) in Fig. 3.11 are now matched by finding the acceptable values (candidates) of the design-manipulated and process-controlled variables. If feasible values cannot be obtained or the values are lying outside of the operational window, a new target is then selected and values of variables are recalculated until a satisfactory match is obtained. The acceptable values (candidates) of design-manipulated and process-controlled variables are calculated using the steady state process model of Eqs. (3.77)-(3.80) with the constitutive models of Eqs. (3.81)-(3.83). The results are given in Table 3.5.

Table 3.5
Values of residence time with the corresponding process-controlled and design-manipulated variables at different reactor designs for a conceptual single reactor design.

Reactor Design	Residence time (τ) (h)	Process-Controlled (**y**)			Manipulated	Design
		C_A (kmol/m^3)	C_B (kmol/m^3)	h_r (m)	F (m^3/h)	V_r (m^3)
A	0.59	0.26	0.4665	0.616	10.0	5.86
B	1.29	0.10	0.4411	0.800	10.0	12.86
C	0.36	0.40	0.3936	0.523	10.0	3.60

From Table 3.5, it can be seen that values of reactor volume V_r and reactor outlet flowrate F can be obtained for these three candidate reactor designs. Clearly, reactor design A has the highest desired product concentration C_B followed by reactor designs B and C. However, in terms of capital cost, reactor design C has the lowest cost since it has the smallest volume followed by reactor designs A and B. In order to find the best design, the value of a multi-objective function is calculated in the verification stage (see Stage 4). It is important to note here that, the steady state value obtained in this stage becomes an initial value for studying process dynamic in the next stage.

Stage 3: Controller design analysis

The objective of this stage is to evaluate and validate the controllability performance of the feasible candidates in terms of their sensitivities with respect to disturbances and manipulated variables.

Step 3.1: Sensitivity analysis

The process sensitivity is analyzed by calculating the derivative values of the controlled variables with respect to disturbances $d\mathbf{y}/d\mathbf{d}$ with a constant step size using the dynamic process models of Eqs. (3.76)-(3.80) with the constitutive models of Eqs. (3.81)-(3.83). In this case, C_B is the desired product concentration which needs to be maintained at its optimal value (set-point) while F_f and C_{Af} are the potential sources of disturbances in the reactor feed. Fig. 3.11 shows plots of the derivative of C_B with respect to C_A. It can be seen that the derivative value of dC_B/dC_A is smaller for a reactor design A compared to other designs (B and C). According to Eq. (3.33b), at the maximum of the attainable region (Point A), the derivative values of dC_A/dF_f and dC_A/dC_{Af} are smaller since dC_B/dC_A is smaller. Derivative values of dC_A/dF_f and dC_A/dC_{Af} are calculated for all reactor designs and tabulated in Table 3.6. From Table 3.6, it can clearly be seen that derivative values of dC_A/dF_f and dC_A/dC_{Af} are smaller for a reactor design A than other designs. Smaller values of dC_B/dF_f and dC_B/dC_{Af} mean that the desired product concentration C_B is less sensitive to the changes in F_f and C_{Af}. In this case, a reactor design A will be more flexible to the changes in F_f and C_{Af} than reactor designs B and C. Therefore, from a process control point of view, reactor design A is less sensitive to the effect of disturbances which makes it more robust in maintaining its controlled variable despite disturbances. This will be verified in Stage 4.

Table 3.6
Derivatives values of C_B with respect to C_{Af} and F_f at different reactor designs for a conceptual single reactor design.

Reactor Design	Derivative	
	dC_B/dC_{Af}	dC_B/dF_f
A	0.0400	0.0001
B	1.0564	0.0327
C	0.3679	0.0067

Step 3.2: Controller structure selection

Next, the controller structure is selected by calculating the derivative values of controlled variables with respect to the manipulated variable with a constant step size by using the dynamic process models of Eqs. (3.77)-(3.80) with the constitutive models of Eqs. (3.81)-(3.83). The objective of this step is to select the best controller structure (pairing of controlled-manipulated variables) which can satisfy the control objective (maintaining desired product concentration C_B at its optimal set point in the presence of disturbances). From Eq. (3.44), it is possible to maintain C_B at its optimal

set point using concentration control of component A (see Eq. (3.44a)) or using reactor level control (see Eq. (3.44b)). Fig. 3.16 shows plots of derivative of controlled variables C_A and h_r with respect to manipulated variable F, and values of derivatives at different reactor designs are given in Table 3.7.

It can be seen that values of dh_r/dF are higher compared to values of dC_A/dF for all reactor designs. Therefore, it can be clearly seen from Fig. 3.16 and Table 3.7, that the best pairing of controlled-manipulated variable that will able to maintain the desired product concentration C_B at its optimal set point value in the presence of disturbances is h_r-F. This controller structure will show better controllability in maintaining C_B at its optimal set point value at reactor design A compared to other designs which will be verified in Stage 4.
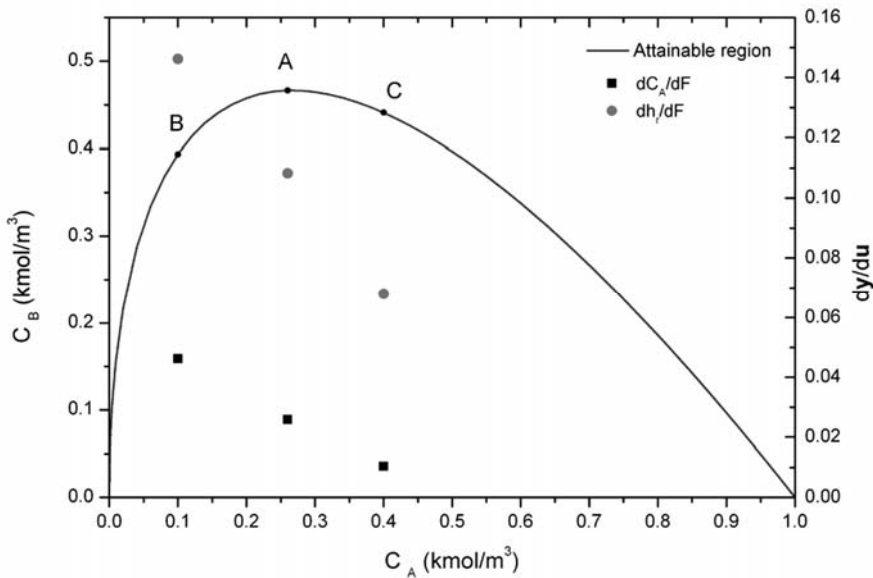
Fig. 3.16. Attainable region diagram for the desired product concentration C_B with respect to reactant C_A, and its corresponding derivatives of the C_A and h_r with respect to manipulated variable F, for a conceptual single reactor design.

Table 3.7
Derivatives values of C_A and h_r with respect to manipulated variable F at different reactor designs for a conceptual single reactor design.

Reactor Design	Derivative	
	dC_A/dF	dh_r/dF
A	0.0175	0.1050
B	0.0391	0.1453
C	0.0011	0.0622

Stage 4: Final selection and verification

The objective of this stage is to select the best candidates by analyzing the value of the multi-objective function, Eq. (3.67).

Step 4.1: Final selection: Verification of design

The value of the multi-objective function, Eq. (3.76) is calculated by summing up each term of the objective function value. In this case, all the objective function terms are weighted equally meaning that the decision-maker does not have any preference for one objective over another. Since the range and unit of each objective function values can be different, an appropriate scaling of each objective function is needed. To this end, each objective value is normalized with respect to its maximum value. Details are given in Table 3.8. $P_{1,1s}$ corresponds to the scaled value of the desired product concentration C_B. $P_{2,1s}$ and $P_{2,2s}$ are scaled values of dC_B/dF_f and dh_r/dF representing the sensitivity of desired product concentration C_B with respect to the disturbance F_f and the sensitivity of the controlled variable h_r with respect to the manipulated variable F, respectively. Whereas, $P_{3,1s}$ is the scaled value of the reactor volume which represents the capital cost. It can be seen that the value of the multi-objective function J for the reactor design A is higher than other designs. Therefore, it is verified that, reactor design A is the optimal solution for the integrated process design and controller design of a conceptual single reactor design problem which satisfies design, control and cost criteria. It should be noted that a qualitative analysis (J highest for point A) is sufficient for the purpose of controller structure selection.

Table 3.8
Multi-objective function calculation. The best candidate is highlighted in bold.

Reactor Design	$P_{1,1}$	$P_{2,1}$	$P_{2,2}$	$P_{3,1}$	
A	0.4665	0.0001	0.1050	5.86	
B	0.3936	0.0067	0.1453	12.86	
C	0.4411	0.0327	0.0622	3.60	
	$P_{1,1s}$	$P_{2,1s}$	$P_{2,2s}$	$P_{3,1s}$	J
A	1.000	0.003	0.723	0.456	**331.01**
B	0.844	0.204	1.000	1.000	7.75
C	0.946	1.000	0.428	0.280	5.95

Step 4.2: Dynamic rigorous simulations: verification of controller performance

In order to further verify the controller structure performances, two closed loop tests are performed; (1) regulator (disturbance rejection) problem, and (2) servo (setpoint tracking) problem using a PI-controller for all designs (Points A, B and C). The value of controller tuning parameters for all designs was calculated using the same standard tuning rules, which in this case is the Ziegler-Nichols tuning method.

In the regulator problem, the closed loop performance in terms of its ability to reject disturbance and to keep C_B at its desired value are verified. To this end, ±10% step changes are applied to the feed flowrate F_f which move the reactor level away from its set points (Points A, B and C). Figs. 3.17-3.19 show the dynamic response of C_B, h_r and F, respectively, when ±10% step changes are applied to the feed flowrate F_f at Points A, B and C. One observes that the effect of the disturbance on C_B is almost negligible at point A, whereas for points B and C are quite significant (see Fig. 3.17) even though the controllers are able to maintain h_r at its desired set points for all reactor designs (Points A, B, C) (see Fig. 3.18). This means that, the process sensitivity at Point A with respect to disturbance F_f is lower than for any other points. As a result, point A offers better robustness (in terms of disturbance rejection) in maintaining its desired product concentration C_B against disturbance. Therefore, it can be verified (albeit empirically) that, designing a reactor at the maximum points of the attainable region leads to a process with lower sensitivity with respect to disturbance.
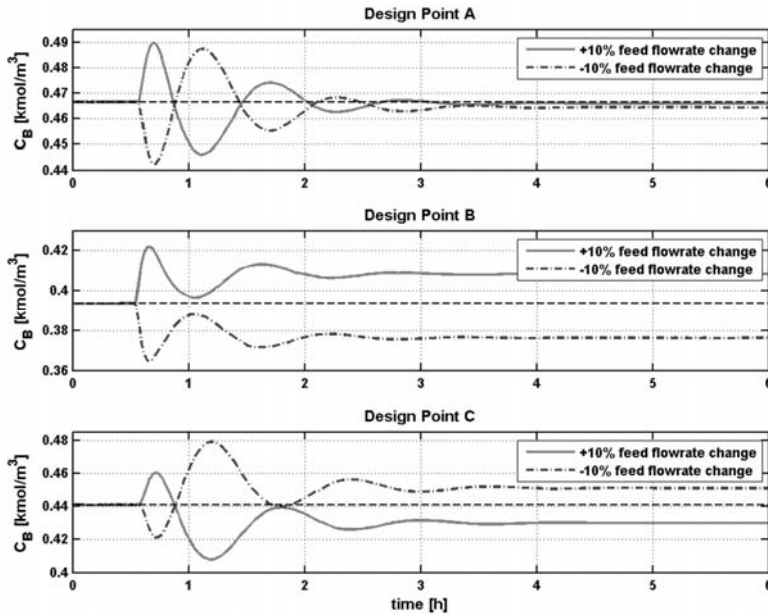
Fig. 3.17. Regulator problem - Dynamic responses of the desired product concentration C_B to ±10% step changes in feed flowrate F_f for different alternative reactor designs.
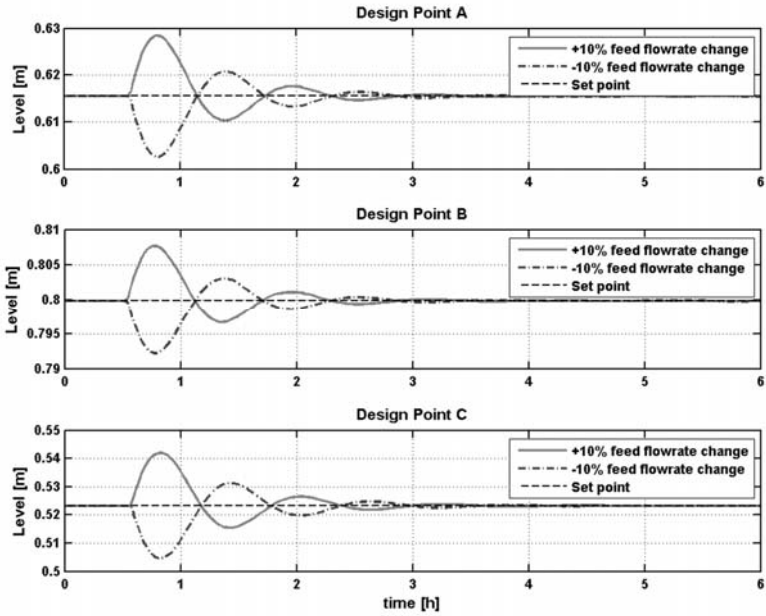
Fig. 3.18. Regulator problem - Closed loop responses of the controlled variable h_r to ±10% step changes in feed flowrate F_f for different alternative reactor designs.
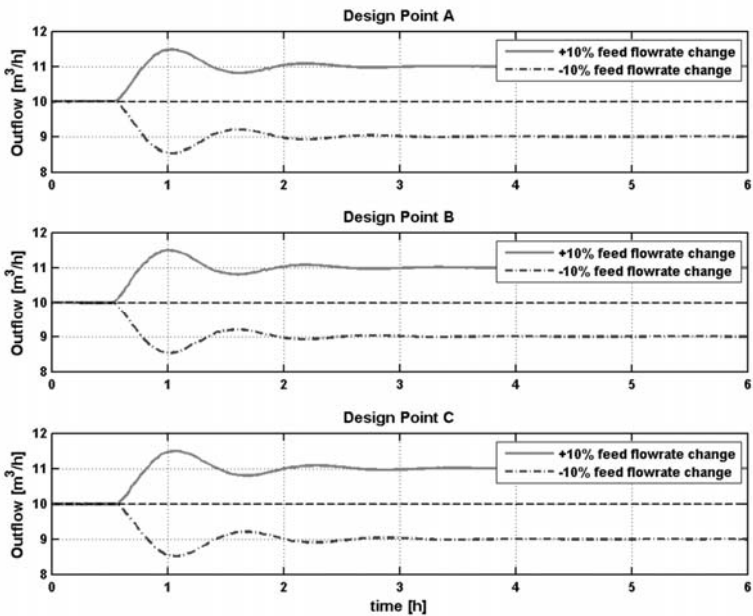
Fig. 3.19. Regulator problem - Dynamic responses of the manipulated variable F to ±10% step changes in feed flowrate F_f for different alternative reactor designs.

In the servo problem, the controller structure performance in terms of its ability to keep tracking the set point changes is verified. To this end, ±10% step changes are applied to the set points of the reactor level h_r (points A, B and C). The dynamic response of C_B, h_r and F are shown in Figs. 3.20-3.22. It can be clearly seen that the controllers (Points A, B and C) successfully managed to follow the changes applied to their set point values (see Fig. 3.21). However, significant changes are observed in the C_B responses for Points B and C, whereas, at Point A changes are negligible (see Fig. 3.20). This means that, process flexibility at Point A is higher than other points. At Point A, the process is able to maintain C_B at its desired value even the set point of h_r is changed compared to Points B and C. Therefore, it can be verified that, designing a reactor at the maximum point of the attainable region leads to a process with higher flexibility.
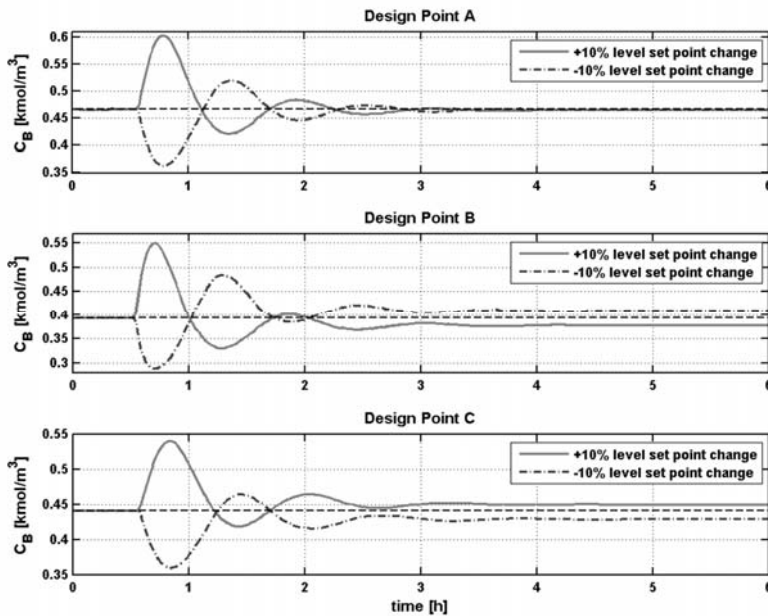
Fig. 3.20. Servo problem - Dynamic responses of the desired product concentration C_B to ±10% step changes in the set point of h_r for different alternative reactor designs.
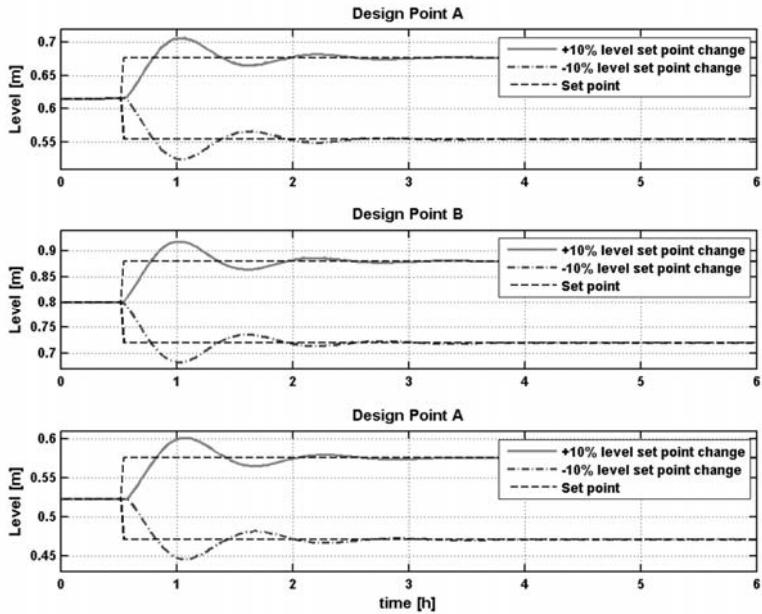
Fig. 3.21. Servo problem - Closed loop responses of the controlled variable h_r to ±10% step changes in the set point of h_r for different alternative reactor designs.
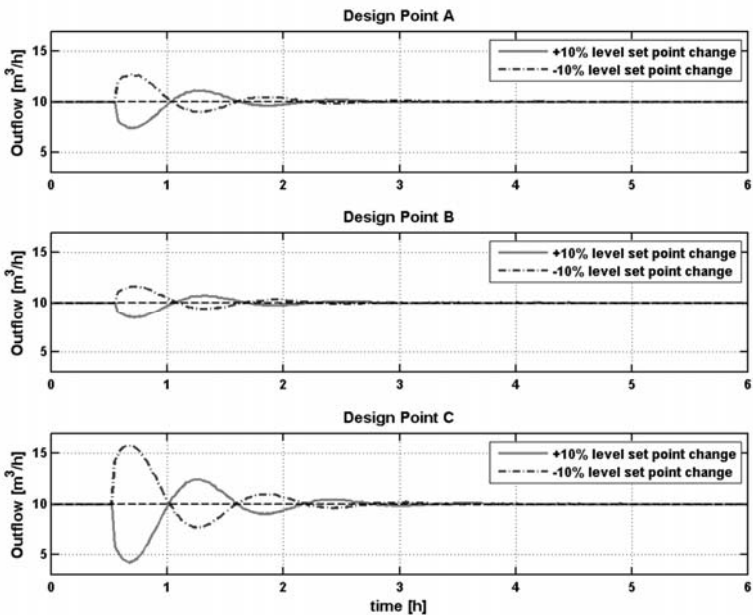
Fig. 3.22. Servo problem - Dynamic responses of the manipulated variable F to ±10% step changes in the set point of h_r for different alternative reactor designs.

As a summary, the results of this simple example illustrate the capability of the proposed *IPDC* methodology to obtain the optimal process-controller design solution of a conceptual single reactor design that satisfies design, control and economic criteria. It was also confirmed that design of a reactor at the maximum point of the attainable region leads to a process with lower sensitivity with respect to disturbances and higher flexibility.

3.5   Conclusion

A generic methodology for the *IPDC* problem of chemical processes has been presented. The proposed methodology is simple to apply, easy to visualize and efficient to solve. Here, the *IPDC* problem is solved by the so-called reverse approach by decomposing it into four sequential hierarchical sub-problems: (i) pre-analysis, (ii) design analysis, (iii) controller design analysis, and (iv) final selection and verification. Using thermodynamic and process insights, a bounded search space is first identified. This feasible solution space is further reduced to satisfy the process design and controller design constraints in sub-problems 2 and 3, respectively, until in the final sub-problem all feasible candidates are ordered according to the defined performance criteria (objective function). The final selected design is verified through rigorous simulation. In the pre-analysis sub-problem, the concepts of the attainable region and driving force are used to locate the optimal design-control solution in terms of optimal conditions of operation from design and control viewpoints. While other optimization methods may or may not be able to find the optimal solution, depending on the performance of their search algorithms and computational demand, the use of the attainable region and the driving force concepts is simple and able to find at least near-optimal designs (if not optimal) to *IPDC* problems. The capability of this methodology is highlighted with a simple conceptual example of a single reactor design.

CHAPTER 4

ICAS-IPDC:

A Software for Model-Based Integrated Process Design and Controller Design of Chemical Processes

A software called *ICAS-IPDC* has been developed in which the new methodology for integrated process design and controller design (*IPDC*) presented in chapter 3 is implemented. The purpose of the software is to support engineers in solving process design and controller design problems in a systematic and efficient way following the methodology presented in chapter 3. In this chapter, first the overview of the software is given in section 4.1 followed by presentation and discussion of the software framework (section 4.2) and the software implementation (section 4.3). The additional features of the software are presented in section 4.4. At the end of this chapter, general conclusions are presented (section 4.5).

4.1   *ICAS-IPDC* Overview

The developed framework for the integrated process design and controller design (*IPDC*) of chemical processes has been implemented into an Excel-based software called *ICAS-IPDC*. It is called *ICAS-IPDC* since it is part of the *ICAS* (Integrated Computer Aided System) software developed at the Computer Aided Process-Product Engineering Center (*CAPEC*), Technical University of Denmark.

A *Start Menu* (see Fig. 4.1) has been created to be the starting User Interface (*UI*) of the software. It can be seen in Fig. 4.1 that the starting point for the software is either to select an already solved case study from which the user will understand different steps or to create a new case study for three different systems; i) a single reactor (*R*) system, ii) a single separator (*S*) system, and iii) a reactor-separator-recycle (*RSR*) system by clicking on the system button. For example, by clicking on a single reactor button, a pop-up menu appears asking the user to choose either to click "Yes" to open a solved case study, or to click "No" to create a new case study. There are also three info buttons located at the left side of the *Start Menu UI*, which are "Software Overview", "User's Manual", and "Tutorials". A "Software Overview" button will show the software framework as shown in Fig. 4.2. This framework, which is based on the developed methodology presented in the previous chapter, illustrates the step-by-step algorithm that has been implemented into this software. The "User's Manual" button will describe the details of each implemented step, whereas the "Tutorials" button will guide the user to understand/apply the software through a solved case study.
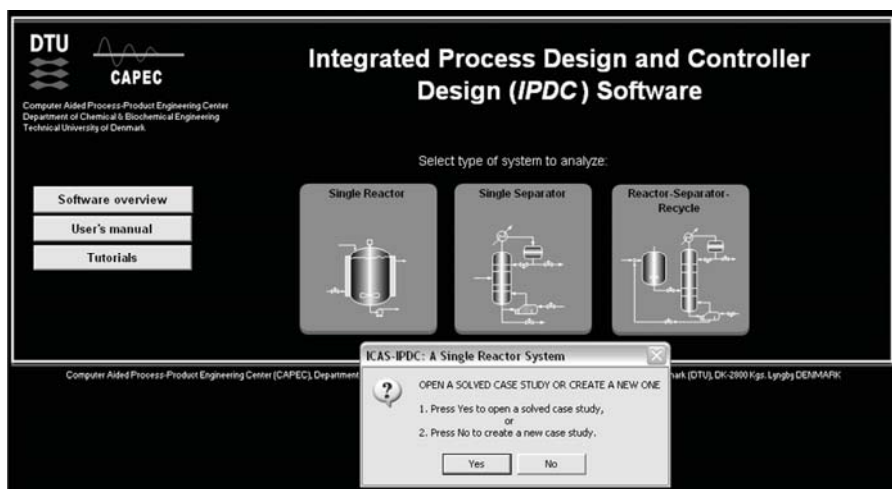
Fig. 4.1. A Start Menu User Interface (*UI*) of the *ICAS-IPDC* software.

4.2 *ICAS-IPDC* Framework

4.2.1 Software Framework Overview

Fig. 4.2 shows the framework overview of the *ICAS-IPDC* software. Once the option either to open/create a case study has been selected from the pop-up view, the user will be guided to the step-by-step algorithm (from step 1 until step 6.2) sequentially. First, the user will define the problem by completing steps 1 and 2. Step 1 is where the user will select components involved in the process. After all components have been selected, the user will then define reactants and products for a reactor system and define top and bottom products for a separator system. Step 2 is where the user will define the feed conditions of the system.

Once the problem has been defined, the user will perform step 3 which consists of three sub-steps: Step 3.1 – Variables analysis, Step 3.2 – Operational window identification, and Step 3.3 – Design-control solution target identification. The objective of this step is to define the operational window and set the targets for the design-control solution. In step 3.1, the user will analyze all variables and classify them as design-manipulated variables, process-controlled variables or disturbances. Then, based on the multi-objective functions, the important variables are short-listed by the software. In step 3.2, the operational window will be identified. Here, the user will define the operational window in terms of process-controlled and design-manipulated variables. Then, design-control solution targets are identified in step 3.3. The software will draw the attainable region (for a reactor design problem) and/or driving force (for a separator design problem) diagrams, and identify design-control targets by locating the maximum points on the attainable region and driving force diagrams.

Targets identified in step 3 will be validated in step 4 by finding acceptable values of design-manipulated and process-controlled variables. If the acceptable values (candidates) cannot be obtained or the values are lying outside the operational window, a new target is selected in step 3.3 and values are recalculated until a satisfactory match is obtained. For a reactor design, values of design-manipulated (reactor volume, reactor outlet flowrate, cooling water flowrate) and process-controlled (reactor temperature, concentrations, pressure) variables that match the target are calculated. For a separator design, values of design variables (feed stage, reflux ratio, reboil ratio) that match the target are calculated. Then values of other design-manipulated (reflux flow, vapor boilup, reboiler and condenser duties) and process-controlled (top and bottom compositions, top and bottom temperature) variables are obtained using the steady state process model.

In step 5, the feasible values (candidates) of design-manipulated and process-controlled variables are evaluated and validated in terms of controllability performances. Two criteria are analyzed: sensitivity of controlled variable with respect to disturbances (in step 5.1) and sensitivity of controlled variables with respect to manipulated variables (in step 5.2). In step 5.2 also, the best pair of controlled-manipulated variables is selected. Finally, in step 6, the best values (candidates) are

selected by analyzing the value of the multi-objective function in step 6.1. The best candidate is then verified using rigorous simulations in step 6.2.

INTEGRATED PROCESS DESIGN AND CONTROLLER DESIGN (IPDC) SOFTWARE FRAMEWORK

MENU:
Select Solved Case Study or Create New
- Single Reactor (R) System
- Single Separator (S) System
- Reactor-Separator-Recycle (RSR) System

1. Problem definition

1.1 **Components selection:**
- Select components
  - ✓ Define reactants and limiting reactant
  - ✓ Define products and desired product

1.2 **For reactor:**
- Select type of reactor
- Select type of reaction
- Define the reaction kinetics

1.3 **For separator:**
- Select type of separator
- Define the relative volatilities
- Define the product purity

$$\max \quad J = \sum_{i=1}^{m}\sum_{j=1}^{s} w_j P_{ij} \qquad (1)$$

subjected to:
Process (dynamic and/or steady state) constraints
$$\frac{d\mathbf{x}}{dt} = f(\mathbf{x}, \mathbf{y}, \mathbf{u}, \mathbf{d}, \boldsymbol{\theta}, Y, t) \qquad (2)$$
Constitutive (thermodynamic) constraints
$$0 = g_1(\mathbf{v}, \mathbf{x}, \mathbf{y}) - \boldsymbol{\theta} \qquad (3)$$
Conditional (process-control) constraints
$$0 = h_1(\mathbf{u}, \mathbf{x}, \mathbf{y}) \qquad (4)$$
$$0 \le h_2(\mathbf{u}, \mathbf{x}, \mathbf{y}, \mathbf{d}) \qquad (5)$$
$$CS = \mathbf{y} + \mathbf{u}^Y \qquad (6)$$

2. Feed and initial conditions definition
- Feed conditions: F, T, P, C_i or z_i
- Initial conditions for dynamic: x_0

		TOOLS USED
STAGE 1: PRE-ANALYSIS		
3.1 Variables analysis	Shortlisted of important y and u	
Eqs. (4) and (5) — 3.2 Operational window identification	$y_{min} \le y \le y_{max}$ $u_{min} \le u \le u_{max}$	
Eq. (3) — 3.3 Design-control solution target identification	AR and DF diagrams	ICAS-MoT / MoT Excel Interface
STAGE 2: DESIGN ANALYSIS		
Eq. (2) in steady state and Eq. (3) — 4 Design (u) and process (y) values calculation	Acceptable value of y and u	ICAS-MoT / MoT Excel Interface

NO — Values found?

NO — Within operational window?

STAGE 3: CONTROLLER DESIGN ANALYSIS		
Eqs. (2) and (3) — 5.1 Sensitivity analysis	dy/dd plots	ICAS-MoT / MoT Excel Interface
Eqs. (2), (3) and (6) — 5.2 Controller structure selection	dy/du plots	ICAS-MoT / MoT Excel Interface
STAGE 4: FINAL SELECTION AND VERIFICATION		
Eq. (1) — 6.1 Multi-objective function calculation	Optimal value of J	
Eqs. (2) - (5) For closed loop: add control law equation — 6.2 Dynamic rigorous simulations	Open and closed loop plots	ICAS-MoT / MoT Excel Interface

Automatically create and store a report of all steps conducted, equations and results

Fig. 4.2. Implementation of the *IPDC* framework into *ICAS-IPDC* software.

4.2.2 Integration of *ICAS-MoT* with the Software

It is important to mention here that, all models used in this software are developed/simulated using *ICAS-MoT* (Sales-Cruz, 2006). *MoT* models simulated using *ICAS-MoT* are integrated with the *ICAS-IPDC* interface using the *MoT* Model Interface as illustrated in Fig. 4.3. The *MoT* Model Interface is an Excel-based interface which is integrated with the *MoT* solver by using a COM object, as well as connected with the *MoT* model.
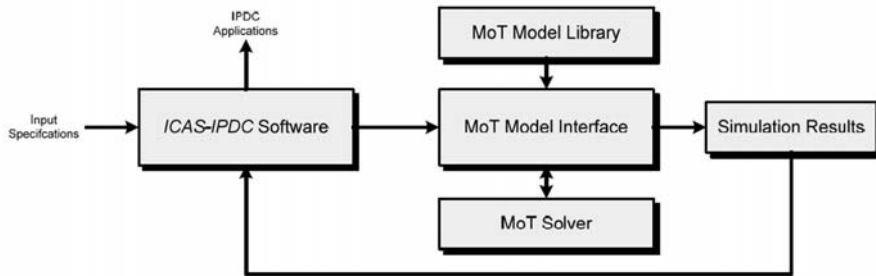
Fig. 4.3. Workflow of the integration of the *ICAS-IPDC* interface with the *MoT* models through *MoT* Model interface.

ICAS-MoT employs a flexible equation-oriented approach. It has been designed to deal effectively with a much wider range of applications, including those with combined discrete and continuous systems, as well as, lumped and distributed parameter systems. It can also perform dynamic optimization, sensitivity analysis and generate statistical reports. Fig. 4.4 shows all the *ICAS-MoT* options available that can be chosen depending on the type of modeling problem that has to be solved. The options include several tools to handle and solve a wide range of problem formulations involving algebraic equations (*AEs*), ordinary differential equations (*ODEs*), differential algebraic equations (*DAEs*), partial differential equations (*PDEs*) and optimization problems. Regarding the model export options, two different modes are available: (a) as a COM-Object that can be used in external applications such as Excel, Virtual C++, Virtual Basic, or Fortran, and (b) as an ICASsim unit process to be incorporated into the ICASsim unit library and used to customize a simulator in steady state or dynamic mode.
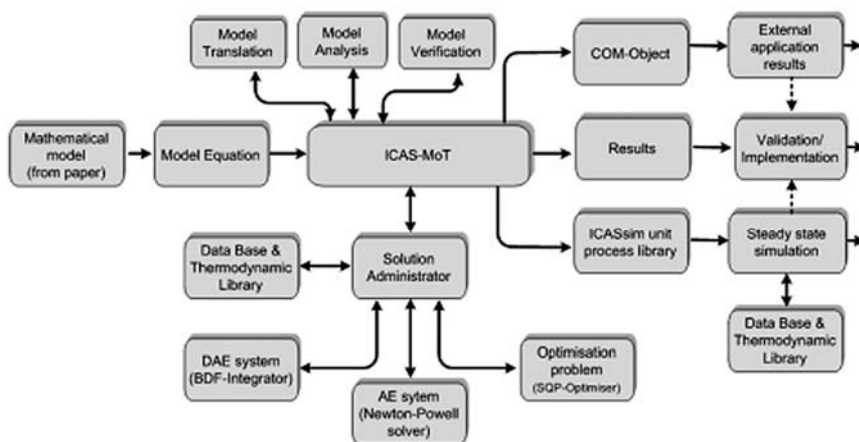
Fig. 4.4. *ICAS-MoT* available options (adapted from Sales-Cruz, 2006).

4.3   *ICAS-IPDC* Implementation

4.3.1   Start of *ICAS-IPDC*

The "Main Menu" of the software is shown in Fig. 4.5 for a single reactor system. The "Main Menu" performs all steps that have been outlined in Fig. 4.2. The "Main Menu" is divided into five sequential parts: Part I – Problem definition, Part II – Pre-analysis stage, Part III – Design analysis stage, Part IV – Controller design analysis stage and Part V – Final selection and verification following the main stages of the methodology (see chapter 3). In order to solve an *IPDC* problem, the user needs to perform all parts sequentially. The built-in color code system together with the conditional logic (if-then rule) guides the user through the different steps.

4.3.2   Part I: Problem Definition

Step 1.1 Problem Definition

The software requires the user to complete Part I first, where the user will be asked to supply some information about the system to be analyzed which can be a single reactor, a single separator or a reactor-separator-recycle system. A "Problem Definition" interface for a single reactor system is shown in Fig. 4.6. There are two frames in the "Problem Definition" interface, which are the "Problem Definition" and the "Process Flow Diagram". The "Problem Definition" frame is where the user will perform selection of components, reactants and products (for a single reactor system) or selection of components, top products and bottom products (for a single separator

system). It can be seen that for a single reactor system, only three buttons which relate to a reactor are active (see fig. 4.6). The second frame is called "Process Flow Diagram" in which the process flow diagram of the analyzed system is shown. In Fig. 4.6, the process flow diagram of a single reactor system is shown.
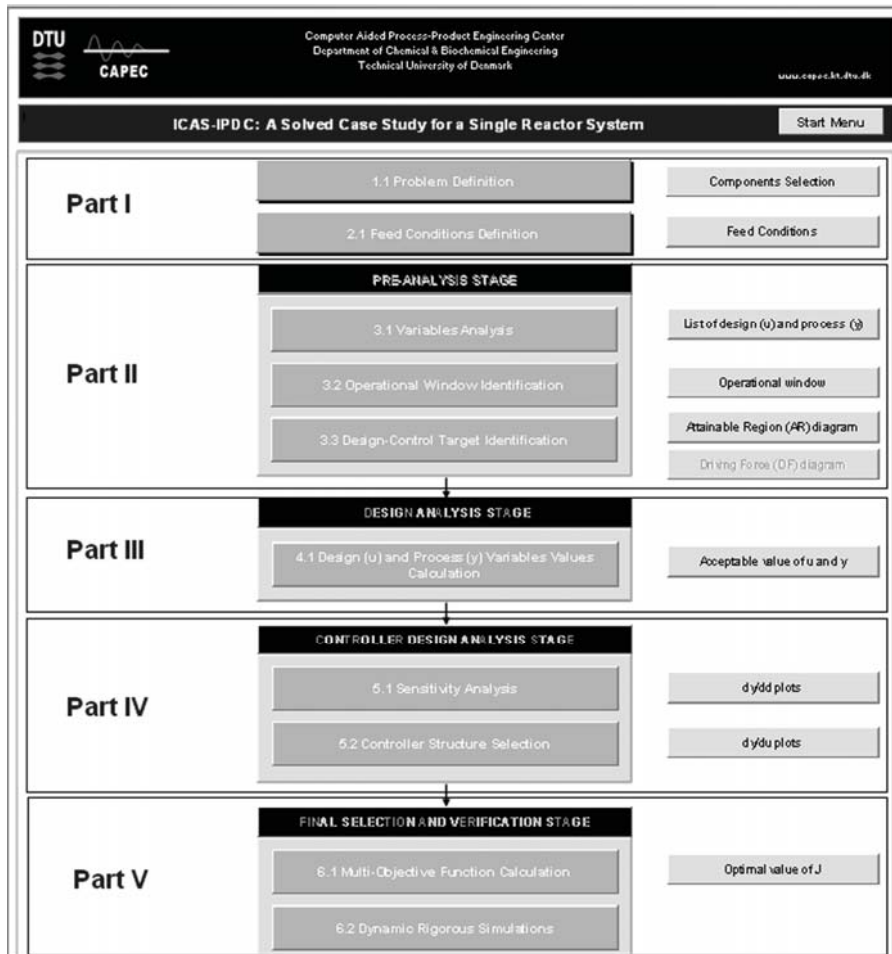
Fig. 4.5. A Main Menu user interface of the *ICAS-IPDC* for a single reactor system.
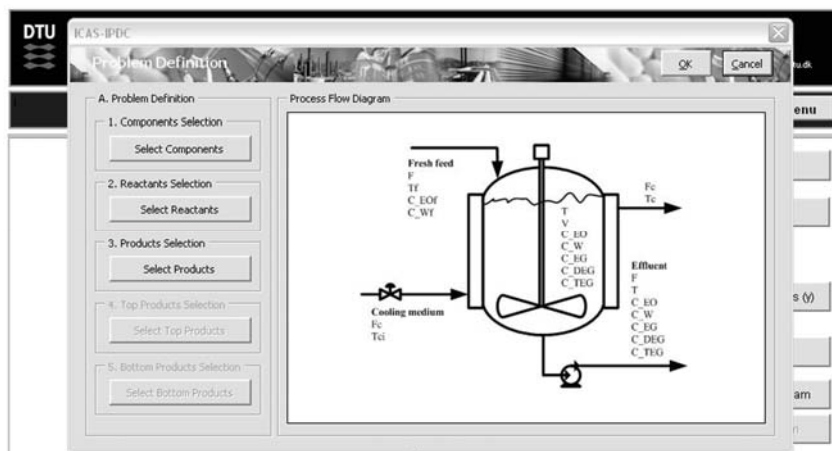
Fig. 4.6. Problem definition user interface for a single reactor system.

Step 2.1 Feed Conditions Definition

A "Feed Conditions Definition" interface is shown in Fig. 4.7. Here the user will define the values of feed conditions.
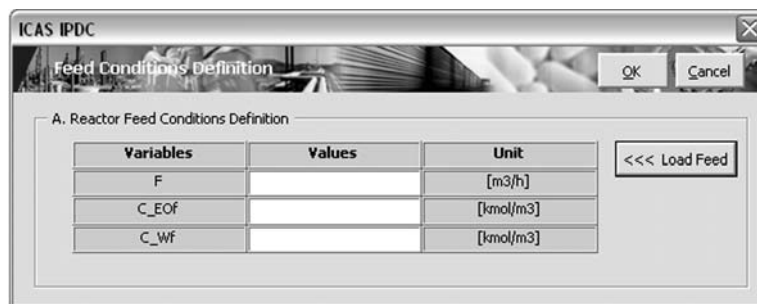
Fig. 4.7. Feed Conditions Definition interface for a single reactor system.

4.3.3   Part II: Pre-analysis Stage

This part consists of three steps: Step 3.1 Variables Analysis, Step 3.2 Operational Window Identification, and Step 3.3 Design-Control Target Identification.

Step 3.1 Variables Analysis

A "Variables Analysis" interface is shown in Fig. 4.8. In this interface, the user will select design-manipulated variables, process-controlled variables and disturbances.
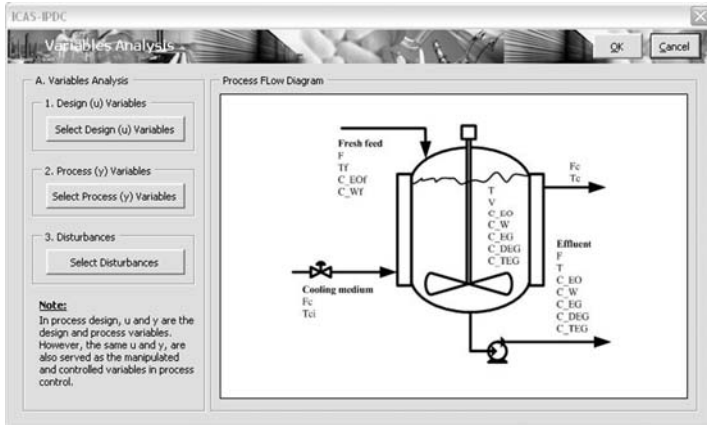
Fig. 4.8. Variables Analysis interface for a single reactor system.

Step 3.2   Operational Window Identification

The second step in the Part II is to identify the operational window. An "Operational Window Identification" interface is shown in Fig. 4.9. In this interface, users are required to define the operational window in terms of design and process variables. For example, the operational window for reactor volume is defined within $3 - 30$ m^3. On the other hand, the operational window for temperature is defined in the range of $273 - 343$ K. The temperature range is defined between the minimum melting point and maximum boiling point of components.
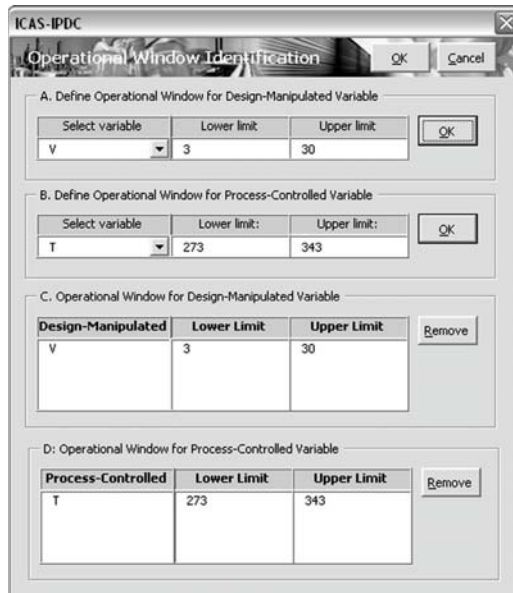
Fig. 4.9. Operational Window Identification interface.

Step 3.3   Design-Control Target Identification

The main objective of this step is to develop the attainable region and driving force diagrams and then to select the design targets at the maximum point of the attainable region and driving force. A "Design-Control Target Identification" interface is shown in Fig. 4.10. For a single reactor system, there are three major sub-steps that need to be performed, i) *MoT* Model Setup, ii) *AR* Calculation Setup, and iii) *AR* Diagram Setup. Fig. 3.10 shows the attainable region diagram with three design alternatives.

Fig. 4.10. Design-Control Target Identification interface for a single reactor system.
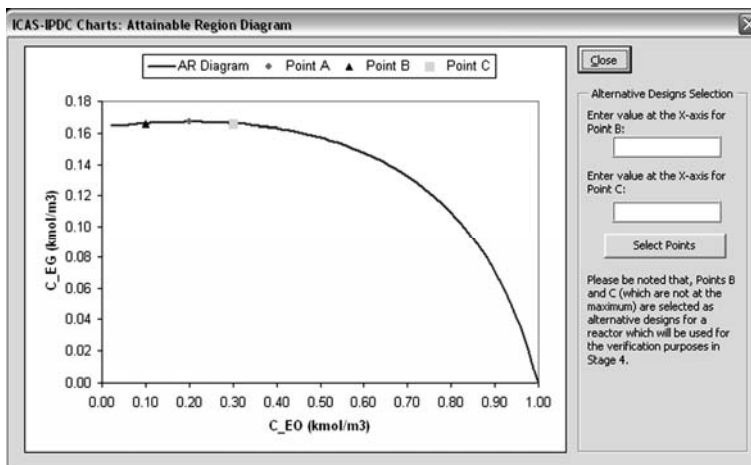
Fig. 4.11. Attainable region diagram with three design alternatives.

4.3.4 Part III: Design Analysis Stage

Step 4.1 Design (u) and Process (y) Variables Values Calculation

A "Design-Process Values Calculation" interface for a single reactor system is shown in Fig. 4.12. Here, users will calculate values of design-process variables at the target identified in the previous stage. There are two main sub-steps in this stage (see Fig. 4.12). The first sub-step is to calculate the reactor volume and the second sub-step is to calculate other design variables.
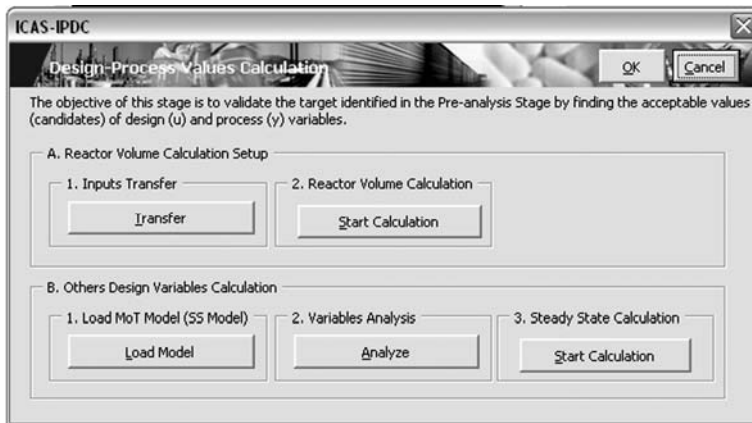
Fig. 4.12. Design-Process Values Calculation interface for a single reactor system.

4.3.5 Part IV: Controller Design Analysis Stage

Part IV of the software consists of two important sub-steps: Step 5.1 Sensitivity Analysis and Step 5.2 Controller Structure Selection.

Step 5.1 Sensitivity Analysis

A "Sensitivity Analysis" interface is shown in Fig. 4.13. Here, the user will load the dynamic process model into the *MoT* Model Interface and then calculate the derivative of controlled variables with respect to disturbances.
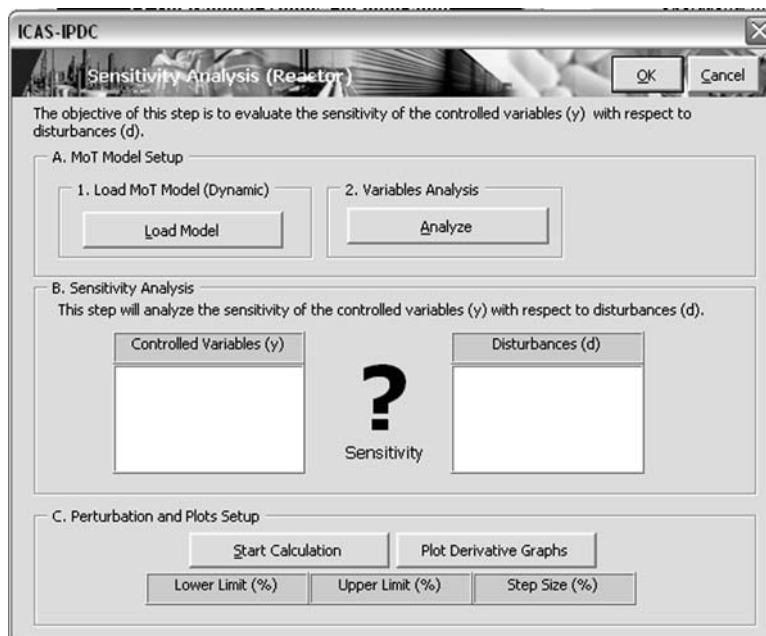
Fig. 4.13. Sensitivity Analysis interface for a single reactor system.

Step 5.2   Controller Structure Selection

A "Controller Structure Selection" interface is shown in Fig. 4.14. In this interface, the user needs to load the dynamic process model into the *MoT* Model Interface. Then, the user will calculate the derivative value of controlled variables with respect to manipulated variables. The user will also identify the best pair of controlled-manipulated variables for controller structure selection.

4.3.6   Part V: Final Selection and Verification Stage

6.1   Multi-Objective Function Calculation

A "Multi-Objective Function Calculation" interface where the user will select the optimal design solution by analyzing the value of the multi-objective function is shown in Fig. 4.15.
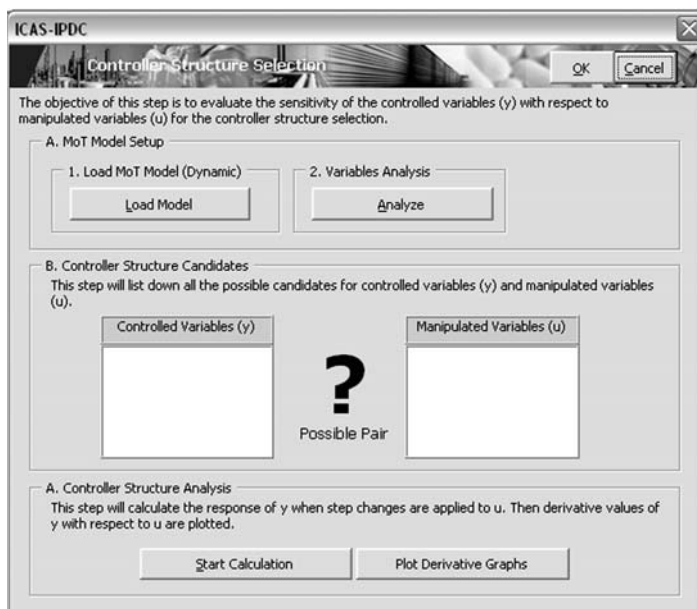
Fig. 4.14. Controller Structure Selection interface for a single reactor system.
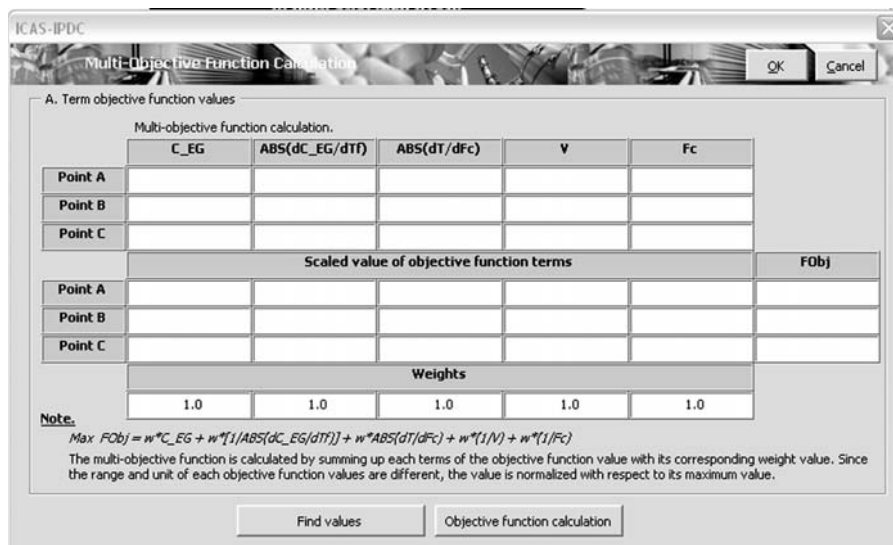
Fig. 4.15. Multi-Objective Function Calculation interface for a single reactor system.

6.2 Dynamic Rigorous Simulations

A "Rigorous Dynamic Simulations" interface is shown in Fig. 4.16. In this interface, there are two options of dynamic simulation for controller structure verification which are open and closed loop dynamic simulations. Fig. 4.17 shows the interface for an open loop dynamic simulation. In the open loop simulation, the user needs to load an open loop model and then set the step change to the disturbance to study the effect of the disturbance on the process especially the controlled variable.
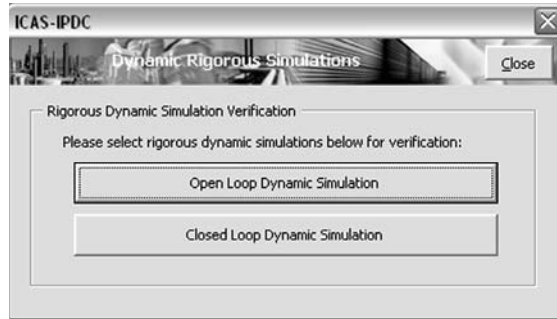
Fig. 4.16. Dynamic Rigorous Simulations interface.

For closed loop simulations, two important steps need to be performed. First, to perform the controller tuning and then the closed loop simulation. The controller tuning interface is shown in Fig. 4.18. Here, the user needs to load an open loop model and then set the step change to the manipulated variable. The first order plus time delay (*FOPTD*) model is calculated and then used to calculate the tuning parameters using the Cohen-Coon tuning method for a PI-controller.
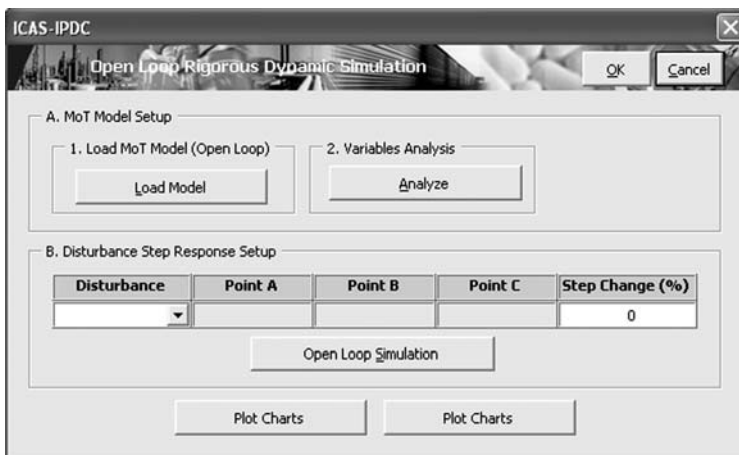
Fig. 4.17. Dynamic open loop rigorous simulations interface.
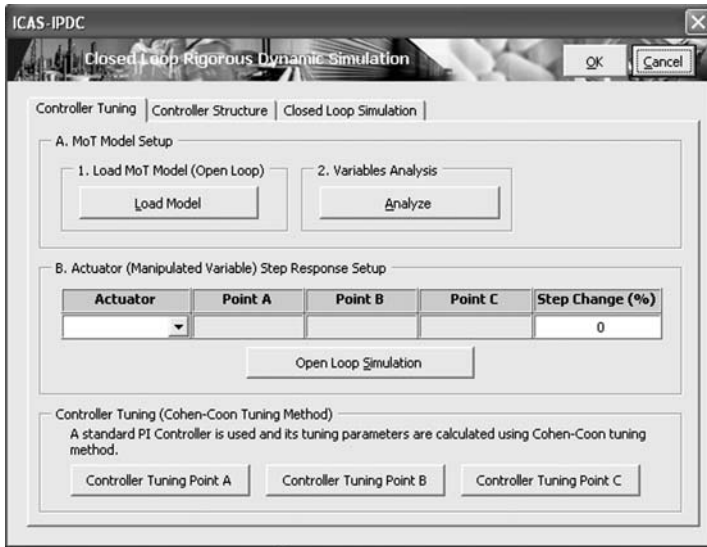
Fig. 4.18. Controller tuning interface.

After the controller tuning parameters are obtained, the closed loop simulations can be performed. The closed loop simulations interface is shown in Fig. 3.19. Here, the user needs to load a closed loop model and then define either a servo or regulator problem to study the controller performances.
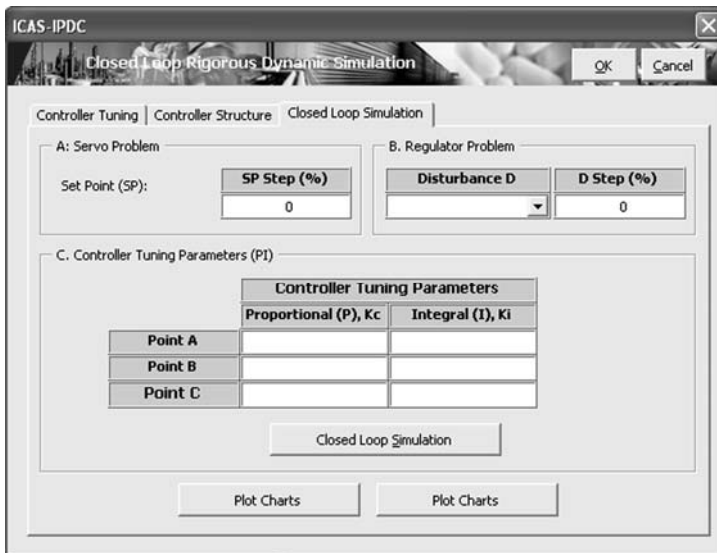
Fig. 4.19. Dynamic closed loop rigorous simulations interface.

4.4   *ICAS-IPDC* Additional Features

User Guide Alerts

This software is able to give users an alert (warning) if the step-by-step procedure is not followed or when the user was accidently clicked the wrong button. An example of a user guide alert is shown in Fig. 4.20. A pop-up alert will appear when the user clicks the wrong button that is not in the sequence. The main idea is to make sure that users follow exactly the software framework, and to guide them in the right way. The alert also provides a suggestion for the users with respect to which step they need to perform.
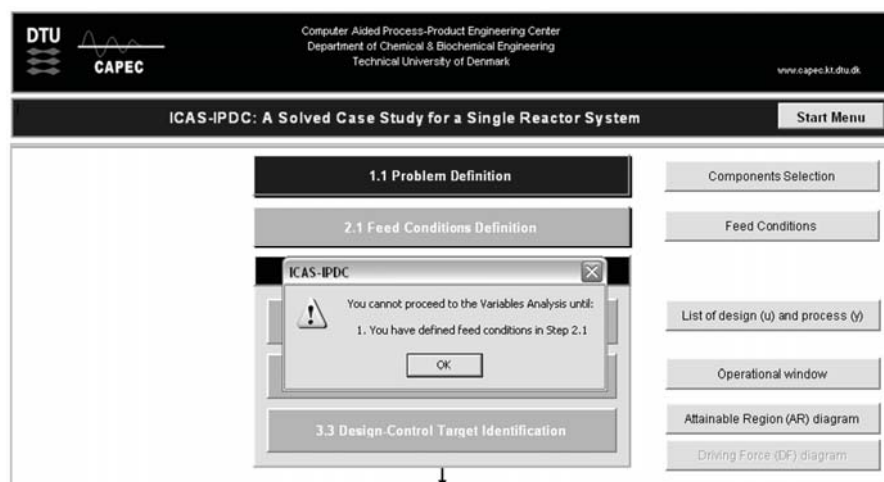
Fig. 4.20. A pop-up alert when the user clicks the wrong button that is not in the sequence.

Results Review

Another feature that is in this software is the option for users to review the results. Once the step is completed, users are able to review the results by just clicking on the button at the right side of the completed step (see Fig. 4.20). In Fig. 4.20, step 1.1 (Problem Definition) is completed (which is indicated by the dark blue color). By clicking on the "Components Selection" button, the results that have been saved can be viewed as shown in Fig. 4.21. The advantage of this feature is that it helps users to review the results easily. This will enable users to verify the results before going further to the next steps.
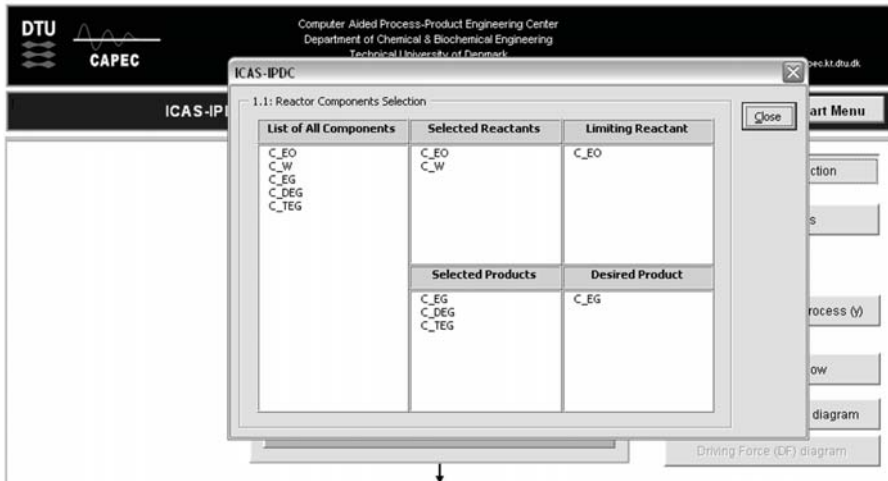
Fig. 4.21. Results review of the completed step.

Controller Tuning Interface

One of the features available within the *ICAS-IPDC* software is called Controller Tuning Interface. This interface helps users to calculate controller tuning parameters for a PI-controller based on the Cohen-Coon tuning method as illustrated in Fig. 4.22. This will require users to calculate the first-order-plus-time-delay (*FOPTD*) model parameters first as shown in Fig 4.22.
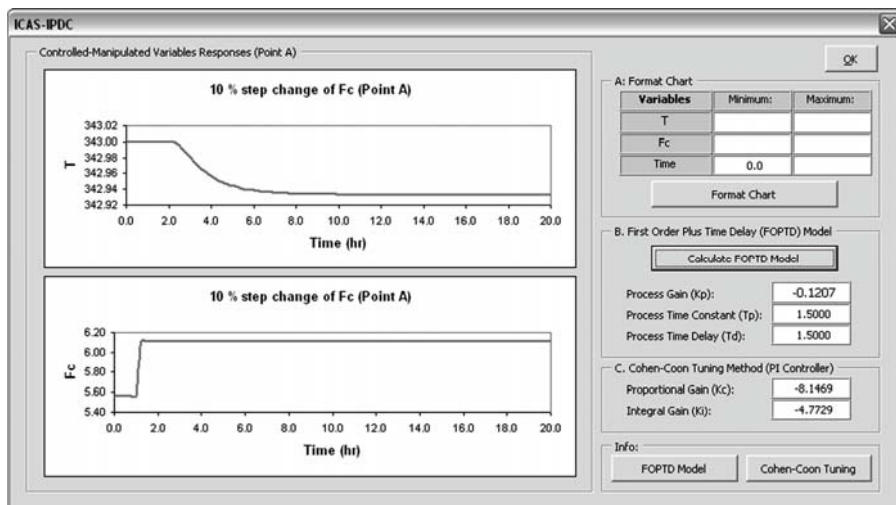
Fig. 4.22. Interface for controller tuning using Cohen-Coon tuning method (PI Controller).

Calculation Progress Monitor

The *ICAS-IPDC* software deals with lots of calculations in which some may require a longer simulation time. Therefore, it is important to monitor the progress of this calculation such that users will have information about the duration or time required to perform such calculation. In this software, all calculations that required the *MoT* model will be monitored as shown in Fig. 4.23.
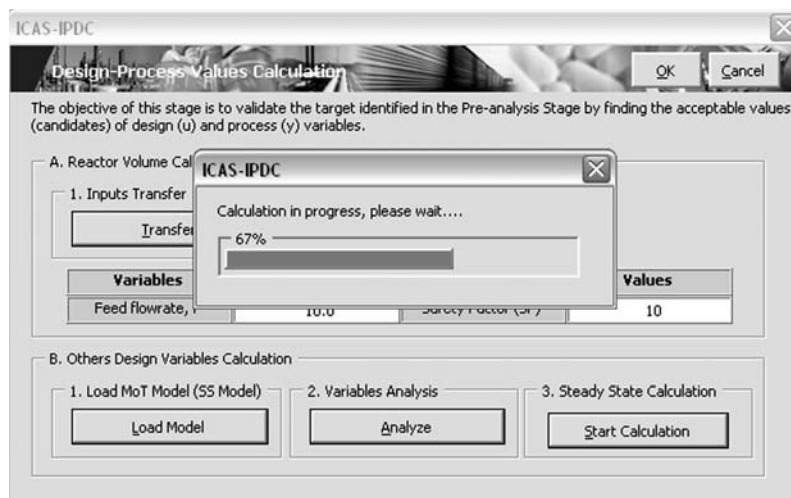
Fig. 4.23. Calculation progress monitor feature within the *ICAS-IPDC* software.

4.5 Conclusion

In this chapter, a software called *ICAS-IPDC* has been presented. *ICAS-IPDC* performs the whole *IPDC* methodology described in Chapter 3, which guides users through each methodology step. The purpose of the software is to guide and help the engineers obtain the optimal solution to *IPDC* problems of chemical processes in a systematic and efficient way. The software has advantages as follows:

- It is a systematic way to solve *IPDC* problems of chemical processes
- It is able to obtain at least a near-optimal solution (if not optimal) to *IPDC* problems
- It makes use of process-thermodynamic insights to locate the optimal design solutions
- It is effective and able to solve *IPDC* problems easily by using a decomposition –based solution strategy

Model-Based Integrated Process Design and Controller Design:

Applications of the Methodology

In this chapter three sections of case studies are presented. The first section (section 5.2) presents the main results for the application of the methodology using *ICAS-IPDC* of a single reactor system. The second section (section 5.3) presents the main *ICAS-IPDC* results for a single separator system whereas in section 5.4, a reactor-separator-recycle system is studied. In the end of the chapter a general conclusion is presented.

5.1 Applications of the Methodology for a Single Reactor System

The application of the methodology (*ICAS-IPDC* application) in solving a single reactor system is illustrated for solving consecutive reactions (see Example 3.3 in Chapter 3). In this section, two industrial case studies where the *ICAS-IPDC* has been applied are presented: an ethylene glycol production process (Hamid et al., 2010a) and a bioethanol production process (Alvarado-Morales et al., 2010). The production of ethylene glycol tests the capability of *ICAS-IPDC* in handling/solving a reaction system with different degrees of difficulty and complexity, whereas the bioethanol production process shows that the *ICAS-IPDC* can also be used in solving biochemical process.

5.1.1 Ethylene Glycol Reaction Process

5.1.1.1 Process Description

The production of Ethylene Glycol (*EG*) has been selected as a case study because of complexity of its reactions (multi-step consecutive-parallel) which provides interesting challenges for *ICAS-IPDC*. The idea is to show that *ICAS-IPDC* is able to handle not only simple reaction systems but also complex reaction systems. We consider the following situation. In a continuous stirred tank reactor (*CSTR*), the product *EG* is to be produced from ethylene oxide (*EO*) and water (*W*). The production of *EG* involves isothermal, irreversible multi-step consecutive-parallel liquid phase reactions and can be represented as follows:

$$\text{EO} + H_2O \xrightarrow{k_1} \text{HO---OH} \tag{5.1}$$

$$\text{EO} + \text{HO---OH} \xrightarrow{k_2} \text{HO---O---OH} \tag{5.2}$$

$$\text{EO} + \text{HO---O---OH} \xrightarrow{k_3} \text{HO---O---O---OH} \tag{5.3}$$
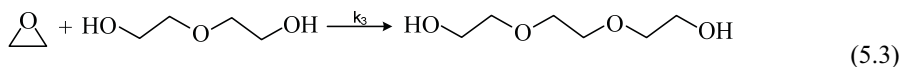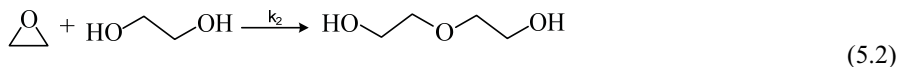
where, *EO* and *W* react to produce *EG* in Eq. (5.1). Eqs. (5.2) - (5.3) are the side-reactions where *EG* reacts with *EO* to produce diethylene glycol (*DEG*), and *DEG* reacts with the remaining *EO* to produce triethylene glycol (*TEG*), respectively. The production of further glycols is comparatively small and is therefore neglected.

$$k_1 = 5.238\exp(30.163 - 10583/T) \, [\text{h}^{-1}]; \quad k_2 = 2.1k_1 \, [\text{h}^{-1}]; \quad k_3 = 2.2k_1 \, [\text{h}^{-1}] \tag{5.4}$$

EO and *W* are considered to be premixed at the same ratio of 1:1, and other component concentrations are zero in the given feed. The kinetic data in Eq. (5.4) for the above reactions are taken from Parker and Prados (1964). The objective is to determine the design-control solution which can satisfy design, control and cost criteria. A scheme of the process is depicted in Fig. 5.1. The process is operated at a nominal operating point as specified in Table 5.1.
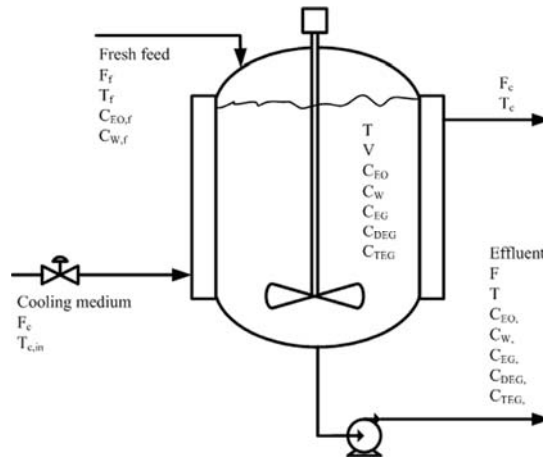
Fig. 5.1. *CSTR* for an ethylene glycol production.

Table 5.1
Nominal operating point of the ethylene glycol reaction process.

Variable	Value	Description
F_f	1000 m³/h	Feed flowrate
$C_{EO,f}$	1 kmol/m³	Concentration of *EO* in the feed
$C_{W,f}$	1 kmol/m³	Concentration of *W* in the feed

5.1.1.2 Problem Formulation

The *IPDC* problem for the process described above is defined in terms of a performance objective (with respect to design, control and cost), and the three sets of constraints (process, constitutive and conditional).

$$\max \quad J = w_{1,1}P_{1,1} + w_{2,1}\left(\frac{1}{P_{2,1}}\right) + w_{2,2}P_{2,2} + w_{3,1}\left(\frac{1}{P_{3,1}}\right) + w_{3,2}\left(\frac{1}{P_{3,2}}\right) \tag{5.5}$$

subjected to:

Process (dynamic and/or steady state) constraints

$$V_r \frac{dC_{EO}}{dt} = F\left(C_{EO,f} - C_{EO}\right) - V_r R_{EO} \tag{5.6}$$

$$V_r \frac{dC_W}{dt} = F\left(C_{W,f} - C_W\right) - V_r R_W \tag{5.7}$$

$$V_r \frac{dC_{EG}}{dt} = -FC_{EG} - V_r R_{EG} \tag{5.8}$$

$$V_r \frac{dC_{DEG}}{dt} = -FC_{DEG} - V_r R_{DEG} \tag{5.9}$$

$$V_r \frac{dC_{TEG}}{dt} = -FC_{TEG} - V_r R_{TEG} \tag{5.10}$$

$$V_r \frac{dT}{dt} = F\rho c_p \left(T_f - T\right) - \sum R_i \Delta H_i V_r - UA\left(T_c - T\right) \tag{5.11}$$

$$V_c \frac{dT_c}{dt} = F_c \rho_c c_{pc} \left(T_{ci} - T_c\right) + UA\left(T_c - T\right) \tag{5.12}$$

Constitutive (thermodynamic) constraints

$$R_{EO} = k_1 C_{EO} C_W + k_2 C_{EO} C_{EG} + k_3 C_{EO} C_{DEG} \tag{5.13}$$

$$R_W = k_1 C_{EO} C_W \tag{5.14}$$

$$R_{EG} = k_2 C_{EO} C_{EG} - k_1 C_{EO} C_W \tag{5.15}$$

$$R_{DEG} = k_3 C_{EO} C_{DEG} - k_2 C_{EO} C_{EG} \tag{5.16}$$

$$R_{TEG} = -k_3 C_{EO} C_{DEG} \tag{5.17}$$

Conditional (process-control) constraints

$$30 \geq V_r \tag{5.18}$$

$$3 \leq V_r \tag{5.19}$$

$$\sum_i x_i T_i^m < T(K) < \sum_i x_i T_i^b \tag{5.20}$$

$$P^{opt} \geq P - \sum_{i=1}^{NC} x_i P_i^* \tag{5.21}$$

$$CS = \mathbf{y} + \mathbf{u}Y \tag{5.22}$$

Eq. (5.5) represents the multi-objective function, where $w_{1,1}$, $w_{2,1}$, $w_{2,2}$, $w_{3,1}$ and $w_{3,2}$ are the weight factors assigned to objective function terms $P_{1,1}$, $P_{2,1}$, $P_{2,2}$, $P_{3,1}$ and $P_{3,2}$, respectively. The first objective function term $P_{1,1}$ is the performance criterion for the reactor design, which in this problem is the concentration of the desired product (C_{EG}). $P_{2,1}$ and $P_{2,2}$ are the sensitivities of the controlled variables $\mathbf{y}$ with respect to disturbances $\mathbf{d}$ and manipulated variables $\mathbf{u}$, respectively, which represent control objective functions. Lastly, $P_{3,1}$ is the real reactor volume V_r which

represents the capital cost and $P_{3,2}$ is the cooling water flowrate F_c which represents the operating cost, for the economic objective function.

Eqs. (5.6) – (5.12) together represent the dynamic process model for the reactor from which the steady-state models are obtained by setting the left hand side of the equations equal to zero. Eqs. (5.6) – (5.10) represent the mass balances for all components. Eq. (5.11) represents an energy balance for a reactor whereas Eq. (5.12) represents an energy balance for a cooling jacket. Eqs. (5.13) - (5.17) represent reaction rates of all components.

Eqs. (5.18) - (5.19) represent the real reactor volume V_r, by summing the reaction volume V_R with the headspace, where the headspace is calculated as 10% of the reaction volume (safety factor). The acceptable value of V_r for a *CSTR* is $3 \leq V_r$ (m^3) ≤ 30 (as defined in Table 6.2 of Sinnot (2005) as a relation between capacity and cost for estimation of purchased equipment costs). The allowable operating temperature is calculated using Eq. (5.20) where, x_i is the mole fraction of component i, and T_i^m and T_i^b are the melting and boiling points, respectively, of component i. The reactor optimal pressure is calculated by analyzing the vapor pressure for all components at the optimal operating temperature using Eq. (5.21). The optimal pressure P^{opt} that is greater than the operating pressure P is selected in order to have all components in the liquid phase. Eq. (5.22) represents the controller structure selection superstructure where $Y \in \{0,1\}$, which select the pairs of controlled-manipulated variables.

The *IPDC* problem formulated above is then solved using the proposed decomposition-based solution strategy as shown below.

5.1.1.3 Decomposition-based solution strategy

The summary of the decomposition-based solution strategy for this problem is shown in Table 5.2 and Fig. 5.2. It can be seen that the constraints in the *IPDC* problem are decomposed into four sub-problems which correspond to the four hierarchical stages. In this way, the solution of the decomposed set of sub-problems is equal to that of the original problem. The *IPDC* problem formulated above is then solved using the developed *ICAS-IPDC* software.

Table 5.2
Mathematical equations and decomposition-based solution for an ethylene glycol reactor design.

Mathematical equations	Decomposition method	Corresponding variables

Multi-objective function: Eq. (5.5) *Process constraints:*
 	
 Eqs. (5.6)-(5.12)
 Constitutive constraints: Eqs. (5.13)-(5.17)
 Conditional constraints: Volume range: Eqs. (5.18)-(5.19)
 Temp range: Eq. (5.20)
 Pressure range: Eq. (5.21)
 Controller structure: Eq. (5.22)
	Stage 1: Pre-analysis.
	 a. Variable analysis
	 b. Operational window: Eqs. (5.18)-(5.19) and (5.20)
	 c. Design-control target
	   Attainable region: Eqs. (5.13)-(5.17)
	 Stage 2: Design analysis.
	   Eqs. (5.13)-(5.17) and Eqs. (5.6)-(5.12) in steady state
	 Stage 3: Controller design analysis:
	   Sensitivity analysis: Eqs. (5.6)-(5.17)
	   Controller structure selection: Eqs. (5.6)-(1.7) and Eq. (5.22)
	 Stage 4: Final selection and verification
	   Final selection: Eq. (5.5)
	   Dynamic simulations verification: Eqs. (5.6)-(5.17)
		C_{EO}, C_W, C_{EG}, T, V_r, F_c
		 $3 \leq V_r \leq 30$
		 $T_{min} \leq T \leq T_{max}$
		
		 C_{EG}/C_{EO}
		
		 T, V_r, F_c
		
		 dC_{EG}/dC_{EO}, dC_{EO}/dT_f
		 dT/dF_c, dC_{EO}/dF_c,
		 dC_{EG}/dF_c
		
		 J
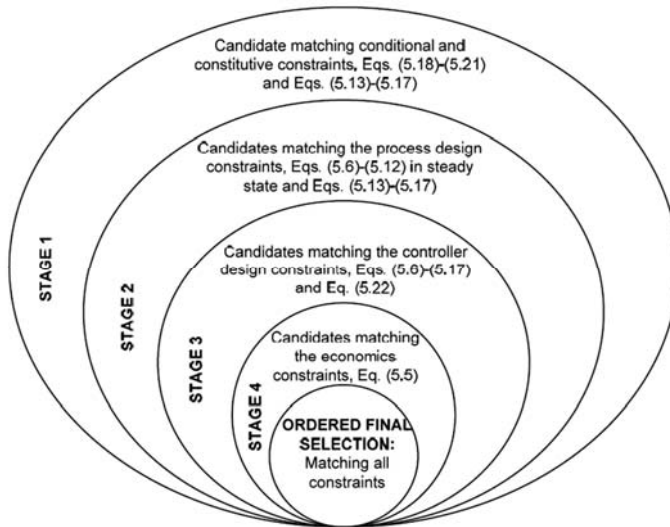
Fig. 5.2. Decomposition-based solution for an ethylene glycol reactor design.

Stage 1: Pre-analysis

The main objective of this stage is to define the operational window within which the optimal solution is located and set the targets for the optimal design-controller solution.

Step 1.1: Variables analysis

The first step in *Stage 1* is to perform variables analysis. All variables involved in this process are analyzed and classified as design and manipulated variables **u**, process-controlled variables **y**, and disturbances **d** as shown in Table 5.3. Then, the important **u** and **y** are selected with respect to the multi-objective function, Eq. (5.5), and tabulated in Table 5.4. In this case study, V is selected as an important design variable since it is directly related to the capital cost and F_c is selected as an important manipulated variable since it is the available manipulated variable and also directly related to the operating cost. On the other hand, process-controlled variables **y** = [C_{EO}, C_{EG}, T] are selected since they are the important variables that need to be monitored and controlled in order to obtain a smooth, operable and controllable process.

Table 5.3
List of all design and manipulated variables, process-controlled variables and disturbances for an ethylene glycol reactor design.

Design variable (**u**$_d$)	V
Manipulated variable (**u**$_m$)	F, F_c
Process-Controlled variables (**y**)	C_{EO}, C_W, C_{EG}, C_{DEG}, C_{TEG}, T, T_c
Disturbances (**d**)	T_f, C_{EOf}

Table 5.4
List of important design and manipulated and process-controlled variables for an ethylene glycol reactor design.

Design variable (**u**$_d$)	V
Manipulated variable (**u**$_m$)	F_c
Process-Controlled variables (**y**$_m$)	C_{EO}, C_W, C_{EG}, T

Step 1.2: Operational window identification

The operational window is identified based on reactor volume and operating temperature constraints. For a single reactor, its volume should satisfy the sizing and costing constraints as defined in Eqs. (5.18)–(5.19). The temperature range is defined between the minimum melting point and maximum boiling point of components, Eq. (5.20). Therefore, the operational window (feasible solutions) within which the optimal solution is likely to exist, is given by $3 \leq V_r(m^3) \leq 30$ and $161 \leq T(K) \leq 562$.

Step 1.3: Design-control target identification

For a reactor design, the attainable region diagram is drawn and the location of the maximum in the attainable region is selected as the reactor design target. The attainable region is drawn from the feed points using Eqs. (5.23a)-(5.23d), which are derived from Eqs. (5.13)-(5.17). Detailed derivations are given in Appendix B.

$$\frac{C_{EG}}{C_W} = \frac{\left(\dfrac{C_W^0}{C_W}\right) - 1}{2.1\left(\dfrac{C_W^0}{C_W}\right) - 1.1} \tag{5.23a}$$

$$\frac{C_{DEG}}{C_W} = \frac{2.1\left(\dfrac{C_{EG}}{C_W}\right)\left[\left(\dfrac{C_W^0}{C_W}\right) - 1\right]}{2.2\left(\dfrac{C_W^0}{C_W}\right) - 1.2} \tag{5.23b}$$

$$\frac{C_{TEG}}{C_W} = 2.2\left(\frac{C_{DEG}}{C_W}\right)\left[\left(\frac{C_W^0}{C_W}\right) - 1\right] \tag{5.23c}$$

$$\frac{C_{EO}}{C_W} = \left(\frac{C_{EO}^0}{C_W}\right) - \left(\frac{C_W^0}{C_W}\right) + 1 + \left[2.1\left(\frac{C_{EG}}{C_W}\right) + 2.2\left(\frac{C_{DEG}}{C_W}\right)\right]\left[\left(\frac{C_W^0}{C_W}\right) - 1\right] \tag{5.23d}$$

Solving Eqs. (5.23a)-(5.23d) for specified values of C_W with $C_W^0 = 1.00$ kmol/m^3 and $C_{EO}^0 = 1.00$ kmol/m^3, values for C_{EG}, C_{DEG}, C_{TEG} and C_{EO} are calculated. Then, the attainable region is created by plotting the concentration of C_{EG} with respect to the concentration of C_W as shown in Fig. 5.3. The location of the maximum point in the attainable region (Point A) is selected as the reactor design target. It can easily be seen from Fig. 5.3 that a maximum of 0.1667 kmol/m^3 of C_{EG} can be achieved using a CSTR with 0.59 kmol/m^3 of C_W in the outflow. The calculation is repeated for different ratios of initial concentration of EO and W of 1:2, 1:10, and 1:20. It was found that by increasing the ratio of C_W in the feed, the concentration of C_{EG} is also increasing. This is because by adding more C_W, the side reactions are suppressed and make the main reaction more active, thus more C_{EG} is produced. However, the normalized value of C_{EG} with respect to C_W^0 is still the same as shown in Fig. 5.3 for all ratios. Besides, it was found that there is an operation constraint of C_W for all ratios (see Fig. 5.3). For a ratio of 1:1, the range of operation with respect to C_W was $0.54 \leq C_W$ (kmol/m^3) ≤ 1.0. When $C_W \leq 0.54$, C_{EO} was all exhausted, thereby, turning off the operation. For other ratios, the operation ranges of C_W were $0.72 \leq C_W$ (kmol/m^3) ≤ 1.0 for ratio 1:2, $0.92 \leq C_W$ (kmol/m^3) ≤ 1.0 for ratio 1:10, and $0.96 \leq C_W$ (kmol/m^3) ≤ 1.0 for ratio 1:20. For ratios higher than 1:1, the maximum point (Point A) was located outside the operation range (see Fig. 5.3). The initial design of the reactor is made at the maximum point of the attainable region for a C_{EO}:C_W ratio of 1:1.
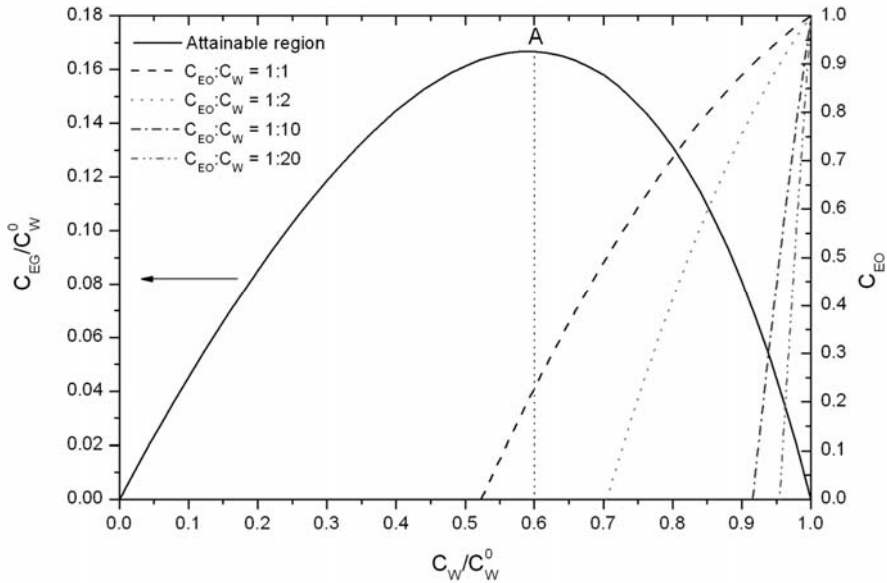
Fig. 5.3. Normalized plot of the desired product concentration C_{EG} and C_{EO} with respect to C_W for different C_{EO}:C_W.

Stage 2: Design analysis

The objective of this stage is to validate the target identified in *Stage 1* by finding the acceptable values of **y** and **u**. In this stage, the search space defined in *Stage 1* is further reduced.

Step 2.1: Design-manipulated and process-controlled variables value calculation

In this stage, the search space defined in Stage 1 is further reduced using design analysis. The established target (Point A) in Fig. 5.4(a) is now matched by finding the acceptable values (candidates) of the design/manipulated and process/controlled variables. If feasible values cannot be obtained or the variable values are lying outside of the operational window, a new target is selected and variables are recalculated until a satisfactory match is obtained. At Point A, the allowable operating temperature is calculated using Eq. (5.20). The feasible solution search space for temperature is now reduced to $251 \leq T(K) \leq 406$ from $161 \leq T(K) \leq 562$. At this range, a feasible pressure range of $1.0 \leq P(atm) \leq 5.8$ is predicted using Eq. (5.21).

With this new range, the feasible solution range for the volume ($11.78 < V_r$ $(m^3) < 1.082 \times 10^8$) is calculated. However, the upper limit of the volume is more than what was defined in Stage 1. Therefore, a volume that is more than 30 m³ and its corresponding temperature are eliminated. For that reason, the search space for temperature is further reduced to $394 \leq T(K) \leq 406$. After Stage 2, the region of the feasible solutions is now between $394 \leq T(K) \leq 406$ and $11.78 \leq V_r(m^3) \leq 26.89$ with a

feasible pressure of $4.5 \leq P(atm) \leq 5.8$. Within the feasible solutions for temperature $394 \leq T(K) \leq 406$, different feasible candidates can be enumerated. For illustration purposes, only four feasible candidates are considered with the scale of temperature decreasing by 4K. Candidates of design/manipulated and process/controlled variables for stage 2 are tabulated in Table 5. In principle, if the design is repeated for higher amounts of C_W and fixed C_{EO}, the pressure would decrease but the size parameters would increase.
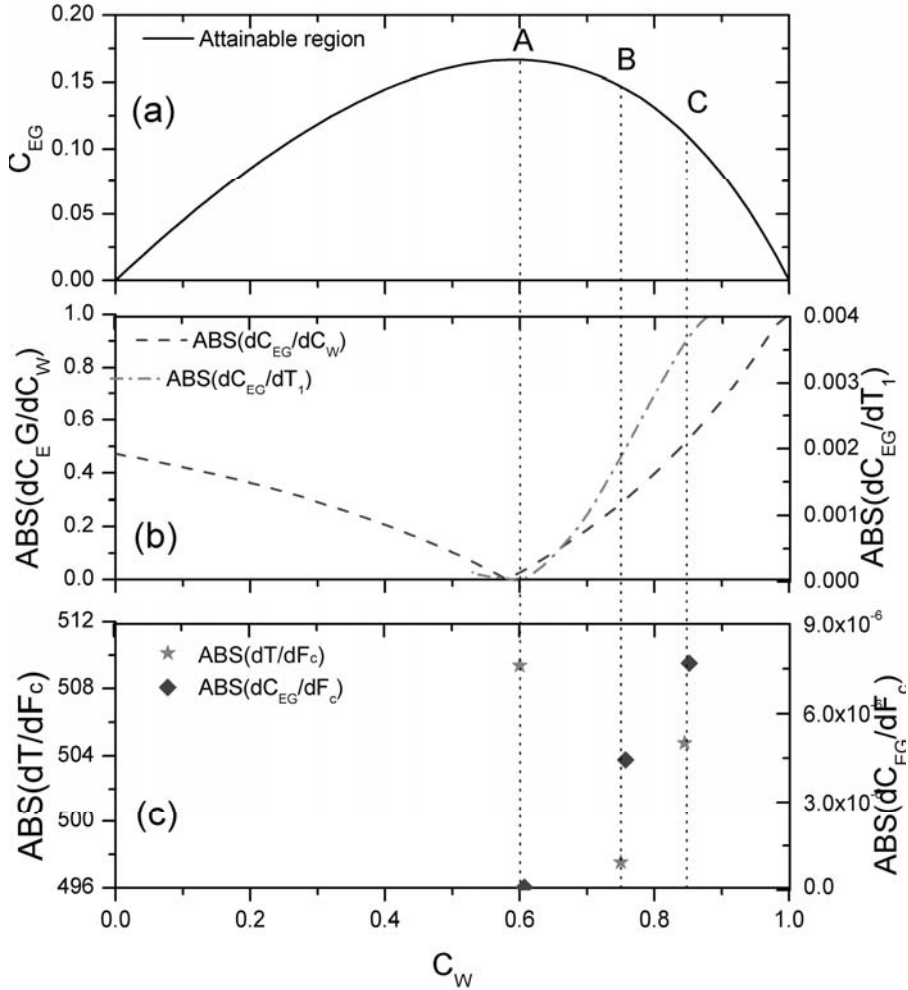
Fig. 5.4. (a) Attainable region diagram for the desired product concentration C_{EG} with respect to C_W for C_{EO}:C_W of 1:1, (b) corresponding derivatives of C_{EG} with respect to C_W and T, and (c) corresponding derivatives of T and C_{EG} with respect to F_c.

Table 5.5.
Candidates of design/manipulated-process/controlled variables for Stage 2 of the *EG* reaction process.

| Candidates | Process-Controlled | | | | Design | Manipulated |
| | C_W | C_{EG} | T | P | V | F_c |
	(kmol/m³)	*(kmol/m³)*	*(K)*	*(atm)*	*(m³)*	*(m³/h)*
1	0.59	0.1667	406	5.8	11.78	1388.31
2	0.59	0.1667	402	5.3	15.76	1388.22
3	0.59	0.1667	398	4.9	20.53	1388.26
4	0.59	0.1667	394	4.5	26.89	1388.34

Stage 3: Controller design analysis

The objective of this stage is to evaluate and validate the controllability performances of the feasible candidates in terms of their sensitivities with respect to disturbances and manipulated variables.

Step 3.1: Sensitivity analysis

The search space is further reduced by considering the feasibility of the process control. The feasible candidates from stage 2 are evaluated in terms of controllability performance. The process sensitivity is analyzed by calculating the derivative of the controlled variables with respect to disturbances. In this case, C_{EOf} and T_f are potential sources of disturbance in the reactor feed while C_{EG} is the controlled variable which needs to be maintained at its optimal value (set point). Accordingly, dC_{EG}/dC_{EOf} and dC_{EG}/dT_f can be expressed as

$$\frac{dC_{EG}}{dC_{EOf}} = \left(\frac{dC_{EG}}{dC_W}\right)\left(\frac{dC_W}{dC_{EOf}}\right) \tag{5.24}$$

$$\frac{dC_{EG}}{dT_f} = \left(\frac{dC_{EG}}{dC_W}\right)\left(\frac{dC_W}{dT_f}\right) \tag{5.25}$$

Fig. 5.4(b) shows plots of the derivative of C_{EG} with respect to C_W and feed temperature T_f. Note that in Fig. 5.4, two other points (Points B and C) which are not at the maximum are identified as candidate alternative designs for a reactor. Those points will be used for verification purposes later on.

Consider the effect of disturbances C_{EOf} and T_f that will move values of C_{EG} away from their setpoints (at Points A, B, C). Since at Point A the value of dC_{EG}/dC_W is smaller, therefore, any significant changes in C_W will give smaller changes in C_{EG} compared to Points B and C – see Fig. 5.4(b). On the other hand, since the value of dC_{EG}/dC_W is larger at Points B and C, therefore, any smaller changes in C_W will significantly move C_{EG} away from its desired value. According to Russel et al. (2002), the process with lower sensitivity will have higher process flexibility. In this case,

reactor design A will be more flexible to the changes in T_f and C_{EOf} than reactor designs B and C. Therefore, from control point of view, reactor design A is less sensitive and more flexible to the disturbances. This will be verified in Stage 4.

Step 3.2: Controller structure selection

Next, the controller structure is selected by calculating the derivative values of potential controlled variables (C_W, C_{EG}, T) with respect to the manipulated variable F_c with a constant step size. The objective of this step is to select the best controller structure (pairing of controlled-manipulated variables) which can satisfy the control objective (maintaining desired product concentration C_{EG} at its optimal set point in the presence of disturbances).

Accordingly, dC_{EG}/dF_c can be represented as:

$$\frac{dC_{EG}}{dF_c} = \left(\frac{dC_{EG}}{dC_W}\right)\left(\frac{dC_W}{dF_c}\right) \tag{5.26}$$

$$\frac{dC_{EG}}{dF_c} = \left(\frac{dC_{EG}}{dC_W}\right)\left(\frac{dC_W}{dT}\right)\left(\frac{dT}{dF_c}\right) \tag{5.27}$$

From Eqs. (5.26)-(5.27), it can be concluded that it is possible to maintain C_{EG} at its optimal set point using concentration control of component W (see Eq. (5.26)) or using temperature control (see Eq. (5.27)). However, it can be seen that values of dT/dF_c are higher compared to values of dC_W/dF_c for all reactor designs – see Fig. 5.4(c). Higher derivative value of controlled variables with respect to manipulated variables means that the process has a higher process gain (Russel et al., 2002). From a process control point of view, a process with a large process gain will require a small change in the manipulated variable (control action) in order to maintain the controlled variable at its set point value in the presence of disturbance. Conversely, a process with a small process gain will require a large change in the manipulated variable (control action) for controlling its controlled variable in the presence of the same disturbance. Therefore, it can be clearly seen from Fig. 5.4(c) that the best pairing of controlled-manipulated variable that will be able to maintain the desired product concentration C_{EG} at its optimal set point value in the presence of disturbances is T-F_c. This controller structure will require less control action compared to the C_W-F_c structure for maintaining C_{EG} at its optimal set point value for all reactor designs. Therefore, the concentration-to-temperature cascade control is proposed. In this structure, the concentration C_{EG} controller is the primary (master or outer loop) controller, while the reactor temperature controller is the secondary (slave or inner loop) controller. The proposed control structure for an ethylene glycol process is shown in Fig. 5.5. The performance of the controller structure obtained in this stage will be verified in Stage 4 in terms of closed loop performance, especially steady state offset of C_{EG}.
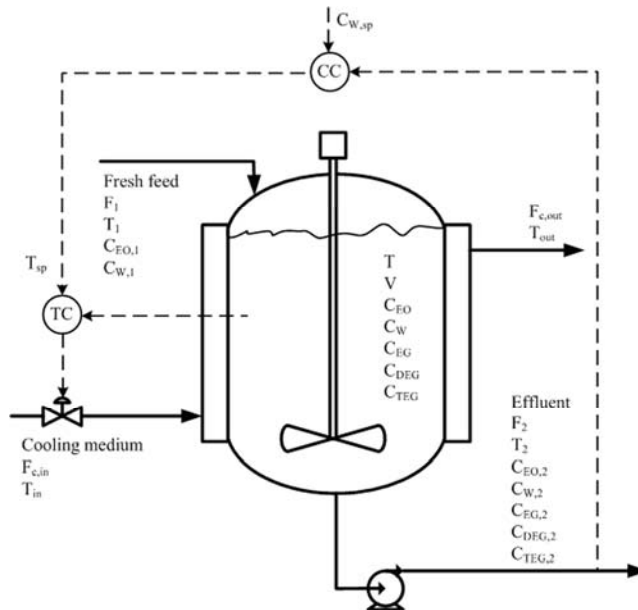
Fig. 5.5. Proposed reactor control structure for an ethylene glycol process.

Stage 4: Final selection and verification

The objective of this stage is to select the best candidates by analyzing the value of the multi-objective function, Eq. (5.5).

Step 4.1: Final selection: Verification of design

The multi-objective function, Eq. (5.5) is calculated by summing up each term of the objective function value. In this case, all the objective function terms are weighted equally meaning that the decision-maker does not have any preference for one objective over another. Since the range and unit of each objective function value can be different, each objective value is normalized with respect to its maximum value. Details are given in Table 5.6. $P_{1,1s}$ corresponds to the scaled value of the desired product concentration C_{EG}. $P_{2,1s}$ and $P_{2,2s}$ are scaled values of dC_{EG}/dT_f and dT/dF_c representing the sensitivity of the desired product concentration C_{EG} with respect to the disturbance T_f and the sensitivity of the controlled variable T with respect to the manipulated variable F_c, respectively. $P_{3,1s}$ is the scaled value of the reactor volume which represents the capital cost and $P_{3,2s}$ is the scaled value of the cooling water flowrate which represent the operating cost. Since all candidates in Table 5.6 are at the maximum point of the attainable region (Point A), values for $P_{1,1s}$, $P_{2,1s}$ and $P_{2,2s}$ are the same. It can be seen that value of J for Candidate 1 is higher than for the other candidates. Therefore, it is verified that Candidate 1 is the optimal solution for the integrated process design and controller design of an ethylene glycol reactor design

problem which satisfies design, control and cost criteria. It should be noted that a qualitative analysis (J highest for point A) is sufficient for the purpose of controller structure selection.

Table 5.6.
Objective function calculation at different operating points of the *EG* reaction process.

Candidate	$P_{1,1s}$	$P_{2,1s}$	$P_{2,2s}$	$P_{3,1s}$	$P_{3,2s}$	J
1	1.00	1.00	1.00	0.44	0.96	**6.34**
2	1.00	1.00	1.00	0.59	0.96	5.74
3	1.00	1.00	1.00	0.76	0.98	5.33
4	1.00	1.00	1.00	1.00	1.00	5.00

Step 4.2: Dynamic rigorous simulations: verification of controller performance

As explained earlier, when a reactor is designed corresponding to the maximum point of the attainable region (Point A), the controllability of the system is also best satisfied. This is verified by selecting two sub-optimal points in the attainable region (see Fig. 5.4(a)). From a design point of view, they are not feasible since Points B and C generate lower *EG* concentrations. From a control point of view, the derivative values of the desired product C_{EG} with respect to disturbances (T_f and C_{EOf}) at Point A is smaller than those at Points B and C, as shown in Fig. 5.4(b). This in turn means that any changes in disturbances will give smaller changes in C_{EG} at Point A compared to Points B or C.

To further verify the controllability aspects, a disturbance (+10% step change in feed temperature T_f) moves reactor temperature T away from its set point (points A, B, C). According to Fig. 5.4(b), any changes in T_f at points B and C will easily move the desired product concentration C_{EG} away from its steady state value and as a result, it will be more difficult to maintain C_{EG} at is set points at these points than at Point A.

Fig. 5.6 shows the open-loop output response of T and C_{EG} when +10% step change in feed temperature T_f is applied at points A, B, and C, respectively. One observes that the effect of the disturbance on C_{EG} is negligible at Point A, whereas for points B and C the effect is quite significant (see Fig. 5.6(a)). This means that, process sensitivity at Point A is lower than at other points. As a result, Point A offers better robustness in maintaining its desired product concentration C_{EG} in the presence of disturbances. Therefore, it can be verified (albeit empirically) that, designing a reactor at the maximum point of the attainable region leads to a process with lower sensitivity with respect to disturbances.
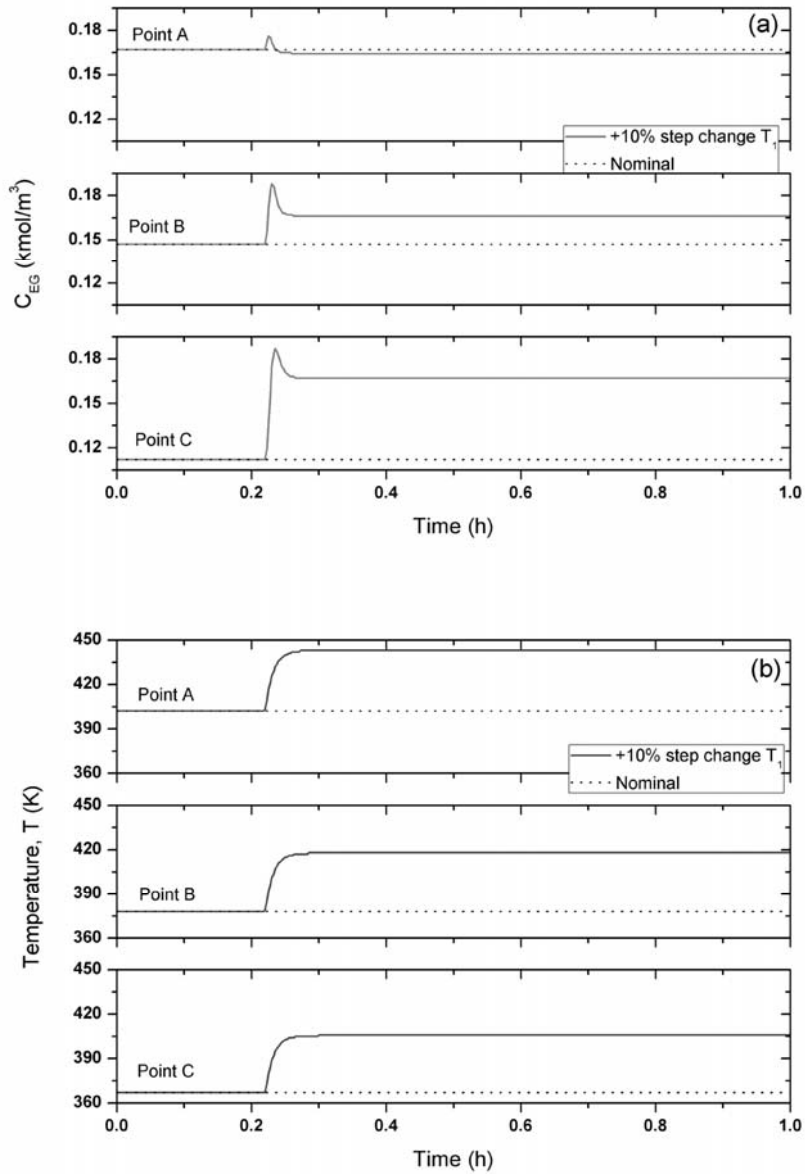
Fig. 5.6. Dynamic open loop responses of: (a) desired product concentration C_{EG}, and (b) reactor temperature, T to a +10% step change in the feed temperature T_f for different alternative reactor design for an ethylene glycol production process.

The closed loop responses, with a PI control, to a +10% step change in the feed temperature for all reactor designs, are shown in Fig. 5.7. The controller parameters are tuned using the same standard Cohen-Coon tuning method for all reactor designs. Closed loop responses of temperature for all reactor designs are shown in Fig. 5.7(b). It can be seen that responses of temperature at all points are not oscillatory and the controller is able to keep temperature at its set-point value.

In Fig. 5.7(a), closed loop responses of C_{EG} for all reactor designs are shown. It can be seen that responses of C_{EG} are less oscillatory. For a reactor design at Point A, C_{EG} settles much faster than for other points. It can also be seen that the overshoot at Point A is the smallest. It is important to verify here that the closed loop performance in Point A is much better than for Points B and C.

Based on the closed loop simulation results obtained in this step, it can be verified that the reactor designed at Point A (at the maximum point of the attainable region) not only has the highest desired product concentration and better capital and operating costs, but also has a better closed loop performance.
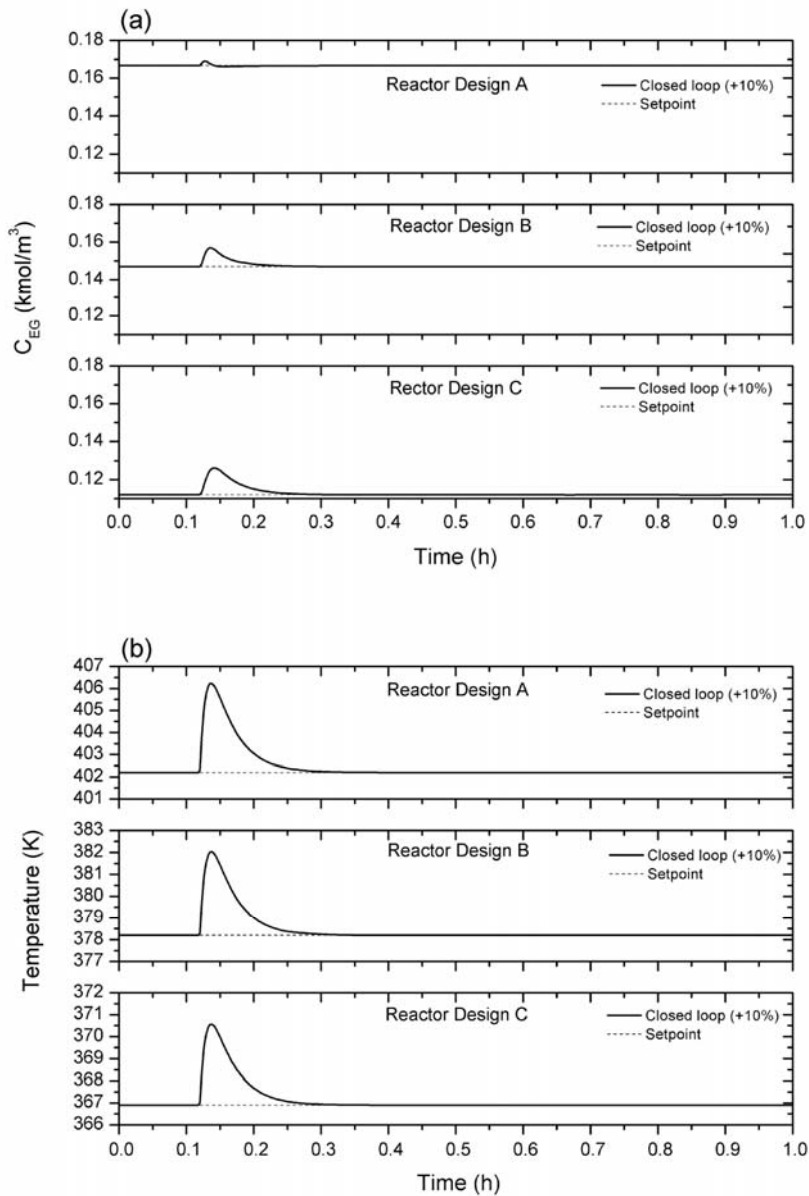
Fig. 5.7. Dynamic closed loop responses of: (a) desired product concentration C_{EG}, and (b) reactor temperature, T to a +10% step change in the feed temperature T_f for different alternative reactor design for an ethylene glycol production process.

5.1.2   Bioethanol Production Process

5.1.2.1 Process Description

The production of bioethanol has been selected as a case study in this section in order to show the capability of the methodology in solving *IPDC* problem for biochemical processes. This case study is a part of the work presented in Alvarado-Morales et al. (2010). The production of ethanol from cellulose is based on the simultaneous saccharification and fermentation (*SSF*) reaction scheme expressed in Eq. (5.28).

$$Cellulose \rightarrow Cellobiose \rightarrow Glucose \rightarrow Ethanol + Cell\ mass \qquad (5.28)$$
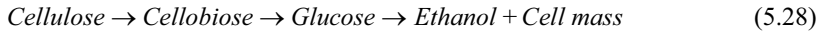
Details of the rate equations and kinetic models for the *SSF* process are given in the Appendix C. The objective here is to determine the optimal design-control solution in which the multi-objective function with respect to design, control and costs is optimal subject to process (dynamic and steady state) constraints, constitutive (thermodynamic states) constraints and conditional (process−controller specification) constraints.

5.1.2.2 Application of the Methodology

The step-by-step methodology for this case study is summarized as follows:

Stage 1: Pre−analysis

First, all variables are analyzed and the important ones are shortlisted. For design (manipulated) variables, reactor volume (V) and enzyme loading (ENZ) are shortlisted since V will determine the capital cost and ENZ will determine the operating cost. For process (controlled) variables, ethanol ($C_{Ethanol}$) and cellulose ($C_{Cellulose}$) concentrations are shortlisted since $C_{Ethanol}$ is the desired product and $C_{Cellulose}$ is the limiting reactant.

The optimal solution with respect to the process-controller design targets is first identified using attainable region analysis by locating the maximum point in the attainable region diagram as the basis for the reactor design. In order to have a graphical representation of the attainable region analysis for the bioreactor unit, kinetic models describing a simultaneous saccharification and fermentation (*SSF*) process were taken from South et al. (1995). The objective here is to identify the optimum concentration of ethanol at the maximum concentration of glucose at different values of enzyme loading. Results are listed in Table 5.7 and shown in Fig. 5.8.

Table 5.7.
Values of process variables for ethanol production at different enzyme loading.

ENZ (*FPU/g*)	Cellulose (*g/l*)	Glucose (*g/l*)	Cell mass (*g/l*)	Ethanol (*g/l*)
100	4.12	0.0076	10.84	44.96
150	7.41	0.0092	10.79	43.54
200	8.66	0.0104	10.77	42.99
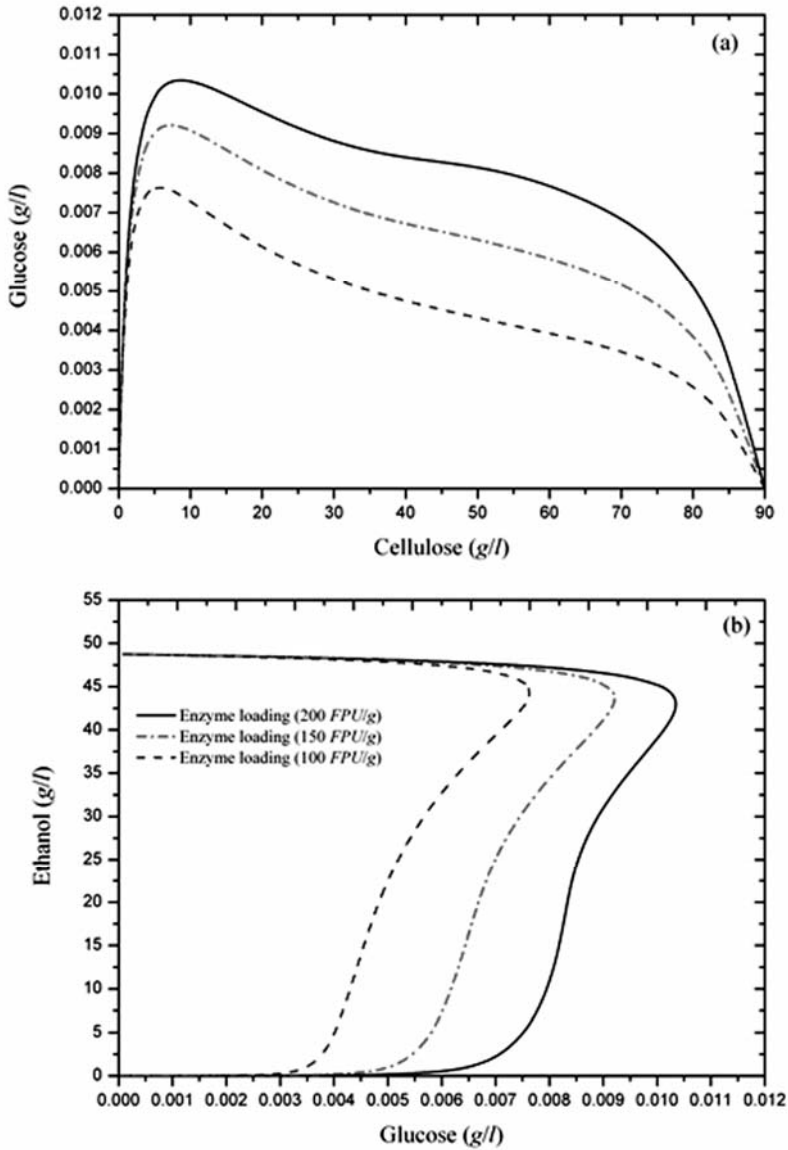
Fig. 5.8. Attainable region space–concentration diagram for: a) cellulose–glucose and b) glucose–ethanol.

Note that an *SSF* bioreactor is considered instead of a simultaneous saccharification and co-fermentation (*SSCF*) bioreactor, because of the large uncertainties of the experimental data as well as the current lack of reliable kinetic models for the *SSCF* process. Nevertheless, the design analysis with the attainable region based method for the *SSF* bioreactor model perfectly serves the purpose of

illustrating the main steps of the *IPDC* methodology. From Fig. 5.8, for an enzyme loading of 100 *FPU*/*g*, an ethanol concentration of 44.96 *g*/*l* is obtained at a maximum concentration of glucose of 0.0076 *g*/*l*. Here, the enzyme activity is expressed in terms of filter paper units (*FPU*) (Adney & Baker, 1996). Ethanol concentrations of 43.54 *g*/*l* and 42.99 *g*/*l* respectively are obtained at the maximum concentrations of glucose of 0.0092 *g*/*l* and 0.0104 *g*/*l* for enzyme loadings of 150 *FPU*/*g* and 200 *FPU*/*g*, respectively. From here, the operational window for the enzyme loading is identified ($100 \leq ENZ$ (*FPU*/*g*) ≤ 200). For an industrial or production bioreactor, the operational window for the volume is assumed to be between 100 m^3 and 500 m^3 (Okafor, 2007).

Stage 2: Design Analysis

The established targets (maximum point in the attainable region diagram) are now validated by finding the feasible values (candidates) of design that match the target. The feasible values lying outside the operational window are eliminated. Results are tabulated in Table 5.8.

Table 5.8.
Values of process variables for ethanol production at different enzyme loading and reactor volume.

Design variables		Process variables		
ENZ (*FPU*/*g*)	V_R (m^3)	Cellulose (*g*/*l*)	Glucose (*g*/*l*)	Ethanol (*g*/*l*)
100	677	4.12	0.0076	44.96
150	541	7.41	0.0092	43.54
200	**440**	**8.66**	**0.0104**	**42.99**

Since the largest volumes are higher than those set in Stage 1, these solutions together with their corresponding enzyme loading are therefore eliminated. For that reason, design options with enzyme loadings of 100 and 150 *FPU*/*g* are rejected. The optimal value of enzyme loading which gives the optimal value of reactor volume is 200 *FPU*/*g*. At this value of enzyme loading, the optimum concentration of ethanol obtained at the maximum concentration of glucose corresponds to 42.99 *g*/*l*.

Stage 3: Controller Design Analysis

a.   <u>Sensitivity analysis</u>

The feasible candidate from Stage 2 is evaluated in terms of process sensitivity with respect to disturbances. The process sensitivity is analyzed by calculating the derivative of glucose concentration $C_{Glucose}$ with respect to cellulose concentration $C_{Cellulose}$, $dC_{Glucose}/dC_{Cellulose}$ with a constant step size. Values of $dC_{Glucose}/dC_{Cellulose}$ are plotted against the concentration of cellulose (Fig. 5.9(a)). In Fig. 5.9(a), the feasible candidate from Stage 2 that is at the maximum point in the attainable region diagram

is shown as Point A. In Fig. 5.9(a) also, two other points are considered (B and C) representing two alternative operating points which are below the maximum point in the attainable region diagram. However, from the viewpoint of design, they are infeasible since Point B generates a lower ethanol concentration and Point C requires a larger residence time. In this case study, inlet cellulose concentration $C_{Cellulose,f}$ and flowrate $F_{Cellulose,f}$ are the potential sources of disturbances. Accordingly, the derivatives of $C_{Glucose}$ with respect to disturbances can be expressed as

$$\frac{dC_{\text{Glucose}}}{dC_{\text{Cellulose,f}}} = \left(\frac{dC_{\text{Glucose}}}{dC_{\text{Cellulose}}} \right) \left(\frac{dC_{\text{Cellulose}}}{dC_{\text{Cellulose,f}}} \right) \tag{5.29}$$

$$\frac{dC_{\text{Glucose}}}{dF_{\text{Cellulose,f}}} = \left(\frac{dC_{\text{Glucose}}}{dC_{\text{Cellulose}}} \right) \left(\frac{dC_{\text{Cellulose}}}{dF_{\text{Cellulose,f}}} \right) \tag{5.30}$$

Consider the effect of disturbances $C_{Cellulose,f}$ and $F_{Cellulose,f}$ that will move values of $C_{Cellulose}$ away from their setpoints (Points A, B, C). Since at Point A, the value of $dC_{Glucose}/dC_{Cellulose}$ is smaller (see Fig. 5.9(a)), therefore, any big changes in $C_{Cellulose}$ will give smaller changes in $C_{Glucose}$ compared to Points B and C. On the other hand, since the value of $dC_{Glucose}/dC_{Cellulose}$ is higher at Points B and C, therefore, smaller changes in $C_{Cellulose}$ will significantly move $C_{Glucose}$ away from its desired value. Thus, smaller values of the derivative with respect to disturbance means process sensitivity is lower (Russel et al., 2002), hence the process is more robust with respect to feed concentration and flowrate variations. Therefore, at the highest of the attainable region point (Point A), the process is more robust to disturbances compared to Points B and C. This will be verified in Stage 4.

b.   Controller Structure Selection

Next, the controller structure is selected by calculating the derivative value of the controlled variables with respect to the manipulated variable. Since there is only one manipulated variable (enzyme loading, ENZ) available, thus in order to maintain $C_{Cellulose}$ and $C_{Ethanol}$ at their desired values the enzyme loading needs to be manipulated. The values of $dC_{Cellulose}/dENZ$ and $dC_{Ethanol}/dENZ$ are calculated with a constant step size and plotted in Fig. 5.8(b). It can be seen that the value of $dC_{Cellulose}/dENZ$ is high for all points, hence it is feasible to manipulate ENZ in order to control $C_{Cellulose}$ at its optimal value (setpoint). It can also be seen that $dC_{Ethanol}/dENZ$ is lower for all points. From Eq. (5.31), since $dC_{Ethanol}/dENZ \approx 0$, it makes sense to control $C_{Cellulose}$ by manipulating ENZ in order to maintain $C_{Ethanol}$ at its optimal set point.

$$\frac{dC_{\text{Ethanol}}}{dENZ} = \left(\frac{dC_{\text{Ethanol}}}{dC_{\text{Glucose}}} \right) \left(\frac{dC_{\text{Glucose}}}{dC_{\text{Cellulose}}} \right) \left(\frac{dC_{\text{Cellulose}}}{dENZ} \right) \approx 0 \tag{5.31}$$

Therefore, the controller structure is as follows: primary controlled variable: $C_{Ethanol}$; secondary controlled variable: $C_{Cellulose}$; manipulated variable: ENZ; primary set point: 42.99 g/l; secondary set point: 8.66 g/l.
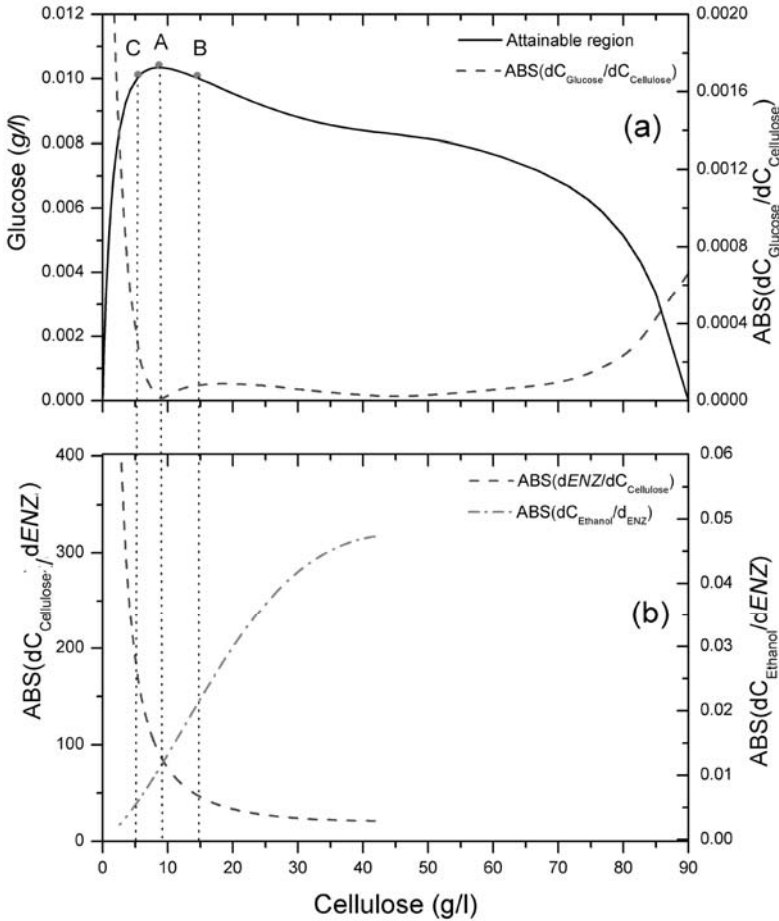
Fig. 5.9.   (a) Attainable region space–concentration diagram for glucose–cellulose and its corresponding derivative with respect to cellulose concentration, (b) Derivatives of cellulose concentration and ethanol concentration with respect to enzyme loading.

Since the value of $dC_{Glucose}/dC_{Cellulose}$ at point A is smaller than at points B and C (see Fig. 5.9(a)), any significant changes in cellulose concentration (because of disturbance or changes in setpoint) will give smaller changes in glucose concentration for Point A. Therefore, by maintaining the cellulose concentration at Point A, the glucose concentration can be more easily maintained than at other points, and consequently, the desired ethanol concentration can more easily be controlled. By controlling $C_{Cellulose}$ at its optimal setpoint at Point A, the robust performance of a controller in order to maintain $C_{Ethanol}$ at its desired optimal value in the presence of a disturbance can be assured. This means that among the many controlled-manipulated variables that could be paired, this is the pairing that should be tried first.

Stage 4: Final Selection and Verification

Final selection: Verification of design

The multi−objective function Eq. (5.5) is calculated by summing up each term of the objective function value. In this case, all the objective function terms are weighted equally meaning that the decision−maker does not have any preference of one objective over another. Since the range and unit of each objective function values can be different, an appropriate scaling of each objective function is needed. To this end, each objective value is normalized with respect to its maximum value. Those results are given in Table 5.9. $P_{1,1s}$ corresponds to the scaled value of the desired product concentration, $C_{Ethanol}$. $P_{2,1,s}$ and $P_{2,2,s}$ are scaled values of $dC_{Glucose}/dC_{Cellulose}$ and $dC_{Cellulose}/dENZ$, representing the process sensitivity with respect to disturbance and manipulated variable, respectively. Whereas, $P_{3,1,s}$ and $P_{3,2,s}$ are the scaled values of the reactor volume and the enzyme loading, respectively, which represent capital and operating costs. It can be seen that the value of J for the design Point A is higher than for the other points. Therefore, it is verified that, design point A is the optimal solution for integrated process design and controller design of a bioreactor which satisfies the design, control and cost criteria. It should be noted that a qualitative analysis (J highest for Point A) is sufficient for the purpose of controller structure selection.

Table 5.9.
Multi-objective function calculation at different operating points for the bioreactor.

Point	$P_{1,1s}$	$P_{2,1s}$	$P_{2,2s}$	$P_{3,1s}$	$P_{3,2s}$	J
A	0.95	0.03	0.54	0.65	1.00	**33.1**
B	0.87	0.24	0.28	0.40	1.00	8.8
C	1.00	1.00	1.00	1.00	1.00	5.0

Dynamic rigorous simulations: verification of controller performance

In order to further verify the controllability aspects, a set of disturbance (±10% changes in inlet cellulose flowrate) is applied to all designs (Points A, B, C). According to Fig. 5.9(a), any changes in the cellulose concentration at Points B and C will easily move the glucose concentration away from its steady state value and as a result, it will be more difficult to maintain glucose and ethanol at these points (Points B and C) than at Point A. Fig. 5.10 shows the open loop response of cellulose and ethanol concentrations when ±10% changes in inlet cellulose flowrate are applied at Points A, B, and C. Since the effect of the disturbance to the glucose concentration at Point A is negligible, thereby, the process sensitivity with respect to the disturbance at Point A is lower compared to the other points. Therefore, these open loop simulations in Fig. 5.9(a) have shown that, designing a reactor at the maximum point of the attainable region diagram leads to a process with lower sensitivity with respect to disturbances.
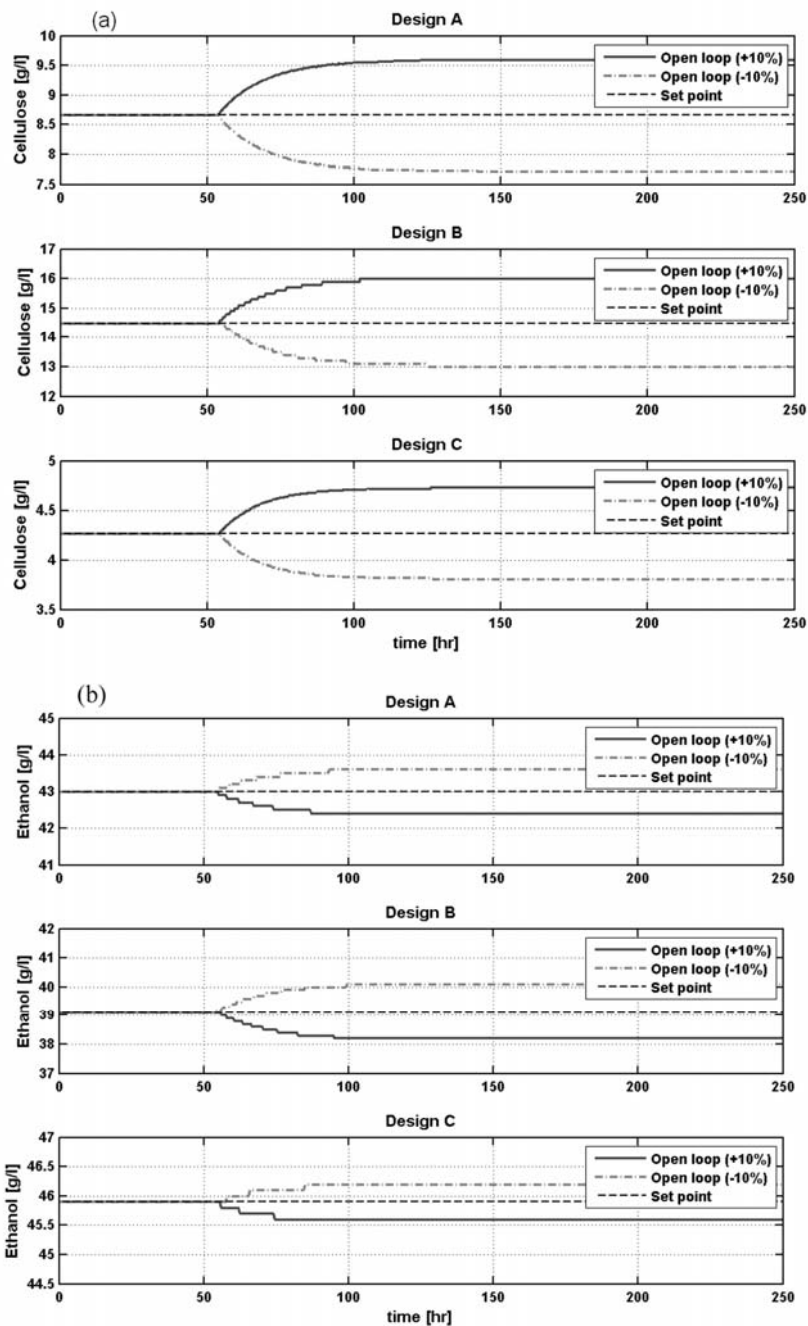
Fig. 5.10. Open loop dynamic behavior of: (a) cellulose and (b) ethanol concentrations when ±10% change in the inlet cellulose flowrate is applied.

Next, the closed loop analysis was performed to verify the controller performance in rejecting the effect of disturbance and also maintaining the ethanol concentration at its set point using a PI−controller for all designs (Points A, B and C). The values of controller tuning parameters for all designs were calculated using the same standard tuning rules (Cohen-Coon tuning method). Fig. 5.11 shows closed loop responses of cellulose and ethanol concentrations at Points A, B, and C. It can be observed that by allowing the set point of the cellulose concentration to change (increase or decrease) when a ±10% change in the inlet cellulose flowrate is applied, maintains the ethanol concentration at its set point. These results show that this control strategy (allowing set point to change) is effective in rejecting the effect of disturbance and also to maintain the ethanol concentration at its desired value for all reactor designs (Points A, B, C). It can also be observed that, the overshoot at Point A for ethanol is much smaller than for the other points which indicates much better closed loop performance.

As a summary, the results illustrate the capability of the *IPDC* methodology to obtain the optimal process-controller design solution that satisfies design, control and cost criteria for a bioethanol production process. It was also confirmed that design of a reactor at the maximum point of the attainable region leads to a process with lower sensitivity with respect to disturbance and better controller performance in terms of rejecting the effect of disturbance and maintaining its desired product concentration.
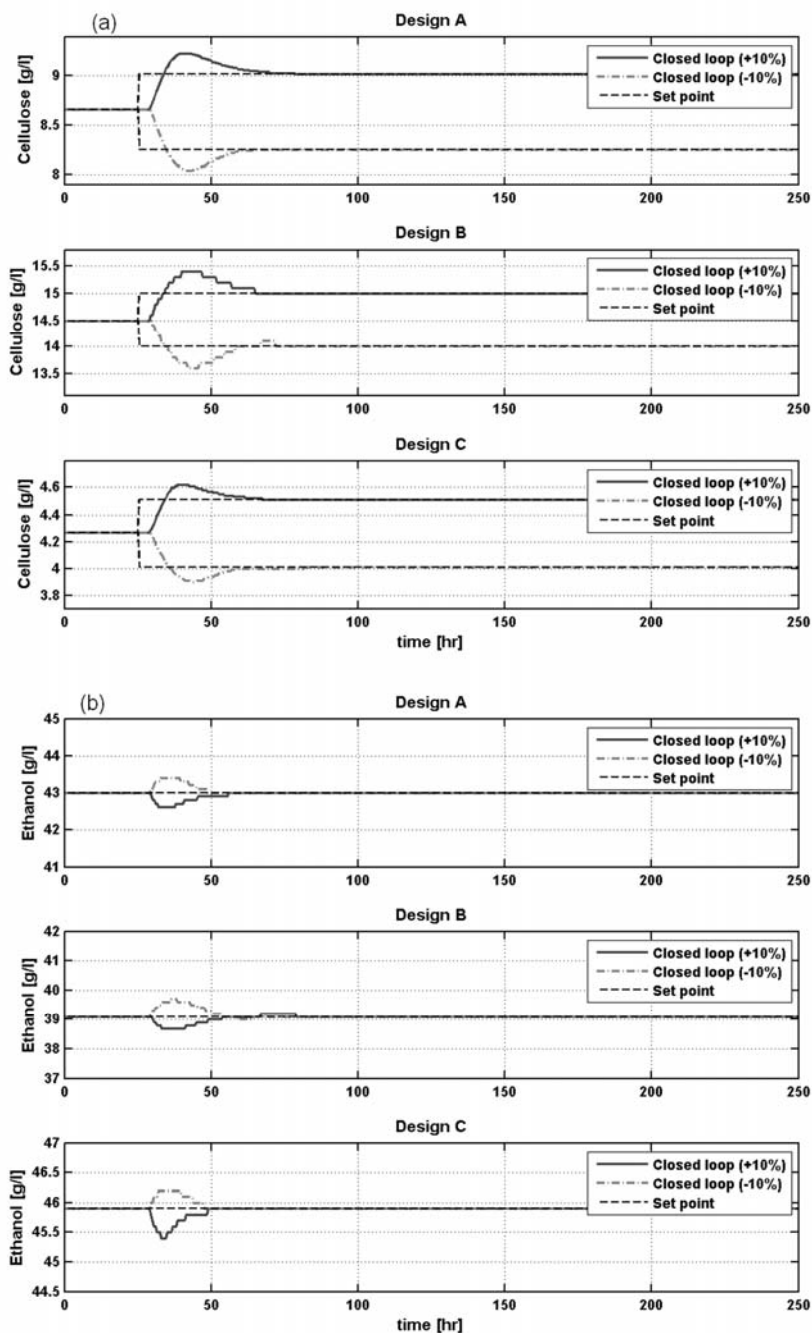
Fig. 5.11. Closed loop analysis with a PI-controller – response of (a) cellulose and (b) ethanol concentrations to ±10% change in the inlet cellulose flowrate.

5.2 Applications of the Methodology for a Single Separator System

The application of the methodology in solving a single separator system is illustrated in this section. The application of the *ICAS-IPDC* is illustrated for solving the separation system using a distillation column. Two case studies have been implemented to illustrate the capability of the proposed methodology which are an ethylene glycol separation process (will be discussed in details in this section) and a methyl acetate separation process (only the results are summarized in this section).

5.2.1 Ethylene Glycol Separation Process

5.2.1.1 Process Description

The application of the *ICAS-IPDC* is illustrated for the separation system of an ethylene glycol (*EG*) process. We consider the following situation. The effluent stream from an *EG* reactor is fed to a distillation column where it is split into two streams of specified purity – bottom product (stream B with mainly *EG*, Diethylene Glycol, *DEG* and Triethylene Glycol, *TEG*) and distillate product (stream D containing 99.5% of unreacted water, *W* and 100% Ethylene Oxide, *EO*). A scheme of the process is depicted in Fig. 5.12. The process is operated at a nominal operating point as specified in Table 5.10.

The objective is then to determine the design-control solution in which the multi-objective function with respect to design, control and cost criteria is optimal. This can be achieved by formulating the above problem as an *IPDC* problem as shown below.

5.2.1.2 Problem formulation

The *IPDC* problem for the process described above is defined in terms of a performance objective (with respect to design, control and cost), and the three sets of constraints (process, constitutive and conditional).
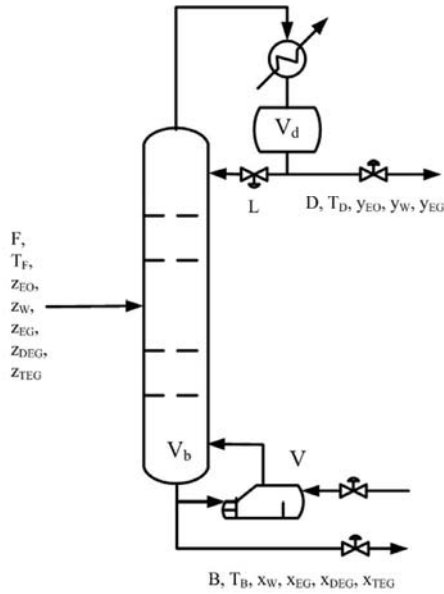
Fig. 5.12. Distillation column for an ethylene glycol process.

Table 5.10
Nominal operating point of the ethylene glycol separation process.

Variable	Value	Description
F	12.279	Feed flowrate (kmol/h)
B	4.00	Bottom flowrate (kmol/h)
T_F	343	Feed temperature (K)
P	5	Feed pressure (atm)
z_{EO}	0.1856	Feed EO composition
z_W	0.4886	Feed W composition
z_{EG}	0.1358	Feed EG composition
z_{DEG}	0.0770	Feed DEG composition
z_{TEG}	0.1130	Feed TEG composition
N	10	Number of stages

$$\max \quad J = w_{1,1}P_{1,1} + w_{2,1}\left(\frac{1}{P_{2,1}}\right) + w_{2,2}P_{2,2} + w_{3,1}\left(\frac{1}{P_{3,1}}\right) + w_{3,2}\left(\frac{1}{P_{3,2}}\right) \tag{5.32}$$

subjected to:

Process (dynamic and/or steady state) constraints

Total mass balance for each stage:

$$\frac{dM_1}{dt} = L_2 - V_1 - L_1 + F_1 \tag{5.33}$$

$$\frac{dM_j}{dt} = V_{j-1} + L_{j+1} - V_j - L_j + F_j \tag{5.34}$$

$$\frac{dM_N}{dt} = V_{N-1} - V_N - D - L_N + F_N \tag{5.35}$$

Component balance for each stage:

$$\frac{dM_{i,1}}{dt} = L_2 x_{i,2} - V_1 y_{i,1} - L_1 x_{i,1} + F_1 z_{i,1} \tag{5.36}$$

$$\frac{dM_{i,j}}{dt} = V_{j-1} y_{i,j-1} + L_{j+1} x_{i,j+1} - V_j y_{i,j} - L_j x_{i,j} + F_j z_{i,j} \tag{5.37}$$

$$\frac{dM_{i,N}}{dt} = V_{N-1} y_{i,N-1} - V_N y_{i,N} - D x_{i,N} - L_N x_{i,N} + F_N z_{i,N} \tag{5.38}$$

Energy balance for each stage:

$$\frac{dU_1}{dt} = L_2 h_2^l - V_1 h_1^v - L_1 h_1^l + F_1 h_1^f + Q_r \tag{5.39}$$

$$\frac{dU_j}{dt} = V_{j-1} h_{j-1}^v + L_{j+1} h_{j+1}^l - V_j h_j^v - L_j h_j^l + F_j h_j^f \tag{5.40}$$

$$\frac{dU_N}{dt} = V_{N-1} h_{N-1}^v - V_N h_N^v - D h_N^l - L_N h_N^l + F_N h_N^f - Q_c \tag{5.41}$$

Constitutive (thermodynamic) constraints

$$F_{Di} = y_{i,j} - x_{i,j} \tag{5.42}$$

$$y_{i,j} = \frac{\alpha_{i,jk} x_{i,j}}{1 + x_{i,j}(\alpha_{i,jk} - 1)} \tag{5.43}$$

$$\alpha_{i,jk} = \frac{K_{i,j}}{K_{j,k}} \tag{5.44}$$

$$K_{i,j} = K_i(T_j, P_j) \tag{5.45}$$

Conditional (process-control) constraints

$$x_W \leq 0.05 \tag{5.46}$$

$$CS = \mathbf{y} + \mathbf{u}Y \tag{5.47}$$

Eq. (5.32) represents the multi-objective function, where $w_{1,1}$, $w_{2,1}$, $w_{2,2}$, $w_{3,1}$ and $w_{3,2}$ are the weight factors assigned to objective function terms $P_{1,1}$, $P_{2,1}$, $P_{2,2}$, $P_{3,1}$ and $P_{3,2}$, respectively. The first objective function term $P_{1,1}$ is the performance criterion for the distillation column design which in this problem is the value of the driving force (F_{Di}). $P_{2,1}$ and $P_{2,2}$ are the sensitivities of the controlled variables $\mathbf{y}$ with respect to disturbances $\mathbf{d}$ and manipulated variables $\mathbf{u}$, respectively, which represent control objective functions. Lastly, $P_{3,1}$ and $P_{3,2}$ represent reboiler and condenser duty, respectively, which determine the operating cost, for the economic objective function.

We assume potential feeds on all of the stages and adopt the following set notation. The number of stages in the column is assumed to be N including both the reboiler and condenser, with stages numbered from the bottom to top. The set $STAGES := \{1, ..., N\}$ will denote the numbered stages and the index, j subscripted to a quantity associated with stage, j. The set $COMP$ denotes the components in the column. The superscripts l and v refer to the quantities associated with the liquid and vapor phases, respectively. Eqs. (5.33)-(5.35) represent the total mass balance for each stage where M_j, L_j, V_j, F_j are the holdup, liquid flowrate, vapor flowrate and feed rate for the jth stage, respectively. Eqs. (5.36)-(5.38) represent the component balance around each stage where $M_{i,j}$, $z_{i,j}$, $x_{i,j}$, $y_{i,j}$ represent the hold-up, feed, liquid and vapor composition of component i for the jth stage, respectively ($i \in COMP$). Eqs. (5.39)-(5.41) represent the energy balance for each stage where the following $U_j(x_j, y_j, T_j)$, $h_j^l(x_j, T_j)$ and $h_j^v(y_j, T_j)$ define the stage holdup internal energy and the specific heat content of liquid and vapor starting from stage j. These are functions of composition of the mixture and stage temperature. h_j^f is the specific enthalpy of the feed stream to stage j and Q_r and Q_c are the reboiler and condenser heat duties, respectively.

Eqs. (5.42)-(5.45) represent the constitutive (thermodynamic) constraints. Eq. (5.42) defines the driving force, which is the difference in composition of component i in two co-existing phases. Eq. (5.43) is the expression for the vapor composition of component i, where $\alpha_{i,jk}$ is the relative volatility of component i with respect to component k as expressed in Eq. (5.44). Eq. (5.45) represents the equilibrium constant of component i which is as a function of temperature and pressure.

Eqs. (5.46)-(5.47) represent conditional (process-control) constraints. Eq. (5.46) is the maximum allowable composition of W at the bottom product stage which determines the quality of the product. Eq. (5.47) represents the controller structure selection.

The *IPDC* problem formulated above is then solved using the proposed decomposition-based solution strategy as shown below.

5.2.1.3 Decomposition-based solution strategy

The summary of the decomposition-based solution strategy for this problem is shown in Table 5.11 and Fig. 5.13. Details of the step-by-step solutions are shown below.

Stage 1: Pre-analysis

The main objective of this stage is to define the operational window within which the optimal solution is located and set the targets for the optimal design-controller solution.

Table 5.11
Mathematical equations and decomposition-based solution for an ethylene glycol distillation column design.

Mathematical equations	Decomposition method	Corresponding variables
Multi-objective function: Eq. (5.32) *Process constraints:* Eqs. (5.33)-(5.41) *Constitutive constraints:* Eqs. (5.42) – (5.45) *Conditional constraints* Product purity: Eq. (5.46) Controller structure: Eq. (5.47)	*Stage 1: Pre-analysis.* a. Variable analysis b. Operational window: Eq. (5.46) c. Design-control target Driving force Eq. (5.42) *Stage 2: Design analysis.* Step-by-step algorithm for a simple distillation design (Gani & Bek-Pedersen, 2000) Eqs. (5.42)-(5.45) and Eqs. (5.33)-(5.41) in steady state *Stage 3: Controller design analysis:* Sensitivity analysis: Eqs. (5.33)-(5.45) Controller structure selection: Eqs. (5.33)-(5.45) and Eq. (5.47). *Stage 4: Final selection and verification* Final selection: Eq. (5.32) Dynamic simulations verification: Eqs. (5.33)-(5.45), (5.47)	N_F, L, V, Q_r, Q_c, y_W, y_{EG}, T_D, x_W, x_{EG}, T_B $x_W \leq 0.05$ $FD = y_W - x_W$, x_W N_F, RR, RB D, L, V, Q_r, Q_c, T_D, T_B dFD/dx_W, dFD/dT dT_B/dV, dx_W/dV, dx_{EG}/dV, dT_D/dL, dy_W/dL, dy_{EG}/dL J
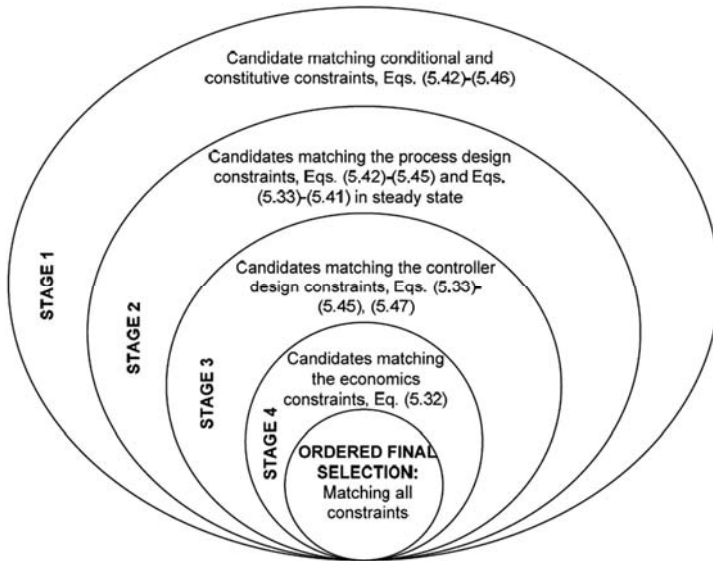
Fig. 5.13. Decomposition-based solution for an ethylene glycol distillation column design.

Step 1.1: Variables analysis

The first step in Stage 1 is to perform variable analysis. All variables involved in this process are analyzed and classified as design and manipulated variables **u**, process-controlled variables **y**, and disturbances **d** as shown in Table 5.12. Then, the important **u** and **y** are selected with respect to the multi-objective function, Eq. (5.32), and tabulated in Table 5.13. Design variables $\mathbf{u}_d = [N_F, Q_r, Q_c]$ are important because by knowing the optimal N_F, the optimal Q_r and Q_c can be obtained which are directly related to the operating costs ($P_{3,1}$ and $P_{3,2}$). On the other hand, manipulated variables $\mathbf{u}_m = [V, L]$ are selected since they are the potential candidates for the manipulated variables and directly related to the objective function $P_{2,2}$. Process-controlled variables $\mathbf{y}_m = [x_{D,W}, x_{D,EG}, x_{B,W}, x_{B,EG}, T_D, T_B]$, are selected since they are the important variables that need to be monitored and controlled in order to obtain the smooth, operable and controllable process, which is also directly related to the objective function $P_{2,1}$.

Table 5.12
List of all design and manipulated variables, process-controlled variables and disturbances for an ethylene glycol distillation column design.

Design variable ($\mathbf{u}_d$)	N_F, RR, RB, Q_r, Q_c
Manipulated variable ($\mathbf{u}_m$)	B, D, V, L
Process-Controlled variables (**y**)	$x_{D,EO}$, $x_{D,W}$, $x_{D,EG}$, $x_{D,DEG}$, $x_{D,TEG}$, $x_{B,EO}$, $x_{B,W}$, $x_{B,EG}$, $x_{B,DEG}$, $x_{B,TEG}$, T_D, T_B
Disturbances (**d**)	T, z_W, z_{EG}

126

Table 5.13
List of important design and manipulated and process-controlled variables for an ethylene glycol distillation column design.

Design variable ($\mathbf{u}_d$)	N_F, Q_r, Q_c
Manipulated variable ($\mathbf{u}_m$)	V, L
Process-Controlled variables ($\mathbf{y}_m$)	$x_{D,W}$, $x_{D,EG}$, $x_{B,W}$, $x_{B,EG}$, T_D, T_B

Step 1.2: Operational window identification

The operational window is identified based on bottom and top product purity. Since the desired product is recovered at the bottom, for that reason, its quality should be monitored and controlled. On the other hand, since most of the unreacted reactants are recovered at the top, their purity will not be monitored and controlled because this stream will be recycled back to the reactor. In order to satisfy product quality, the bottom water composition x_W should be less than 0.05.

Step 1.3: Design-control target identification

The step-by-step algorithm for a simple distillation column proposed by Gani and Bek-Pedersen (2000) is implemented here. The driving force diagram for the *W-EG* (key component of the binary pair) system at $P = 5$ atm is drawn as shown in Fig. 5.14. Driving force is a measure of the relative ease of separation. The larger the driving force, the easier the separation is. In this graphical method, the target for the optimal process-controller design solution for the distillation column is identified at the maximum point of the driving force (Point A) (see Fig. 5.14). In Fig. 5.14 also, two other points which are not at the maximum are identified as candidate alternative designs. From a process design point of view, they are not optimal since at these points the value of the driving force is smaller hence separation at these points is more difficult. Therefore, from a design perspective, Point A is the optimal solution for distillation column design (this claim will be verified in Stage 4).
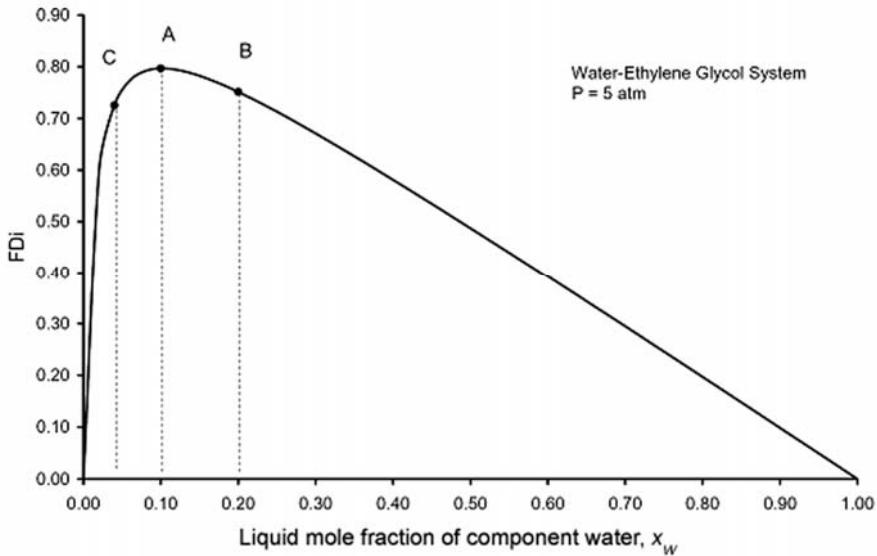
Fig. 5.14. Driving force diagram for the separation of Water-Ethylene Glycol by a distillation column.

Stage 2: Design analysis

The objective of this stage is to validate the target identified in Stage 1 by finding the acceptable values of **y** and **u**. In this stage, the search space defined in Stage 1 is further reduced.

Step 2.1: Design-manipulated and process-controlled variables value calculation

The established targets (points A, B, C) in Fig. 5.14 are now matched by finding the acceptable values of design variables (e.g. feed stage, N_F and reflux ratio, RR). The values of the design variables are determined graphically as shown in Fig. 5.15. Table 5.14 summarizes the results obtained graphically with respect to design variables for three different design alternatives. With specified values of N, N_F, RR, product purity, and feed conditions, the design of distillation column is verified using a steady state process model - Eqs. (5.33)-(5.45), to find values of other design-process variables. Results of the steady state simulation for different design alternatives are tabulated in Table 5.15. It can be noted that design at the maximum point of driving force (Point A) corresponds to the minimum with respect to energy consumption compared to other points, which is also confirmed by Gani and Bek-Pedersen (2000).

Table 5.14
Values of design variables for different design alternatives of ethylene glycol distillation column design.

Point	Design Variables					
	N	N_F	RR_{min}	RB_{min}	RR	RB
A	10	9	0.94	15.93	1.12	19.12
B	10	8	1.00	5.01	1.20	6.00
C	10	10	0.80	72.51	0.96	87.01

Table 5.15
Steady state simulation results for different design alternatives of ethylene glycol distillation column design.

Variables	Point A	Point B	Point C
	Feed		
F (kmol/h)	12.279	12.279	12.279
T (K)	343	343	343
P (atm)	5	5	5
N_F	9	8	10
z_{EO}	0.1856	0.1856	0.1856
z_W	0.4886	0.4886	0.4886
z_{EG}	0.1358	0.1358	0.1358
z_{DEG}	0.0770	0.0770	0.0770
z_{TEG}	0.1130	0.1130	0.1130
	Distillate		
D (kmol/h)	8.28	8.28	8.28
L (kmol/h)	9.31	9.95	62.62
T_D (K)	338	343	363
$x_{D,EO}$	0.2753	0.2753	0.2753
$x_{D,W}$	0.7247	0.7231	0.7214
$x_{D,EG}$	0.0152	0.0004	0.0241
$x_{D,DEG}$	0.0008	0.0000	0.0134
$x_{D,TEG}$	0.0003	0.0000	0.0196
Q_c (kJ/h)	663.06	667.74	2081.57
	Bottom		
B (kmol/h)	4.00	4.00	4.00
V (kmol/h)	45.48	34.18	111.54
T_B (K)	343	353	329
$x_{B,EO}$	0.0000	0.0000	0.0000
$x_{B,W}$	0.0000	0.0032	0.0068
$x_{B,EG}$	0.3853	0.4161	0.3670
$x_{B,DEG}$	0.2347	0.2364	0.2287
$x_{B,TEG}$	0.3463	0.3469	0.3464
Q_r (kJ/h)	25.72	41.53	68.05
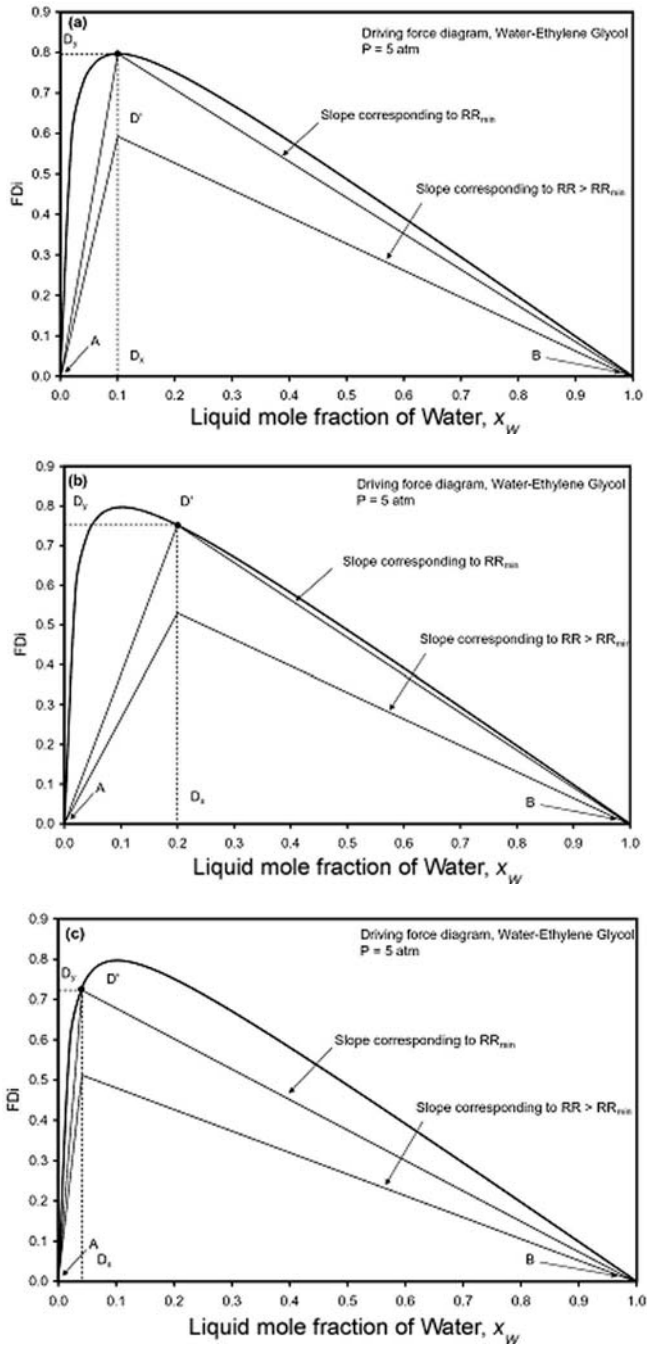
Fig. 5.15. Driving force diagram with illustration of the distillation design parameters at: (a) Point A; (b) Point B; and (c) Point C for the separation of Water-Ethylene Glycol.

Stage 3: Controller design analysis

The objective of this stage is to evaluate and validate the controllability performance of the feasible candidates in terms of their sensitivities with respect to disturbances and manipulated variables.

Step 3.1: Sensitivity analysis

The process sensitivity is analyzed by calculating the derivative values of the controlled variables with respect to disturbances $d\mathbf{y}/d\mathbf{d}$ with a constant step size using the dynamic process models of Eqs. (5.33)-(5.41) with the constitutive model of Eqs. (5.42)-(5.45). Fig. 5.16(b) shows plots of the derivative of F_{Di} with respect to x_W and T, and values of derivatives for different designs are given in Table 5.16.

Fig. 5.16. (a) Driving force diagram for the separation of Water-Ethylene Glycol by distillation; (b) corresponding derivatives of the driving force with respect to composition and temperature.

It can be seen that the derivative values are smaller for reactor design A compared to other designs (B and C). A smaller value of the derivative means that the process sensitivity is lower (Russel et al., 2002) hence, from a process control point of view, reactor design A is less sensitive to the effect of disturbances which makes it more robust in maintaining its controlled variables in the presence of disturbances.

Table 5.16
Derivatives values of F_{Di} with respect to x_W and T at different distillation designs for an ethylene glycol separation system.

Distillation Design	Derivative	
	dF_{Di}/dx_W	dF_{Di}/dT
A	0.1259	0.0004
B	0.7354	0.0028
C	2.3975	0.0058

According to Russel et al. (2002), the derivative of θ with respect to $\mathbf{x}$, $d\theta/d\mathbf{x}$ indirectly influences process sensitivity and controller structure selection. In this example, $d\theta/d\mathbf{x}$ is represented by dF_{Di}/dx_w. Accordingly, $dx_{B,W}/dT_f$ and $dx_{D,EG}/dT_f$ can be represented as:

$$\frac{dx_{B,W}}{dT_f} = \left(\frac{dx_{B,W}}{dF_{Di}} \right) \left(\frac{dF_{Di}}{dx_W} \right) \left(\frac{dx_W}{dT_f} \right) \tag{5.48}$$

$$\frac{dx_{D,EG}}{dT_f} = \left(\frac{dx_{D,EG}}{dF_{Di}} \right) \left(\frac{dF_{Di}}{dx_W} \right) \left(\frac{dx_W}{dT_f} \right) \tag{5.49}$$

Since values for dF_{Di}/dx_W are readily obtained (see Fig. 5.16b), values for $dx_{B,W}/dF_{Di}$ and $dx_{D,EG}/dF_{Di}$ can be obtained from Eqs. (5.42)-(5.43) and also values for dx_W/dT_f can be obtained from Eqs. (5.39)-(5.41), it is possible to gain useful insights related to process sensitivity. It can clearly be seen from Fig. 5.16b and from Table 5.16, that the value of dF_{Di}/dx_W is smaller for distillation design A compared to other designs. Since dF_{Di}/dx_W is smaller at design A, therefore, for any values of $dx_{B,W}/dF_{Di}$, $dx_{D,EG}/dF_{Di}$ and dx_W/dT_f will result in smaller value of $dx_{B,W}/dT_f$ and $dx_{D,EG}/dT_f$. Small value of $dx_{B,W}/dT_f$ and $dx_{D,EG}/dT_f$ mean that the bottom and top product purity is less sensitive to the changes in T_f. According to Russel et al. (2002), a process with lower sensitivity will have a higher process flexibility. In this case, distillation design A will be more flexible to adsorb the changes in disturbances than distillation designs B and C. Therefore, from a control point of view, distillation design A is less sensitive and more flexible to adsorb the disturbances. This will be verified in Stage 4.

Step 3.2: Controller structure selection

Next, the controller structure is selected by calculating the derivative values of potential controlled variables ($x_{B,W}$, $x_{B,EG}$, T_B, $x_{D,W}$, $x_{D,EG}$, T_D) with respect to the

potential manipulated variables (V and L) with a constant step size by using the dynamic process models of Eqs. (5.33)-(5.41) with the constitutive model of Eqs. (5.42)-(5.45). The objective of this step is to select the best controller structure (pairing of controlled-manipulated variables) which can satisfy the control objective (maintaining top and bottom product purity which are represented by $x_{D,EG}$ and $x_{B,W}$ purity at their optimal set point in the presence of disturbances). All values of derivatives at different distillation designs are tabulated in Table 5.17. Fig. 5.17 shows derivative plots of T_B-V and T_D-L for three distillation design alternatives.

According to Russel et al. (2002), $dx_{B,W}/dV$ and $dx_{D,EG}/dL$ can be represented as:

$$\frac{dx_{B,W}}{dV} = \left(\frac{dx_{B,W}}{dF_{Di}}\right)\left(\frac{dF_{Di}}{dx_W}\right)\left(\frac{dx_W}{dT_B}\right)\left(\frac{dT_B}{dV}\right) \approx 0 \tag{5.50}$$

$$\frac{dx_{D,EG}}{dL} = \left(\frac{dx_{D,EG}}{dF_{Di}}\right)\left(\frac{dF_{Di}}{dx_W}\right)\left(\frac{dx_W}{dT_D}\right)\left(\frac{dT_D}{dL}\right) \approx 0 \tag{5.51}$$

Since $dx_{B,W}/dV \approx 0$ and $dx_{D,EG}/dL \approx 0$, it is possible to maintain $x_{B,W}$ and $x_{D,EG}$ at their optimal set point using concentration control or temperature control. On the other hand, since values for dF_{Di}/dx_W are readily obtained (see Fig. 5.16b), values for $dx_{B,W}/dF_{Di}$ and $dx_{D,EG}/dF_{Di}$ can be obtained from Eqs. (5.42)-(5.43) and also values for dT_B/dV and dT_D/dL can be obtained from Eqs. (5.39)-(5.41), it is possible to gain useful insights related to controller structure.

Table 5.17
Derivative values of potential controlled variables with respect to potential of manipulated variables at different distillation designs for an ethylene glycol separation system.

Distillation Design	Derivatives with respect to V					
	$dx_{B,W}/dV$	$dx_{B,EG}/dV$	dT_B/dV	$dx_{D,W}/dV$	$dx_{D,EG}/dV$	dT_D/dV
A	0.0000	0.0004	0.3154	0.0000	0.0002	0.1500
B	0.0005	0.0000	0.0889	0.0002	0.0000	0.1333
C	0.0004	0.0000	0.7059	0.0002	0.0000	0.0911
Distillation Design	Derivatives with respect to L					
	$dx_{B,W}/dL$	$dx_{B,EG}/dL$	dT_B/dL	$dx_{D,W}/dL$	$dx_{D,EG}/dL$	dT_D/dL
A	0.0000	0.0016	0.2679	0.0000	0.0016	23.43
B	0.0015	0.0002	1.417	0.0007	0.0001	23.17
C	0.0015	0.0007	4.029	0.0007	0.0003	4.4504

It can clearly be seen from Fig. 5.17 and from Table 5.17, that derivative values of dT_B/dV and dT_D/dL are higher than other derivatives. Higher values of this derivative mean that the process has higher process gain. From a process control point of view, a process with a large process gain will require a small control action in order

to maintain the controlled variable at its optimal set point value. Therefore, it can clearly be seen from Table 5.17, that the best pairing of controlled-manipulated variable that will able to maintain product purity at the bottom of the distillation column is T_B-V, whereas the best pairing for controlling product purity at the top of the distillation column is T_D-L. These controller structures will require less control action in maintaining column product purity compared to controller structures that control the product compositions directly. It should be noted that, at point A, the controller action and performance are at the best. This claim will be verified in Stage 4 using closed loop dynamic simulations and relative gain array (*RGA*) tests.

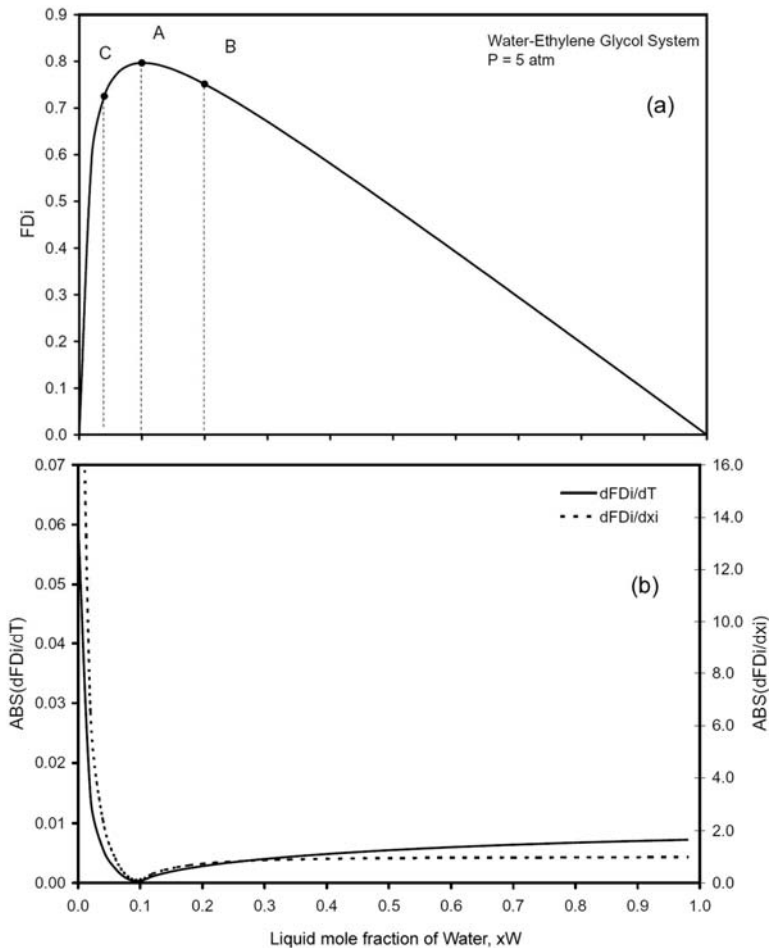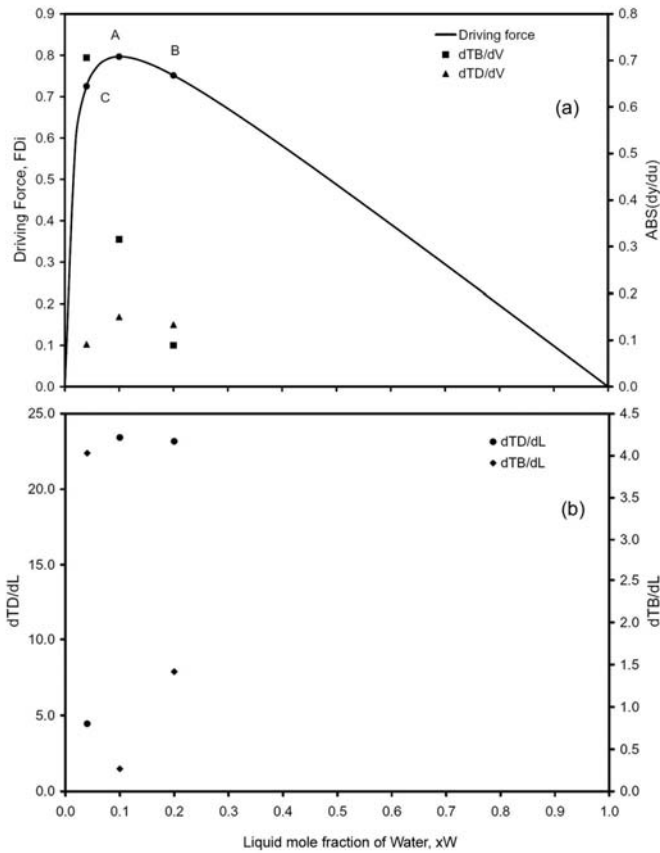**Fig. 5.17.** (a) Driving force diagram for the separation of Water-Ethylene Glycol by distillation with corresponding derivatives of T_B and T_D with respect to V; (b) corresponding derivatives of T_B and T_D with respect to L.

Stage 4: Final selection and verification

The objective of this stage is to select the best candidates by analyzing the value of the multi-objective function, Eq. (5.32).

Step 4.1: Final selection: Verification of design

The multi-objective function, Eq. (5.32) is calculated by summing up each terms of the objective function value. In this case, all the objective function terms are weighted equally meaning that the decision-maker does not have any preference for one objective over another. Since the range and unit of each objective function values can be different, each objective value is normalized with respect to its maximum value. Details are given in Table 5.18. $P_{1,1s}$ corresponds to the scaled value of the driving force, F_{Di}. $P_{2,1s}$ and $P_{2,2s}$ are scaled values of dF_{Di}/dx_W and dT_D/dL representing the sensitivity of F_{Di} with respect to T and the sensitivity of the top column temperature T_D with respect to L, respectively. $P_{3,1s}$ is the scaled value of the condenser duty Q_c and $P_{3,2s}$ is the scaled value of the reboiler duty Q_r, which represent the operating cost. It can be seen that the value of the multi-objective function J for the distillation column design A is higher than other designs. Therefore, it is verified that, distillation column design A is the optimal solution for the integrated process design and controller design of an ethylene glycol separation process which satisfies design, control and cost criteria. It should be noted that a qualitative analysis (J highest for point A) is sufficient for the purpose of controller structure selection.

Table 5.18
Multi-objective function calculation. The best candidate is highlighted in bold.

Distillation Design	$P_{1,1}$	$P_{2,1}$	$P_{2,2}$	$P_{3,1}$	$P_{3,2}$	
A	0.7967	0.0004	23.43	663.06	25.72	
B	0.7513	0.0028	23.17	667.74	41.53	
C	0.7251	0.0058	4.45	2081.57	68.05	
	$P_{1,1s}$	$P_{2,1s}$	$P_{2,2s}$	$P_{3,1s}$	$P_{3,2s}$	J
A	1.0000	0.0648	1.0000	0.3185	0.3780	**23.21**
B	0.9430	0.4910	0.9892	0.3208	0.6103	8.72
C	0.9101	1.0000	0.1900	1.0000	1.0000	4.10

Step 4.2: Dynamic rigorous simulations: verification of controller performance

In order to further verify the controller structure performances, simulations of a closed loop regulator problem using a PI-controller for all distillation designs (points A, B and C) are performed. The value of controller tuning parameters for all designs was calculated using the same standard tuning rules. The closed loop responses are shown in Figs. 5.18-5.19.
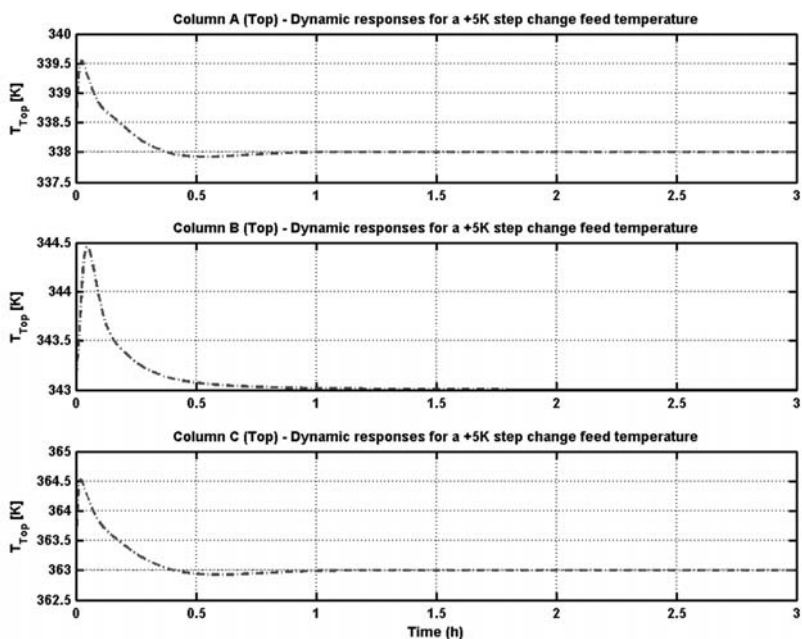
(a)
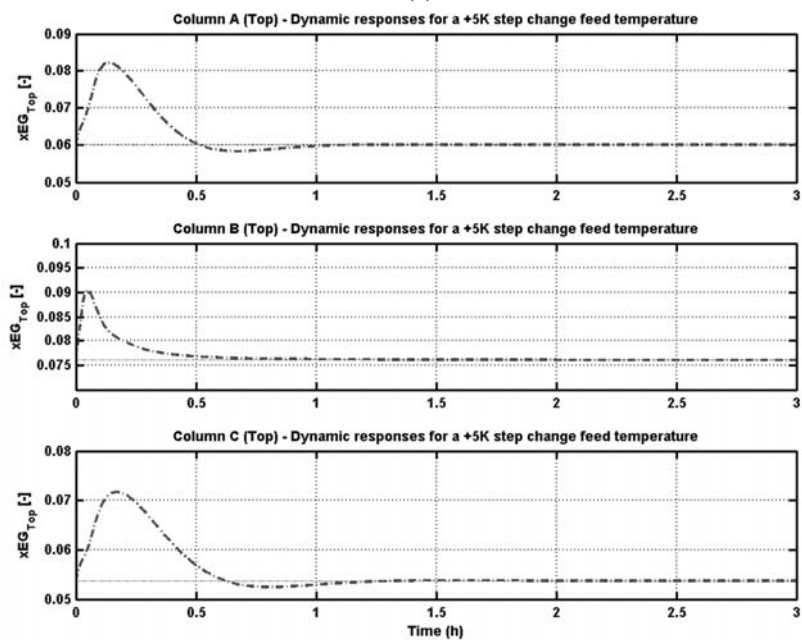
(b)

Fig. 5.18. Regulator problem – Closed loop responses of (a) top column temperature; and (b) top ethylene glycol composition to a +5K step change in feed temperature for different distillation designs.

In the regulator problem, the closed loop performance in terms of its ability to reject disturbance and to keep the minimum $x_{D,EG}$ and $x_{B,W}$ steady state offsets are verified. To this end, a +5K step change is applied to the feed temperature T_f which moves the top and bottom reactor temperatures away from their set points (points A, B and C). According to Fig. 5.16b, any changes in the T at points B and C will easily move $x_{D,EG}$ and $x_{B,W}$ away from their steady state values and as a result, it will be more difficult to maintain $x_{D,EG}$ and $x_{B,W}$ at these points compared to at point A.

Fig. 5.18 shows the closed loop responses of top column temperature and ethylene glycol composition, when a +5K step change is applied to the feed temperature at points A, B and C. One can observe that the effect of the disturbance is successfully rejected by the controller at all points (see Fig. 5.18a). This result shows that the selected controller structure (pairing of T_D-L) is the best pair that performs very well in rejecting the effect of disturbance. It can also be seen that all top temperature responses settle after t = 1 h. The same percentage of overshoot was observed for all responses. The results of closed loop performances are tabulated in Table 5.19.

Table 5.19
Closed loop performances (top control loop) of regulator problem for ethylene glycol separation process.

Distillation Design	Top Temperature Response		
	Settling time (h)	*Overshoot (%)*	*Offset*
A	1	0.44	-
B	1	0.44	-
C	1	0.41	-
Distillation Design	Top $x_{D,EG}$ Response		
	Settling time (h)	*Overshoot (%)*	*Offset*
A	1	30	-
B	1	20	-
C	1.2	33	-

From Fig. 5.18b, it can be clearly seen that no steady state offset is observed for the product $x_{D,EG}$ composition, for all points. This shows the effectiveness of the controller (controller structure) in maintaining its desired product concentration in the presence of disturbance. It can also be seen that the $x_{D,EG}$ response at point C settles after t = 1.2 h, whereas at points A and B it settles after t = 1 h. In terms of overshoot, bigger percentages are observed for all points which is exceeded the maximum percentage suggested by Skogestad and Postlethwaite (2007) (maximum value is 20%). It should be noted here that, although a bigger percentage of overshoot is observed, it will not affect the overall performance of the process since the top product will be recycled back to the reactor. Therefore, the top composition is loosely controlled here.
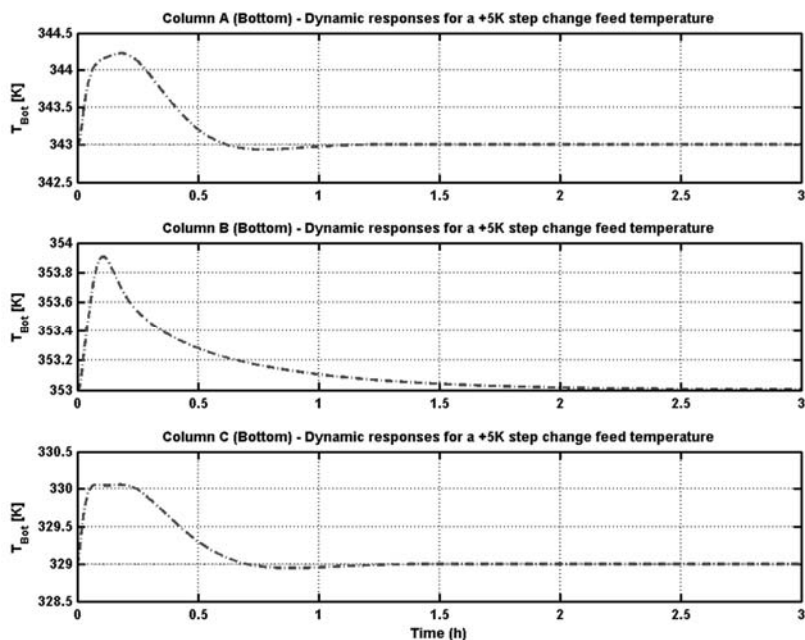
(a)
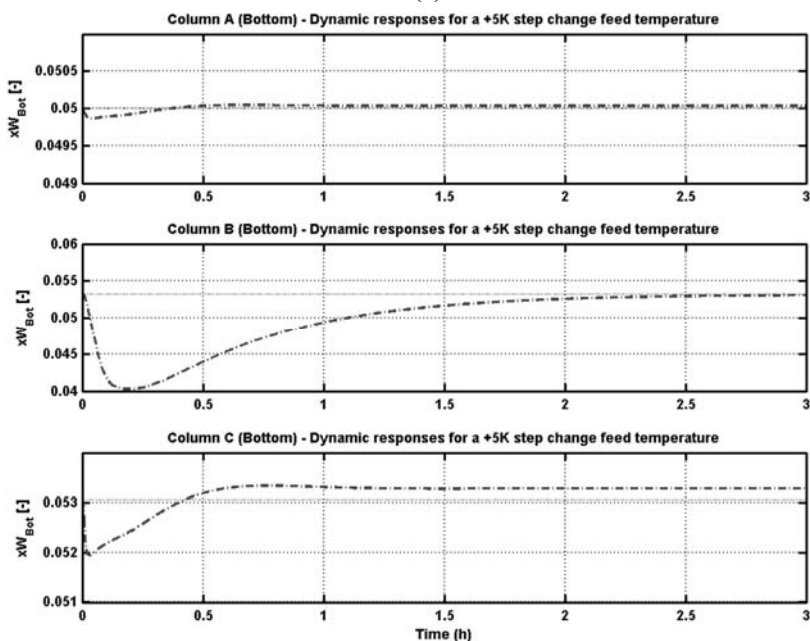
(b)

Fig. 5.19. Regulator problem – Closed loop responses of (a) bottom column temperature; and (b) bottom water composition to a +5K step change in feed temperature for different distillation designs.

Fig. 5.19 shows the closed loop responses of bottom column temperature and water composition, when a +5K step change is applied to the feed temperature at points A, B and C. One can observe that the effect of the disturbance is successfully rejected by the controller at all points (see Fig. 5.19a). This result shows that the selected controller structure (pairing of T_B-V) is the best pair that performs very well in rejecting the effect of disturbance. The results of closed loop performances for bottom temperature control are tabulated in Table 5.20.

Table 5.20
Closed loop performances (bottom control loop) of regulator problem for the ethylene glycol separation process.

Distillation Design	Bottom Temperature Response		
	Settling time (h)	Overshoot (%)	Offset
A	1.2	0.38	0.00
B	2.5	0.25	0.00
C	1.5	0.30	0.00
Distillation Design	Bottom $x_{B,W}$ Response		
	Settling time (h)	Overshoot (%)	Offset
A	0.5	0.40	0.00
B	2.5	26	0.00
C	1.0	2.0	0.01

From Fig. 5.19b, it can be clearly seen that no steady state offset is observed for the product $x_{B,W}$ composition, for all points. This shows the effectiveness of the controller (controller structure) in maintaining its desired product concentration in the presence of disturbances. It can also be seen that the closed loop performance of point A is much better than at other points. For example, the settling times and the bottom $x_{B,W}$ response overshoot are much smaller. The reason for this better performance is that, at point A, which is at the maximum point of the driving force, the control action required is at minimum since at that point, the process has minimum sensitivity with respect to the disturbance. To further verify this statement, a relative gain array (*RGA*) has been calculated for all design points as follows:

We consider this case study as a 2 x 2 distillation system where the input **u** = [V L] and the output **y** = [$x_{B,W}$ $x_{D,EG}$] for which we have a steady state gain for all points taken from Table 5.17. The general expression of steady state gain is

$$G = \begin{matrix} & V & L \\ T_B & \begin{bmatrix} K_{11} & K_{12} \\ T_D & K_{21} & K_{22} \end{bmatrix} \end{matrix}$$

$$G_A = \begin{bmatrix} -0.3154 & -0.2679 \\ 0.1500 & 23.43 \end{bmatrix}, \; G_B = \begin{bmatrix} -0.0889 & -1.417 \\ 0.1333 & 23.17 \end{bmatrix}, \; G_C = \begin{bmatrix} 0.7059 & -4.029 \\ 0.0911 & 4.4504 \end{bmatrix}$$

The corresponding *RGA* is calculated as

$$\Lambda(G_A) = \begin{bmatrix} 1.006 & -0.006 \\ -0.006 & 1.006 \end{bmatrix}, \ \Lambda(G_B) = \begin{bmatrix} 1.101 & -0.101 \\ -0.101 & 1.101 \end{bmatrix}, \ \Lambda(G_C) = \begin{bmatrix} 0.895 & 0.105 \\ 0.105 & 0.895 \end{bmatrix}$$

It was suggested to pair the controlled and manipulated variables so that the corresponding relative gains are positive and as close to one as possible. It can clearly be seen that *RGA* element at point A is close to one, while for other points they are much further from one. Since the *RGA* element at point A is close to one, interactions between two closed loops are negligible. This explains why the closed loop performance at point A is much better than at other points.

5.2.1.4 Summary

As a summary, the results of this case study reveal the potential use of the methodology in solving *IPDC* problem of a single distillation column with the help of the driving force diagram. It was confirmed that designing a distillation column at the maximum point of the driving force leads to a process with lower energy requirements and much better closed loop performances than any other points. In general, this application has shown that the methodology is viable and provides an optimal solution of the *IPDC* problem for a single separator system in a systematic way.

5.2.2   Methyl Acetate Separation Process

5.2.1.1 Process Description

We consider the following situation. The effluent from the methyl acetate reactor is fed to a distillation column where it is then split into two streams of specified purities – bottom product (stream B with mainly Water, *W* and Acetic Acid, *HOAc*) and distillate product (stream D containing 99.5% of unreacted Methanol, *MeOH* and 100% of product Methyl Acetate, *MeOAc*). The process is operated at a nominal operating point as specified in Table 5.21. The objective is then to determine the design-control solution in which the multi-objective function with respect to design, control and cost criteria is optimal.

The *IPDC* problem is formulated in terms of a performance objective (with respect to design, control and cost), and a set of constraints: process (dynamic and/or steady state), constitutive (thermodynamic) and conditional (process-control specification) as expressed in Eqs. (5.32)-(5.47).

Table 5.21
Nominal operating point of the methyl acetate separation process.

Variable	Value	Description
F	60.00	Feed flowrate (kmol/h)
B	30.00	Bottom flowrate (kmol/h)
T_F	303	Feed temperature (K)
P	1	Feed pressure (atm)
z_{MeOAc}	0.1508	Feed *MeOAc* composition
z_{MeOH}	0.3492	Feed *MeOH* composition
z_W	0.1508	Feed *W* composition
z_{HOAc}	0.3492	Feed *HOAc* composition
N	22	Number of stages

5.2.1.2 Summary of the Decomposition-based Solution Strategy

Stage 1: Pre-analysis

First, all variables are analyzed and the important ones are shortlisted with respect to the multi-objective function, Eq. (5.32), and tabulated in Table 5.22. Design variables $\mathbf{u}_d = [N_F, Q_r, Q_c]$ are important because by knowing the optimal N_F, the optimal Q_r and Q_c can be obtained which are directly related to the operating costs ($P_{3,1}$ and $P_{3,2}$). On the other hand, manipulated variables $\mathbf{u}_m = [V, L]$ are selected since they are the potential candidate for the manipulated variables and directly related to the objective function $P_{2,2}$. Process-controlled variables $\mathbf{y}_m = [x_{D,W}, x_{D,MeOH}, x_{B,W}, x_{B,MeOH}, T_D, T_B]$, are selected since they are the important variables that need to be monitored and controlled for the smooth, operable and controllable process, which also directly related to the objective function $P_{2,1}$.

Table 5.22
List of important design and manipulated and process-controlled variables for a methyl acetate distillation column design.

Design variable ($\mathbf{u}_d$)	N_F, Q_r, Q_c
Manipulated variable ($\mathbf{u}_m$)	V, L
Process-Controlled variables ($\mathbf{y}_m$)	$x_{D,W}, x_{D,MeOH}, x_{B,W}, x_{B,MeOH}, T_D, T_B$

The optimal solution with respect to the process-controller design target is first identified using the driving force analysis by locating the maximum point in the driving force diagram as the basis for the separator design. The step-by-step algorithm for a simple distillation column proposed by Gani and Bek-Pedersen (2000) are implemented here. The driving force diagram for the *MeOH-W* (key component of binary pair) system at $P = 1$ atm is drawn as shown in Fig. 5.20.
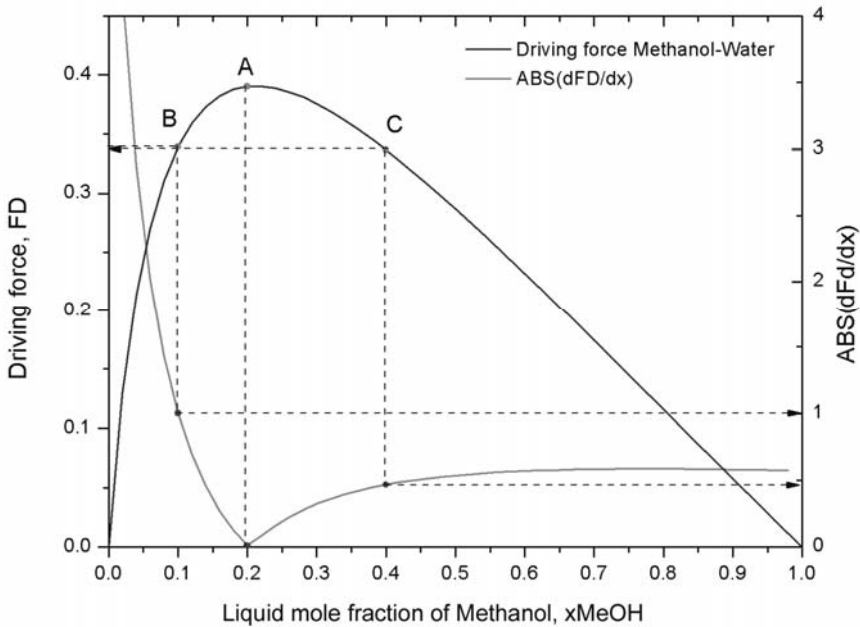
Fig. 5.20. Plot of driving force and derivative of driving force with respect to composition as a function of composition for methanol-water at P = 1 atm.

In this graphical method, the target for the optimal process-controller design solution for distillation column is identified at the maximum point of the driving force (Point A) (see Fig. 5.20). In Fig. 5.20 also, two other points which are not at the maximum are identified as candidate alternative designs. From a process design point of view, they are not optimal since at these points the value of the driving force is smaller hence separation at these points is more difficult. Therefore, from a design perspective, Point A is the optimal solution for distillation column design (this claim will be verified in Stage 4).

Stage 2: Design analysis

The objective of this stage is to validate the target identified in Stage 1 by finding the acceptable values of **y** and **u**. The established targets (points A, B, C) in Fig. 5.20 are now matched by finding the acceptable values of design variables (e.g. feed stage, N_F and reflux ratio, RR). Table 5.23 summarizes the results obtained graphically with respect to design variables for three different design alternatives.

Table 5.23.
Value of design variables of for different design alternatives of a methyl acetate distillation column.

Point	No. Stage	Feed Stage	RB_{min}	RR_{min}	RR
A	22	17	1.9845	0.5505	0.6606
B	22	20	2.6383	0.2800	0.3361
C	22	13	1.7665	1.1727	1.4073

With specified values of N, N_F, RR, product purity, and feed conditions, the design of the distillation column is verified using a steady state process model - Eqs. (5.33)-(5.45), to find values of other design-process variables. Results of the steady state simulation at different design alternatives are tabulated in Table 5.24. It can be noted that design at the maximum point of the driving force (point A) corresponds to the minimum with respect to energy consumption compared to other points, which was also confirmed by Gani and Bek-Pedersen (2000).

Table 5.24.
Steady-state simulation for different design alternatives of a methyl acetate distillation column.

Point	Feed Stage	RR	D (kmol/h)	T_D (K)	T_B (K)	Q_r (MJ/h)	Q_c (MJ/h)
A	17	0.6606	30.82	330.35	384.30	20.95	17.52
B	20	0.3361	47.15	338.81	390.81	23.33	19.94
C	13	1.4073	48.12	328.10	372.57	21.21	19.07

Stage 3: Controller design analysis

The objective of this stage is to evaluate and validate the controllability performance of the feasible candidates in terms of their sensitivities with respect to disturbances and manipulated variables.

Sensitivity analysis

The process sensitivity is analyzed by calculating the derivative values of the controlled variables with respect to disturbances $d\mathbf{y}/d\mathbf{d}$ with a constant step size using the dynamic process models of Eqs. (5.33)-(5.41) with the constitutive model of Eqs. (5.42)-(5.45). Fig. 5.20 shows plots of the derivative of F_{Di} with respect to x_{MeOH}.

Accordingly, $dx_{B,MeOH}/dT_f$ and $dx_{D,W}/dT_f$ can be represented as:

$$\frac{dx_{B,MeOH}}{dT_f} = \left(\frac{dx_{B,MeOH}}{dF_{Di}} \right)\left(\frac{dF_{Di}}{dx_{MeOH}} \right)\left(\frac{dx_{MeOH}}{dT_f} \right) \tag{5.52}$$

$$\frac{dx_{D,W}}{dT_f} = \left(\frac{dx_{D,W}}{dF_{Di}}\right)\left(\frac{dF_{Di}}{dx_{MeOH}}\right)\left(\frac{dx_{MeOH}}{dT_f}\right) \tag{5.53}$$

It can clearly be seen from Fig. 5.20 that the value of dF_{Di}/dx_{MeOH} is smaller for distillation design A compared to other designs. Since dF_{Di}/dx_{MeOH} is smaller at design A, therefore, for any values of $dx_{D,W}/dF_{Di}$, $dx_{B,MeOH}/dF_{Di}$ and dx_{MeOH}/dT_f will result in smaller value of $dx_{B,MeOH}/dT_f$ and $dx_{D,W}/dT_f$. Small value of $dx_{B,MeOH}/dT_f$ and $dx_{D,W}/dT_f$ mean that the bottom and top product purity is less sensitive to the changes in T_f. In this case, the distillation design A will be more flexible to the changes in disturbances than distillation designs B and C. Therefore, from a control point of view, distillation design A is less sensitive and more flexible to the disturbances. This will be verified in Stage 4.

Controller structure selection

Next, the controller structure is selected by calculating the derivative values of potential controlled variables ($x_{B,W}$, $x_{B,MeOH}$, T_B, $x_{D,W}$, $x_{D,MeOH}$, T_D) with respect to the potential manipulated variables (V and L). Fig. 5.21 shows derivative plots of T_B-V and T_D-L for three distillation design alternatives.

According to Russel et al. (2002), $dx_{B,W}/dV$ and $dx_{D,EG}/dL$ can be represented as:

$$\frac{dx_{B,MeOH}}{dV} = \left(\frac{dx_{B,MeOH}}{dF_{Di}}\right)\left(\frac{dF_{Di}}{dx_{MeOH}}\right)\left(\frac{dx_{MeOH}}{dT_B}\right)\left(\frac{dT_B}{dV}\right) \approx 0 \tag{5.54}$$

$$\frac{dx_{D,W}}{dL} = \left(\frac{dx_{D,W}}{dF_{Di}}\right)\left(\frac{dF_{Di}}{dx_{MeOH}}\right)\left(\frac{dx_{MeOH}}{dT_D}\right)\left(\frac{dT_D}{dL}\right) \approx 0 \tag{5.55}$$

Since $dx_{B,MeOH}/dV \approx 0$ and $dx_{D,W}/dL \approx 0$, it is possible to maintain $x_{B,MeOH}$ and $x_{D,W}$ at their optimal set point using concentration control or temperature control.

It can clearly be seen from Fig. 5.21 that derivative values of dT_B/dV and dT_D/dL are higher. Higher values of the derivative mean that the process has a higher process gain. From a process control point of view, a process with a large process gain will require a small control action in order to maintain the controlled variable at its optimal set point value. Therefore, the best pairing of controlled-manipulated variable that will able to maintain product purity at the bottom of the distillation column is T_B-V, whereas the best pairing for controlling product purity at the top of the distillation column is T_D-L.
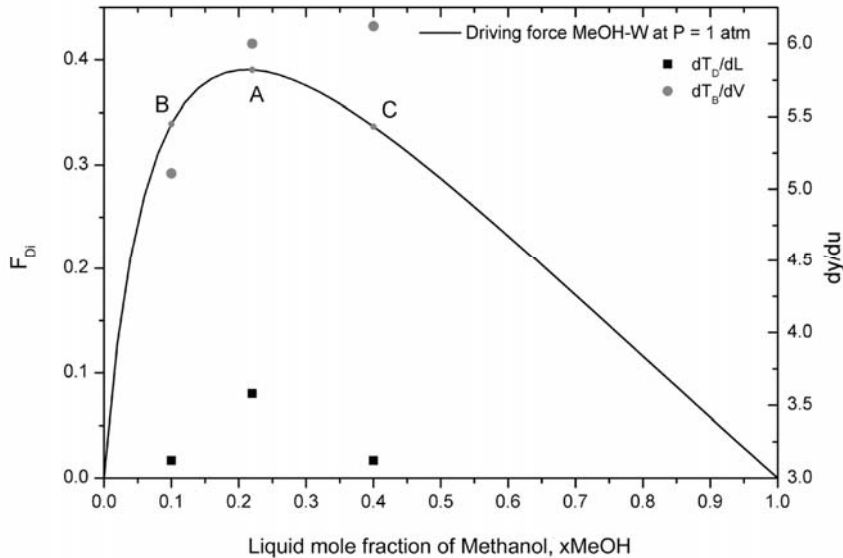
Fig. 5.21. Driving force diagram for the separation of Methanol-Water by distillation with corresponding derivatives of T_B and T_D with respect to V and L.

Stage 4: Final selection and verification

The objective of this stage is to select the best candidates by analyzing the value of the multi-objective function, Eq. (5.32).

Final selection: Verification of design

The multi-objective function, Eq. (5.32) is calculated by summing up each terms of the objective function value as shown in Table 5.25. $P_{1,1s}$ corresponds to the scaled value of the driving force, F_{Di}. $P_{2,1s}$ and $P_{2,2s}$ are scaled values of dF_{Di}/dx_{MeOH} and dT_B/dV, respectively. $P_{3,1s}$ is the scaled value of the condenser duty Q_c and $P_{3,2s}$ is the scaled value of the reboiler duty Q_r, which represent the operating cost. It can be seen that the value of the multi-objective function J for the distillation column design A is higher than other designs. Therefore, it is verified that, distillation column design A is the optimal solution for the integrated process design and controller design of an ethylene glycol separation process which satisfies design, control and cost criteria. It should be noted that a qualitative analysis (J highest for point A) is sufficient for the purpose of controller structure selection.

Table 5.25
Multi-objective function calculation. The best candidate is highlighted in bold.

Distillation Design	$P_{1,1}$	$P_{2,1}$	$P_{2,2}$	$P_{3,1}$	$P_{3,2}$	
A	0.3905	0.0004	6.00	20.95	17.52	
B	0.3392	0.0034	5.11	23.33	19.94	
C	0.3368	0.0045	6.12	21.21	19.07	
	$P_{1,1s}$	$P_{2,1s}$	$P_{2,2s}$	$P_{3,1s}$	$P_{3,2s}$	J
A	1.0000	0.0648	1.0000	0.3185	0.3780	**26.73**
B	0.9430	0.4910	0.9892	0.3208	0.6103	6.35
C	0.9101	1.0000	0.1900	1.0000	1.0000	6.01

Dynamic rigorous simulations: verification of controller performance

In order to further verify the controller structure performances, simulations of a closed loop regulator problem using a PI-controller for all distillation designs (points A, B and C) are performed. The value of controller tuning parameters for all designs was calculated using the same standard tuning rules. The closed loop responses are shown in Figs. 5.22-5.23.

Fig. 5.22 shows the closed loop responses of top column temperature and methanol composition, when a +5K step change is applied to the feed temperature at points A, B and C. One can observe that the effect of the disturbance is successfully rejected by the controller at all points (see Fig. 5.22). This result shows that the selected controller structure (pairing of T_D-L) is the best pair that performs very well in rejecting the effect of disturbances. It can also be seen that the design A requires less time (t = 0.3 h) to settle while other designs require longer time.

Fig. 5.23 shows the closed loop responses of bottom column temperature and water composition, when a +5K step change is applied to the feed temperature at points A, B and C. One can observe that the effect of disturbance is also successfully rejected by the controller at all points (see Fig. 5.23) which shows that the selected controller structure (pairing of T_B-V) is the best pair that performs very well in rejecting the effect of disturbance. It can also be seen that the design A requires less time (t = 0.4 h) to settle while other designs require longer time.

Therefore, it is verified that distillation design at the maximum point of the driving force leads to a process with lower energy required and much better closed loop closed performances in maintaining its controlled variables than any other points.
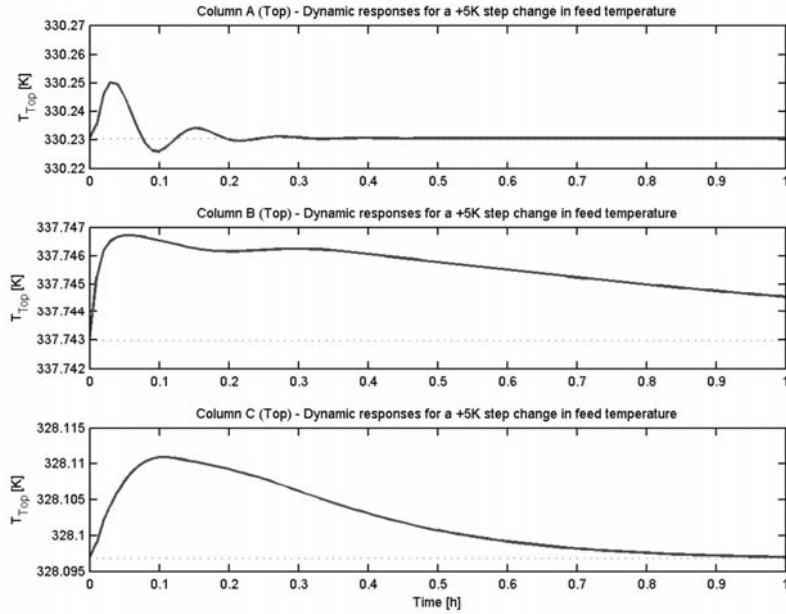
(a)
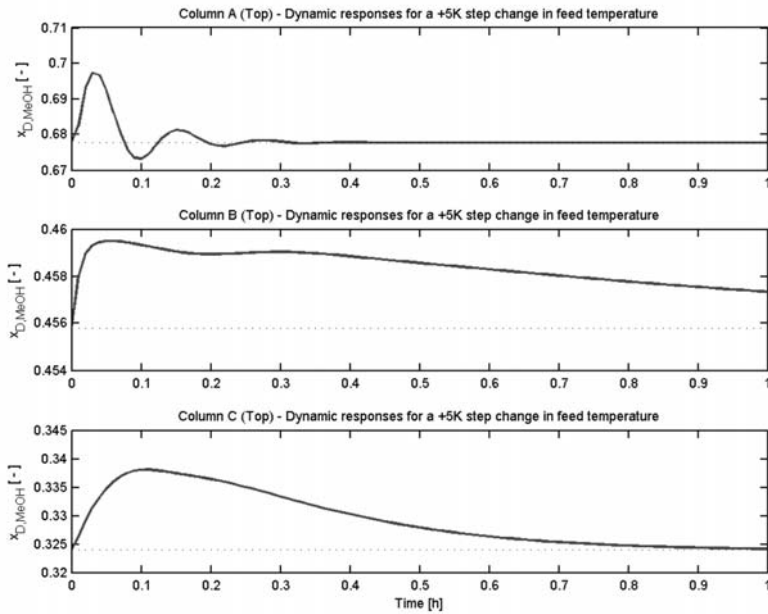
(b)

Fig. 5.22. Regulator problem – Closed loop responses of (a) top column temperature; and (b) top methanol composition to a +5K step change in feed temperature for different distillation designs.
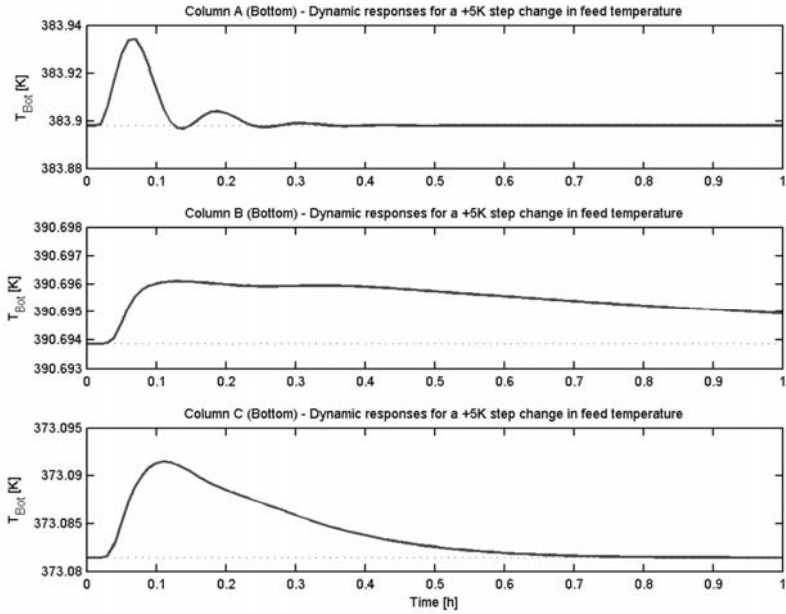
(a)
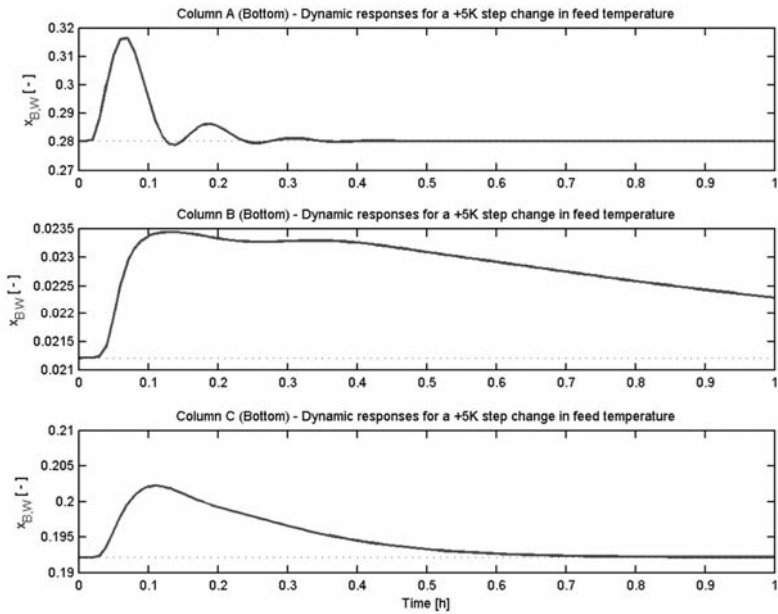
(b)

Fig. 5.23. Regulator problem – Closed loop responses of (a) bottom column temperature; and (b) bottom water composition to a +5K step change in feed temperature for different distillation designs.

5.3 Applications of the Methodology for a Reactor-Separator-Recycle System

The application of the methodology in solving a reactor-separator-recycle (*RSR*) system is illustrated in this section. The section starts with a theoretical consecutive reactions system in which a design of a single reactor that has been illustrated in Example 3.3 is analyzed together with a splitter in section 5.3.1. Then, an ethylene glycol process in which a design of a single reactor that has been analyzed in section 5.1.1 is analyzed together with a distillation column (see section 5.2.1) in order to produce higher and controllable desired product and also to avoid the so-called snowball effect due to recycle of the unreacted reactant back to the reactor.

5.3.1 Theoretical Consecutive Reactions (Conceptual Examples 3.1 and 3.3 Revisited)

In this section, the application of the *IPDC* methodology in solving theoretical consecutive reactions of a *RSR* system is presented (Hamid et al., 2010b). We considered the following situation. In a *CSTR* (let us revisit Examples 3.1 and 3.3), liquid phase, constant density, isothermal reactions described in Eq. (3.8) are taking place. The kinetics and initial feed concentrations are given in Table 3.1. The objective of the reactor is to produce component B ($z_{B,F}$) as high as possible, while the objective of the column is to keep 99.9% of component A in the bottom ($x_{A,R}$) (and 1% of component A in the top, $x_{A,D}$), i.e., $\mathbf{y} = [z_{B,F}, x_{A,D}, x_{A,R}]$. The reactant-rich stream F_R is recycled back to the reactor to increase the conversion. The main disturbances for the reactor are the feed flowrate (F_0) and feed composition ($z_{A,0}$), i.e., $d_R = [F_0 \ z_{A,0}]$, whereas the main disturbances for the column are reactor effluent temperature (T) and component B ($z_{B,F}$), i.e., dc = $[T \ z_{B,F}]$. The objective here is to determine the *IPDC* solution in which the multi-objective function defined in Eq. (5.46) is optimal – that is to produce higher and controllable product B and also to avoid the so-called snowball effect. The pure component properties are given in Table 3.2.

5.3.1.1 Problem formulation

The *IPDC* problem for the process described above is defined in terms of a performance objective (with respect to design, control and cost), and the three sets of constraints (process, constitutive and conditional).

$$Max \quad J = w_{1,l}P_{1,l} + w_{2,1}\left(\frac{1}{P_{2,1}}\right) + w_{2,2}P_{2,2} + w_{3,l}\left(\frac{1}{P_{3,l}}\right) \quad l = 1,2 \qquad (5.56)$$

subjected to:

Process (dynamic and/or steady state) constraints

$$\frac{dV_r}{dt} = F_1 - F_2 \qquad (5.57)$$

$$\frac{dV_r C_{i,2}}{dt} = F_1 C_{i,1} - F_2 C_{i,2} - R_i V_r \quad i = 1, NC \tag{5.58}$$

$$\frac{dM_1}{dt} = L_2 - V_1 - L_1 + F_1 \tag{5.59}$$

$$\frac{dM_j}{dt} = V_{j-1} + L_{j+1} - V_j - L_j + F_j \quad j \in STAGES \setminus \{1, N\} \tag{5.60}$$

$$\frac{dM_N}{dt} = V_{N-1} - V_N - D - L_N + F_N \tag{5.61}$$

$$\frac{dM_{i,1}}{dt} = L_2 x_{i,2} - V_1 y_{i,1} + F_1 z_{i,1} \tag{5.62}$$

$$\frac{dM_{i,j}}{dt} = V_{j-1} y_{i,j-1} + L_{j+1} x_{i,j+1} - V_j y_{i,j} - L_j x_{i,j} + F_j z_{i,j} \tag{5.63}$$

$$\frac{dM_{i,N}}{dt} = V_{N-1} y_{i,N-1} - V_N y_{i,N} - D x_{i,N} - R x_{i,N} + F_N z_{i,N} \tag{5.64}$$

$$0 = F_0 + D - F_1 \tag{5.65}$$

$$0 = F_0 z_{i,0} + D x_{i,D} - F_1 z_{i,1} \quad i = 1, NC \tag{5.66}$$

Constitutive (thermodynamic) constraints

$$0 = R_i - k\{T\} C_{i,2} \quad i = 1, NC \tag{5.67}$$

$$F_{Di} = y_i - x_i \tag{5.68}$$

$$y_i = \frac{\alpha_{i,k} x_i}{\sum_i \alpha_{i,k} x_i} \tag{5.69}$$

Conditional (process-control) constraints

$$30 \geq V_R - (V_r + 0.1 V_r) \tag{5.70}$$

$$3 \leq V_R - (V_r + 0.1 V_r) \tag{5.71}$$

$$x_{A,D} \leq 0.01 \tag{5.72}$$

$$CS = \mathbf{y} + \mathbf{u} Y \tag{5.73}$$

Eq. (5.56) is the multi-objective function in terms of design, control and cost, where w is the weight factor assigned to each objective term P. $P_{1,1}$ is the performance

criteria for reactor design and $P_{1,2}$ is the performance criterion for separator design. In order to achieve process design objectives, $P_{1,1}$ is maximized. On the other hand, in order to achieve controller design objectives, $P_{2,1}$ is minimized by minimizing $d\mathbf{y}/d\mathbf{d}$, and $P_{2,2}$ is maximized by maximizing $d\mathbf{u}/d\mathbf{y}$. $d\mathbf{y}/d\mathbf{d}$ is the sensitivity of controlled variables $\mathbf{y}$ with respect to disturbances $\mathbf{d}$, and $d\mathbf{y}/d\mathbf{u}$ is the sensitivity of the controlled variables $\mathbf{y}$ with respect to manipulated variables $\mathbf{u}$ for the best controller structure. To achieve economic objectives, $P_{3,1}$ is minimized, where $P_{3,1}$ is the capital cost and $P_{3,2}$ is the operating costs.

Eq. (5.57) is the mass balance for the reactor and Eq. (5.58) is the component i balance (there are $i = 1$, NC equations, where NC is the total number of components). Eqs. (5.59)-(5.61) are the total mass balance on each stage for the distillation column, where M_j, L_j, V_j, and F_j are the holdup, liquid flowrate, vapor flowrate and feed rate on the jth stage, respectively. The number of stages in the column is assumed to be N including both the reboiler and the condenser, with stages numbered from the bottom to top. The set $STAGES := \{1, N\}$ denotes the numbered stages and the index, j subscripted to a quantity associated with stage j. Eqs. (5.62)-(5.64) are the component balance on each stage for the distillation column, where $M_{i,j}$, $z_{i,j}$, $x_{i,j}$, and $y_{i,j}$ represent the holdup, liquid and vapor composition of component i on the jth stage, respectively. Eq. (5.65) is the mass balance for the mixer and Eq. (5.66) is the component i balance.

Eq. (5.67) represents the phenomena model for the reaction rate for the reactor. By assuming equilibrium holds for each stage, Eq. (5.68) represents the driving force, defined as the difference in composition of a component i between the vapor phase and the liquid phase in the column. The vapor composition of component i is represented in Eq. (5.69). Eqs. (5.70)-(5.71) are the sizing equations for a single reactor, represent the real reactor volume, V_r by summing the reaction volume, V_R with the head space, where the head space is calculated as 10% of the reaction volume. The acceptable value of V_r for a jacketed reactor is $3 \leq V_r \leq 30$ m^3. Eq. (5.72) is the product quality constraint for the distillation column. Eq. (5.73) presents the controller structure selection constraint. Y is the set of binary decision variables for the controller structure selection which corresponds to whether a controlled variable is paired with a particular manipulated variable or not.

The *IPDC* problem formulated above is then solved using the proposed decomposition-based solution strategy as shown below.

5.3.1.2 Decomposition-based solution strategy

The summary of the decomposition-based solution strategy for this problem is shown in Table 5.26 and Fig. 5.24. It can be seen that the constraints in the *IPDC* problem are decomposed into four sub-problems which correspond to the four hierarchical stages. In this way, the solution of the decomposed set of sub-problems is equal to that of the original problem. Details of the step-by-step solutions are shown below.

Table 5.26
Mathematical equations and decomposition-based solution for a conceptual *RSR* system.

Mathematical equations	Decomposition method	Corresponding variables
Multi-objective function: • Eq. (5.56) *Process constraints:* • *Reactor :* Eqs. (5.57)-(5.58) • *Distillation :*Eqs. (5.59)-(5.64) • *Mixer :*Eqs. (5.65)-(5.66) *Constitutive constraints:* • Eq. (5.67) • Eqs. (5.68) – (5.69) *Conditional constraints :* • Reactor sizing: Eqs. (5.70)-(5.71) • Product purity: Eq. (5.72) • Controller structure: Eq. (5.73)	*Stage 1: Pre-analysis.* a. Variable analysis b. Operational window: • Reactor: Eqs. (5.70)-(5.71) • Distillation: Eq. (5.72) c. Design-control target • Attainable region: Eq. (5.67) • Driving force Eqs. (5.68)-(5.69) *Stage 2: Design analysis.* • Step-by-step algorithm for a simple distillation design (Gani & Bek-Pedersen, 2000) • Eqs. (5.67)-(5.69) and Eqs. (5.57)- (5.66) in steady state *Stage 3: Controller design analysis:* • Sensitivity analysis: Eqs. (5.57)-(5.69) • Controller structure selection: Eqs. (5.57)-(5.69) and Eq. (5.73) *Stage 4: Final selection and verification* • Final selection: Eq. (5.56) • Dynamic simulations verification: Eqs. (5.57)-(5.69), Eq. (5.73)	$3 \leq V_R \leq 30$ $x_{A,D} \leq 0.01$ z_B/z_A $FD = y_B - x_B, x_B$ N_F, RR, RB V_r, D, L, V $dFD/dx_B, dFD/dT, dz_B/dz_A, dz_A/dh$ $dx_{A,D}/dV, dx_{A,R}/dV, dx_{A,D}/dL, dx_{A,R}/dL, dh/dF, dz_A/dF$ J

Stage 1: Pre-analysis

The main objective of this stage is to define the operational window within which the optimal solution is located and set the targets for the optimal design-controller solution.

Step 1.1: Variables analysis

The first step in Stage 1 is to perform variable analysis. All variables involved in this process are analyzed and classified as design and manipulated variables **u**, process-controlled variables **y**, and disturbances **d** as shown in Table 5.27. Then, the important **u** and **y** are selected with respect to the multi-objective function, Eq. (5.56), and tabulated in Table 5.28. Design variables $\mathbf{u}_d = [V_r, N_F]$ are important since V_r and N_F are related to capital and operating costs ($P_{3,1}$ and $P_{3,2}$). On the other hand, manipulated variables $\mathbf{u}_m = [F, V, L]$ are selected since they are the potential candidates for the manipulated variables and directly related to the objective function $P_{2,2}$. Process-controlled variables $\mathbf{y}_m = [z_B, z_A, x_{A,D}, x_{BD}, x_{A,R}, x_{A,R}]$, are selected since they are the important variables that need to be monitored and controlled in order to obtain the smooth, operable and controllable process, which is also directly related to the objective function $P_{2,1}$.
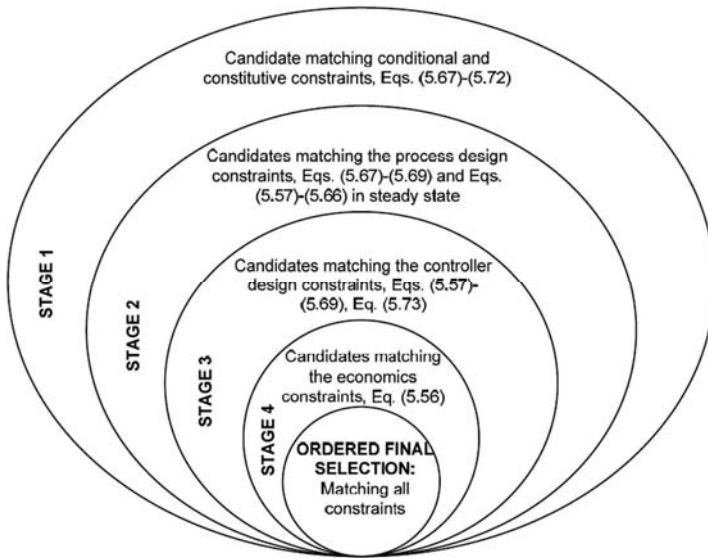
Fig. 5.24. Decomposition-based solution for a conceptual *RSR* system.

Table 5.27
List of all design and manipulated variables, process-controlled variables and disturbances for a conceptual *RSR* system.

Design variable ($\mathbf{u}_d$)	V_r, N, N_F, RR, RB
Manipulated variable ($\mathbf{u}_m$)	F, B, D, V, L
Process-Controlled variables ($\mathbf{y}$)	$z_B, z_A, z_C, x_{A,D}, x_{B,D}, x_{C,D}, x_{A,R}, x_{A,R}, x_{C,R}$
Disturbances ($\mathbf{d}$)	F_0, T, z_A, z_B

Table 5.28
List of important design and manipulated and process-controlled variables for a conceptual *RSR* system.

Design variable ($\mathbf{u}_d$)	V_r, N_F
Manipulated variable ($\mathbf{u}_m$)	V, L, F
Process-Controlled variables ($\mathbf{y}_m$)	$z_B, z_A, x_{A,D}, x_{BD}, x_{A,R}, x_{A,R}$

Step 1.2: Operational window identification

The operational window is identified based on the bottom and the top products purity in the distillation column. In order to satisfy product quality, the component A composition at the bottom $x_{A,R}$ should be more than 0.99 (and less than 0.01 at the top).

Step 1.3: Design-control target identification

The attainable region diagram is generated by plotting the response of the desired product $z_{B,F}$ with respect to the response of reactant $z_{A,F}$ as shown in Fig. 5.25. Fig. 5.26 shows the plot of the driving force against composition for distillation design. The target for the optimal process-controller design solution is then identified at the maximum point of the attainable region (point A) for a reactor and the driving force (point D) for distillation. Note that, in Fig.5.25, two other points which are not at the maximum are identified as candidate alternative designs for a reactor which will be used for verification purposes (see stage 4).

Stage 2: Design analysis

The objective of this stage is to validate the target identified in Stage 1 by finding the acceptable values of **y** and **u**. In this stage, the search space defined in Stage 1 is further reduced.
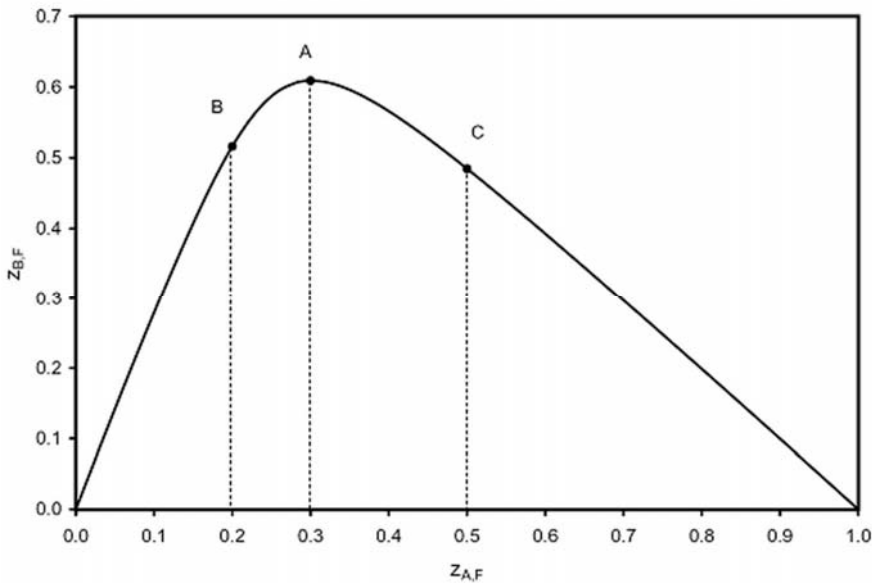
Fig. 5.25. Attainable region diagram for the desired product composition $z_{B,F}$ with respect to $z_{A,F}$ for a conceptual *RSR* system.
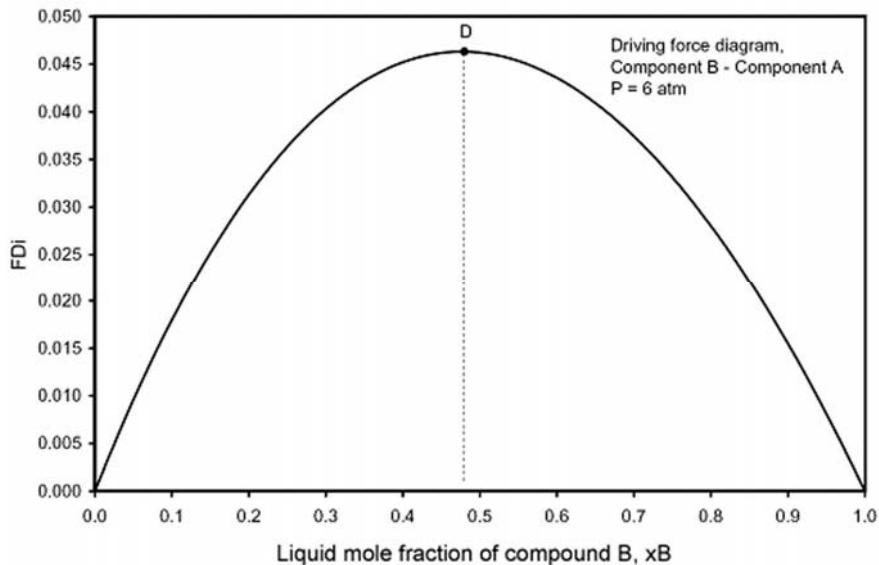
Fig. 5.26. Driving force diagram for the separation of component *B* and *A* by distillation for a conceptual *RSR* system.

Step 2.1: Design-manipulated and process-controlled variables value calculation

Before calculating the value of design variables, it is important to define the feasible range of operation with respect to manipulated (design) and controlled (process) variables within which the snowball effect will not appear and the desired product composition will be high. Therefore, it is important to define the feasible range of operation with respect to manipulated (design) and controlled (process) variables where the snowball effect can be avoided.

To define the feasible range we need the process model and a set of conditional constraints which is derived for the *RSR* system under following assumptions:

A_0 The reaction is considered to take place isothermally in a continuously stirred tank reactor (*CSTR*),

A_1 The separation section will be modelled as a component sharp splitter unit with recovery of component *A* ($\alpha_{Y,S} = 0.99$),

A_2 A fraction of the unreacted reactant is recycled back to the reactor through a mixer unit,

A_3 No recovery of products *B* and *C* ($\beta_{Y,S} = \gamma_{Y,S} = 0$),

A_4 Pure A is fed to the system ($F_B = F_C = 0$) and no purge ($\sigma = 0$).

Through manipulation of the mass balance equations, the set of conditional constraints are obtained in terms of dimensionless variables (Damköhler number, $Da = k_1 C_{A,F} V/F$). The detailed derivation for these equations are given in the Appendix D.

$$0 = \xi_{v,1} - \xi_{v,3} - \Omega \left[\left(1 - \xi_{v,1} + \xi_{v,3}\right) - k_1^* \left(\xi_{v,1} - \xi_{v,2} - \xi_{v,3}\right)\left(1 - \alpha_{Y,S}\right) \right] \qquad (5.74)$$

$$0 = \left(\xi_{v,3} + \xi_{v,2} - \xi_{v,1}\right) - \Omega \left[\left(k_1^* + k_2^*\right)\left(\xi_{v,1} - \xi_{v,2} - \xi_{v,3}\right)\left(1 - \alpha_{Y,S}\right) - \left(1 - \xi_{v,1} + \xi_{v,3}\right) \right] \qquad (5.75)$$

$$0 = \xi_{v,2} - \Omega k_2^* \left(\xi_{v,1} - \xi_{v,2} - \xi_{v,3}\right)\left(1 - \alpha_{Y,S}\right) \qquad (5.76)$$

where

$$\Omega = \frac{D_a}{1 - \alpha_{Y,S}\left(\xi_{v,1} - \xi_{v,3}\right)}$$

In this *IPDC* problem, we want to identify the feasible range of operation in terms of dimensionless design variable Da and ξ within which the highest composition of product B can be obtained and the snowball effect can be eliminated. Eqs. (5.74)-(5.76) can be written in compact from as

$$0 = f\begin{bmatrix} \xi & u \end{bmatrix} \qquad (5.77)$$

where

$$\mathbf{u} = [Da, \alpha_{Y,S}]$$

Vector $\mathbf{u}$ represents the set of design variables. Once the vector $\mathbf{u}$ has been determined, Eq. (6.77) is solved for ξ and using Eqs. (5.78)-(5.80) (representing the steady state process model) the values of the important process variables are obtained:

$$z_{A,S} = \frac{1 - \xi_{v,1} + \xi_{v,3}}{1 - \alpha_{Y,S}\left(\xi_{v,1} - \xi_{v,3}\right)} \qquad (5.78)$$

$$z_{B,S} = \frac{\left(\xi_{v,1} - \xi_{v,2} - \xi_{v,3}\right)\left(1 - \alpha_{Y,S}\right)}{1 - \alpha_{Y,S}\left(\xi_{v,1} - \xi_{v,3}\right)} \qquad (5.79)$$

$$z_{C,S} = \frac{\xi_{v,2}\left(1 - \alpha_{Y,S}\right)}{1 - \alpha_{Y,S}\left(\xi_{v,1} - \xi_{v,3}\right)} \qquad (5.80)$$

The dimensionless equations with respect to F_R and reactor effluent compositions ($z_{i,F}$) are obtained and solved. Results are plotted in Fig. 5.27.
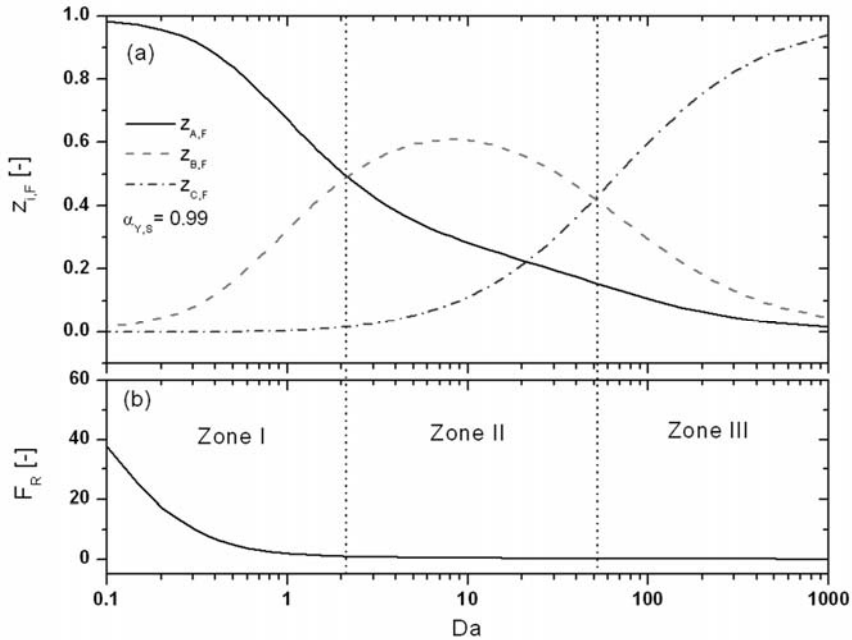
Fig. 5.27. Operational windows for; (a) reactor outlet composition, and (b) recycle flowrate F_R as a function of Da number.

In Fig. 5.27(a), it can be observed that a higher value of $z_{B,F}$ can be achieved within the range $2<Da<50$ (Zone II). But, when $Da<2$ (Zone I), the F_R increases significantly indicating a possible snowball effect, as shown in Fig. 5.27(b). In order to avoid the snowball effect, the reactor should be operated at the higher value of Da (for example $Da>2$). However, for large values of $Da>50$ (Zone III), there appears more $z_{C,F}$ in the reactor. Therefore, in order to obtain high $z_{B,F}$ and also to eliminate the snowball effect, the feasible operational window for Da is identified within the range of $2<Da<50$.

Once the feasible range of Da has been established, design targets identified earlier at the maximum points of the attainable region (see Fig. 5.25) and the driving force (see Fig. 5.26), for reactor and separator designs, respectively, are used to determine the remaining design variables and controller structure design. The results are given in Table 5.29 and Table 5.30 for reactor and distillation, respectively.

Table 5.29
Values of residence time with the corresponding process-controlled and design-manipulated variables for different conceptual reactor designs.

Reactor Design	Da	Process-Controlled (**y**)			Manipulated	Design
		$z_{A,F}$	$z_{B,F}$	F (kmol/min)	F_R (kmol/min)	V (m^3)
A	8.2	0.30	0.61	71.6	25.5	8.2
B	26.0	0.21	0.53	67.3	15.5	26.0
C	2.0	0.50	0.48	84.6	59.3	2.0

From Table 5.29, it can be seen that values of reactor volume and corresponding flow rates can be obtained for these three candidate reactor designs. In Table 5.30, values of distillation design variables corresponding to the maximum point of the driving force (point D) for three different reactor designs are obtained.

Table 5.30
Values of process/controlled and design/manipulated variables for distillation at point D for different conceptual reactor designs.

Reactor Design	Process/controlled			
	$x_{A,D}$	$x_{B,D}$	$x_{A,R}$	$x_{B,R}$
A	0.01	0.87	0.99	0.01
B	0.01	0.67	0.99	0.01
C	0.01	0.91	0.99	0.01

Reactor Design	Design/manipulated			
	N_S	N_F	L (kmol/min)	V (kmol/min)
A	65	34	730.8	337.5
B	65	34	730.8	204.7
C	65	34	730.8	784.3

In Table 5.29 reactor design A has the highest product composition $z_{B,F}$, followed by reactor designs B and C. However, in terms of capital cost, reactor design C has the lowest cost since it has the smallest volume followed by reactor designs A and B. The distillation capital costs for the three reactor designs are the same since they have the same number of stages. However, in terms of operating cost for recycle (see Table 5.29), reactor design B has the lowest cost since its recycle flow rate (reactor design C has the highest operating costs while reactor design A has moderate operating costs). To find the best alternative, the value of a multi-objective function is calculated in the verification stage (see stage 4).

Stage 3: Controller design analysis

The objective of this stage is to evaluate and validate the controllability performance of the feasible candidates in terms of their sensitivities with respect to disturbances and manipulated variables.

Step 3.1: Sensitivity analysis

The process sensitivity is analyzed by calculating the derivative values of the controlled variables with respect to disturbances $d\mathbf{y}/d\mathbf{d}$ with a constant step size. Fig. 5.28(b) shows plots of the derivative of $z_{B,F}$ with respect to $z_{A,0}$ and F_0 at different reactor designs. It can be seen that the derivative values are smaller for reactor design A compared to other designs (B and C). Fig. 5.29(b) shows plots of the derivative of the driving force with respect to composition of B and temperature.
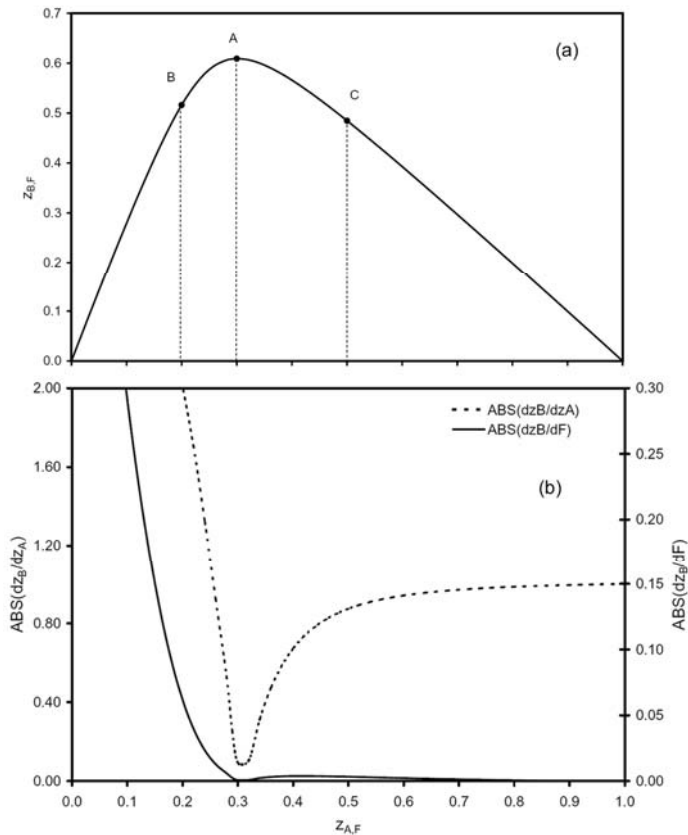
Fig. 5.28. (a) Attainable region diagram for the desired product composition $z_{B,F}$ with respect to $z_{A,F}$, (b) Corresponding derivatives of $z_{B,F}$ with respect to $z_{A,0}$ and F_0 of a conceptual reactor design.

It can be seen that derivative values are smaller at the maximum point of the driving force. Hence, from a control point of view, reactor design A and column design D are less sensitive to the effect of disturbances, which makes them more robust in maintaining their controlled variables against disturbances. As shown in Fig. 5.28(b), the value of $dz_{B,F}/dz_{A,0}= (dz_{B,F}/dh)(dh/dz_{A,0})\approx 0$ and $dz_{B,F}/dF_0=(dz_{B,F}/dh)(dh/dF_0)\approx 0$, thus from a control perspective, composition and level control are feasible for this reactor design. For distillation design, as shown in Fig, 5.29(b), the value of $dF_{Di}/dT=dF_{Di}/dx_B\approx 0$, thus composition and temperature control are feasible. At the highest attainable region point (design A) and driving force point (design D), the controller performance will be the best. At these points, any major changes to the disturbances will result in smaller changes in the controlled variables. Therefore, at these points the desired controlled variables can more easily be controlled at their optimal set points. This is verified in step 4.2.
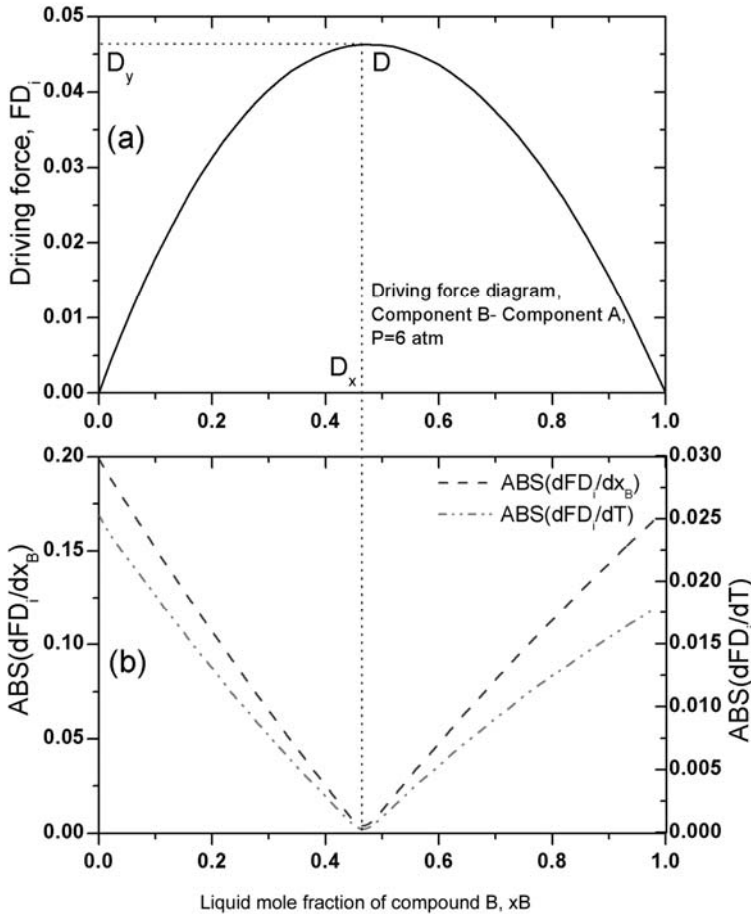
Fig. 5.29. (a) Driving force diagram for the separation of components *B* and *A* by distillation, (b) Corresponding derivatives of the driving force with respect to composition and temperature of a conceptual reactor design.

Step 3.2: Controller structure selection.

Next the controller structure is selected by calculating the derivative value of controlled variables with respect to manipulated variables $d\mathbf{y}/d\mathbf{u}$. Since there is only one manipulated variable (F) available for controlling $z_{B,F}$ and h_r for reactor design, therefore $z_{B,F}$ and h_r can be controlled by manipulating F. The derivative values of $dz_{B,F}/dF$ and dh_r/dF are calculated and plotted in Fig. 5.30b.
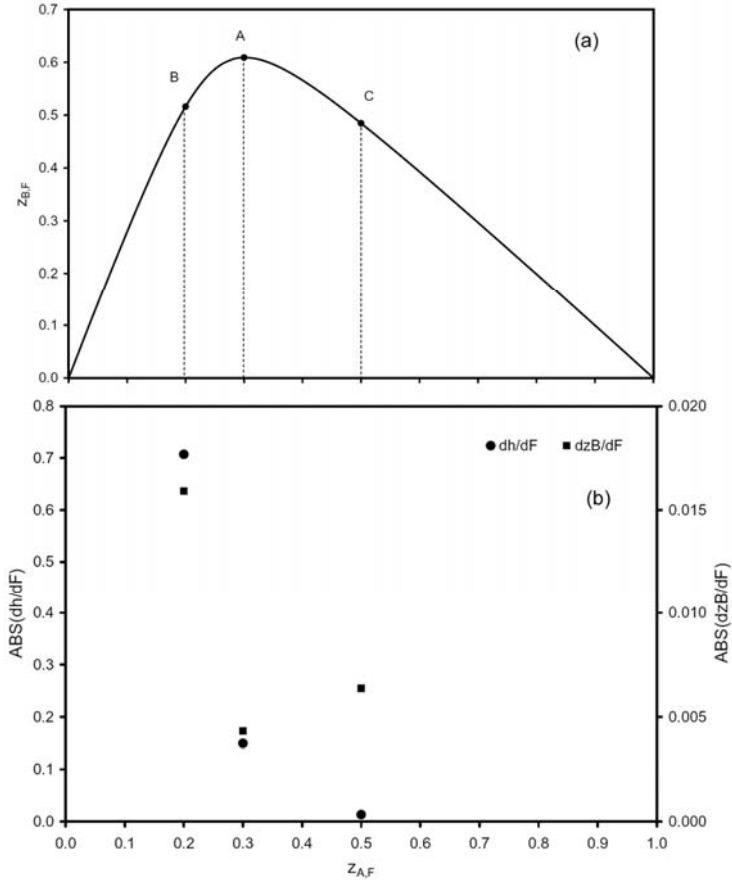
Fig. 5.30. (a) Attainable region diagram for the desired product composition $z_{B,F}$ with respect to $z_{A,F}$, (b) Corresponding derivatives of the potential controlled variables with respect to manipulated variables for a conceptual reactor design.

Accordingly, $dz_{B,F}/dF$ can be represented as:

$$\frac{dz_{B,F}}{dF} = \left(\frac{dz_{B,F}}{dz_{A,F}}\right)\left(\frac{dz_{A,F}}{dh_r}\right)\left(\frac{dh_r}{dF}\right) \approx 0 \tag{5.81}$$

Since $dz_{B,F}/dF \approx 0$, it is possible to maintain $z_{B,F}$ at its optimal set point using level control. From Fig. 5.30b and Table 5.31, it can be seen that values of dh_r/dF are higher compared to values of $dz_{B,F}/dF$ for all reactor designs. A higher derivative value of controlled variables with respect to manipulated variables means that the process has a higher process gain (Russel et al., 2002). From a process control point of view, a process with a large process gain will require a small change in the manipulated variable (control action) in order to maintain the controlled variable at its set point value in the presence of disturbances. Therefore, it can be clearly seen from Fig. 5.30 and Table 5.31, that the best pairing of controlled-manipulated variable that will able to maintain the desired product composition $z_{B,F}$ at its optimal set point value in the presence of disturbances is h_r-F. This controller structure will require less control action compared to the other structure ($z_{B,F}$ -F) for maintaining $z_{B,F}$ at its optimal set point value for all reactor designs. It should be noted that, the objective of this step is not to find the optimal value of controller tuning parameters or type of controller, but to generate the feasible controller structure.

Table 5.31
Derivatives values of $z_{B,F}$ and h_r with respect to F at different conceptual reactor designs.

Reactor Design	Derivative	
	dh_r/dF	$dz_{B,F}/dF$
A	0.1492	0.0043
B	0.7072	0.0159
C	0.0134	0.0064

Stage 4: Final selection and verification

The objective of this stage is to select the best candidates by analyzing the value of the multi-objective function, Eq. (5.56).

Step 4.1: Final selection: Verification of design

The multi-objective function, Eq. (5.56) is calculated by summing up each term of the objective function value. In this case, all the objective function terms are weighted equally meaning that the decision-maker does not have any preference for one objective over another. Since the range and unit of each objective function value can be different, each objective value is normalized with respect to its maximum value. Details are given in Table 5.32. $P_{1,1s}$ and $P_{1,2s}$ correspond to the scaled value of the attainable region and the driving force, F_{Di}. $P_{2,1s}$ and $P_{2,2s}$ are scaled values of dF_{Di}/dT and dh_r/dF representing the process sensitivity and the controller structure selection criteria. Whereas, $P_{3,1s}$, $P_{3,2s}$, are the scaled value of the reactor volume and the recycle flow rate, respectively, which represent capital and operating costs. It can be seen that, the value of J at reactor design A is higher than for the other designs. Therefore, it is verified that the optimal solution for process-controller design of a *RSR* system which satisfies the design, control and cost criteria is given by reactor design A.

Table 5.32
Multi-objective function calculation. The best candidate is highlighted in bold.

Reactor Design	$P_{1,1}$	$P_{1,2}$	$P_{2,1}$	$P_{2,2}$	$P_{3,1}$	$P_{3,2}$	
A	0.609	0.046	0.000	0.149	16.00	4.26	
B	0.529	0.037	0.009	0.707	50.53	2.59	
C	0.483	0.040	0.038	0.013	4.00	9.89	
	$P_{1,1s}$	$P_{1,2s}$	$P_{2,1s}$	$P_{2,2s}$	$P_{3,1s}$	$P_{3,2s}$	J
A	1.00	1.00	0.01	0.21	0.32	0.43	**103**
B	0.87	0.81	0.24	1.00	1.00	0.26	12
C	0.79	0.87	1.00	0.02	0.08	1.00	16

Step 4.2: Dynamic rigorous simulations: verification of controller performance

In this closed loop simulation, we use the conventional control structure (control of reactor level by manipulating F, and control of both product compositions of the column) to verify results obtained in the previous steps in terms of controller performance. It is assumed that the bottom and distillate compositions of the distillation are perfectly controlled, as we want to focus on the effect of the recycle on the system. Hence the reactor control structure/strategy is analyzed in detail here (see Fig. 5.31) to obtain controllable desired product as well as to eliminate the snowball effect. Values of tuning parameters are calculated using the Ziegler-Nichols tuning method for all reactor design alternatives. Figs. 5.32-5.34 shows the results when a +5% step change is applied to the F_f.
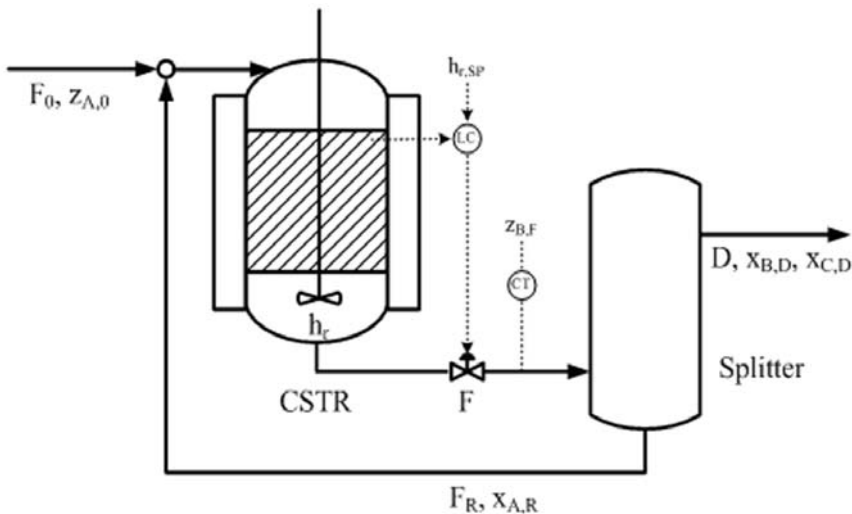
Fig. 5.31. Schematic diagram of reactor/distillation column plant with perfect control of both column bottom and top levels and both column product compositions.

Fig. 5.32. Dynamic responses of the desired product composition $z_{B,F}$ to a +5% step change in F_f for different alternative reactor designs.

Fig. 5.33. Closed loop dynamic responses of the reactor level h_r to a +5% step change in F_f for different alternative reactor designs.

Fig. 5.34. Dynamic responses of the recycle flow rate F_R to a +5% step change in F_f for different alternative reactor designs.

From the results, it can be seen that the reactor level (see Fig. 5.33) can be maintained at its set-point after a +5% step change is applied to the feed flowrate for all reactor design alternatives. These results show that the controller structure selected using this methodology is able to maintain the controlled variable for this process in the presence of the disturbance.

It is also important to note that, the control structure selected in this case study is the same as the conventional control structure (control of reactor level by manipulating reactor outflow F, and control of both column product compositions). According to Luyben (1994) and Larsson et al., (2003), this conventional control structure will exhibit a snowball effect. The same results are also obtained in this case study. The results in Fig. 5.34 show that, the snowball effect is observed in the recycle flowrate F_R when a +5% step change is applied to the feed flowrate. These results confirm the results obtained in the previous studies (Luyben, 2004; Larsson et al., 2003).

However as proposed by Wu and Yu (1996), this snowball effect can be eliminated by changing both reactor holdup and recycle flow rate. In the conventional control structure, it is not possible to change the recycle flow rate since it is already manipulated to control condenser holdup. Therefore, we implemented a new strategy to change the reactor holdup by allowing the reactor level controller set point to change. The idea is to reject the effect of disturbances and also to maintain the recycle flow by changing the set point of the reactor level controller. This will allow changes in the reactor holdup. Figs. 5.35-5.37 show the closed loop dynamic responses in $z_{B,F}$,

reactor level h_r and recycle flow F_R to a +5% step increase in the F_f using this new control strategy.
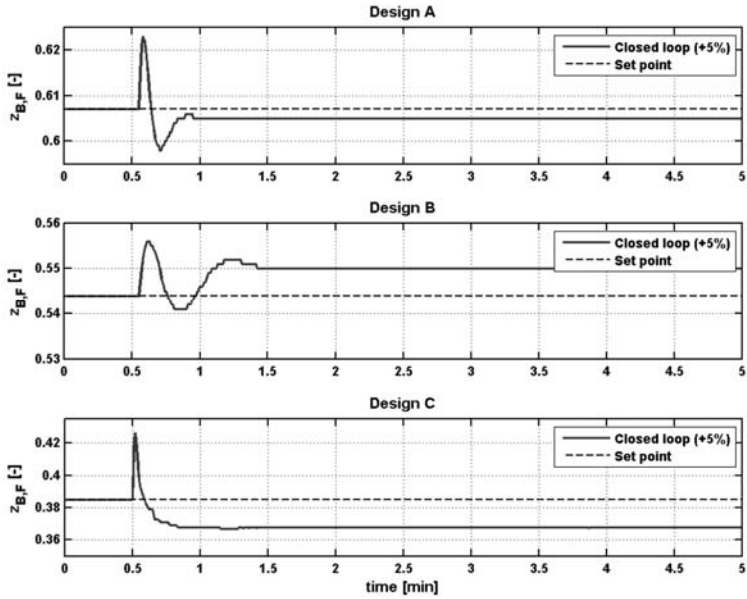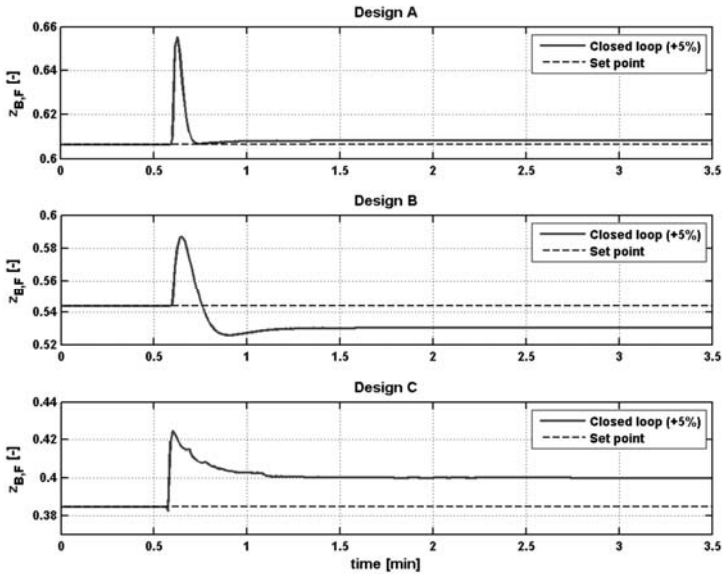

Fig. 5.35. Dynamic responses of the desired product composition $z_{B,F}$ to a +5% step change in the F_f for different alternative reactor designs (new control strategy).
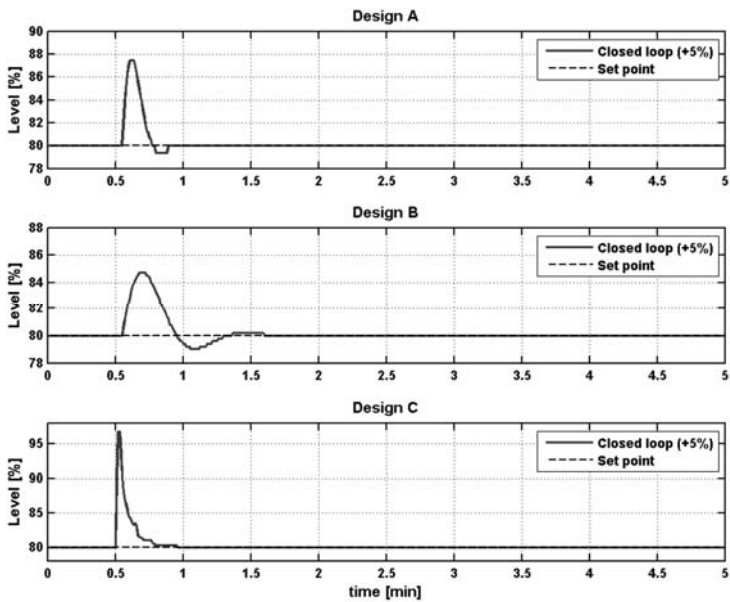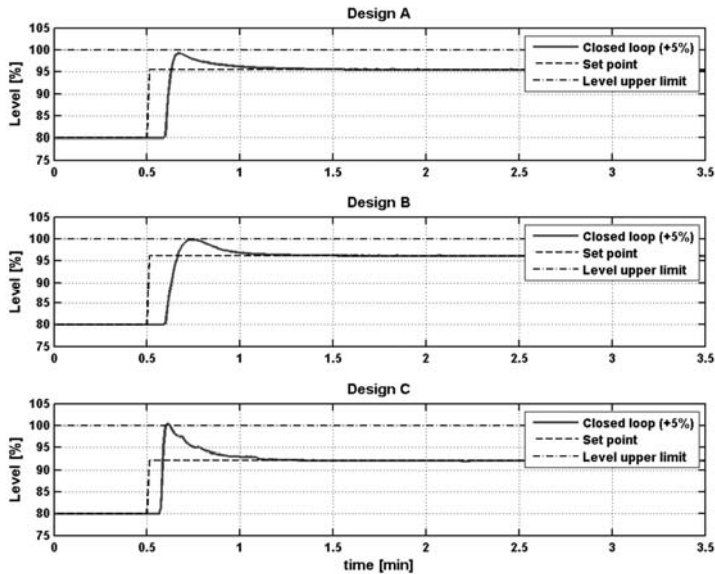

Fig. 5.36. Closed loop dynamic responses of the reactor level h_r to a +5% step change in the F_f for different alternative reactor designs (new control strategy).
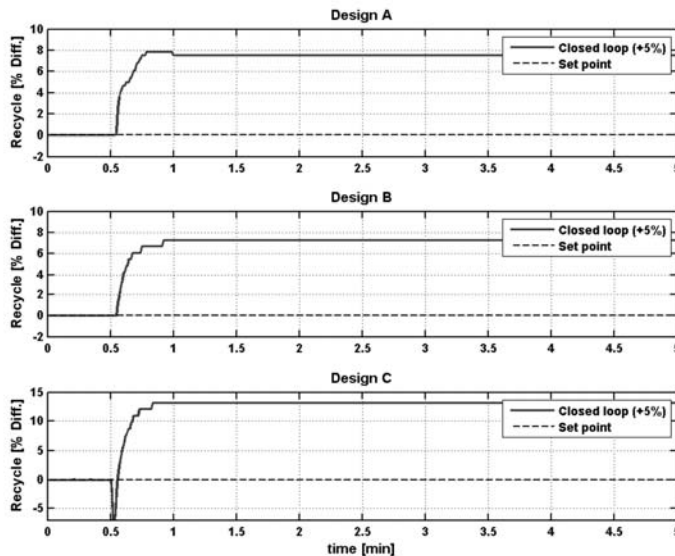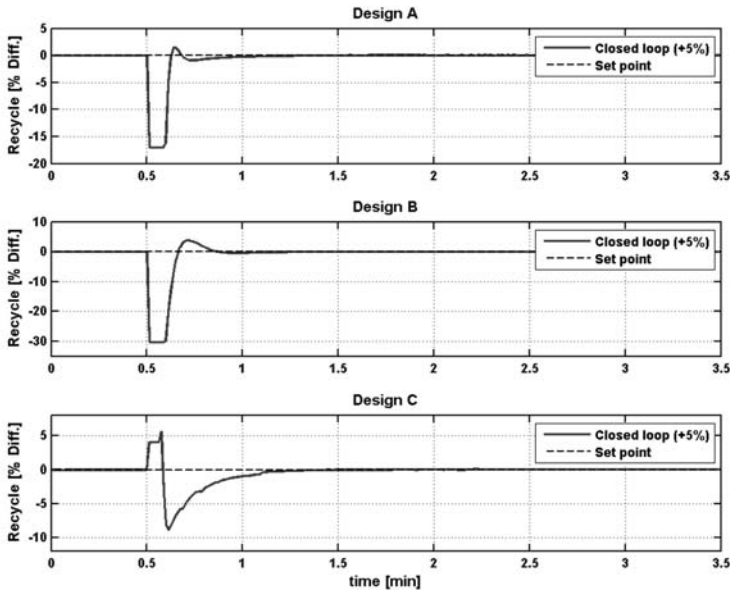
Fig. 5.37. Dynamic responses of the recycle flow rate F_R to a +5% step change in the F_f for different alternative reactor designs (new control strategy).

One can clearly see that by implementing a strategy where the reactor holdup is allowed to change by changing the reactor level controller set-point, the snowball effect can be eliminated. This can be seen in Fig. 5.37 where the dynamic responses of the recycle flowrate F_R for all reactor design alternatives are shown. It can clearly be seen that by increasing the reactor level set-point to a certain value of ΔSP, since the controller is able to keep track of this increment (see Fig. 5.36), the reactor volume is increased. Since the reactor volume is now large, therefore, the snowball effect in the recycle flowrate disappears (see Fig. 5.37). These results verify the effectiveness of the new control strategy in solving the snowball effect problem.

The most important results from this case study are shown in Fig. 5.35 where the responses of the desired product composition z_B are shown for all reactor design alternatives. It can be seen that, the presence of disturbances in the feed flowrate and also changes in the reactor level set-point, did not produce any undesired effect on the desired product composition z_B at the reactor design Point A compared to the other designs (Points B and C). It can be observed that the steady state offset of the desired product composition z_B is smaller at the reactor design Point A (see Fig. 5.35) while for other designs a larger steady state offset is seen. These results shown that z_B is less sensitive to the effect of disturbances at the reactor design Point A than at other designs as mentioned in stage 3.

5.3.2 Ethylene Glycol Reactor-Separator-Recycle System

This section demonstrates the application of the *ICAS-IPDC* software in solving an integrated design and control problem for the reactor-separator-recycle system as illustrated in Fig. 5.38. We consider the following situation. The effluent from the *CSTR* (case study in section 5.1.1) is fed to a distillation column (case study in section 5.2.1) where it is split into two streams of specified purity. The reactant rich stream D is recycled back to the reactor, to improve the process economy when the conversion is low. The objective here is to determine the *IPDC* solution in which the multi-objective function defined in Eq. (5.56) is optimal, that is, to produce higher and controllable desired product *EG* and also to avoid the so-called snowball effect.

The *IPDC* problem for the process described above is defined in terms of a performance objective (with respect to design, control and cost), and the three sets of constraints (process, constitutive and conditional) as expressed in Eqs. (5.56)-(5.73).

5.3.2.1 Application of ICAS-IPDC

The *IPDC* problem formulated above is then solved using the developed *ICAS-IPDC* software as shown below.

Starting of *ICAS-IPDC*
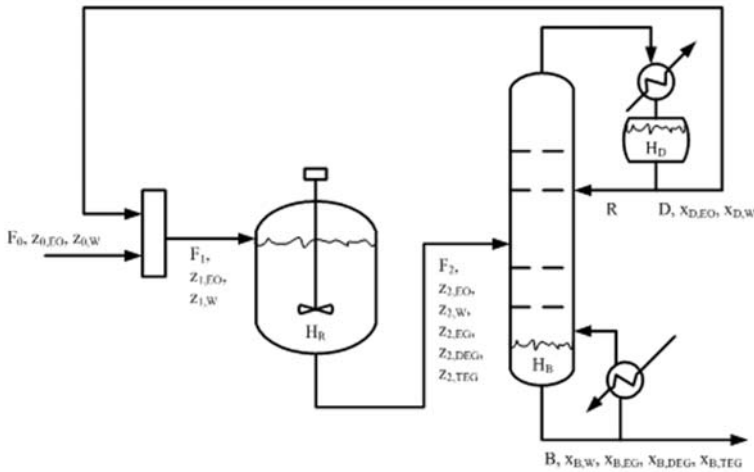
Fig. 5.38 Flowsheet of an Ethylene Glycol reactor-separator-recycle system.

After opening *ICAS-IPDC*, the start menu as shown in Fig. 5.39 is displayed. The user should select a Reactor-Separator-Recycle system and then click on the "Reactor-Separator-Recycle" button. The pop-up menu will appear asking the user to choose either to click "Yes" to open a solved case study, or to click "No" to create a new case study. Click "Yes" to open a solved case study and the screen shot as shown in Fig. 5.40 will come up, which shows the steps that need to be followed sequentially.
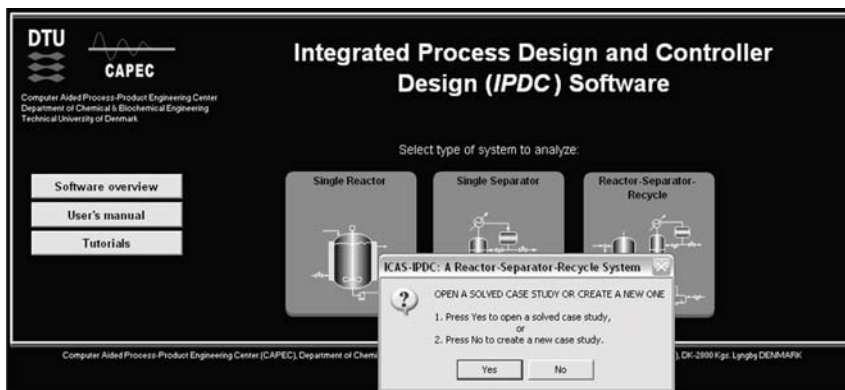
Fig. 5.39. A Start Menu interface for an ethylene glycol *RSR* system.
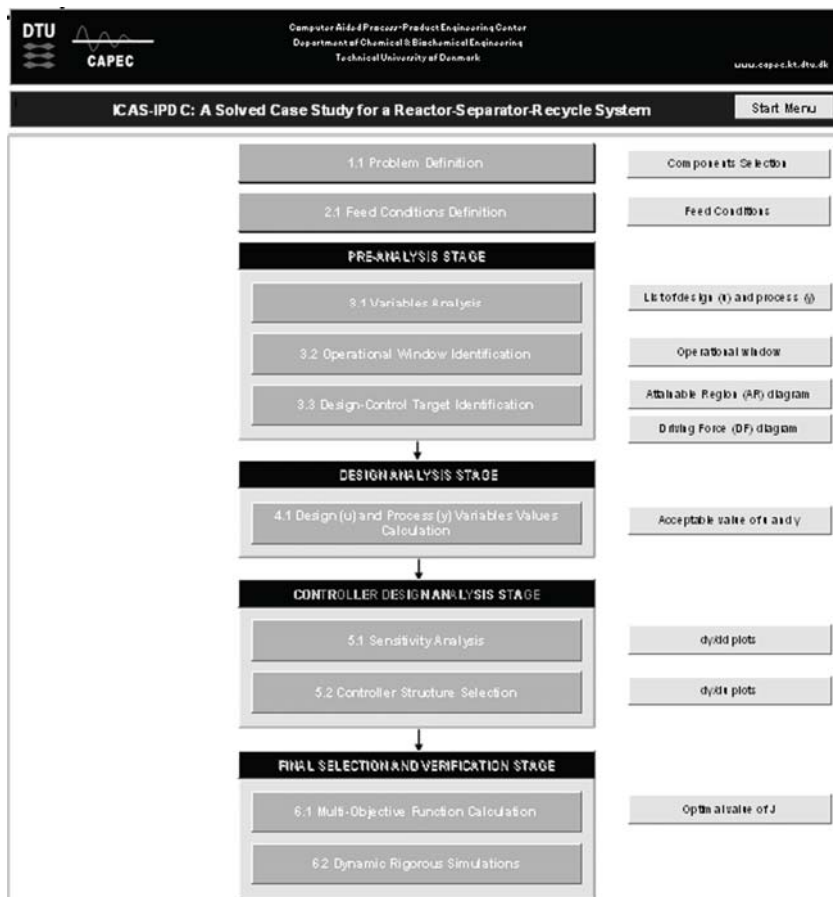
Fig. 5.40. A Main Menu interface for an ethylene glycol *RSR* system.

Part I: Problem Definition

Step 1.1 Problem Definition

A "Problem Definition" interface is shown Fig. 5.41. In this interface, the user needs to complete five sub-steps which are "Components Selection", "Reactants Selection", "Products Selection", "Top Products Selection" and "Bottom Products Selection".
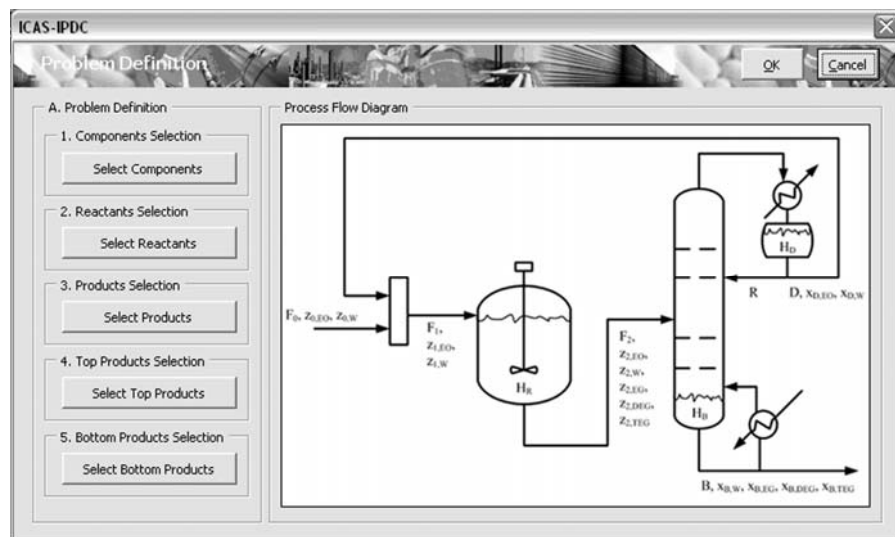
Fig. 5.41. Problem definition interface for an ethylene glycol *RSR* system.

Components Selection: A "Components Selection" interface is shown in Fig. 5.42. In this interface, the user needs to define components used in this process.
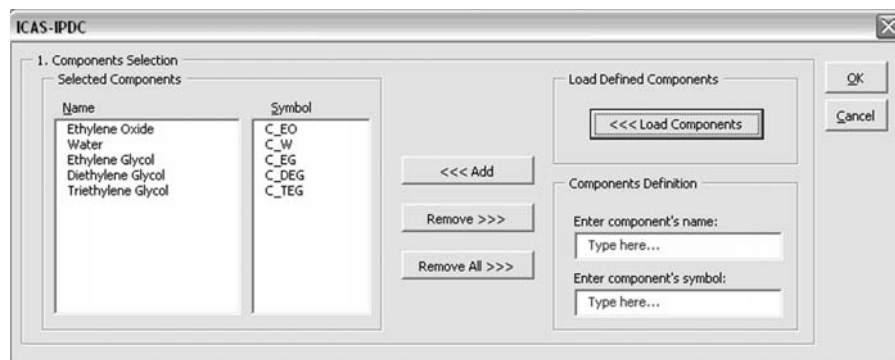
Fig. 5.42. Components Selection interface for an ethylene glycol *RSR* system.

Reactants Selection: A "Reactant Selection" interface where the user should select a list of reactants and the limiting reactant is shown in Fig. 5.43.
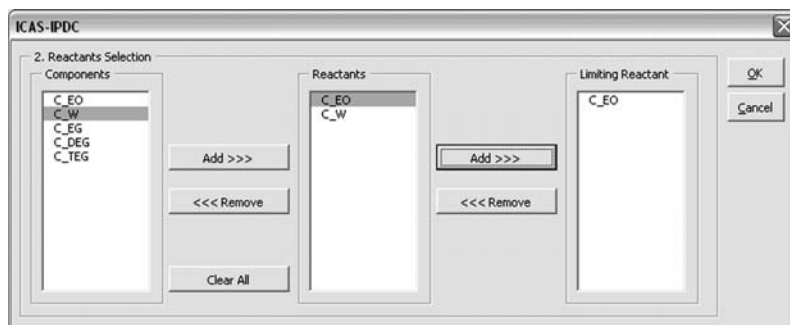
Fig. 5.43. Reactants Selection interface for an ethylene glycol *RSR* system.

Products Selection: A "Product Selection" interface is displayed as shown in Fig. 5.44. Here, the user needs to select a list of products and desired product.
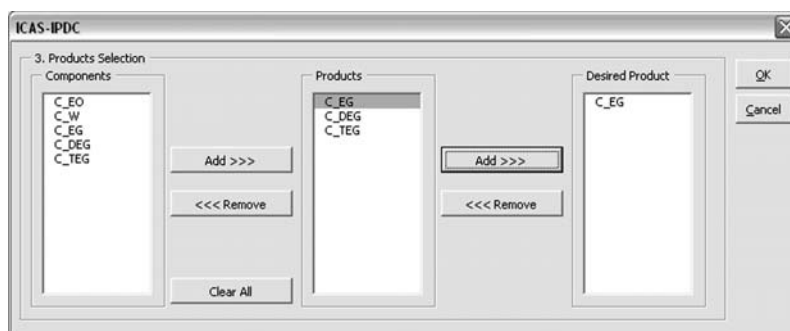
Fig. 5.44. Products Selection interface for an ethylene glycol *RSR* system.

Top Products Selection: A "Top Product Selection" interface where the user needs to select a list of top products and an important top product is shown in Fig. 5.45.
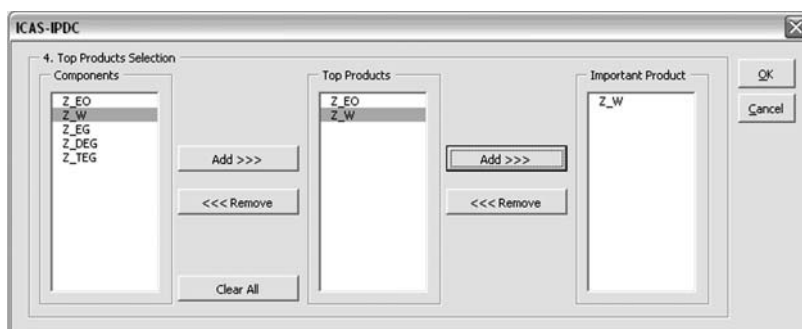
Fig. 5.45. Top Products Selection interface for an ethylene glycol *RSR* system.

Bottom Products Selection: A "Top Product Selection" interface is shown in Fig. 5.46. Here, the user needs to select a list of bottom products and an important bottom product.
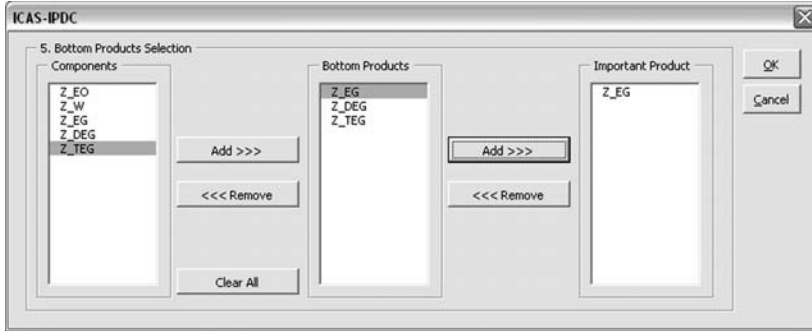
Fig. 5.46. Bottom Products Selection interface for an ethylene glycol *RSR* system.

Step 2.1 Feed Conditions Definition

A "Feed Conditions Definition" interface is shown in Fig. 5.47.
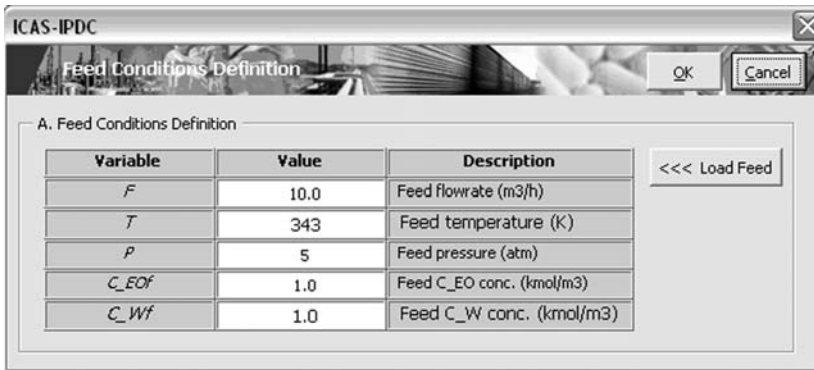
Fig. 5.47. Feed Conditions Definition interface for an ethylene glycol *RSR* system.

Part II: Pre-analysis Stage

This part consists of three steps; Step 3.1 Variables Analysis, Step 3.2 Operational Window Identification, and Step 3.3 Design-Control Target Identification.

Step 3.1 Variables Analysis

A "Variables Analysis" interface is displayed as shown in Fig. 5.48. Here, the user needs to select design variables, process variables and disturbances.
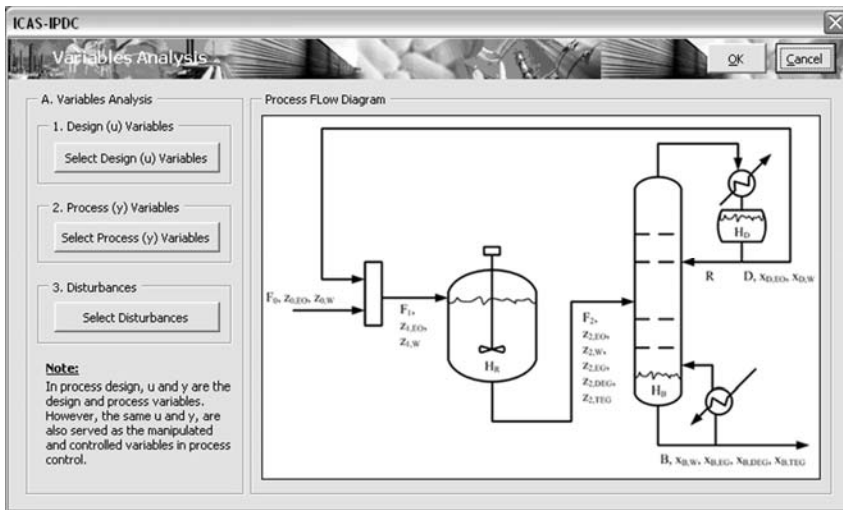
Fig. 5.48. Variables Analysis interface for an ethylene glycol *RSR* system.

Design Variables Selection: A "Selection of Important Design and Manipulated Variables" interface is shown in Fig. 5.49.
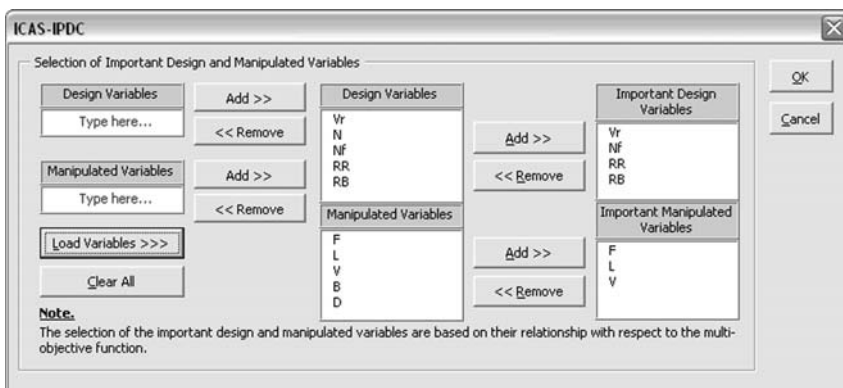
Fig. 5.49. Selection of the Important Design and Manipulated Variables interface for an ethylene glycol *RSR* system.

Process Variables Selection: A "Selection of Important Process-Controlled Variables" interface is shown in Fig. 5.50.
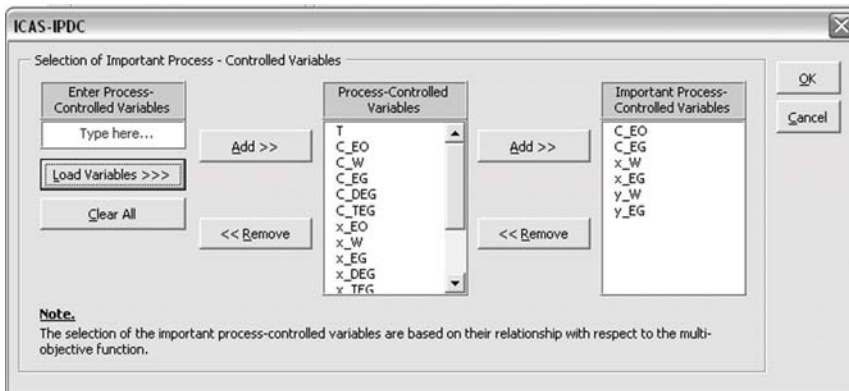
Fig. 5.50. Selection of Important Process-Controlled Variables interface for an ethylene glycol *RSR* system.

Disturbances Selection: A "Selection of Disturbances" interface is shown in Fig. 5.51.
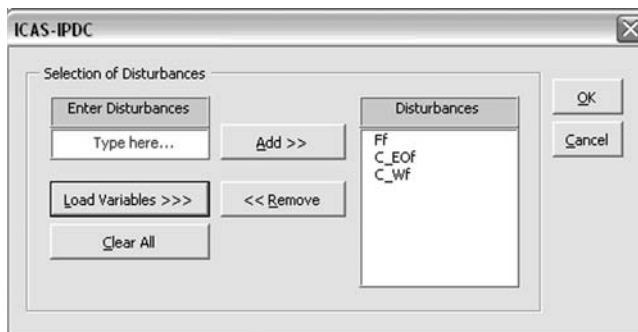
Fig. 5.51. Selection of Disturbances interface for an ethylene glycol *RSR* system.

Step 3.2   Operational Window Identification

The second step in Part II is to identify the operational window. A "Operational Window Identification" interface is shown in Fig. 5.52. In this step, the software helps the user to define the operational window in terms of design and process variables. For this example, the operational window for reactor volume is defined within $3 - 30$ m^3. On the other hand, to satisfy product quality, the water composition at the bottom $x_{W,D}$ should be less than 0.05.

Fig. 5.52. Operational Window Identification interface for an ethylene glycol *RSR* system.

Step 3.3   Design-Control Target Identification

The main objective of this step is to develop the attainable region and driving force diagrams for reactor and separator design problem, respectively, and then to select the design target at the maximum point of the attainable region and driving force. A "Design-Control Target Identification" interface is shown in Fig. 5.53.

Fig. 5.53. Design-Control Target Identification interface for an ethylene glycol *RSR* system.

Attainable Region Development: The calculated attainable region diagram is shown in Fig. 5.54.
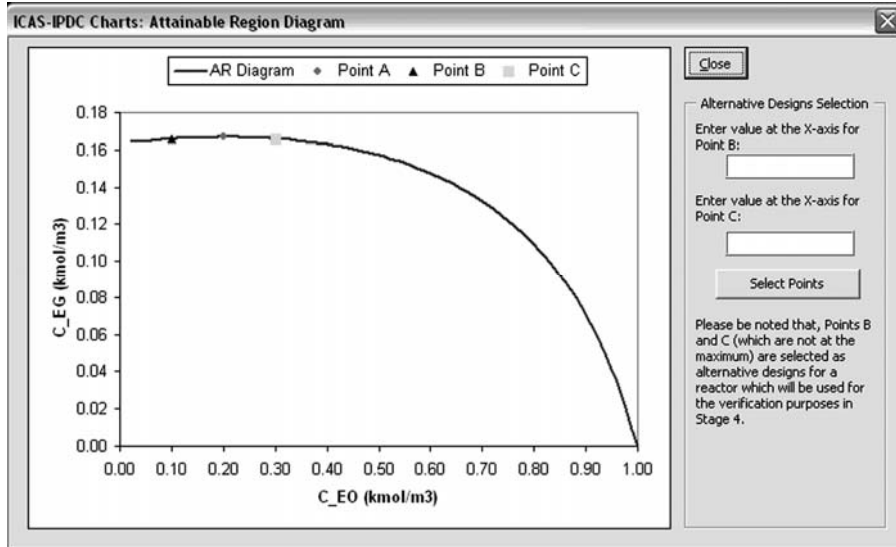
Fig. 5.54. Attainable region diagram with three design alternatives.

Driving Force Development: The calculated driving force diagram is shown in Fig. 5.55.
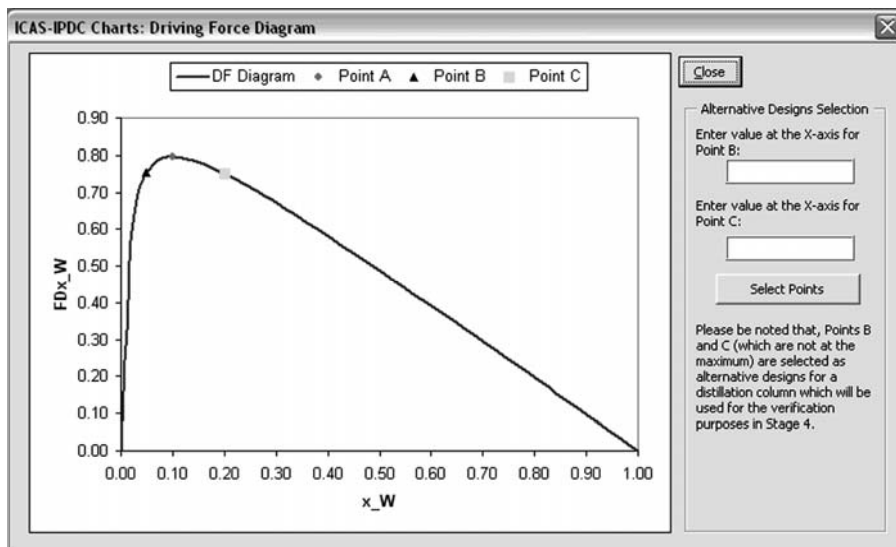
Fig. 5.55. Driving force diagram with three design alternatives.

Part III: Design Analysis Stage

Step 4.1   Design (u) and Process (y) Variables Values Calculation

Before calculating the values of design variables, it is important to define the feasible range of operation with respect to manipulated (design) and controlled (process) variables within which the snowball effect will not appear and desired product composition will be high. Therefore, it is important to define the feasible range of operation with respect to manipulated (design) and controlled (process) variables where the snowball effect can be avoided.

To define the feasible range we need the process model and the set of conditional constraints which is derived for the *RSR* system. Through manipulation of the mass balance equations, the following set of conditional constraints are obtained in terms of dimensionless variables ξ, $\beta_{Y,S}$, Da and variables m_{EO}, f_W. The detailed derivation for these equations is given in the Appendix E.

$$0 = (1 - \beta_{Y,S})\xi_{v,1} - \Omega(1 + y_{EO} - \xi_{v,1} - \xi_{v,2} - \xi_{v,3})(f_W - \xi_{v,1}) \tag{5.82}$$

$$0 = (1 - \beta_{Y,S})(\xi_{v,2} - \xi_{v,1}) - \Omega(1 + y_{EO} - \xi_{v,1} - \xi_{v,2} - \xi_{v,3})\dots$$
$$\dots[2.1(1 - \beta_{Y,S})(\xi_{v,1} - \xi_{v,2}) - (f_W - \xi_{v,1})] \tag{5.83}$$

$$0 = (\xi_{v,3} - \xi_{v2}) - \Omega(1 + y_{EO} - \xi_{v,1} - \xi_{v,2} - \xi_{v,3})[2.2(\xi_{v,2} - \xi_{v,3}) - 2.1(\xi_{v,1} - \xi_{v,2})] \tag{5.84}$$

where

$$\Omega = \frac{Da}{[1 + y_{EO} + (f_W - \xi_{v,1})/(1 - \beta_{Y,S}) - (\xi_{v,2} + \xi_{v,3})]^2}$$

In this *IPDC* problem, we want to identify the feasible range of operation in terms of dimensionless design variable *Da* and ξ within which the highest composition of desired product C_{EG} can be obtained and the snowball effect can be avoided. Eqs. (5.82)-(5.84) can be written in compact from as

$$0 = f[\xi \quad u] \tag{5.85}$$

where

$$\mathbf{u} = [Da, \beta_{Y,S}, m_{EO}, f_W]$$

Vector **u** represents the set of design variables. Once the vector **u** has been determined, Eq. (5.85) is solved for ξ and using Eqs. (5.86)-(4.32) (representing the steady state process model) the values of the important process variables are obtained:

$$S = 1 + y_{EO} + \left(\frac{f_W - \xi_{v,1}}{1 - \beta_{Y,S}}\right) - (\xi_{v,2} + \xi_{v,3}) \tag{5.86}$$

$$z_{EO,S} = \frac{1 + y_{EO} - \left(\xi_{v,1} + \xi_{v,2} + \xi_{v,3}\right)}{1 + y_{EO} + \left(f_W - \xi_{v,1}\right)/\left(1 - \beta_{Y,S}\right) - \left(\xi_{v,2} + \xi_{v,3}\right)} \qquad (5.89)$$

$$z_{W,S} = \frac{\left(f_W - \xi_{v,1}\right)/\left(1 - \beta_{Y,S}\right)}{1 + y_{EO} + \left(f_W - \xi_{v,1}\right)/\left(1 - \beta_{Y,S}\right) - \left(\xi_{v,2} + \xi_{v,3}\right)} \qquad (5.90)$$

$$z_{EG,S} = \frac{\xi_{v,1} - \xi_{v,2}}{1 + y_{EO} + \left(f_W - \xi_{v,1}\right)/\left(1 - \beta_{Y,S}\right) - \left(\xi_{v,2} + \xi_{v,3}\right)} \qquad (5.91)$$

$$z_{DEG,S} = \frac{\xi_{v,2} - \xi_{v,3}}{1 + y_{EO} + \left(f_W - \xi_{v,1}\right)/\left(1 - \beta_{Y,S}\right) - \left(\xi_{v,2} + \xi_{v,3}\right)} \qquad (5.92)$$

$$z_{TEG,S} = \frac{\xi_{v,3}}{1 + y_{EO} + \left(f_W - \xi_{v,1}\right)/\left(1 - \beta_{Y,S}\right) - \left(\xi_{v,2} + \xi_{v,3}\right)} \qquad (5.93)$$

A "Design-Process Values Calculation" interface is shown in Fig. 5.56.
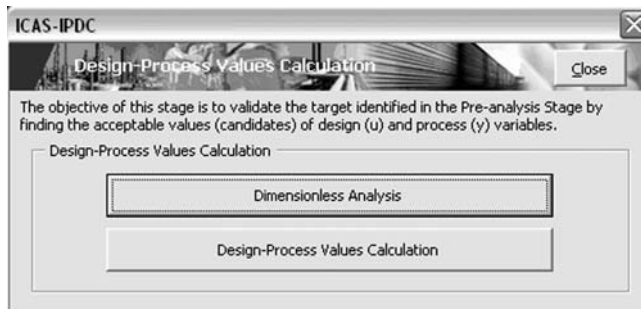
Fig. 5.56. Design-Process Values Calculation menu for an ethylene glycol *RSR* system.

Dimensionless Analysis: Here, the user should define the feasible range of operation with respect to manipulated (design) and controlled (process) variables. A "Dimensionless Analysis" results is shown in Fig. 5.57.
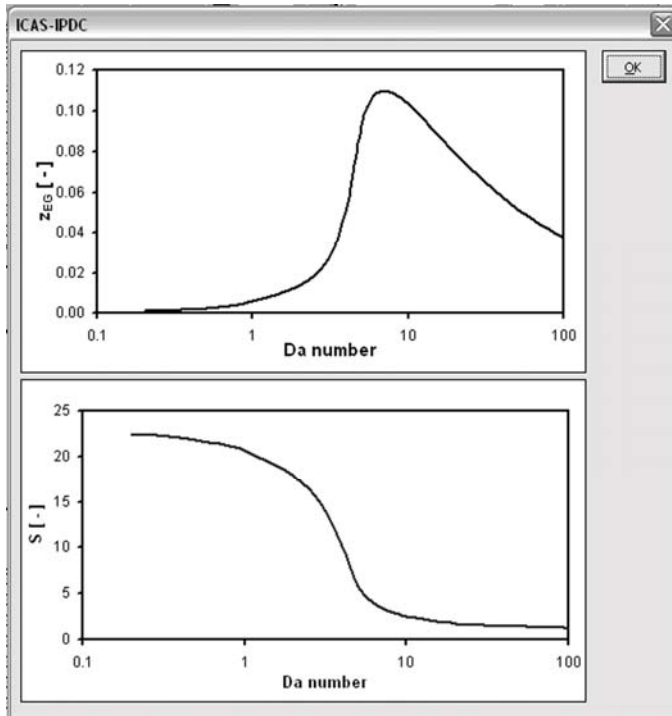
Fig. 5.57. Product composition of *EG* and reactor outlet flowrate, *S*, as a function of *Da*.

In Fig. 5.57, it can be observed that the maximum values of z_{EG} are within the range of of $3 < Da < 10$. But, when $Da < 5$, the S increases significantly indicating a possible snowball effect. In order to avoid the snowball effect, the reactor should be operated at higher value of *Da* (for example $Da > 4$). Therefore, for the maximum values for the production of *EG* and also to eliminate the snowball effect, the feasible operational window for *Da* is identified within the range of $5 < Da < 10$.

Design-Process Values Calculation: Results of the reactor volume calculation are shown in Fig. 5.58. For distillation design variables calculation, results are shown in Fig. 5.59.

Fig. 5.58. Interface for Da number and corresponding reactor volume for a reactor.

Fig. 5.59. Values of design variables at different distillation design alternatives for an ethylene glycol RSR system.

It is important to mention that, in practice, the separation section is efficient and robust. It can deliver the product and recycle streams of relatively high purities, even when the flow or composition of the separator feed changes. Therefore, here, we only consider a distillation column at point A (at the maximum point of driving force diagram) for further analysis with other reactor design alternatives. The objective is to obtain higher desired product composition and also to avoid the snowball effect through an appropriate reactor design. The steady state simulation results are shown in Fig. 5.60. It should be noted here that the steady state simulation results obtained in this step will be used as initial values for controlled and manipulated variables in the dynamic simulation.

Fig. 5.60. Steady state simulation results at different reactor design alternatives for an ethylene glycol RSR system.

<u>Part IV: Controller Design Analysis Stage</u>

Part IV of the methodology consists of two important steps, Step 5.1 Sensitivity Analysis and Step 5.2 Controller Structure Selection.

Step 5.1   Sensitivity Analysis

Derivative plots are shown in Fig. 5.61 for reactor design and Fig. 5.62 for distillation design.
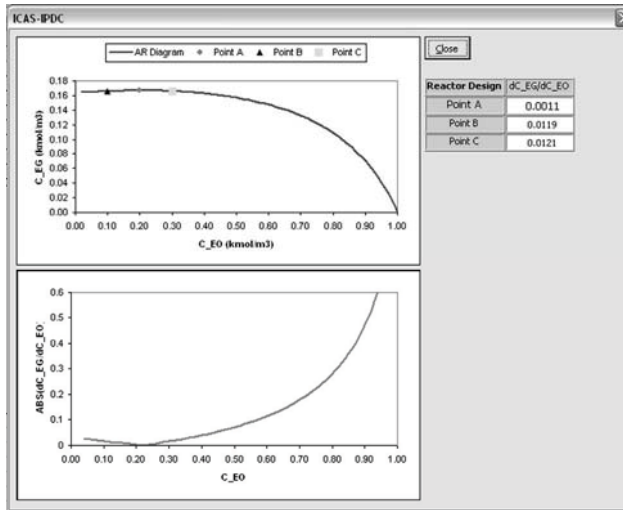
Fig. 5.61. Plot of derivative of C_{EG} with respect to C_{EO} for sensitivity analysis.
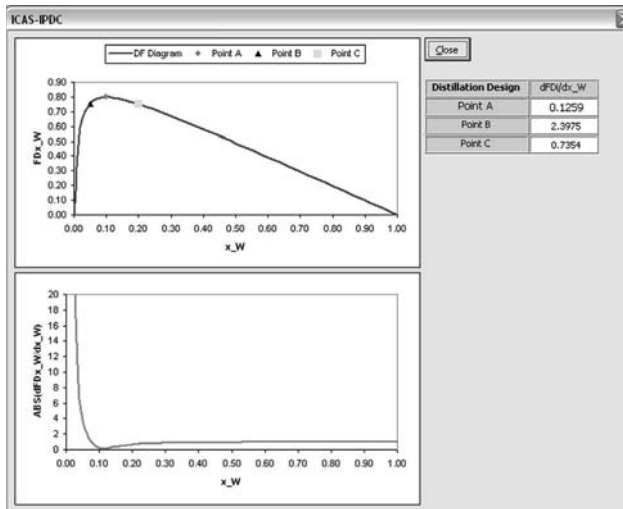
Fig. 5.62. Plot of derivative of FD_i with respect to x_W for sensitivity analysis.

Accordingly, dC_{EG}/dF_f and dC_{EG}/dC_{EOf} can be represented as:

$$\frac{dC_{EG}}{dF_f} = \left(\frac{dC_{EG}}{dC_{EO}}\right)\left(\frac{dC_{EO}}{dF_f}\right) \tag{5.95}$$

$$\frac{dC_{EG}}{dC_{EOf}} = \left(\frac{dC_{EG}}{dC_{EO}}\right)\left(\frac{dC_{EO}}{dC_{EOf}}\right) \tag{5.96}$$

It can be seen from Fig. 5.61 that the value of dC_{EG}/dC_{EO} is smaller for reactor design A compared to other designs. Since dC_{EG}/dC_{EO} is smaller at design A, therefore, will result in a smaller value of dC_{EG}/dF_f and dC_{EG}/dC_{EOf}. A small value of dC_{EG}/dF_f and dC_{EG}/dC_{EOf} mean that the desired product C_{EG} is less sensitive to the changes in F_f and C_{EOf}. In this case, reactor design A will be more robust to the changes in disturbances than reactor designs B and C.

For a distillation column design, $d\theta/d\mathbf{x}$ is represented by dF_{Di}/dx_W. Accordingly, $dx_{B,W}/dF$ and $dx_{D,EG}/dF$ can be represented as:

$$\frac{dx_{B,W}}{dF} = \left(\frac{dx_{B,W}}{dF_{Di}}\right)\left(\frac{dF_{Di}}{dx_W}\right)\left(\frac{dx_W}{dF}\right) \tag{5.97}$$

$$\frac{dx_{D,EG}}{dF} = \left(\frac{dx_{D,EG}}{dF_{Di}}\right)\left(\frac{dF_{Di}}{dx_W}\right)\left(\frac{dx_W}{dF}\right) \tag{5.98}$$

It can be seen from Fig. 5.62, that the value of dF_{Di}/dx_W is smaller for distillation design A, therefore, will result in a smaller value of $dx_{B,W}/dF$ and $dx_{D,EG}/dF$. A small value of $dx_{B,W}/dF$ and $dx_{D,EG}/dF$ means that the bottom and top product purity are less sensitive to the changes in F.

Step 5.2   Controller Structure Selection

The objective of this step is to select the best controller structure (pairing of controlled-manipulated variables) that can satisfy the control objective (maintaining desired product composition z_{EG} in the reactor, and top and bottom product purity for the distillation column, which is represented by $x_{D,EG}$ and $x_{B,W}$, at their optimal set point in the presence of disturbances). Results are shown in Fig. 5.63.

According to Russel et al. (2002), dC_{EG}/dF, $dx_{B,W}/dV$ and $dx_{D,EG}/dL$ can be represented as:

$$\frac{dC_{EG}}{dF} = \left(\frac{dC_{EG}}{dC_{EO}}\right)\left(\frac{dC_{EO}}{dh_r}\right)\left(\frac{dh_r}{dF}\right) \approx 0 \tag{5.99}$$

$$\frac{dx_{B,W}}{dV} = \left(\frac{dx_{B,W}}{dF_{Di}}\right)\left(\frac{dF_{Di}}{dx_W}\right)\left(\frac{dx_W}{dV}\right) \approx 0 \tag{5.100}$$

$$\frac{dx_{D,EG}}{dL} = \left(\frac{dx_{D,EG}}{dF_{Di}}\right)\left(\frac{dF_{Di}}{dx_W}\right)\left(\frac{dx_W}{dL}\right) \approx 0 \tag{5.101}$$

Since $dC_{EG}/dF \approx 0$, $dx_{B,W}/dV \approx 0$ and $dx_{D,EG}/dV \approx 0$, it is possible to maintain C_{EG} at its optimal set point using concentration control or level control (see Eq. (5.99)) and $x_{B,W}$ and $x_{D,EG}$ at their optimal set point using concentration control (see Eqs. (5.100)-(5.101)).
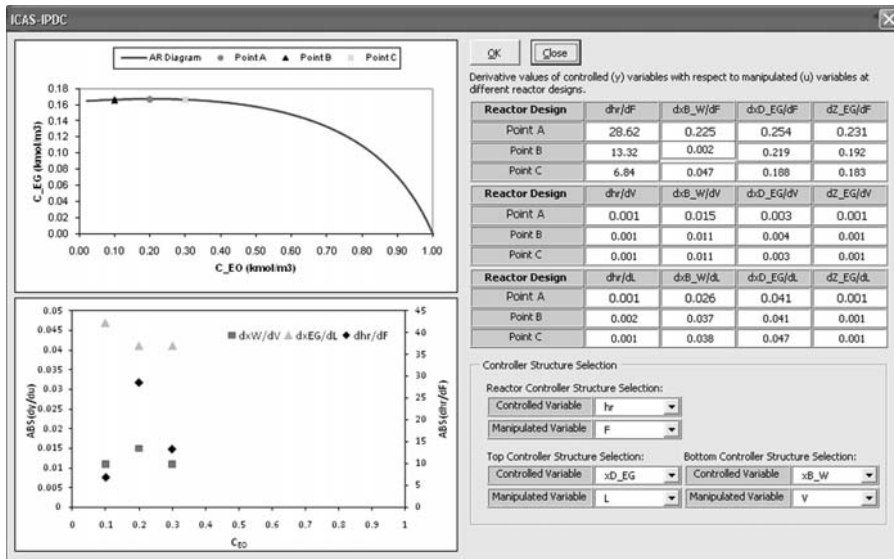
Fig. 5.63. Plot of the derivative of controlled variables with respect to manipulated variables for controller structure selection.

It can clearly be seen from Fig. 5.63, that the derivative values of dh_r/dF, $dx_{B,W}/dV$ and $dx_{D,EG}/dL$ are higher than the other derivatives. Therefore, the best pairing of controlled-manipulated variable that will able to maintain C_{EG} in the reactor is h_r-F and for product purity at the bottom of distillation column is $x_{B,W}$-V, whereas the best pairing for controlling product purity at the top of the distillation column is $x_{D,EG}$-L. These controller structures will require less control action in maintaining their controlled variables compared to other controller structures. It should be noted that, at point A, the controller action and performance are the best.

Part V: Final Selection and Verification

Step 6.1   Multi-Objective Function Calculation

The objective of this step is to select the best design candidates by analyzing the value of the multi-objective function by summing up each term of the objective function value. Results are shown in Fig. 5.64. It can be seen that the value of F_{Obj} for Point A is higher than for Points B and C. This verifies that Point A corresponds to the optimal reactor design and satisfies design, control and cost criteria.

ICAS-IPDC										
Multi-Objective Function Calculation									OK	Cancel

A. Term objective function values

Multi-objective function calculation.

	C_EG	FDi	dC_EG/dC_EO	dFDi/dx_W	dhr/dF	dxD_EG/dL	dxB_W/dV	Vr	D	
Point A	0.1522	0.7967	0.0011	0.1259	28.62	0.015	0.041	13.01	2.57	
Point B	0.1398	0.7251	0.0120	2.3975	13.32	0.011	0.041	29.64	1.57	
Point C	0.1279	0.7513	0.0121	0.7354	6.84	0.011	0.047	7.46	3.64	
Scaled value of objective function terms										FObj
Point A	1.000	1.000	0.088	0.053	1.000	1.000	0.872	0.435	0.706	39.05
Point B	0.919	0.910	0.989	1.000	0.465	0.733	0.872	1.000	0.431	9.23
Point C	0.840	0.943	1.000	0.307	0.239	0.733	1.000	0.249	1.000	13.03
Weights										
1.0	1.0	1.0	1.0	1.0	1.0	1.0	1.0	1.0	

Note.

Max FObj = w*C_EG + w*FDi + w*(1/dC_EG/dC_EO) + w*(1/dFDi/dx_W) + w*dhr/dF + w*dxD_EG/dL + w*dxB_W/dV + w*(1/Vr) + w*(1/D)

The multi-objective function is calculated by summing up each terms of the objective function value with its corresponding weight value.

Since the range and unit of each objective function values are different, the value is normalized with respect to its maximum value.

Find values	Objective function calculation

Fig. 5.64. Multi-Objective Function Calculation interface for a RSR system.

Step 6.2 Dynamic Rigorous Simulations

Closed loop dynamic simulations results are shown in Figs. 5.65-5.69. From the results, it can be seen that the reactor level (see Fig. 5.66), bottom water composition (see Fig. 5.67) and top ethylene glycol composition (see Fig. 5.69) can be maintained at their setpoints after a +2% step change is applied to a feed flowrate for all reactor design alternatives. These results shown that the controller structures selected using this methodology are able to maintain the controlled variables for this process in the presence of the disturbances.
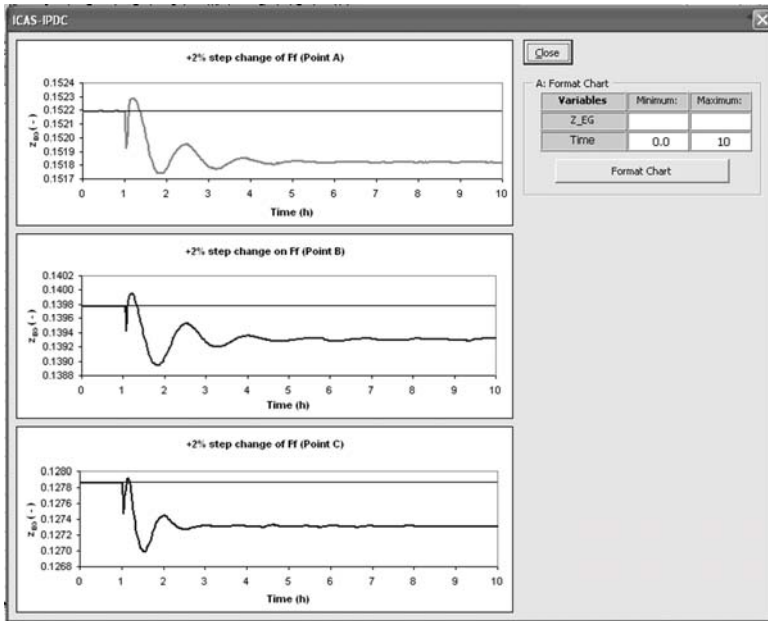
Fig. 5.65. Dynamic response of the desired product composition z_{EG} to a +2% step change of F_f for different reactor design alternatives.
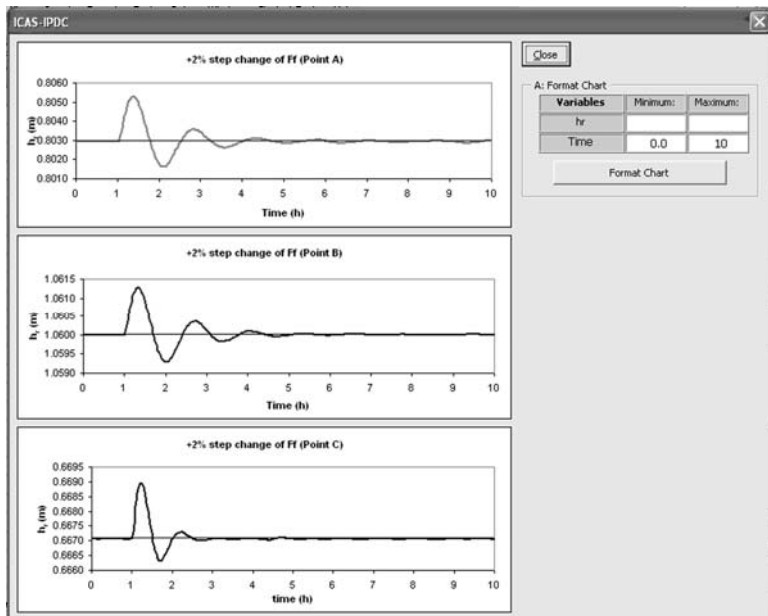
Fig. 5.66. Closed loop dynamic response of the reactor level h_r to a +2% step change of F_f for different reactor design alternatives.
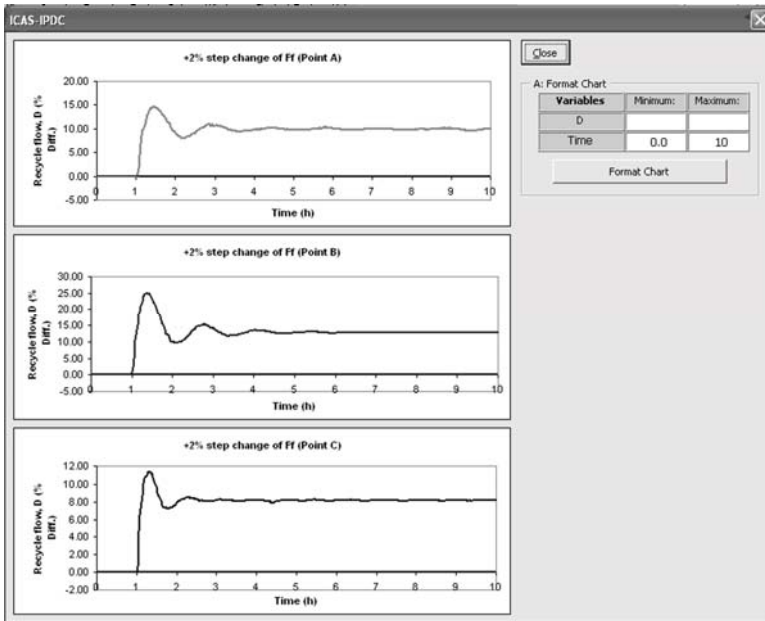
Fig. 5.67. Dynamic response of the recycle flowrate D to a +2% step change of F_f for different reactor design alternatives.
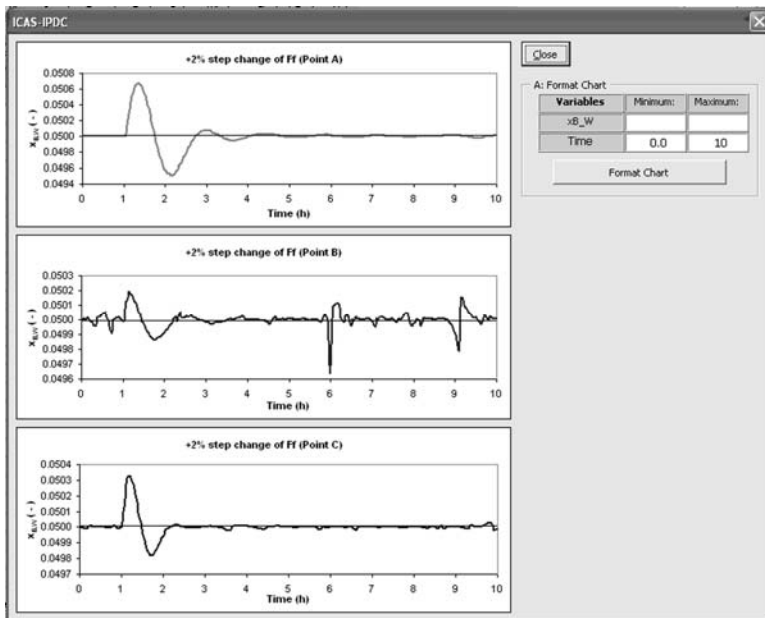
Fig. 5.68. Closed loop dynamic response of the bottom column water composition $x_{B,W}$ to a +2% step change of F_f for different reactor design alternatives.
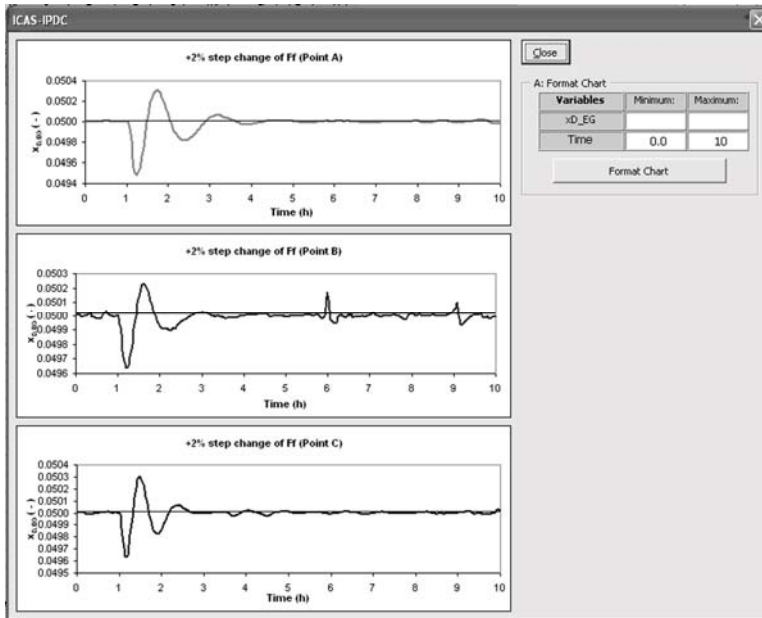
Fig. 5.69. Closed loop dynamic response of the top column ethylene glycol composition $x_{D,EG}$ to a +2% step change of F_f for different reactor design alternatives.

Results in Fig. 5.67 show that, the snowball effect is observed in the recycle flowrate D when a 2% step change is applied to the feed flowrate. These results confirm the results obtained in previous studies (Luyben, 2004; Larsson et al., 2003). To eliminate the snowball effect, in this case study, we proposed a new strategy to change the reactor holdup by allowing the reactor level controller setpoint to change at a certain value of ΔSP.

By implementing a strategy in where the reactor holdup is allowed to change by changing the reactor level controller setpoint, the snowball effect is eliminated as shown in Fig. 5.72. These results verify the effectiveness of the new control strategy in solving the snowball effect problem. The most important results from this case study are shown in Fig. 5.70 where the responses of the desired product composition z_{EG} are shown for all reactor design alternatives. It can be seen that, disturbances in the feed flowrate and also for changes in the reactor level setpoint did not give any effect on the desired product composition z_{EG} at the reactor design Point A compared to other designs (Points B and C). It can be observed that the steady state offset of the desired product composition z_{EG} is almost negligible at the reactor design Point A (see Fig. 5.70) while for other designs a larger steady state offset is found. These results show that z_{EG} is less sensitive to the effect of disturbances at reactor design Point A than for other designs.

Model-Based Integrated Process Design and Controller Design of Chemical Processes
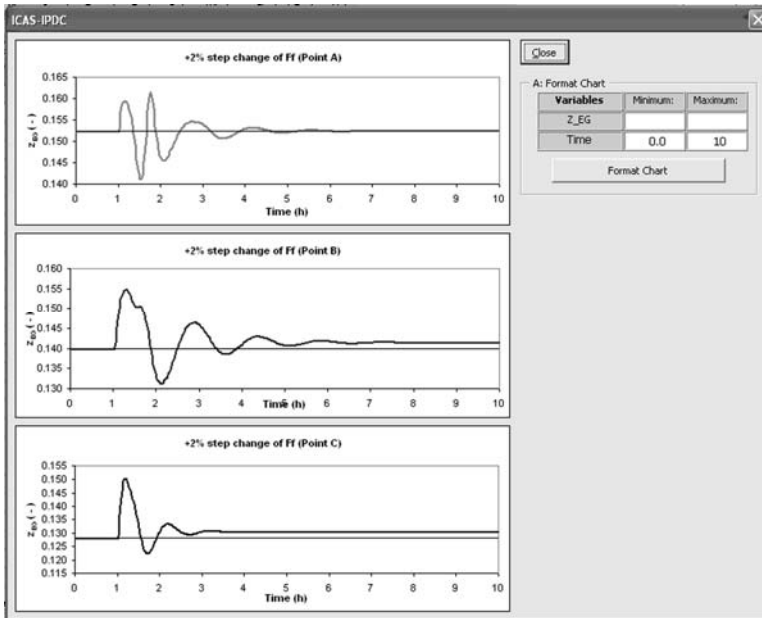
Fig. 5.70. Dynamic response of the desired product composition z_{EG} to a +2% step change of F_f for different reactor design alternatives (new control strategy).
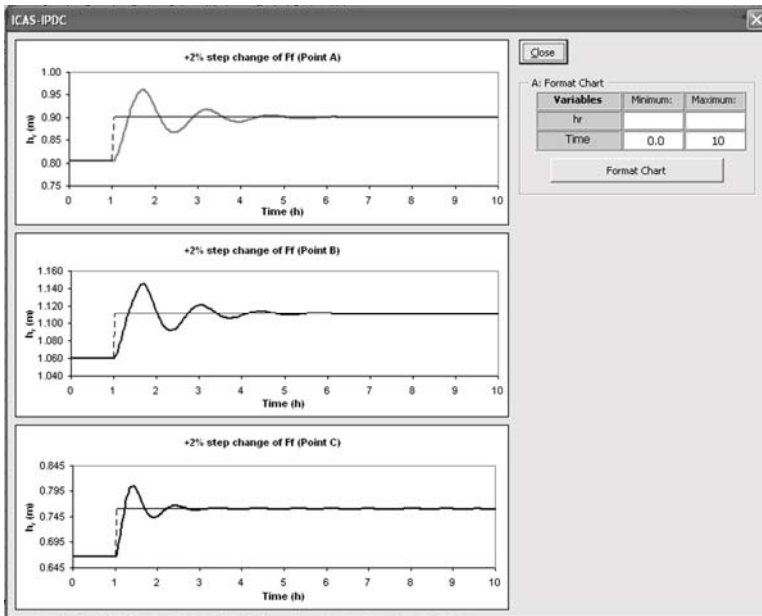
Fig. 5.71. Closed loop dynamic response of the reactor level h_r to a +2% step change of F_f for different reactor design alternatives (new control strategy).
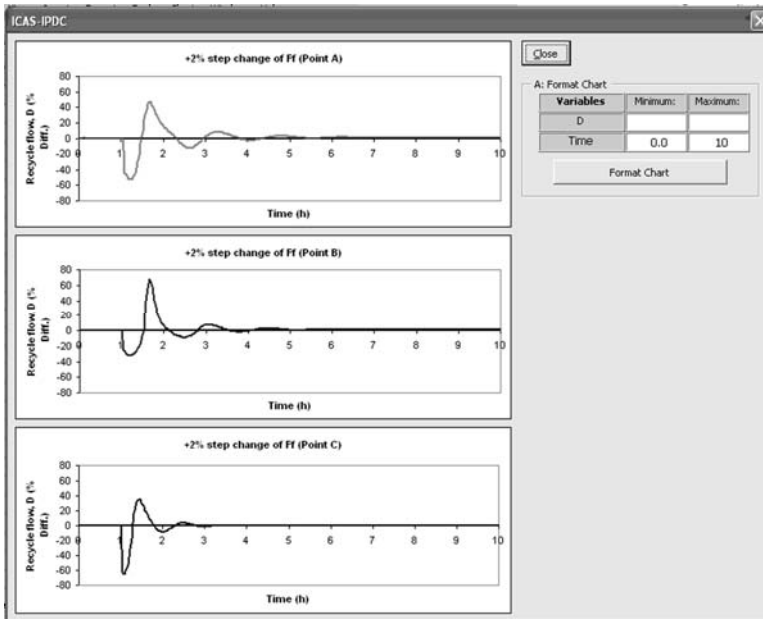
Fig. 5.72. Dynamic response of the recycle flowrate D to a +2% step change of F_f for different reactor design alternatives (new control strategy).
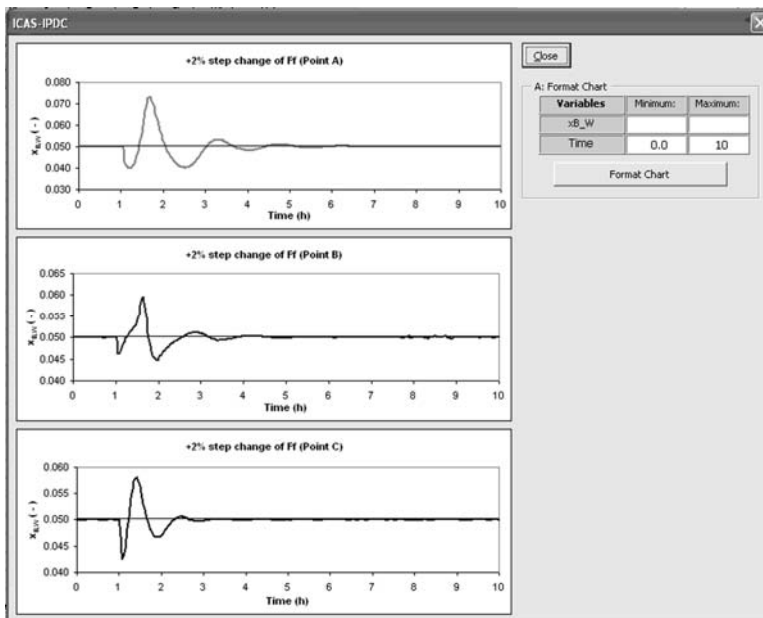
Fig. 5.73. Closed loop dynamic response of the bottom column water composition $x_{B,W}$ to a +2% step change of F_f for different reactor design alternatives (new control strategy).
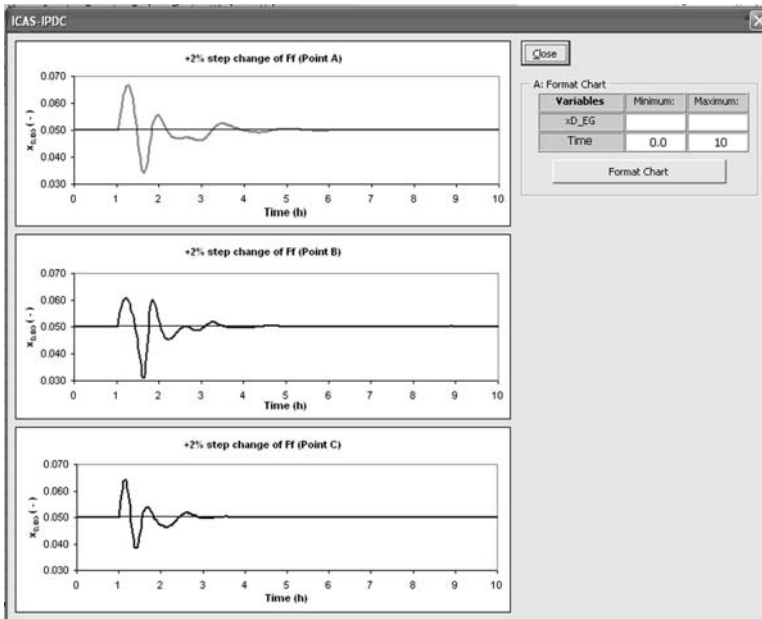
Fig. 5.74. Closed loop dynamic response of the top column ethylene glycol composition $x_{D,EG}$ to a +2% step change of F_f for different reactor design alternatives (new control strategy).

5.4 Conclusion

This section presented the applications of the proposed *IPDC* methodology in solving various types of *IPDC* problems in chemical processes. Six different types of case studies have been presented representing three different systems.

For a single reactor system, an ethylene glycol and a bioethanol production have been used as case studies to verify the capability of the proposed methodology in solving a design of a reactor system involving complex reactions. By using the proposed methodology, an optimal solution with respect to design and also controller structure has been obtained.

For a single separator design, ethylene glycol and methyl acetate separation systems were used to illustrate the capability of the proposed methodology in solving a single separator process-controller design problem. It was confirmed that designing a distillation column at the maximum point of the driving force leads to a process with lower energy consumption and much better closed loop performances in maintaining its controlled variables than at any other points.

For a reactor-separator-recycle system, a conceptual case study has been used to illustrate the effectiveness of the proposed methodology in solving process-

controller design problems. The results confirm that by applying the proposed methodology, a reactor-separator-recycle system with higher productivity and a controllable process can be designed. The results also show not only that the optimal solution for the process-controller design can be obtained at the maximum points of the attainable region and driving force for reactor and separator design, respectively, but also that the snowball effect can be avoided.

Application of the developed *ICAS-IPDC* software has been illustrated for solving a process-controller design problem of a reactor-separator-recycle system for the ethylene glycol system. By using the developed software, faster and more efficient solution of the integrated design-control problem can be obtained in a systematic way.

CHAPTER 6

Conclusions and
Future Work

6.1   **Achievements**

6.2   **Future Work**

6.1   Achievements

In this work, a systematic model-based methodology has been developed for integrated process design and controller design (*IPDC*) of chemical processes. The methodology has been applied and verified for a single reactor system, a single separator system and a reactor-separator-recycle system. A software called *ICAS-IPDC*, which step-by-step applies the described methodology has also been developed. The purpose of the software is to guide and help the engineers obtain the optimal solution to *IPDC* problems of chemical processes in a systematic and efficient way.

The main achievements that have been obtained from this work are summarized as follows:

1. This methodology is a step-by-step procedure, which allows a systematic analysis at every stage. Each step of the design methodology is clear with respect to calculations/analysis and generic in terms of application range which makes the application of the methodology quite easy.

2. This methodology is based on a decomposition solution strategy where the main idea is to decompose the complexity of the *IPDC* problem into four hierarchical stages (sub-problems): (i) pre-analysis; (ii) design analysis, (iii) controller design analysis, and (iv) final selection and verification. Using thermodynamic and process insights, a bounded search space is first identified. This feasible solution space is further reduced to satisfy the process design and controller design constraints in sub-problems (ii) and (iii), respectively, until

in the final sub-problem all feasible candidates are ordered according to the defined performance criteria (objective function). As each sub-problem is being solved, a large portion of the infeasible solution of the search space is identified and eliminated, thereby leading to a final sub-problem that is significantly smaller, which can be solved more easily.

3. In the pre-analysis of this methodology, the concepts of attainable region and driving force are used to locate the optimal design-control solution in terms of optimal condition of operation from process design and process control viewpoints. The idea is to locate the maximum point of the attainable region diagram as a solution target for the reactor design and maximum point of the driving force diagram as a solution target for the separator design. From these targets, values of others design-manipulated and process-controlled variables that match those targets are calculated using the reverse solution approach. Using model analysis, controllability issues are incorporated to pair the identified manipulated variables with the corresponding controlled variables While other optimization methods may or may not be able to find the optimal solution, depending on the performance of their search space algorithms and computational demand, the use of attainable region and driving force concepts is simple and able to find at least near-optimal designs (if not optimal) to *IPDC* problems.

4. A software called *ICAS-IPDC* has been developed and is able to perform a systematic model-based analysis to find the optimal solution of *IPDC* problems. By using *ICAS-IPDC,* the optimal solution of the complex *IPDC* problem can easily and accurately be obtained in a systematic way. *ICAS-IPDC* allows simple, accurate and faster analysis of any chemical process even in a complex process such a reactor-separator-recycle. The software is generic and its applicability can be extended to any chemical (biochemical) process by adding the necessary models to the model library.

5. The methodology has been applied to several case studies. For all presented case studies, an optimal solution with respect to design, control and cost has been obtained in a efficient and systematic way.

6.2   Future Work

A systematic methodology for solving integrated process design and controller design (*IPDC*) has been developed successfully in this work. However, there are still a number of opportunities for further developments and improvements. Several suggestions for future work are given in terms of:

1. Scientific Challenges:

    a. In order to ensure robust operability of the optimal designed process, the effect of uncertainties will need to be incorporated during the analysis (sub-problem 1 – 3). The effect of uncertainties such as those related to the operating conditions (i.e., feed flowrates and concentrations, and catalyst activity), model parameters (i.e., heat transfer coefficients and kinetic constants) and the costs or prices of materials is an important issue to analyze. It is possible that an optimal design under nominal conditions would show poor operability performances under uncertainties.

    b. The case studies indicate a wide range of complex problems, but the real industrial problems have not been tackled. However, the suggestion is to partition the industrial problems into smaller sub-sets and apply the methodology for each partition.

    c. The *IPDC* solution obtained in this methodology is guaranteed optimal (or near optimal if not optimal). However, it is advisable to compare results obtained in this methodology with other solution approaches to identify their difficulties and give suggestions to improve their performance.

    d. The validation of the designed process using *ICAS-IPDC* is presently based on process models. However, it would be interesting to include experimental validations to validate the designed process.

    e. In the objective function calculation, all the objective function terms are weighted equally meaning that the decision-maker does not have any preference for one objective over another. However, it would be interesting to use different value of the weights to study their impact on the *IPDC* solution especially in the controller structure selection.

2. Software Development: More options and analysis tools could be added to the software to make it more flexible, reliable and comprehensive such as:

    a. The connection with a reaction database is required in order to extract the reactions information automatically.

b. The main interface of *ICAS-IPDC* might be connected to the commercial simulators (*Aspen*, *PRO II*, *ICAS*, *HYSYS*, etc.) for verification using rigorous simulation.

c. The connection with some commercial simulator/databases is required in *ICAS-IPDC* in order to extract the component properties automatically.

d. Presently, *ICAS-IPDC* only considered a simple *SISO* (single-input-single-output) feedback control system to verify the designed process in terms of closed loop performances. However, it is advisable to extend to more advance control systems such as *MIMO* (multi-input-multi-output) controller or *MPC* (model predictive control) to be integrated in the software.

Nomenclature

$\mathbf{d}$	=	Vector of disturbances
f_W		Dimensionless feed water flowrate
h_r	=	Reactor level
h_j^l	=	Specific heat content of liquid emanating from stage j
h_j^v	=	Specific heat content of vapour emanating from stage j
k	=	Kinetic constant
m_{EO}	=	Dimensionless reactor inlet ethylene oxide flowrate
$\mathbf{r(C)}$	=	Vector of reaction rate
r_A	=	Reaction rate for Component A
r_B	=	Reaction rate for Component B
r_P	=	Reaction rate for desired product
r_R	=	Reaction rate for limiting reactant
t	=	time
$\mathbf{u}$	=	Vector of design (manipulated) variables
$\mathbf{u}_0$	=	Vector of initial conditions of the design (manipulated) variables
x_B	=	Bottom composition
$x_{B,MeOH}$	=	Methanol bottom composition
$x_{B,W}$	=	Water bottom composition
x_D	=	Distillate composition
$x_{D,EG}$	=	Ethylene glycol distillate composition
$x_{D,MeOH}$	=	Methanol distillate composition
$x_{D,W}$	=	Water distillate composition
x_i	=	Liquid composition of Component i
$x_{i,j}$	=	Liquid mole fraction for component i on the jth stage
x_W	=	Liquid Water composition
$\mathbf{x}$	=	Vector of state variables
$\mathbf{x}_0$	=	Vector of initial conditions of the state variables
$\mathbf{x}^*, \mathbf{y}^*, \mathbf{u}^*$	=	Optimal steady state solutions
$\mathbf{v}$	=	Vector if chemical system variables
w	=	Weight factor
$\mathbf{y}$	=	Vector of process (controlled) variables
y_i	=	Vapour composition of Component i
$y_{i,j}$	=	Vapour mole fraction for component i on the jth stage
z_A	=	Reactor composition of Component A
y_1	=	Primary controlled variable
y_2	=	Secondary controlled variable
$z_{A,F}$	=	Feed composition of Component A
$z_{B,F}$	=	Feed composition of Component B
z_{DEG}	=	Diethylene glycol reactor composition

z_{EO}	=	Ethylene oxide reactor composition
z_{EG}	=	Ethylene glycol reactor composition
z_{HOAc}	=	Acetic acid reactor composition
z_{MeOAc}	=	Methyl acetate reactor composition
z_{MeOH}	=	Methanol reactor composition
z_{TEG}	=	Triethylene glycol reactor composition
z_W	=	Water reactor composition
A	=	Cross sectional area
B	=	Bottom flowrate
$C_{Cellulose}$	=	Cellulose concentration
$C_{Ethanol}$	=	Ethanol concentration
$C_{Glucose}$	=	Glucose concentration
C_A	=	Concentration of Component A
$C_{A,0}$	=	Feed concentration of Component A
C_B	=	Concentration of Component B
$C_{B,0}$	=	Feed concentration of Component B
C_{DEG}	=	Concentration of Diethylene Glycol
C_{EG}	=	Concentration of Ethylene Glycol
C_{EO}	=	Concentration of Ethylene Oxide
C_P	=	Concentration of desired product
$C_{P,0}$	=	Feed concentration of desired product
C_R	=	Concentration of limiting reactant
$C_{R,0}$	=	Feed concentration of limiting reactant
C_{TEG}	=	Concentration of Triethylene Glycol
C_W	=	Concentration of Water
$\mathbf{C}$	=	Vector of concentrations
D	=	Distillate flowrate
Da	=	Damköhler number
F	=	Outlet flowrate
F_c	=	Cooling water flowrate
F_{Di}	=	Driving force
F_f	=	Feed flowrate
F_R	=	Recycle flowrate
J	=	Multi-objective function
$K_{i,j}$	=	Equilibrium constant of component i on the jth stage
L	=	Reflux flowrate
L_j	=	Liquid flowrate on the jth stage
$M_{i,j}$	=	Holdup of component i on the jth stage
M_j	=	Holdup on the jth stage
N	=	Number of stages
N_F	=	Feed stage
P	=	Pressure
P^*	=	Vapor pressure
$P_{i,j}$	=	Objective function terms (i=1,3; j=1,2)
$P_{i,js}$	=	Scaled objective function terms (i=1,3; j=1,2)
Q_c	=	Condenser heat duty
Q_r	=	Reboiler heat duty
R_i	=	Net reaction rate of reaction i

RB	=	Reboil ratio
RB_{min}	=	Minimum reboil ratio
RR	=	Reflux ratio
RR_{min}	=	Minimum reflux ratio
T	=	Temperature
T_b^i	=	Boiling point
T_m^i	=	Melting point
T_B	=	Bottom column temperature
T_c	=	Coolant temperature
T_{ci}	=	Coolant inlet temperature
T_D	=	Top column temperature
T_f	=	Feed temperature
T_{max}	=	Maximum temperature
T_{min}	=	Minimum temperature
U	=	Overall heat transfer coefficient
V	=	Vapour boilup
V_R	=	Reaction volume
V_r	=	Real reactor volume
V_j	=	Vapour flowrate on the $_j$th stage
Y	=	Binary decision variables

Greek Symbols

$\alpha_{i,j}$	=	Relative volatility
$\alpha_{Y,S}$	=	Recovery of ethylene oxide at stream Y with respect to stream S
c_p	=	Heat capacity
c_{pc}	=	Coolant heat capacity
$\delta_{Y,S}$	=	Recovery of diethylene glycol at stream Y with respect to stream S
$\varepsilon_{Y,S}$	=	Recovery of triethylene glycol at stream Y with respect to stream S
ρ	=	Liquid density
ρ_c	=	Coolant liquid density
τ	=	Residence time
$\beta_{Y,S}$	=	Recovery of water at stream Y with respect to stream S
$\chi_{Y,S}$	=	Recovery of ethylene glycol at stream Y with respect to stream S
$\boldsymbol{\theta}$	=	Vector of constitutive variables
ΔH_i	=	Heat of reaction i
ξ_i	=	Dimensionless extent of reaction of component i

Acronyms

BB	=	Branch and Bound
CAMD	=	Computer Aided Molecular/Mixture Design
CSTR	=	Continuous Stirred Tank Reactor
CVP	=	Control Vector Parameterization
DAEs	=	Differential Algebraic Equations
DEG	=	Diethylene Glycol

DO	=	Dynamic Optimization
EG	=	Ethylene Glycol
ENZ	=	Enzyme loading
FOPTD	=	First Order Plus Time Delay
FPU	=	Filter paper units
GBD	=	Generalized Benders Decomposition
HOAc	=	Acetic Acid
ICAS	=	Integrated Computer Aided System
IPDC	=	Integrated Process Design and Controller Design
LMI	=	Linear Matrix Inequalities
LQR	=	Linear Quadratic Regulator
MeOAc	=	Methyl Acetate
MeOH	=	Methanol
mLQR	=	Modified Linear Quadratic Regulator
MIDO	=	Mixed Integer Dynamic Optimization
MIMO	=	Multi Input Multi Output
MINLP	=	Mixed Integer Non-Linear Program
MoT	=	Modeling Testbed
MPC	=	Model Predictive Control
NLP	=	Non-Linear Program
OA	=	Outer Approximation
ODEs	=	Ordinary Differential Equations
PDEs	=	Partial Differential Equations
PFR	=	Plug Flow Reactor
PI	=	Proportional-Integral
PSO	=	Particle Swarm Optimization
RGA	=	Relative Gain Array
RSR	=	Reactor-Separator-Recycle
SISO	=	Single Input Single Output
SSCF	=	Simultaneous Saccharification and Co-Fermentation
SSF	=	Simultaneous Saccharification and Fermentation
TEG	=	Triethylene Glycol
UI	=	User Interface
W	=	Water

References

Adney, B., & Baker, J. (1996). Measurement of Cellulase Activities. (National Renewable Energy Laboratory, Golden Colorado, USA)

Allgor, R. J., & Barton, P. I. (1999). Mixed-integer dynamic optimizaton. I. Problem formulaton. *Computers and Chemical Engineering*, 23(4-5), 567-584.

Alhammadi, H. Y., & Romagnoli, J. A. (2004). Process design and operation incorporating environmental, profitability, heat integration and controllability considerations. In P. Seferlis, & M. C. Georgiadis (Eds.), *The integration of process design and control* (pp. 264-305-41). Amsterdam: Elsevier B. V.

Altimari, P., & Bildea, C. S. (2009). Integrated design and control of plantwide systems coupling exothermic and endothermic reactions. *Computers and Chemical Engineering*, 33(4), 911-923.

Alvarado-Morales, M., Hamid, M. K. A., Sin, G., Gernaey, K. V., Woodley, J. M., & Gani, R. (2010). A model-based methodology for simultaneous design and control of a bioethanol production process. *Computers and Chemical Engineering*, 23(12), 2043-2061.

Androulakis, I. (2000). Kinetic mechanism reduction based on an integer programming approach. *AIChE Journal*, 46(2), 361-371.

Avraam, M., Shah, N., & Pantelides, C. C. (1998). Modeling and optimization of general hybrid systems in the continuous time domain. *Computers and Chemical Engineering*, 22(Suppl.), S221-S228.

Avraam, M., Shah, N., & Pantelides, C. C. (1999). A decomposition algorithm for the optimization of hybrid dynamic processes. *Computers and Chemical Engineering*, 23(Suppl.), S451-S454.

Bahri, P., Bandoni, J. A., & Romagnoli, J. A. (1997). Integrated flexibility and controllability analysis in design of chemical processes. *AIChE Journal*, 43(4), 997-1015.

Balakrishna, S., & Biegler, L. T. (1993). A unified approach for the simultanoues synthesis of reaction energy and separation system. *Industrial and Engineering Chemistry Research*, 32(7), 1372-1382.

Banga, J. R., Moles, C. G., & Alonso, A. A. (2003). Global optimization of bioprocess using stochastic and hybrid methods. In C. A. Floudas, & P. M. Pardalos (Eds.), *Frontier in global optimization, nonconvex optimization and its applications* (pp. 45-70). Kluver Academic Publishers.

Bansal, V., Perkins, J. D., Pistikopoulos, E. N., Ross, R., & Van Schijndel, J. M. G. (2000). Simultaneous design and control optimization under uncertainty. *Computers and Chemical Engineering*, 24, 261-266.

Bansal, V., Perkins, J. D., & Pistikopoulos, E. N. (2002). A case study in simultaneous design and control using rigorous, mixed-integer dynamic optimization models. *Industrial and Engineering Chemistry Research*, 41(4), 760-778.

Bansal, V., Sakizlis, V., Ross, R., Perkins, J. D., & Pistikopoulos, E. N. (2003). New algorithms for mixed-integer dynamic optimization. *Computers and Chemical Engineering*, 27, 647-668.

Bek-Pedersen, E. (2002). *Synthesis and design of distillation based separation scheme*. Ph.D. Dissertation Thesis, Technical University of Denmark.

Bek-Pedersen, E., & Gani, R. (2004). Design and synthesis of distillation systems using a driving force based approach. *Chemical Engineering and Processing*, 43(3), 251-262.

Carvalho. A., Gani, R., & Matos, H. (2008). Design of sustainable chemical processes: Systematic retrofit analysis generation and evaluation of alternatives. *Process Safety and Environmental Protection*, 86(5), 328-346.

Chachuat, B., Singer, A. B., & Barton, P. I. (2005). Global mixed-integer dynamic optimization. *AIChE Journal*, 51(8), 2235-2253.

Chawankul, N., Ricardez-Sandoval, L. A., Budman, H., & Douglas, P. L. (2007). Integration of design and control: A robust control approach using MPC. *Canadian Journal of Chemical Engineering*, 85, 433-446.

Conte, E., Gani, R., & Malik, T. I. (2010), The virtual product-process laboratory applied to personal care formulations, *Computer Aided Chemical Engineering*, 28, 1297-1302.

d'Anterroches, L., & Gani, R. (2006). Computer aided methodology for simultaneous synthesis, design and analysis of chemical products-processes. *Computer Aided Chemical Engineering*, 21, 853-858.

Dimitriadis, V., & Pistikopoulos, E. N. (1995). Flexibility analysis of dynamic system. *Industrial and Engineering Chemistry Research*, 34(12), 4451-4462.

Douglas, J. M. (1988). *Conceptual design of chemical processes*. New York: McGraw-Hill.

Esposito, W. R., & Floudas, C. A. (2000). Deterministic global optimization in nonlinear optimal control problems. *Journal of Global Optimization*, 17, 245-255.

Exler, O., Antelo, L. T., Egea, J. A., Alonso, A. A., & Banga, J. R. (2008). A Tabu search-based algorithm for mixed-integer nonlinear problems and its application to integrated process and control system design. *Computers and Chemical Engineering*, 32, 1877-1891.

Gani, R., & Bek-Pedersen, E. (2000). A simple new algortihm for distillation column design. *AIChE Journal*, 46(6), 1271-1274.

Gani, R., Gómez, P. A., Folić, M., Jiménez-González, C., & Constable, D. J. C. (2008). Solvents in organic síntesis: Replacement and multi-step reaction systems. *Computers and Chemical Engineering*, 32(10), 2420-2444.

Ghose, T. K., & Tyagi, R. D. (1979). Rapid ethanol fermentation of cellulose hydrolysate. II. Product and substrate inhibition and optimization of fermentor design. *Biotechnology and Bioengineering*, 21(8), 1401-1420.

Glasser, D., Hildebrandt, D., & Crowe, C. (1987). A geometric approach to steady flow reactors: The attainable region and optimization in concentration space. *Industrial and Engineering Chemistry Research*, 26(9), 1803-1810.

Glasser, D., Hildebrandt, D., & Crowe, C. (1990). Geometry of the attainable region generated by reaction and mixing: With and without constraints. *Industrial and Engineering Chemistry Research*, 29(1), 49-58.

Godorr, S. A., Hildebrandt, D., & Glasser, D. (1994). The attainable region for systems with mixing and multiple-rate processes: finding optimal reactor structures. *The Chemical Engineering Journal and the Biochemical Engineering Journal*, 54(3), 175-186.

Gusakov, A. V., Sinitsyn, A. P., & Klyosov, A. A. (1985). Kinetics of the enzymatic hydrolysis of cellulose. 1. A mathematical model for a batch rector process. *Enzyme Microb. Technol.*, 7, 346-352.

Hamid, M. K. A., Sin, G., & Gani, R. (2009A). A new model-based methodology for simultaneous design and control of reaction-separation system with recycle. *Computer Aided Chemical Engineering*, 26, 839-845.

Hamid, M. K. A., Sin, G., & Gani, R. (2009B). Determination of optimal design and control decisions for reactor-separator systems with recycle. In M. M. El-Halwagi, & A. A. Linninger (Eds.), *Design for energy and the environment* (pp. 593-602). Breckenridge, Colorado: CRC Press

Hamid, M. K. A., Sin, G., & Gani, R. (2010A). Integration of process design and controller design for chemical processes using model-based methodology. *Computers and Chemical Engineering*, 34(5), 683-699.

Hamid, M. K. A., Sin, G., & Gani, R. (2010B). Application of decomposition methodology to solve integrated process design and controller design problems for reactor-separator-recycle systems. In M. Kothare, M. Tade, A. Vande Wouwer, & I. Smets (Eds.), *Proceedings of the 9th International Symposium on Dynamics and Control of Process Systems* (DYCOPS 2010) (pp. 449-454). Lueven, Belgium.

Hildebrandt, D., & Glasser, D. (1990). The attainable region and optimal reactor structures. *Chemical Engineering Science*, 45(8), 2161-2168.

Karunanithi, A. P. T., Achenie, L. E. K., & Gani, R. (2005). A new decomposition-based computer-aided molecular/mixture design methodology for the design of optimal solvents and solvent mixtures. *Industrial and Engineering Chemistry Research*, 44, 4785-4797.

Karunanithi, A. P. T., Achenie, L. E. K., & Gani, R. (2006). A computer-aided molecular design framework for crystallization solvent design. *Chemical Engineering Science,* 61(4), 1247-1260.

Kookos, I. K., & Perkins, J. D. (2001). An algorithm for simultaneous process design and control. *Industrial and Engineering Chemistry Research*, 40, 4079-4088.

Larsson, T., & Skogestad, S. (2000). Plantwide control – A review and a new design procedure. *Modeling, Identification and Control*, 21(4), 209-240.

Larsson, T., Govatsmark, M. S., Skogestad, S., & Yu, C. C. (2003). Control structure selection for reactor, separator, and recycle processes. *Industrial and Engineering Chemistry Research*, 42, 1225-1234.

Lee, C. –G., Kim, C. H., & Rhee, S. K. (1992). A kinetic model and simulation of starch saccharification and simulateneous ethanol fermentation by amyloglucosidase and Zymomonas mobilis. *Bioprocess and Biosystems Engineering*, 7(8), 335-341.

López-Negrete, R., & Flores-Tlacuahuac, A. (2009). Integrated design and control using a simultaneous mixed-integer dynamic optimization approach. *Industrial and Engineering Chemistry Research*, 48, 1933-1943.

Lu, X. J., Li, H.-X., & Yuan, X. (2010). PSO-based intelligent integration of design and control for one kind of curing process. *Journal of Process Control*, 20, 1116-1125.

Lutze, P., Gani, R., & Woodley, J. M. (2010). Process intensification: A perspective on process synthesis. *Chemical Engineering and Processing: Process Intensification*, 49(6), 547-558

Luyben, W. L. (2004). The need for simultaneous design education. In P. Seferlis, & M. C. Georgiadis (Eds.), *The integration of process design and control* (pp. 10-41). Amsterdam: Elsevier B. V.

Luyben M. L., & Floudas, C. A. (1994). Analyzing the interaction of design and control. 1. A multiobjective framework and application to binary distillation synthesis. *Computers and Chemical Engineering*, 18(10), 933-969.

Malcom, A., Polan, J., Zhang, L., Ogunnaike, B. A., & Linninger, A. (2007). Integrating systems design and control using dynamic flexibility analysis. *AIChE Journal*, 53(8), 2048-2061.

Meeuse, F. M., & Grievink, J. (2004). Thermodynamic controllability assessment in process synthesis. In P. Seferlis, & M. C. Georgiadis (Eds.), *The integration of process design and control* (pp. 146-167). Amsterdam: Elsevier B. V.

Milne, D., Glasser, D., Hildebrandt, D., & Hausberger, B. (2006). Graphically assess a reactor's characteristics. *Chemical Engineering Progress*, 102(3), 46-51.

Miranda, M., Reneaume, J. M., Meyer, X., Meyer, M., & Szigeti, F. (2008). Integrating process design and control: An application of optimal control to chemical processes. *Chemical Engineering and Processing*, 47, 2004-2018.

Mohideen, M., Perkins, J. D., & Pistikopoulos, E. N. (1996). Optimal design of dynamic system under uncertainty. *AIChE Journal*. 42(8), 2251-2272.

Mohideen, M., Perkins, J. D., & Pistikopoulos, E. N. (1997). Towards an efficient numerical procedure for mixed-integer optimal control. *Computers and Chemical Engineering*, 21(Suppl.), S457-S462.

Moles, C. G., Gutierrez, G., Alonso, A. A., & Banga, J. R. (2003). Integrated process design and control via global optimization: A wastewater treatment plant case study. *Chemical Engineering Research and Design*, 81, 507-517.

Moon, H., Kim, J-S., Oh, K-Y., Kim, S-W., & Hong, S-I. (2001). Ethanol production using steam-exploded wood with glucose-and cellobiose fermenting yeast, Brettanomyces custersii. *Journal of Microbiology and Biotechnology*, 11(4), 598-606.

Moon, J., Kim, S, Ruiz, G. J., & Linninger, A., (2009A). Integrated design and control under uncertainty – Algorithm and applications. In M. M. El-Halwagi, & A. A. Linninger (Eds.), *Design for energy and the environment* (pp. 659-668). Breckenridge, Colorado: CRC Press

Moon, J., Kim, S, Ruiz, G. J., & Linninger, A., (2009B). Embedded control for optimizing flexible dynamic process performance. *Computer Aided Chemical Engineering*, 27, 1251-1256.

Okafor, N. (2007). *Modern Industrial Microbiology and Biotechnology*. New Hampshire: Science Publishers.

Ooshima, H., Burns, D. S., & Converse, A. O. (1990). Adsorption of cellulase from Trichoderma reesei on cellulose and lignacious residue in wood pretreated by dilute sulfuric acid with explosive decomposition. *Biotechnology and Bioengineering*, 36, 446-452.

Parker, W. A., & Prados, J. W. (1964). Analog computer design of an ethylene glycol system. *Chemical Engineering Progress*, 60(6), 74-78.

Patel, J., Uygun, K., & Huang, Y. (2008). A path constrained method for integration of process design and control. *Computers and Chemical Engineering*, 32, 1373-1384.

Philippidis, G. P., Spindler, D. D., & Wyman, C. E. (1992). Mathematical modeling of cellulose conversion to ethanol by the simultaneous saccharification and fermentation process. *Applied Biochemistry and Biotechnology*, 34/35, 543-556.

Ricardez-Sandoval, L. A., Budman, H. M., & Douglas, P. L. (2008). Simultaneous design and control of process under uncertainty. *Journal of Process Control*, 18, 735-752.

Ricardez-Sandoval, L. A., Budman, H. M., & Douglas, P. L. (2009A). Application of robust control tools to the simultaneous design and control of dynamic systems. *Industrial and Engineering Chemistry Research*, 48, 801-813.

Ricardez-Sandoval, L. A., Budman, H. M., & Douglas, P. L. (2009B). Integration of design and control for chemical processes: A review of the literature and some recent results. Annual Reviews in Control, 33(2), 158-171.

Ricardez-Sandoval, L. A., Budman, H. M., & Douglas, P. L. (2010). Simultaneous design and control: A new approach and comparisons with existing methodologies. *Industrial and Engineering Chemistry Research*, 49, 2822-2833.

Ross, R., Bansal, V., Perkins, J. D., & Pistikopoulos, E. N. (1998). A mixed-integer dynamic optimization approach to simultaneous design and control. In *AIChE Annual Meeting*, American Institute of Chemical Engineering, Miami Beach, Florida, USA.

Russel, B. M., Henriksen, J. P., Jørgensen, S. B., & Gani, R. (2002). Integration of design and control through model analysis. *Computers and Chemical Engineering*, 26, 213-225.

Sakizlis, V., Perkins, J. D., & Pistikopoulos, E. N. (2004). Recent advances in optimization-based simultaneous process design and control design. *Computers and Chemical Engineering*, 28, 2069-2086.

Sales-Cruz, A. M. (2006). *Development of a computer aided modeling system for bio and chemical process and product design*. Ph.D. Dissertation Thesis, Technical University of Denmark.

Schweiger, C. A., & Floudas, C. A. (1997). Interaction of design and control: Optimization with dynamic models. In W. Hager, & P. Pardalos (Eds.), *Optimal control: Theory, algorithm and applications* (pp. 388-435). Gainesville, USA: Kluver Academic Publishers.

Seferlis, P., & Georgiadis, M. C. (2004). *The integration of process design and control*. Amsterdam: Elsevier B. V.

Sendin, O. H., Moles, C. G., Alonso, A. A., & Banga, J. R. (2004). Multiobjective integrated design and control using stochastic global optimization methods. In P. Seferlis, & M. C. Georgiadis (Eds.), *The integration of process design and control* (pp. 555-581). Amsterdam: Elsevier B. V.

Sharif, M., Shah, M., & Pantelides, C. C. (1998). On the design of multicomponent batch distillation columns. *Computers and Chemical Engineering*, 22(Suppl.) S69-S76.

Sinnot, R. K. (2005). *Chemical Engineering, Vol. 6. Chemical engineering design* (fourth edition). Elsevier Butterworth-Heinemann.

Skogestad, S. (2000a). Plantwide control: The search for the self-optimizing control structure. *Journal of Process Control*, 1085), 487-507.

Skogestad, S. (200b). Self-optimizing control: the missing link between steady state optimization and control. *Computers and Chemical Engineering*, 24(2-7), 569-575.

Skogestad, S. (2002). Plantwide control: Towards a systematic procedure. *Computer Aided Chemical Engineering*, 10, 57-69.

Skogestad, S. (2004). Control structure design for complete chemical plants. *Computers and Chemical Engineering*, 28(1-2), 219-234.

Skogestad, S., & Postlethwaite, I. (2007). *Multivariable Feedback Control – Analysis and Design*, 2nd. Edition, John Wiley& Sons.

South, C. R., Hogsett, D. A. L., & Lynd, L. R. (1995). Modeling simultaneous saccharification and fermentation of lignocellulose to ethanol in batch and continuous reactors. *Enzyme and Microbial Technology, 17*(9), 797–803.

Swartz, C. L. E. (2004). The use of controller parameterization in the integration of design and control. In P. Seferlis, & M. C. Georgiadis (Eds.), *The integration of process design and control* (pp. 239-263). Amsterdam: Elsevier B. V.

Van Uden, N. (1983). Effects of ethanol on the temperature relations of viability and growth in yeast. *Critical Reviews in Biotechnology*, 1(3), 263-272.

Wu, K-L, & Yu, C-C (1996). Reactor/separator processes with recycle – 1. Candidate control structure for operability. *Computers and Chemical Engineering*, 20(11), 1291-1316.

Appendix A

Derivation of an alternative distillation column sensitivity analysis

This Appendix shows the detailed derivation of an alternative way for analyzing the distillation column sensitivity at the maximum driving force. This method indicates half of the driving force area.

Let us consider the effect of the feed composition z to the desired product purity of x_d and x_b. Using the operating line of the rectifying section, the top product purity is expressed as a function of F_D as follows

$$x_d = (RR+1)F_D + x \tag{A1}$$

Differentiating Eq. (A1) with respect to F_D, we get

$$\frac{dx_d}{dF_D} = (RR+1) + \frac{dx}{dF_D} \tag{A2}$$

$$\frac{dx_d}{dF_D} = (RR+1) + \left(\frac{dF_D}{dx}\right)^{-1} \tag{A3}$$

Differentiating Eq. (A1) with respect to x, we get

$$\frac{dx_d}{dx} = (RR+1)\frac{dF_D}{dx} + 1 \tag{A4}$$

For $x = z$, Eq. (A4) is expressed as

$$\frac{dx_d}{dz} = (RR+1)\frac{dF_D}{dz} + 1 \tag{A5}$$

Since $x = z$, that is where the location of the x_{max} is, then $dx/dz = 1$, then Eq. (A5) can be simplified as

$$\frac{dx_d}{dx} = (RR+1)\frac{dF_D}{dx} + 1 \tag{A6}$$

Eq. (A7) is the expressed in terms of dxd/dF_D as follows

$$\frac{dF_D}{dx}\left[\frac{dx_d}{dF_D} - (RR+1)\right] = 1 \tag{A7}$$

The derivative expression of x_d with respect to z is expressed as follows

$$\frac{dx_d}{dz} = \left(\frac{dx_d}{dF_D}\right)\left(\frac{dF_D}{dx}\right)\left(\frac{dx}{dz}\right) \tag{A8}$$

which then can be simplified to

$$\frac{dx_d}{dz} = \left((RR+1) + \left(\frac{dF_D}{dx}\right)^{-1}\right)\left(\frac{dF_D}{dx}\right)\left(\frac{dx}{dz}\right) \tag{A9}$$

At the maximum driving force, $dF_D/dx \approx 0$ and $dx/dz = 1$, then equation (A9) becomes

$$\frac{dx_d}{dz} \approx ((RR+1))(0)(1) \approx [0] \tag{A10}$$

It can be seen that, the effect of the disturbance in the feed can best rejected at the maximum driving force. Using this simple analysis, insight can be gained in terms controllability with respect to disturbance rejection.

Appendix B

Derivation of the attainable region equations for an ethylene glycol reaction system

This Appendix shows the detailed derivation of Eqs. (5.23a)-(5.23d).

The production of ethylene glycol (*EG*) from ethylene oxide (*EO*) and water (*W*) is an isothermal, irreversible liquid phase reactions and can be represented as follows

$$\triangle\!\!\!O + H_2O \xrightarrow{k_1} HO\diagup\diagdown OH \tag{B1}$$

$$\triangle\!\!\!O + HO\diagup\diagdown OH \xrightarrow{k_2} HO\diagup\diagdown O\diagup\diagdown OH \tag{B2}$$

$$\triangle\!\!\!O + HO\diagup\diagdown O\diagup\diagdown OH \xrightarrow{k_3} HO\diagup\diagdown O\diagup\diagdown O\diagup\diagdown OH \tag{B3}$$
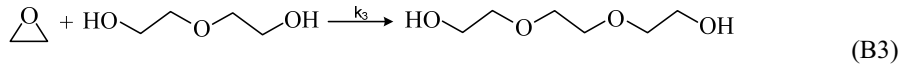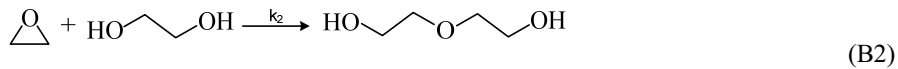
The kinetic data

$$k_1 = 5.238\exp(30.163 - 10583/T) \ ; \ k_2 = 2.1k_1 \ ; \ k_3 = 2.2k_1 \tag{B4}$$

The reaction rates are:

$$r_1 = k_1 C_{EO} C_W \tag{B5}$$

$$r_2 = k_2 C_{EO} C_{EG} \tag{B6}$$

$$r_3 = k_3 C_{EO} C_{DEG} \tag{B7}$$

By taking

$$r_2 = 2.1\left(\frac{C_{EG}}{C_W}\right) r_1 \tag{B8}$$

$$r_3 = 2.2\left(\frac{C_{DEG}}{C_W}\right) r_1 \tag{B9}$$

Substituting Eq. (B8) and Eq. (B9) into species' generation rates yields

$$dC_W = -r_1 ;$$

$$dC_{EG} = r_1 - r_2 = -r_1 \left[2.1 \left(\frac{C_{EG}}{C_W} \right) - 1 \right] ;$$

$$dC_{DEG} = r_2 - r_3 = -r_1 \left[2.2 \left(\frac{C_{DEG}}{C_W} \right) - 2.1 \left(\frac{C_{EG}}{C_W} \right) \right] ;$$

$$dC_{TEG} = r_3 = -r_1 \left[-2.2 \left(\frac{C_{DEG}}{C_W} \right) \right] ;$$

$$dC_{EO} = -r_1 - r_2 - r_3 = -r_1 \left[1 + 2.1 \left(\frac{C_{EG}}{C_W} \right) + 2.2 \left(\frac{C_{DEG}}{C_W} \right) \right]$$

Since *EG* is the desired product and *W* is the reactant, then species' generation rates can be expressed as linear combinations of dC_W and dC_{EG} as follows:

$$\frac{dC_{EG}}{dC_W} = 2.1 \left(\frac{C_{EG}}{C_W} \right) - 1 ;$$

$$\frac{dC_{DEG}}{dC_W} = 2.2 \left(\frac{C_{DEG}}{C_W} \right) - 2.1 \left(\frac{C_{EG}}{C_W} \right) ;$$

$$\frac{dC_{TEG}}{dC_W} = -2.2 \left(\frac{C_{DEG}}{C_W} \right) ;$$

$$\frac{dC_{EO}}{dC_W} = 1 + 2.1 \left(\frac{C_{EG}}{C_W} \right) + 2.2 \left(\frac{C_{DEG}}{C_W} \right)$$

By taking $dC_i = C_i - C_i^0$ results in

$$\frac{C_{EG}}{C_W - C_W^0} = 2.1 \left(\frac{C_{EG}}{C_W} \right) - 1 \tag{5.23a}$$

$$\frac{C_{DEG}}{C_W - C_W^0} = 2.2 \left(\frac{C_{DEG}}{C_W} \right) - 2.1 \left(\frac{C_{EG}}{C_W} \right) \tag{5.23b}$$

$$\frac{C_{TEG}}{C_W - C_W^0} = -2.2\left(\frac{C_{DEG}}{C_W}\right)$$ (5.23c)

$$\frac{C_{EO}^0 - C_{E0}}{C_W - C_W^0} = 1 + 2.1\left(\frac{C_{EG}}{C_W}\right) + 2.2\left(\frac{C_{DEG}}{C_W}\right)$$ (5.23d)

where C_{EO}^0 and C_W^0 are the given feed concentrations, $\left(C_{EG}^0 = C_{DEG}^0 = C_{TEG}^0 = 0\right)$.

Appendix C

Rate of equations and kinetics models for Simultaneous Saccharification and Fermentation (*SSF*) process

This Appendix shows the detailed of the rate equations and kinetic models for the *SSF* process.

Rate equations used to simulate *SSF* are presented below together with the Langmuir adsorption model as presented by Ooshima *et al*. (1990).

The Langmuir affinity constants for cellulose and lignin, respectively, were defined as:

$$K_S = \frac{ES}{E_f \times S_f \times \varsigma_S} \tag{C1}$$

$$K_l = \frac{EL}{E_f \times S_f \times \varsigma_l} \tag{C2}$$

which represent the capacity of substrate and lignin, respectively, to bind enzyme, and may also be interpreted as the ratio of *E* (enzyme) to *S* (cellulose) or *L* (lignin) in each enzyme complex.

Conservation equations for substrate, lignin, and, enzyme respectively are:

$$S = S_f + \frac{ES}{\varsigma_S} \tag{C3}$$

$$L = L_f + \frac{EL}{\varsigma_l} \tag{C4}$$

$$E_t = E_f + ES + EL \tag{C5}$$

Enzyme adsorbed to cellulose and lignin is calculated from E_t, S, and, L, with the adsorption parameters of Ooshima *et al*. (1990). The equations (C1) trough (C5) can readily be solved simultaneously to give ES, for values of initial substrate (cellulose and lignin), E_t, K_S, K_L, ς_S and ς_L.

Rate equations used to simulate are presented below, where r is the rate of formation of the component of interest. Eqs. (C6) and (C7) account for the enzymatic hydrolysis of cellulose and cellobiose, respectively; EQs. (C8) through (C10) account for cell production, substrate uptake, and solvent production by the biocatalyst:

$$r_S = -\left[k\left(1-x\right)^n + c\right] \times \frac{ES}{\varsigma_S} \times \frac{k_{S/C}}{C + k_{S/C}} \times \frac{k_{S/Eth}}{Eth + k_{S/Eth}} \tag{C6}$$

$$r_C = 1.056\left[k\left(1-x\right)^n + c\right] \times \frac{ES}{\sigma_C} \times \frac{k_{S/C}}{C + k_{S/C}} \times \frac{k_{S/Eth}}{Eth + k_{S/Eth}} - \frac{k_C \times C \times B}{K_m \times \left(1 + \left(\dfrac{G}{k_{C/G}}\right)\right) + C} \tag{C7}$$

$$r_X = \frac{X \times \mu_{max} \times G}{G + k_G} \times \left(1 - \frac{Eth}{k_{X/Eth}}\right) \tag{C8}$$

$$r_G = 1.053\left(-1.056 r_S - r_C\right) - \frac{r_X}{Y_{X/G}} \tag{C9}$$

$$r_E = \frac{Y_{E/G}}{Y_{X/G}} r_X \tag{C10}$$

where $x = \left(C_0 - C\right)/C_0$

The parameter values in Eqs. (C1)-(C10) are shown in Table C1.

For the development of the attainable region diagram, Eqs. (C11)-(C15) are used.

$$S^0 - S = t\left[k\left(1-x\right)^n + c\right] \times \frac{ES}{\varsigma_S} \times \frac{k_{S/C}}{C + k_{S/C}} \times \frac{k_{S/Eth}}{Eth + k_{S/Eth}} \tag{C11}$$

$$C - C^0 = t\left(1.056 \times \left[k\left(1-x\right)^n + c\right] \times \frac{ES}{\varsigma_S} \times \frac{k_{S/C}}{C + k_{S/C}} \times \frac{k_{S/Eth}}{Eth + k_{S/Eth}} - \frac{k_C \times C \times B}{K_m \times \left(1 + \left(\dfrac{G}{k_{C/G}}\right)\right) + C}\right) \tag{C12}$$

$$G - G^0 = t\left(1.053 \times \left(-1.056 r_C - r_B\right) - \frac{1}{Y_{X/G}} \times \frac{X \times \mu_{max} \times G}{G + k_G} \times \left(1 - \frac{Eth}{k_{X/Eth}}\right)\right) \tag{C13}$$

$$X - X^0 = t\left(\frac{X \times \mu_{max} \times G}{G + k_G} \times \left(1 - \frac{E}{k_{X/E}}\right)\right) \qquad (C14)$$

$$E - E^0 = t\left(\frac{Y_{Eth/G}}{Y_{X/G}} \times \frac{X \times \mu_{max} \times G}{G + k_G} \times \left(1 - \frac{E}{k_{X/E}}\right)\right) \qquad (C15)$$

Table C1.
Value of parameters

Symbol	Value	Units	Source
C	0.18125	1/h	South *et al*., 1995
K	2.8625	1/h	South *et al*., 1995
k_C	0.020	g/Uh	Gusakov *et al*., 1985
k_G	0.45	g/L	Moon et al., 2001
K_S	1.49	L/U	Ooshima *et al*., 1991
K_l	0.66	L/U	Ooshima *et al*., 1991
K_m	10.56	g/L	Phillippidis *et al*., 1992
$k_{C/G}$	0.62	g/L	Phillippidis *et al*., 1992
$k_{S/C}$	5.85	g/L	Phillippidis *et al*., 1992
$k_{S/Eth}$	50.35	g/L	Phillippidis *et al*., 1992
$k_{X/Eth}$	50.0	g/L	van Uden, 1983
N	5.30		South *et al*., 1995
$Ç_c$	98.3	U/g	Ooshima *et al*., 1991
$Ç_l$	15.0	U/g	Ooshima *et al*., 1991
μ_{max}	0.4	1/h	Ghose and Tyagi, 1979
$Y_{X/G}$	0.02		Lee *et al*., 1992
$Y_{Eth/G}$	0.487		Lee *et al*., 1992

Appendix D

Derivation of the set of conditional constraints for the theoretical consecutive reactions *RSR* system

This Appendix shows the detailed derivation of Eqs. (5.74)-(5.76).

To define the feasible range, we require set of conditional constraints which is derived for the *RSR* system which shown in Fig. D1 under following assumptions:

A_0 The reaction is considered to take place isothermally in a continuous stirred tank reactor (*CSTR*),

A_1 The separation section will be modelled as a component shard splitter unit with recovery of component A ($\alpha_{Y,S} = 0.99$),

A_2 A fraction of the unreacted reactant is recycled back to the reactor through a mixer unit,

A_3 No recovery of products B and C ($\beta_{Y,S} = \gamma_{Y,S} = 0$),

A_4 Pure A feed to the system ($F_B = F_C = 0$) and no purge ($\sigma = 0$).
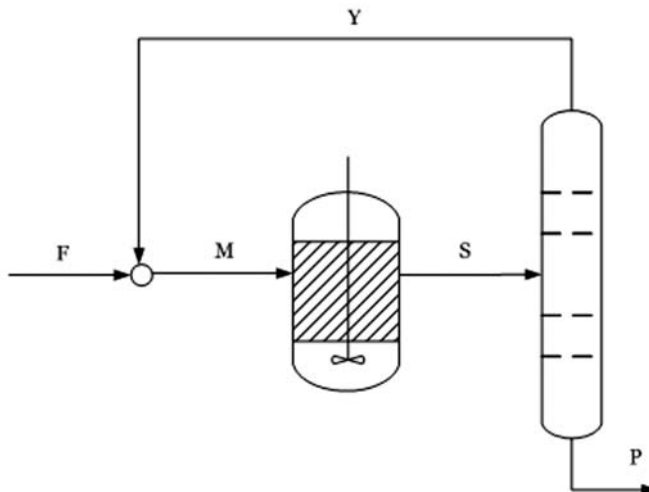
Fig. D1. Simplified flowsheet for the theoretical conceptual reactions.

Based on the simplified flowsheet described in Fig. D1 for the *EG* production and the assumptions given above, the corresponding mass balances are:

Mixer:

$$0 = F_{A,F} + F_{A,Y} - F_{A,M} \tag{D1}$$

$$0 = F_{B,M} \tag{D2}$$

$$0 = F_{C,M} \tag{D3}$$

Separator:

$$0 = F_{A,S} - F_{A,Y} - F_{A,P} \tag{D4}$$

$$0 = F_{B,S} - F_{B,P} \tag{D5}$$

$$0 = F_{C,S} - F_{C,P} \tag{D6}$$

Reactor:

$$0 = F_{A,M} - F_{A,S} - (k_1 C_{A,S} - k_{-1} C_{B,S})V \tag{D7}$$

$$0 = F_{B,M} - F_{B,S} - (k_2 C_{B,S} + k_{-1} C_{B,S} - k_1 C_{A,S})V \tag{D8}$$

$$0 = F_{C,M} - F_{C,S} + k_2 C_{B,S}V \tag{D9}$$

If $F_{A,F}$, k_1 and $C_{A,F}$ are taken as variables of reference, the corresponding mass balance (Eqs. (D1) – (D9)) in terms of dimensionless variables are:

Mixer:

$$0 = 1 + y_A - m_A \tag{D10}$$

$$0 = m_B \tag{D11}$$

$$0 = m_C \tag{D12}$$

Separator:

$$0 = s_A - \alpha_{Y,S} s_A - (1 - \alpha_{Y,S})s_A = s_A - y_A - (1 - \alpha_{Y,S})s_A \tag{D13}$$

$$0 = s_B - p_B \tag{D14}$$

$$0 = s_C - p_C \tag{D15}$$

Reactor:

$$0 = m_A - s_A - D_a(z_{A,S} - k_1^* z_{B,S}) \tag{D16}$$

$$0 = m_B - s_B - D_a [(k_1^* + k_2^*) z_{B,S} - z_{A,S}]$$ (D17)

$$0 = m_C - s_C + D_a k_2^* z_{B,S}$$ (D18)

where

$$D_a = k_1 V C_{A,F} / F_{A,F} \qquad f_i = F_{i,F} / F_{A,F} \qquad y_i = F_{i,Y} / F_{A,F}$$

$$m_i = F_{i,M} / F_{A,F} \qquad s_i = F_{i,S} / F_{A,F} \qquad p_i = F_{i,P} / F_{A,F}$$

$$z_i = C_{i,S} / C_{A,F} \qquad \alpha_{Y,S} = F_{A,Y} / F_{A,S}$$

$$F_{A,P} = (1 - \alpha_{Y,S}) F_{A,S}$$

$$k_1^* = k_{-1} / k_1 \qquad k_2^* = k_2 / k_1$$

In multiple reaction systems, the extent of reaction is an appropriate means to take into account the change in the number moles due to reaction. Table D1 summarizes the corresponding mole fractions $z_{i,S}$ for this reactive system.

Table D1.
Table of moles for simple RSR system

Component	Initial	Final (at stream S)	Mole fraction, $z_{i,S}$
A	$F_{A,M}$	$F_{A,M} - \xi_1 + \xi_3$	$F_{A,M} - \xi_1 + \xi_3 / F_{A,M}$
B	0	$\xi_1 - \xi_2 - \xi_3$	$\xi_1 - \xi_2 - \xi_3 / F_{A,M}$
C	0	ξ_2	$\xi_2 / F_{A,M}$
Total	F_M	$F_{A,M}$	1

Note that ξ_k has unit of flow (kmol/h). Therefore, given that the fresh flowrate of A has been taken as a variable of reference, thus

$$\xi_{v,k} = \xi_k / F_{A,F}, \qquad k = 1 \dots NR$$ (D19)

Eq. (D19) represents the dimensionless extent of reaction for the kth reaction.

From Table D1 it can be seen that the flowrate of A leaving the reactor, in terms of dimensionless variables, is

$$s_A = m_A - \xi_{v,1} + \xi_{v,3}$$

But from Eq. (D13) and $y_A = \alpha_{Y,S} s_A$, hence

$$s_A = (1 - \xi_{v,1} + \xi_{v,3}) / (1 - \alpha_{Y,S})$$ (D20)

Similarly, the flowrate of A into the reactor is

$$m_A = 1 + y_A = 1 + \alpha_{Y,S} s_A$$
$$= 1 - \alpha_{Y,S}\left(\xi_{v,1} - \xi_{v,3}\right)/\left(1 - \alpha_{Y,S}\right) \tag{D21}$$

The reactor outlet flowrate can also be obtained from Table D1, hence

$$S = m_A \tag{D22}$$

Note that only A is fed to the reactor, since this is the only component to be recycled. By substituting Eq. (D22) in the corresponding mole fraction expressions in the reactor $z_{i,S}$, thus

$$z_{A,S} = \frac{1 - \xi_{v,1} + \xi_{v,3}}{1 - \alpha_{Y,S}\left(\xi_{v,1} - \xi_{v,3}\right)} \tag{D23}$$

$$z_{B,S} = \frac{\left(\xi_{v,1} - \xi_{v,2} - \xi_{v,3}\right)\left(1 - \alpha_{Y,S}\right)}{1 - \alpha_{Y,S}\left(\xi_{v,1} - \xi_{v,3}\right)} \tag{D24}$$

$$z_{C,S} = \frac{\xi_{v,2}\left(1 - \alpha_{Y,S}\right)}{1 - \alpha_{Y,S}\left(\xi_{v,1} - \xi_{v,3}\right)} \tag{D25}$$

By substituting Eqs. (D23)-(D25) into Eqs. (D16)-(D18) yields

$$0 = \xi_{v,1} - \xi_{v,3} - \Omega\left[\left(1 - \xi_{v,1} + \xi_{v,3}\right) - k_1^*\left(\xi_{v,1} - \xi_{v,2} - \xi_{v,3}\right)\left(1 - \alpha_{Y,S}\right)\right] \tag{5.74}$$

$$0 = \left(\xi_{v,3} + \xi_{v,2} - \xi_{v,1}\right) - \Omega\left[\left(k_1^* + k_2^*\right)\left(\xi_{v,1} - \xi_{v,2} - \xi_{v,3}\right)\left(1 - \alpha_{Y,S}\right) - \left(1 - \xi_{v,1} + \xi_{v,3}\right)\right] \tag{5.75}$$

$$0 = \xi_{v,2} - \Omega k_2^*\left(\xi_{v,1} - \xi_{v,2} - \xi_{v,3}\right)\left(1 - \alpha_{Y,S}\right) \tag{5.76}$$

where

$$\Omega = \frac{D_a}{1 - \alpha_{Y,S}\left(\xi_{v,1} - \xi_{v,3}\right)}$$

Appendix E

Derivation of the set of conditional constraints for an ethylene glycol *RSR* system

This Appendix shows the detailed derivation of Eqs. (5.82)-(5.84).

To define the feasible range, we require set of conditional constraints which is derived for the *RSR* system which shown in Fig. E1 under following assumptions:

A_0.   Steady-state condition using a CSTR,

A_1.   Complete recovery of *EO* recycled back to the reactor ($\alpha_{Y,S} = 1$),

A_3.   No recycle of *EG*, *DEG* and *TEG* ($\chi_{Y,S} = \delta_{Y,S} = \varepsilon_{Y,S} = 0$),

A_4.   Equimolar feed flowrate of reactants ($F_{A,F} = F_{B,F}$),

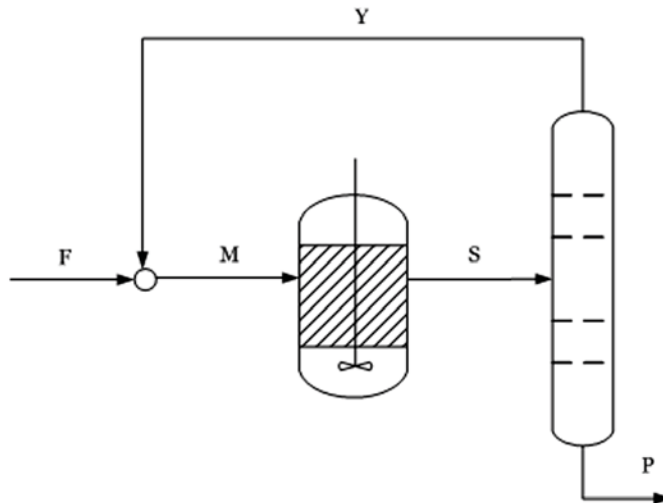A_5.   Isothermal reaction in CSTR.

Fig. E1. Simplified flowsheet for the Ethylene Glycol production.

Based on the simplified flowsheet described in Fig. E1 for the *EG* production and the assumptions given above, the corresponding mass balances are:

Mixer:

$$0 = F_{EO,F} + F_{EO,Y} - F_{EO,M} \tag{E1}$$

$$0 = F_{W,F} + F_{W,Y} - F_{W,M} \tag{E2}$$

$$0 = F_{EG,M} \tag{E3}$$

$$0 = F_{DEG,M} \tag{E4}$$

$$0 = F_{TEG,M} \tag{E5}$$

Separator:

$$0 = F_{EO,S} - F_{EO,Y} \tag{E6}$$

$$0 = F_{W,S} - F_{W,Y} - F_{W,P} \tag{E7}$$

$$0 = F_{EG,S} - F_{EG,P} \tag{E8}$$

$$0 = F_{DEG,S} - F_{DEG,P} \tag{E9}$$

$$0 = F_{TEG,S} - F_{TEG,P} \tag{E10}$$

Reactor:

$$0 = F_{EO,M} - F_{EO,S} - \left(k_1 C_{EO,S} C_{W,S} + k_2 C_{EO,S} C_{EG,S} + k_3 C_{EO,S} C_{DEG,S}\right)V \tag{E11}$$

$$0 = F_{W,M} - F_{W,S} - \left(k_1 C_{EO,S} C_{W,S}\right)V \tag{E12}$$

$$0 = -F_{EG,S} - \left(k_2 C_{EO,S} C_{EG,S} - k_1 C_{EO,S} C_{W,S}\right)V \tag{E13}$$

$$0 = -F_{DEG,S} - \left(k_3 C_{EO,S} C_{DEG,S} - k_2 C_{EO,S} C_{EG,S}\right)V \tag{E14}$$

$$0 = -F_{TEGS} - \left(-k_3 C_{EO,S} C_{DEG,S}\right)V \tag{E15}$$

If $F_{EO,F}$, k_1 and $C_{EO,F}$ are taken as variables of reference, the corresponding mass balance Eqs. (E1)-(E15) in terms of dimensionless variables are:

Mixer:

$$0 = 1 + y_{EO} - m_{EO} \tag{E16}$$

$$0 = f_W + y_W - m_W \tag{E17}$$

$$0 = m_{EG} \tag{E18}$$

$$0 = m_{DEG} \tag{E19}$$

$$0 = m_{TEG} \tag{E20}$$

Separator:

$$0 = s_{EO} - y_{EO} \tag{E21}$$

$$0 = s_W - \beta_{Y,S} s_W - (1 - \beta_{Y,S}) s_W = s_W - y_W - (1 - \beta_{Y,S}) s_W \tag{E22}$$

$$0 = s_{EG} - p_{EG} \tag{E23}$$

$$0 = s_{DEG} - p_{DEG} \tag{E24}$$

$$0 = s_{DEG} - p_{DEG} \tag{E25}$$

Reactor:

$$0 = m_{EO} - s_{EO} - Da\left(z_{EO,S} z_{W,S} + 2.1 z_{EO,S} z_{EG,S} + 2.2 z_{EO,S} z_{DEG,S}\right) \tag{E26}$$

$$0 = m_W - s_W - Da\left(z_{EO,S} z_{W,S}\right) \tag{E27}$$

$$0 = -s_{EG} - Da\left(2.1 z_{EO,S} z_{EG,S} - z_{EO,S} z_{W,S}\right) \tag{E28}$$

$$0 = -s_{DEG} - Da\left(2.2 z_{EO,S} z_{DEG,S} - 2.1 z_{EO,S} z_{EG,S}\right) \tag{E29}$$

$$0 = -s_{TEG} - Da\left(-2.2 z_{EO,S} z_{DEG,S}\right) \tag{E30}$$

where

$$Da = k_1 V C_{EO,F}^2 / F_{EO,F} \qquad f_i = F_{i,F} / F_{EO,F} \qquad y_i = F_{i,Y} / F_{EO,F}$$
$$m_i = F_{i,M} / F_{EO,F} \qquad s_i = F_{i,S} / F_{EO,F} \qquad p_i = F_{i,P} / F_{EO,F}$$
$$z_i = C_i / C_{EO,F} \qquad \beta_{Y,S} = F_{W,Y} / F_{W,S} \qquad F_{W,Y} = \beta_{Y,S} F_{W,S}$$
$$F_{W,P} = (1 - \beta_{Y,S}) F_{W,S} \qquad k_2/k_1 = 2.1 \qquad k_3/k_1 = 2.2$$

In multiple reaction systems, the extent of reaction is an appropriate means to take in account the change in the number of moles due to reaction. In this respect, Table E1 summarizes the corresponding mole fractions $z_{i,S}$ for this reactive system.

Table E1.
Table of moles for ethylene glycol production

Comp.	Initial	Final (at stream S)	Mole fraction, $z_{i,S}$
EO	$F_{EO,M}$	$F_{EO,M} - (\xi_1 + \xi_2 + \xi_3)$	$F_{EO,M} - (\xi_1 + \xi_2 + \xi_3)/F_M - (\xi_1 + \xi_2 + \xi_3)$
W	$F_{W,M}$	$F_{W,M} - \xi_1$	$F_{W,M} - \xi_1/F_M - (\xi_1 + \xi_2 + \xi_3)$
EG	0	$\xi_1 - \xi_2$	$\xi_1 - \xi_2/F_M - (\xi_1 + \xi_2 + \xi_3)$
DEG	0	$\xi_2 - \xi_3$	$\xi_2 - \xi_3/F_M - (\xi_1 + \xi_2 + \xi_3)$
TEG	0	ξ_3	$\xi_3/F_M - (\xi_1 + \xi_2 + \xi_3)$
Total	F_M	$F_M - (\xi_1 + \xi_2 + \xi_3)$	1

Note that ξ_k has unit of flow (kmol/h). Therefore, given that the fresh flowrate of *EO* has been taken as a variable of reference, thus

$$\xi_{v,k} = \xi_k / F_{EO,F}, \qquad k = 1 \dots NR \tag{E31}$$

Eq. (E31) represents the dimensionless extent of reaction for the *k*th reaction.

From Table E1 it can be seen that the flowrate of *W* leaving the reactor, in terms of dimensionless variables, is

$$s_W = m_W - \xi_{v,1}$$

But from Eq. (E17) and $y_W = \beta_{Y,S} s_W$, hence

$$s_W = (f_W - \xi_{v,1})/(1 - \beta_{Y,S}) \tag{E32}$$

Similarly, the flowrate of *W* into the reactor is

$$m_W = f_W + y_W = f_W + \beta_{Y,S} s_W$$

$$= (f_W - \beta_{Y,S}\xi_{v,1})/(1 - \beta_{Y,S}) \tag{E33}$$

The reactor outlet flowrate can also be obtained from Table E1, hence

$$S = m_{EO} + m_W - (\xi_{v,1} + \xi_{v,2} + \xi_{v,3}) \tag{E34}$$

Note that only *EO* and *W* are fed to the reactor, since these are the only components to be recycled. The reactor outlet flowrate S, based on Eqs. (E16) and (E32)-(E33), after rearranging leads to

$$S = 1 + y_{EO} + \left(\frac{f_W - \xi_{v,1}}{1 - \beta_{Y,S}} \right) - \left(\xi_{v,2} + \xi_{v,3} \right) \qquad (E35)$$

By substituting Eq. (E35) in the corresponding mole fraction expressions in the reactor $z_{i,S}$, thus

$$z_{EO,S} = \frac{1 + y_{EO} - \left(\xi_{v,1} + \xi_{v,2} + \xi_{v,3} \right)}{1 + y_{EO} + \left(f_W - \xi_{v,1} \right)/\left(1 - \beta_{Y,S} \right) - \left(\xi_{v,2} + \xi_{v,3} \right)} \qquad (E36)$$

$$z_{W,S} = \frac{\left(f_W - \xi_{v,1} \right)/\left(1 - \beta_{Y,S} \right)}{1 + y_{EO} + \left(f_W - \xi_{v,1} \right)/\left(1 - \beta_{Y,S} \right) - \left(\xi_{v,2} + \xi_{v,3} \right)} \qquad (E37)$$

$$z_{EG,S} = \frac{\xi_{v,1} - \xi_{v,2}}{1 + y_{EO} + \left(f_W - \xi_{v,1} \right)/\left(1 - \beta_{Y,S} \right) - \left(\xi_{v,2} + \xi_{v,3} \right)} \qquad (E38)$$

$$z_{DEG,S} = \frac{\xi_{v,2} - \xi_{v,3}}{1 + y_{EO} + \left(f_W - \xi_{v,1} \right)/\left(1 - \beta_{Y,S} \right) - \left(\xi_{v,2} + \xi_{v,3} \right)} \qquad (E39)$$

$$z_{TEG,S} = \frac{\xi_{v,3}}{1 + y_{EO} + \left(f_W - \xi_{v,1} \right)/\left(1 - \beta_{Y,S} \right) - \left(\xi_{v,2} + \xi_{v,3} \right)} \qquad (E40)$$

By substituting Eqs. (E36)-(E40) into Eqs. (E27)-(E29) yields

$$0 = \left(1 - \beta_{Y,S} \right) \xi_{v,1} - \Omega \left(1 + y_{EO} - \xi_{v,1} - \xi_{v,2} - \xi_{v,3} \right) \left(f_W - \xi_{v,1} \right) \qquad (5.82)$$

$$0 = \left(1 - \beta_{Y,S} \right) \left(\xi_{v,2} - \xi_{v,1} \right) - \Omega \left(1 + y_{EO} - \xi_{v,1} - \xi_{v,2} - \xi_{v,3} \right) \ldots$$
$$\ldots \left[2.1 \left(1 - \beta_{Y,S} \right) \left(\xi_{v,1} - \xi_{v,2} \right) - \left(f_W - \xi_{v,1} \right) \right] \qquad (5.83)$$

$$0 = \left(\xi_{v,3} - \xi_{v2} \right) - \Omega \left(1 + y_{EO} - \xi_{v,1} - \xi_{v,2} - \xi_{v,3} \right) \ldots$$
$$\ldots \left[2.2 \left(\xi_{v,2} - \xi_{v,3} \right) - 2.1 \left(\xi_{v,1} - \xi_{v,2} \right) \right] \qquad (5.84)$$

where

$$\Omega = \frac{Da}{\left[1 + y_{EO} + \left(f_W - \xi_{v,1} \right)/\left(1 - \beta_{Y,S} \right) - \left(\xi_{v,2} + \xi_{v,3} \right) \right]^2}$$

This PhD-project was carried out at CAPEC, the Computer Aided Product-Process Engineering Center. CAPEC is committed to research, to work in close collaboration with industry and to participate in educational activities. The research objectives of CAPEC are to develop computer-aided systems for product/process simulation, design, analysis and control/operation for chemical, petrochemical, pharmaceutical and biochemical industries. The dissemination of the research results of CAPEC is carried out in terms of computational tools, technology and application. Under computational tools, CAPEC is involved with mathematical models, numerical solvers, process/operation mathematical models, numerical solvers, process simulators, process/product synthesis/design toolbox, control toolbox, databases and many more. Under technology, CAPEC is involved with development of methodologies for synthesis/design of processes and products, analysis, control and operation of processes, strategies for modelling and simulation, solvent and chemical selection and design, pollution prevention and many more. Under application, CAPEC is actively involved with developing industrial case studies, tutorial case studies for education and training, technology transfer studies together with industrial companies, consulting and many more.

Further information about CAPEC can be found at www.capec.kt.dtu.dk.